

PERFORMANCE UPGRADING OF
COMMERCIAL VEHICLE REAR
UNDERRIDE GUARDS

Volume 2

Appendices

Prepared for

Bureau of Motor Carrier Safety
Federal Highway Administration
U. S. Department of Transportation

by

Eugene Buth
Research Engineer

T. J. Hirsh
Research Engineer

L. I. Griffin III
Assistant Research Psychologist

and

M. E. James
Associate Research Engineer

Texas A&M Research Foundation
Texas Transportation Institute
Texas A&M University

March 1980

TABLE OF CONTENTS
VOLUME 2 APPENDICES

Appendix	Page
A - COLLISION MECHANICS	A-1
Synthesis of the Problem	A-1
Forces and Deformations During Impact with Underride Guard	A-4
B - ACCIDENT SEVERITY AND IMPACT SPEED RELATIONSHIPS	B-1
A Rational Method for Choosing Closing Speed Which the Underride Guard Should be Able to Withstand	B-1
Illustrative Application of Rational Method for Choosing Vehicle Design Closing Speed	B-7
Using Human Tolerance to Impact Acceleration as a Method for Selecting Vehicle Closing Speed	B-7
Automobile Crashworthiness in Frontal Impacts	B-16
Summary	B-18
C - VEHICLE DATA	C-1
Automobile Data	C-1
Truck and Trailer Data	C-11
D - RECOMMENDED PLASTIC ANALYSIS AND DESIGN PROCEDURE FOR REAR UNDERRIDE GUARDS	D-1

TABLE OF CONTENTS
VOLUME 2 APPENDICES
(continued)

Appendix	Page
E - UNDERRIDE GUARD DESIGN CALCULATIONS	E-1
General	E-1
Rigid Frame Underride Guard 1-ST	E-2
Rigid Frame Underride Guard 1-AL	E-6
Rigid Frame Underride Guard 2-ST	E-11
Rigid Frame Underride Guard 2-AL	E-14
Variable Road Clearance - Truck Underride Guard 3-AL	E-17
Rigid Frame Underride Guard 5-ST	E-24
Guard 7-ST for IH 1610 Truck	E-28
F - DETAILS OF FULL-SCALE CRASH TESTS	F-1
Test Program	F-1
General Test Procedures	F-4
Data Acquisition and Processing	F-4
Test Results	F-12
G - PARAMETRIC STUDY OF GUARD DESIGNS	G-1
Design for Centric Load	G-4
Results	G-7
Eccentric Load Analysis for Diagonally Braced Guards	G-7
Eccentric Load Analysis for Cantilevered Guards	G-10

TABLE OF CONTENTS
VOLUME 2 APPENDICES
(continued)

<u>Appendix</u>	<u>Page</u>
H - ECONOMIC ANALYSIS	H-1
Benefit Cost Analysis of Modified Underride Guards	H-1
Relative Costs of the Four Modified Underride Guards (4ST, 5ST, 6ST, and 2AL)	H-6
Discussion of Results	H-23



APPENDIX A
COLLISION MECHANICS

Synthesis of the Problem

A collision between two automobiles or between an automobile and a barrier may be synthesized with a reasonable degree of accuracy using elementary mechanics or more sophisticated computer simulation models. Both methods use experimentally derived stiffness or force-deformation properties to simulate the crush characteristics of the vehicle front end as input. The accuracy achieved is generally controlled by the accuracy of the input stiffness of the vehicle.

Emori (3) has presented a simple model of an automobile collision wherein the automobile is idealized as a lump mass and a spring as shown in Figure A-1.

The idealized collision in Figure A-1 may be described by the homogeneous linear differential equation:

$$\begin{aligned} - kx &= M\ddot{x} \\ \text{or} & \text{----- Eqn A-1} \\ \ddot{x} + w^2x &= 0 \end{aligned}$$

where:

- x = displacement of automobile (ft)
- M = mass of automobile (slugs)
- \ddot{x} = acceleration of automobile (ft/sec²)
- k = spring stiffness of automobile (g's/ft)
- $w^2 = k/M$

The boundary conditions are:

$$\begin{aligned} \text{at } t &= 0 \\ x &= 0 \text{ and } \dot{x} = V \end{aligned}$$

where:

- t = time after impact
- V = velocity of automobile at impact

The solution is:

$$x = \frac{V}{W} \sin wt \text{----- Eqn A-2}$$

After observing the results of many full-scale crash tests involving a rigid barrier, Emori concluded that a reasonably accurate average value for the spring stiffness, k, was 12.5 times the weight of the impacting

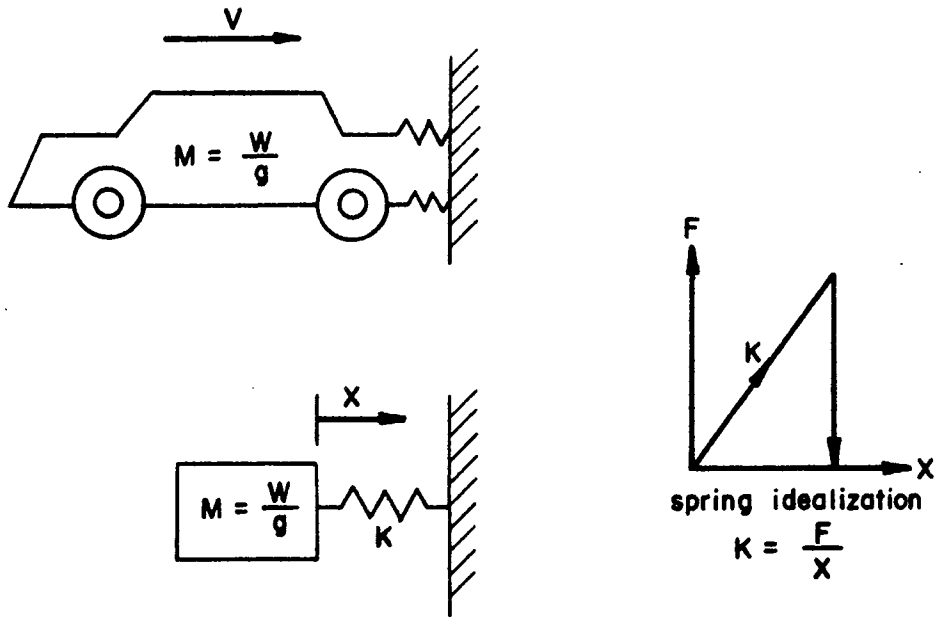


Figure A-1. Simulation of Rigid Barrier Collision.

automobile. This value was based on 1968 models and older full-size automobiles manufactured in the United States. It is further noted that this value was derived from impacts with a flat-faced rigid barrier, wherein the entire cross section of the automobile was deformed. If one differentiates Equation A-2 twice, the result is an expression for acceleration of the automobile:

$$X = -Vw \sin wt \quad \text{--- Eqn A-3}$$

Since V and w are constants, the maximum value of \ddot{x} (max. acceleration) occurs when:

$$\begin{aligned} \sin wt &= 1 \\ \text{or} & \quad \text{--- Eqn A-4} \\ wt &= \pi/2 \end{aligned}$$

Since $w = \sqrt{\frac{k}{m}} = 20.06 \text{ rad/sec}$

$$t = \pi/2 \frac{1}{20.06} = .078 \text{ sec}$$

and

$$\ddot{x}_{\max} = Vw = -V/20.06 \text{ sec}$$

Now, if \ddot{x}_{\max} is in g's and V is in mph,

$$\ddot{x}_{\max} = G_{\max} = -.91 V \quad \text{--- Eqn A-5}$$

$$G_{\max} = -0.91 V$$

or --- Eqn A-6

$$F_{\max} = G_{\max} W$$

and

$$G_{\text{avg}} = -0.58 V$$

or --- Eqn A-7

$$F_{\text{avg}} = G_{\text{avg}} W$$

where:

- V = impact velocity in mph
- G = acceleration in g's

One can readily extend this simulation to that of the vehicle-to-truck collision as shown in Figure A-2. By using Newton's third law (the conservation of momentum), one may state that the momentum before impact must equal the momentum after impact:

$$M_1V_1 + M_2V_2 = M_1V'_1 + M_2V'_2 \quad \text{Eqn A-8}$$

If spring k_1 has no restitution (i.e., plastic impact), then:

$$M_1V_1 + M_2V_2 = V'(M_1 + M_2) \quad \text{Eqn A-9}$$

and

$$V' = \frac{W_1V_1 + W_2V_2}{W_1 + W_2} \quad \text{Eqn A-10}$$

$$\Delta V_1 = -V_1 + V' \quad \text{Eqn A-11}$$

$$\Delta V_2 = -V_2 + V' \quad \text{Eqn A-12}$$

If it is assumed that V_2 is small or zero than:

$$V' = V_1 \left[\frac{W_1}{W_2 + W_1} \right] \quad \text{Eqn A-13}$$

It can then be shown that the accelerations imposed on the automobile are:

$$G_{\max} = 0.91\Delta V_1 \quad \text{Eqn A-14}$$

$$G_{\text{avg}} = 0.58\Delta V_1 \quad \text{Eqn A-15}$$

Forces and Deformations During Impact with Underride Guard

Equations similar to those just presented may be used to (1) define performance criteria for truck underride guards and (2) compute impact forces for guards to meet those criteria.

The value of spring stiffness, k , recommended by Emori was 12.5 W for frontal impacts of average 1968 automobiles into rigid non-moving barriers. For automobiles impacting rear underride guards, the value differs from 12.5 for a number of reasons. The ground clearance of the guard is such that it does not necessarily contact the automobile bumper. In guard impacts where alignment is offset, the full width of the automobile is not involved. Also, the late model automobiles considered in this study have frontal crush characteristics that differ from the earlier models.

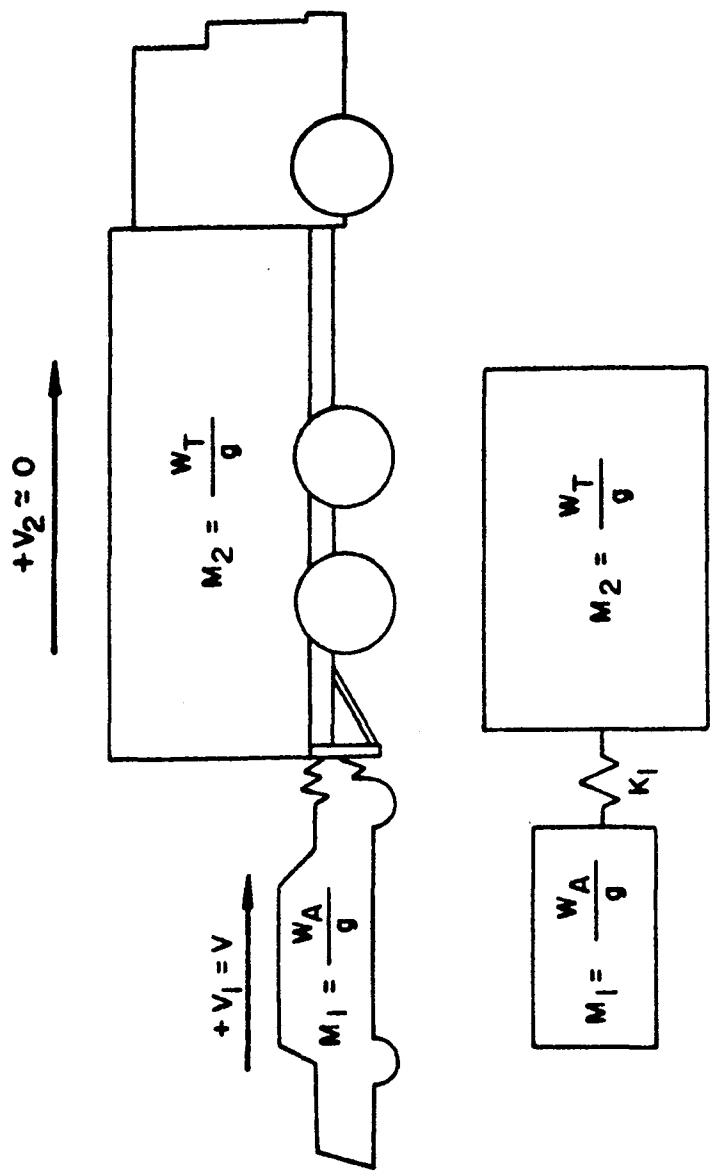


Figure A-2. Simulation of Vehicle to Vehicle Collision.

Table A-1 presents a summary of some recent vehicle crash test results with some late model automobiles into rigid walls and into rigid truck underride guards of various heights. The table shows the computed average stiffness (K) of the vehicle front end. For the seven crash tests into the rigid wall the average K is found to be 12.66 W which is very close to Emori's average value.

The crash test results into rigid guards varying in height from 0.46 m (18 in.) to 0.61 m (24 in.) indicate the stiffness K does decrease as guard ground clearance increases as shown in Figure A-3.

Figure A-3 shows that for guard heights greater than 0.64 m (25 in.) the guard may not contact the engine block and K would be reduced even more. Guard heights greater than 0.81 m (32 in.) may not even contact the hood and K would be essentially zero.

From Figure A-3 the stiffness of the automobile when impacting guards of various heights (H) can be expressed as:

$$K = (26.4 - 0.7 H) W_A \text{ - - - - - Eqn A-16}$$

where:

- K = stiffness in lbs per ft
- H = guard height in in. $16 \leq H \leq 24$, and
- W_A = car weight in lbs

Since the automobile may not have a centric impact with the rigid truck guard, the K value should be reduced further for off center impacts. In the absence of more accurate test data, it will be assumed that the stiffness of the car front end is proportional to the frontal lateral distance of contact with the guard. Thus,

$$K = (26.4 - 0.7 H) W_A \frac{\Delta}{D} \text{ - - - - - Eqn A-17}$$

where:

- Δ = auto-guard contact distance, ft, and
- D = width of automobile in ft

Using the value of K for the automobile, the maximum impact force in an impact with a rigid underride guard would be:

$$F_{\max} = 0.2585 \sqrt{26.4 - 0.7 H} (W_A) V_{\text{mph}} \left[\frac{W_T}{W_T + W_A} \right] \sqrt{\frac{\Delta}{D}} \text{ - - Eqn A-18}$$

The maximum automobile crush distance, X_{\max} , would be:

$$X_{\max} = \frac{F_{\max}}{K} \text{ - - - - - Eqn A-19}$$

Table A-1. Vehicle Front-End Stiffness.

Vehicle Vintage-Make	W = Veh Weight lb	Impact Speed mph	Test Barrier	Max Veh Deformation in.	*3 Vehicle Stiffness K in. lb/ft	*4 Vehicle Stiffness K in. lb/ft	Source of Data
1977 VW Rabbit	2250	40.8	18 in. Rigid Guard	34.8	13.2 W	11.2 W	TTI Test 1
1979 Chev. Imp.	4090	33.8	18 in. Rigid Guard	31.2	11.0 W	10.0 W	TTI Test 3
1977 VW Rabbit	2300	36.3	22 in. Rigid Guard*2	35.04	10.3 W	8.8 W	TTI Test 5
1966 Ford	3750	39.6	18 in. Rigid Guard	40.0	9.4 W		Test No. 7 Calspan Report VJ-2844-V-3
1966 Ford	3460	43.1	24 in. Rigid Guard	47.5	7.9 W*1		Test No. 11 Calspan Report VJ-2844-V-3
1973 Ford	4600	30.0	Wall	29.1	10.2 W		
1974 Ford	4367	31.0	Wall	30.1	10.2 W		
1976 Chevette	2534	30.4	21 in. Rigid Guard	29.2	10.4 W		IIHS Test 3
1975 Plymouth	4560	30.7	Wall	28.0	11.6 W		
1973 AMC Matador	4502	30.0	Wall	25.5	13.3 W		
1973 Chevelle	4625	29.9	Wall	25.1	13.7 W		
1975 Chev. Imp.	4330	29.8	Wall	24.9	13.8 W		
1973 Plymouth	4380	30.2	Wall	23.6	15.8 W		
				Avg K = 11.9 W*5			

*1 - This value is low because of 24 in. guard height. It was not considered in computing avg K.

*2 - Unloaded van raised guard clearance an additional 2 in.

*3 - From equation $K = V^2/gx^2$.

*4 - From acceleration-deformation curves.

*5 - W = weight of car in lbs.

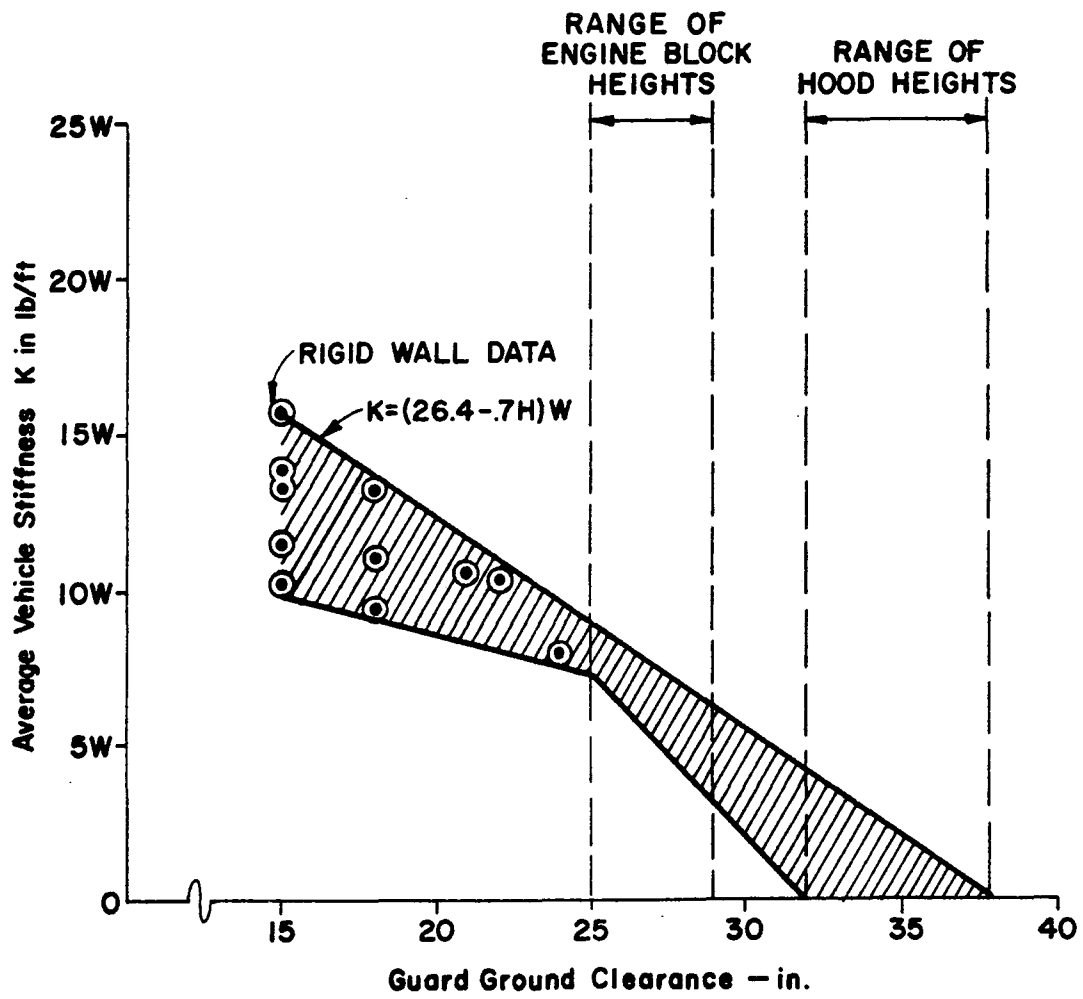


Figure A-3. Variation of Vehicle Front-End Stiffness vs Guard Ground Clearance.

The maximum deceleration (G_{\max}) of the automobile would be:

$$G_{\max} = \frac{F_{\max}}{W_A} \text{ - - - - - Eqn A-20}$$

Equations A-18, A-19 and A-20 can be used to compute the maximum impact force on a rigid underride guard for design purposes. For example, a centric impact involving a 1860 kg (4100 lb) automobile traveling at 56 km/h (35 mph) into a 0.51 m (20 in.) high guard on a 24,970 kg (55,000 lb) truck/trailer yields a maximum impact force of 121,562 lbs.

$$F_{\max} = 0.2585 \sqrt{26.4 - .7 \times 20} \times 4100 \text{ lbs} \times 35 \times \left(\frac{55,000}{55,000 + 4100} \right)$$

$$F_{\max} = 121,562 \text{ lbs}$$

The maximum automobile crush distance would be:

$$X_{\max} = \frac{121,562}{(26.4 - .7 \times 20) \times 4100 \text{ lbs}}$$

$$X_{\max} = 2.39 \text{ ft}$$

And the maximum deceleration on the car would be:

$$G_{\max} = \frac{F_{\max}}{W} = \frac{121,562}{4100} = 29.6 \text{ g's}$$

If the automobile had impacted the guard with a 1.07 m (42 in.) offset (center line to center line) the ratio of Δ/D would be 0.5 for a 2.13 m (7 ft) wide guard and 1.83 m (6 ft) wide car and the maximum impact force would be:

$$F_{\max} = 121,562 \text{ lbs} \sqrt{.5} = 85,944 \text{ lbs}$$



APPENDIX B

ACCIDENT SEVERITY AND IMPACT SPEED RELATIONSHIPS

A Rational Method for Choosing the Closing Speed Which the Underride Guard Should be Able to Withstand

In the analysis to follow, it will be assumed that the underride guard is rigid, i.e. the guard will not be deformed or destroyed by the impact of a striking automobile at closing speeds below a stated amount. Secondly, it will be assumed that the guard is positioned sufficiently close to the ground to insure that it contacts the engine block (and ideally the bumper and frame) of the striking automobile. Thirdly, it is assumed that the mass of the truck or trailer to which the underride guard is attached is infinite -- i.e. the truck or trailer is not displaced during impact. With these three assumptions in mind, the question can reasonably be asked: What closing speeds should the underride guard be able to withstand before deforming or breaking away?

If the guard were designed to withstand impacts of up to 16 km/h (10 mph), and then break away, it seems reasonable to believe that the guard would be of relatively little benefit. At such a low design speed, the occupants of automobiles striking the guard at higher speeds would receive little or no protection from the device. That is to say, at impact speeds above 16 km/h (10 mph), the guard would not significantly reduce the probability of fatality.

Going to the other extreme, imagine that the underride guard was designed to withstand impacts at closing speeds of up to 145 km/h (90 mph). In this case, the driver of an automobile striking the guard at a speed of 137 km/h (85 mph) would be prevented from riding beneath or beyond the guard. Death due to passenger compartment penetration by truck/trailer parts would be avoided. However, at this speed death would have occurred anyway, due to the decelerations on the occupant and/or to penetration of the passenger compartment by frontal components (e.g., the hood or engine) of the impacting automobile itself.

As the design speed of the underride guard rises, the cost, weight, and complexity of the device will also rise. Additionally, as the design speed of the underride guard rises, reductions in fatalities will also rise, then begin to taper off, and finally approach an asymptote at closing speeds in excess of say 80 or 96 km/h (50 or 60 mph). See Figure B-1. This figure is hypothetical, but theoretically justifiable.

Consider the information contained in Figure B-2. This function (f_1) indicates, not surprisingly, that as impact speeds rise, the probability of a fatality also rises. At high speeds, the probability of a fatality approaches certainty, 1.0.

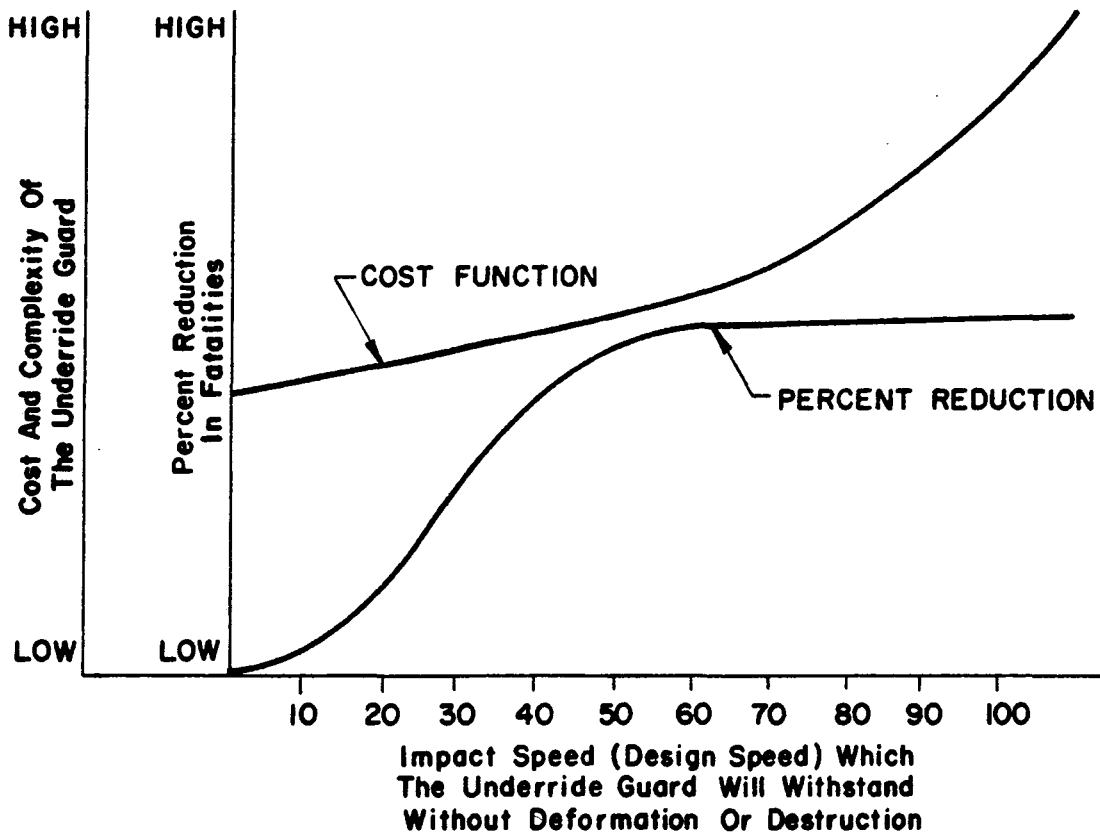


Figure B-1 . Relationship Between Design Speed of the Underride Guard and Cost and Reduction in Fatalities.

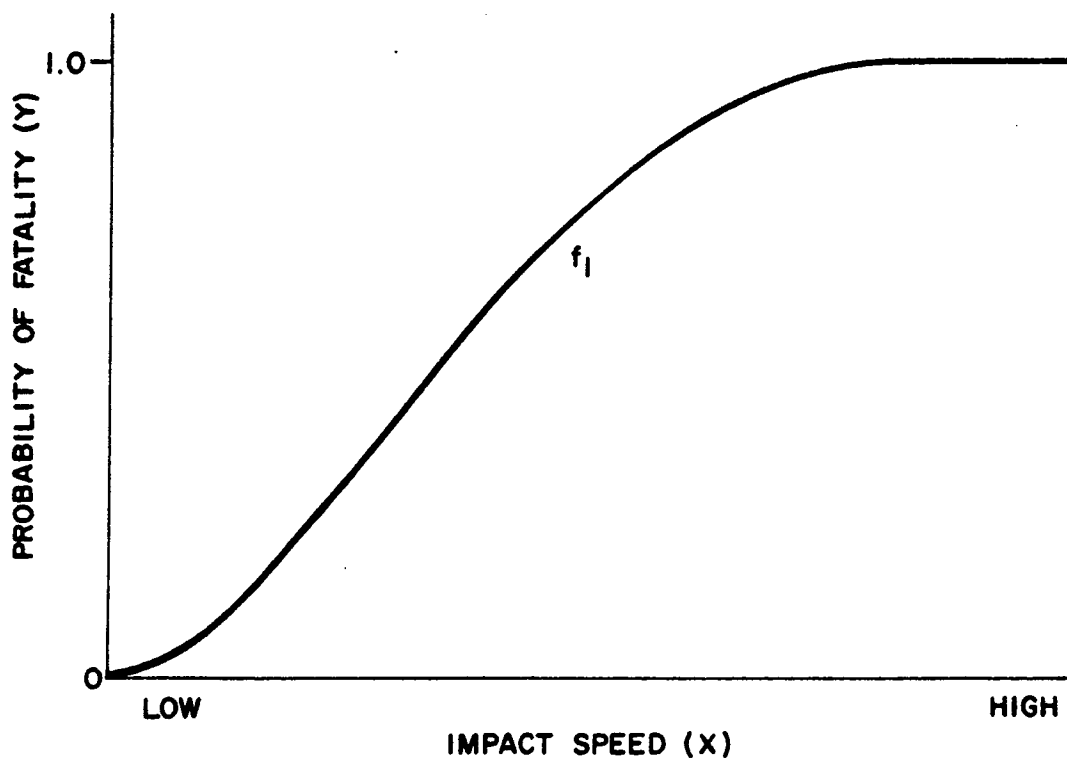


Figure B-2 . Impacts of Passenger Cars into the Rear End of Presently Equipped Trucks and Trailers.

Now consider another figure, Figure B-3. Again, probability of fatality is located along the Y axis and impact speed is located along the X axis. The function from the previous figure, f_1 , is redrawn in Figure B-3A. A second function, f_2 , depicts the probability of a fatality as a function of impact speed when passenger cars strike a truck or trailer equipped with a new proposed underride guard. Note that the design speed (break away speed) for the guard is X_i . At speeds up to X_i , the device restrains the passenger car, prevents penetration beneath the truck/trailer, and reduces the probability of fatality. At speeds in excess of X_i , the device will fail, and the passenger car will penetrate beneath the truck or trailer to which it is attached. We will assume that at impact speeds in excess of X_i , f_1 and f_2 are synonymous, i.e., at speeds in excess of X_i the modified guard does not reduce the probability of fatality*.

Figure B-3B depicts the reduction in the probability of fatality (f_3) which is attributable to the modified guard as a function of impact speed. The reduction in the probability of fatality (f_3) is nothing more than the vertical distance between f_1 and f_2 in the previous figure (B-3A).

In order to determine the effectiveness of the modified guard in reducing fatalities (not probability of fatality), one more function is needed. This function, f_4 , is depicted in Figure B-4. From this figure it can be seen that f_4 is the distribution of impact speeds for passenger cars colliding with the rear ends of truck/trailers.

Now, by multiplying f_1 (Figure B-2) by f_4 (Figure B-4) and integrating the resultant function from 0 to infinity, we can determine the number of lives currently being lost due to passenger cars impacting the rear ends of existing trucks and trailers. By multiplying f_3 by f_4 (Figures B-3B and B-4) and integrating the resultant function from 0 to X_i , we can determine the number of lives which could be saved, if all presently existing trucks and trailers were equipped with modified guards. To determine the degree (percentage) by which the modified guard reduces fatalities, the following equation would be appropriate:

$$\begin{array}{l} \text{Effectiveness of} \\ \text{the Modified} \\ \text{Guard in Reducing} \\ \text{Fatalities} \\ \text{(Expressed as a Percent)} \end{array} = \left[\frac{\int_0^{X_i} (f_3 \times f_4) \, dx}{\int_0^{\infty} (f_1 \times f_4) \, dx} \right] \quad - - - \text{Eqn B-1}$$

* At impact speeds slightly above X_i , it is conceivable that f_2 will lie below f_1 . The reason for this is fairly straight forward. If present underride guards fail easily at speeds in excess of X_i , penetration beneath the truck/trailer will be large, and the probability of fatality will be high. If the modified guard fails at speeds in excess of X_i , but in the process of failing reduces the speed of the car, penetration beneath the truck/trailer will be reduced, and the probability of fatality may be reduced.

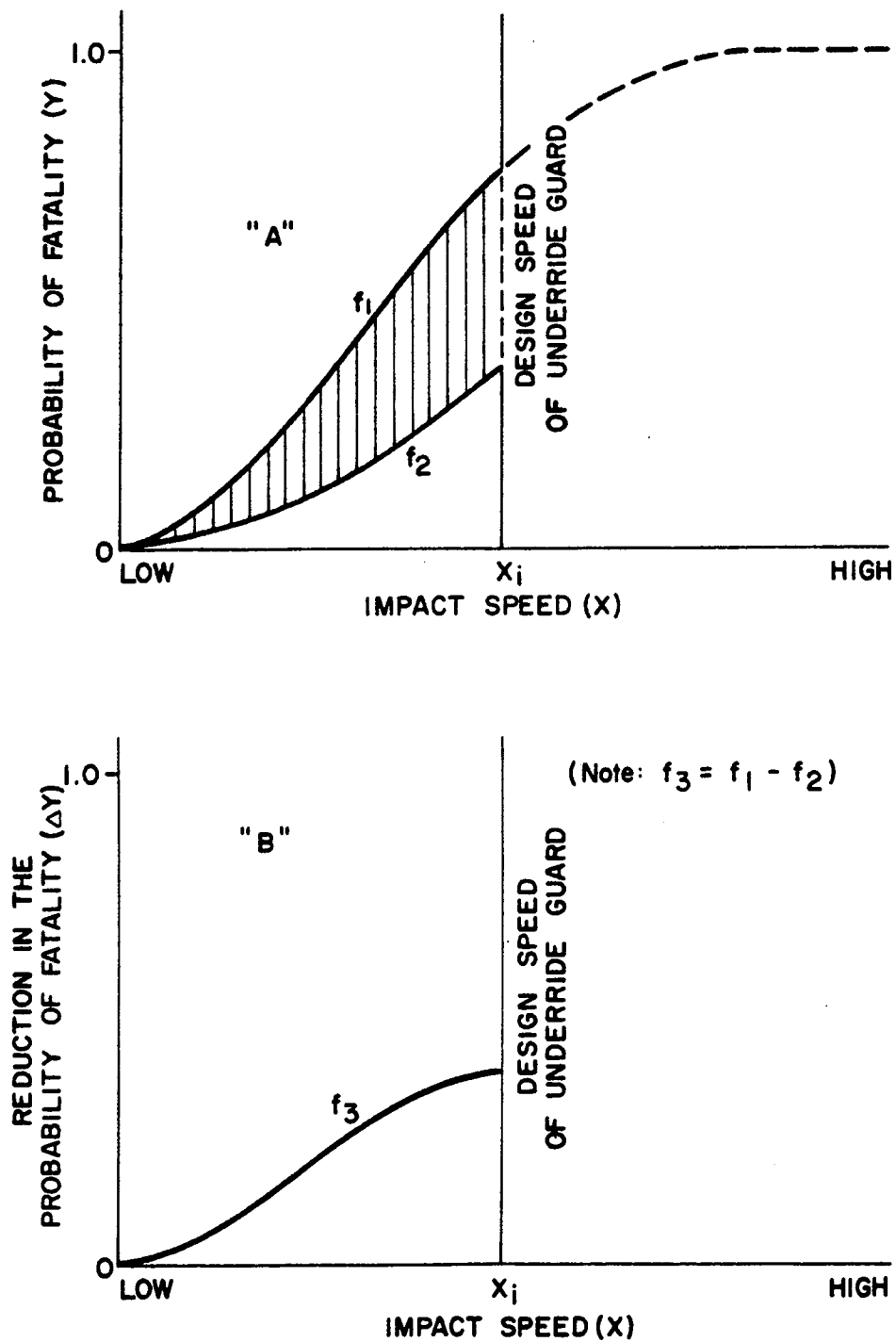


Figure B-3. Impacts of Passenger Cars into the Rear End of Presently Equipped and Modified Trucks and Trailers.

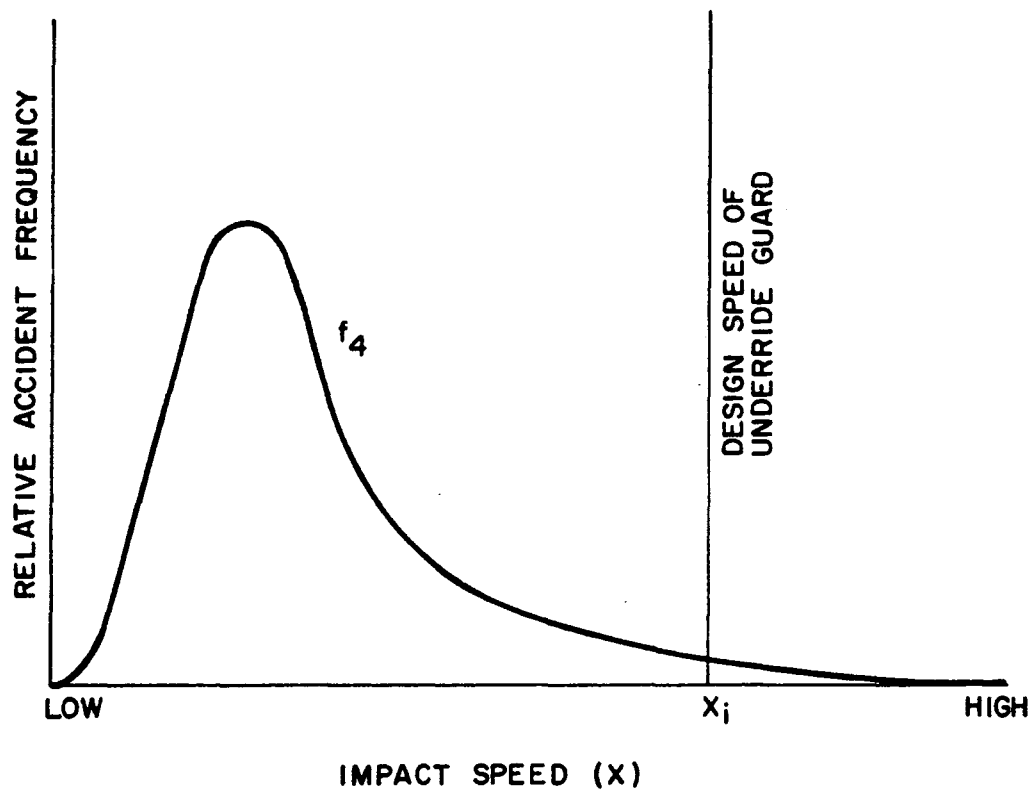


Figure B-4 . Impact of Passenger Cars into the Rear End of Trucks and Trailers During a Given Time Period.

By repeatedly solving the equation shown above with a variety of X_i 's, the lower function depicted in Figure B-1 can be produced. With the aid of this last function, a maximum design speed for the underride guard can be defensibly and rationally specified.

Illustrative Application of Rational Method for Choosing Vehicle Design Closing Speed

Unfortunately, the statistical accident data required to use the rational method just presented are not available. To illustrate the method and to get a feel for what the results might look like, some engineering estimates have been made.

Figure B-5 presents an estimate of what the probability of a fatality with a present underride guard (f_1) might look like. The curve for f_1 is based upon the literature and the experience of the authors. The curve for f_2 is also strictly the opinion of the authors. Using the estimated curves for f_1 and f_2 , f_3 was calculated -- f_3 equals f_1 minus f_2 . Figure B-6 presents an estimate of what f_3 would look like.

Figure B-7 depicts what the accident frequency distribution of passenger cars into the rear end of trucks (f_4) might look like. These data, in fact, represent all types of front distributed accidents (e.g. head-on crashes, crashes into fixed objects, etc.), not just collisions with the rear ends of trucks or trailers. These data are simply assumed to be appropriate for defining f_4 .

These values of f_1 , f_2 , f_3 and f_4 were used to compute the percent reduction in fatalities which might be achieved if a rigid barrier underride device were used. These results are shown in Figure B-8. The curve on Figure B-8 indicates that a design closing or impact speed greater than 97 km/h (60 mph) would not reduce truck/trailer rear end fatalities to any further extent. The curve seems to indicate that the desirable design impact speed might be around 64 or 80 km/h (40 or 50 mph). The curve further indicates the maximum possible reduction in truck underride fatalities which could be achieved by a rigid device is around 22.4 percent.

Using Human Tolerance to Impact Acceleration as a Method for Selecting Vehicle Closing Speed

By definition, acceleration is a time rate of change in velocity. Linear acceleration is the rate of change in the linear velocity of a mass, the direction of which is kept constant. One approach in selecting a design closing speed for a truck underride device would be to determine a range of linear accelerations which are tolerable to the human body. In other words, what upper limit of acceleration can a person in an automobile experience and still not sustain serious injury. As of this time, no definite levels of human tolerance to acceleration have

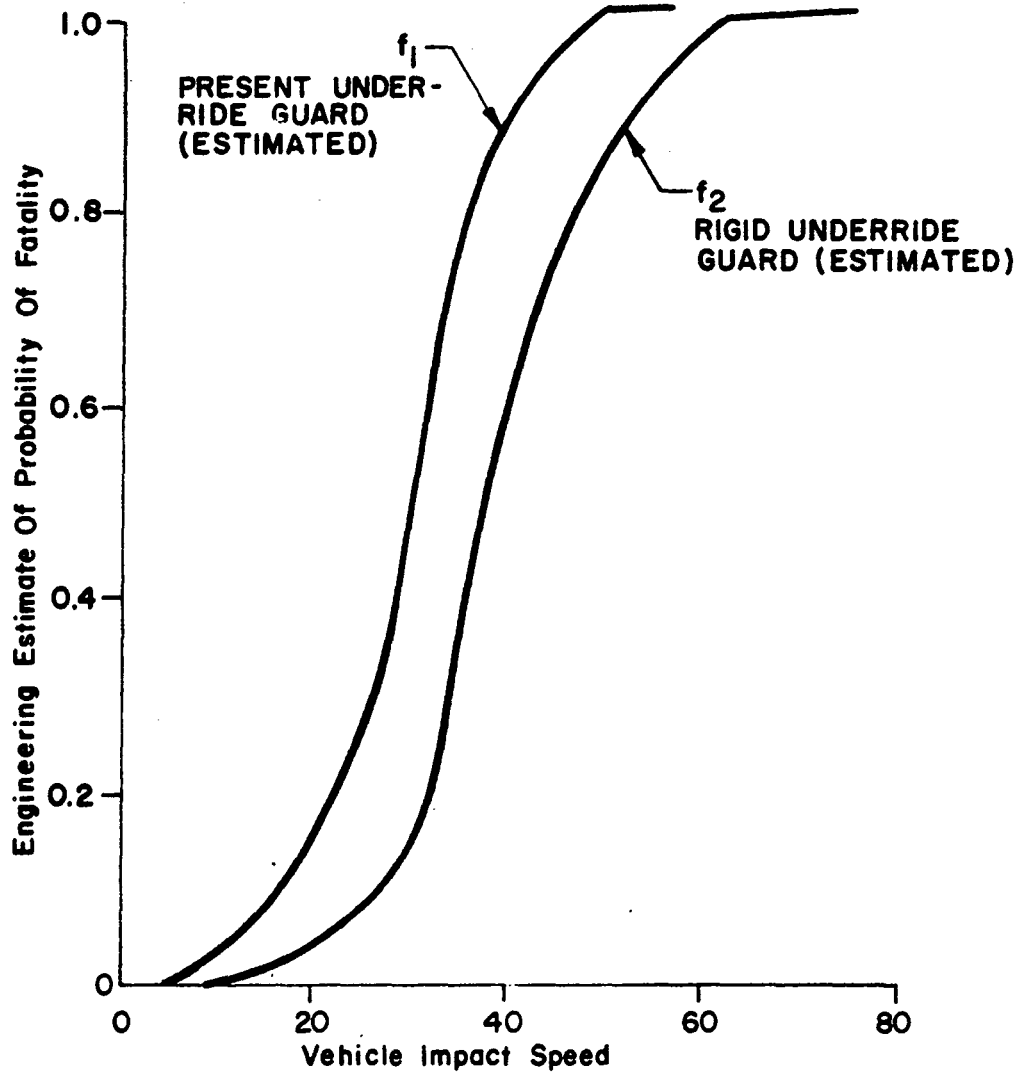


Figure B-5 . Engineering Estimate of What the Probability of Fatality with a Passenger Car Collision With a Present Underride Guard and a Proposed Rigid Underride Guard.

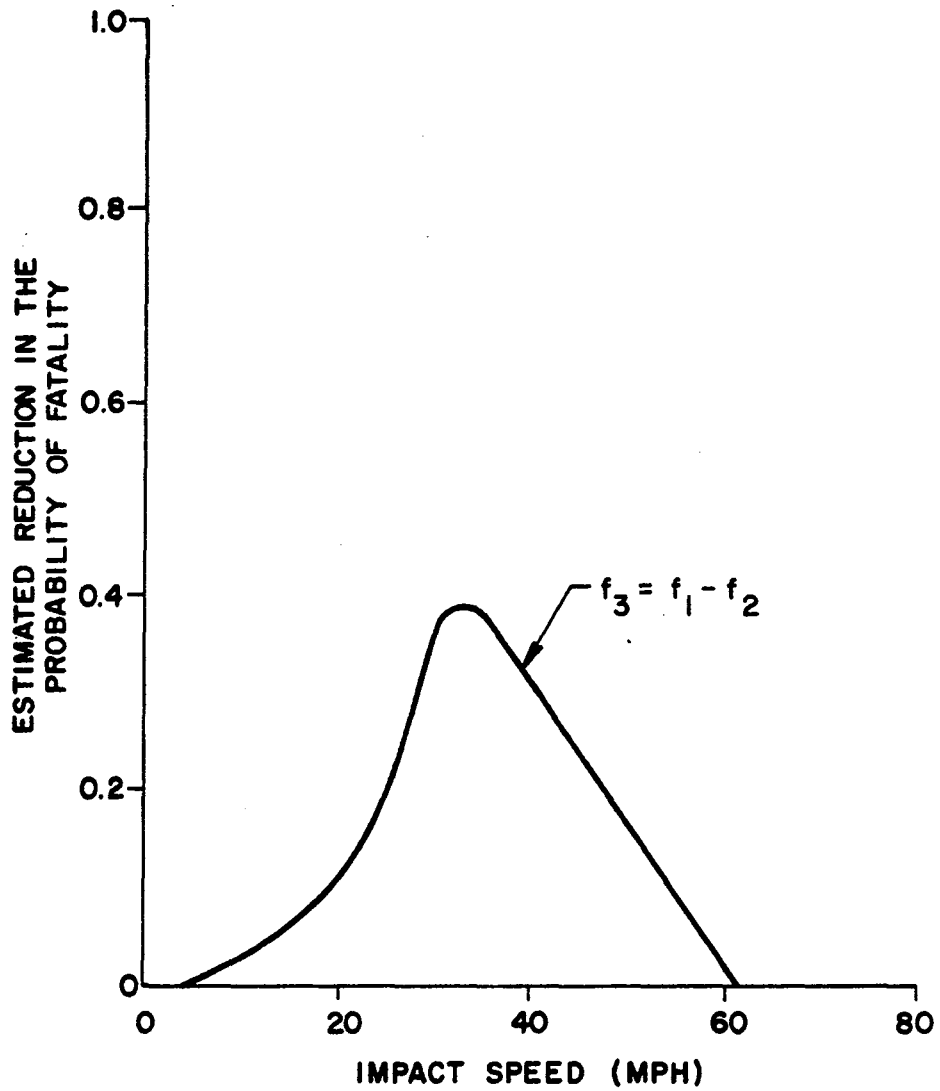


Figure B-6 . Estimated Reduction in the Probability of Fatality. Data from Figure B-5 . Strictly an Engineering Estimate.

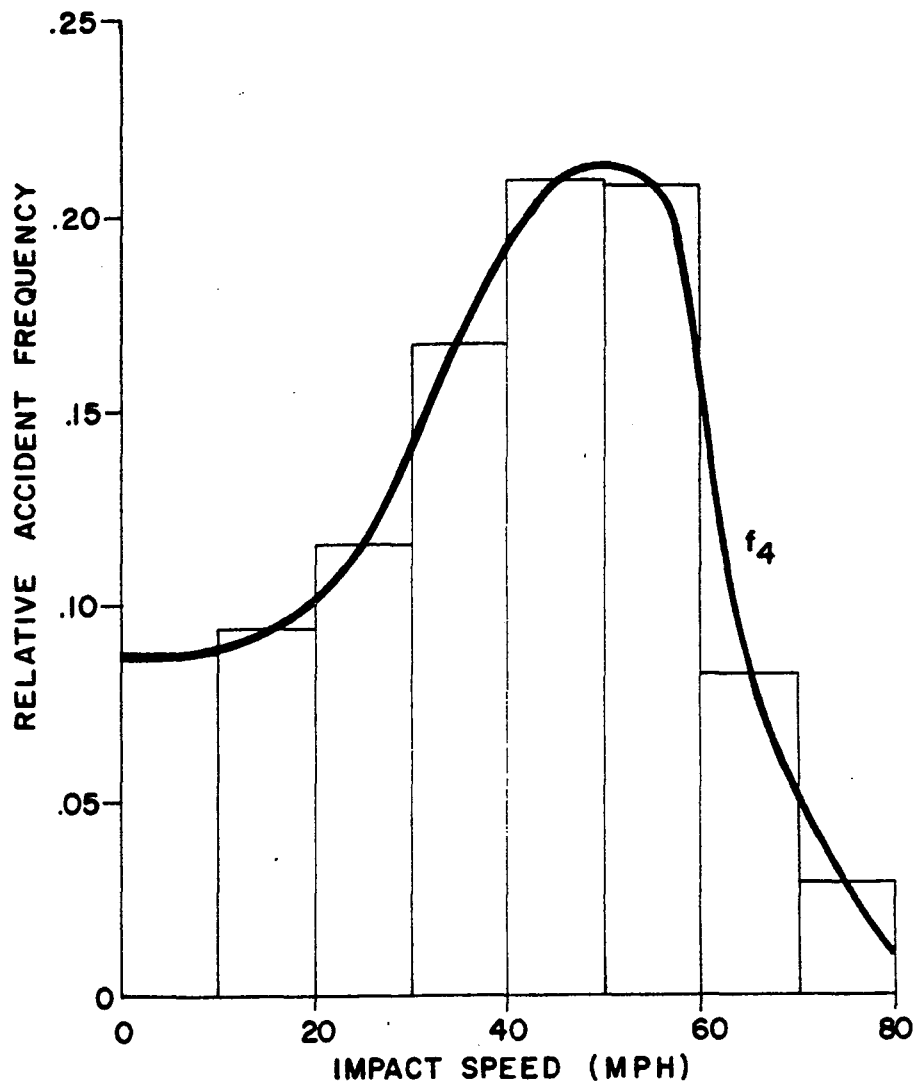


Figure B-7 . Relative Accident Frequency by Impact Speed. Data from 8,481 Vehicle Frontal Distributed Accidents in North Carolina 1972-73 taken from University of North Carolina's Highway Safety Research Center's Accident Data Base.

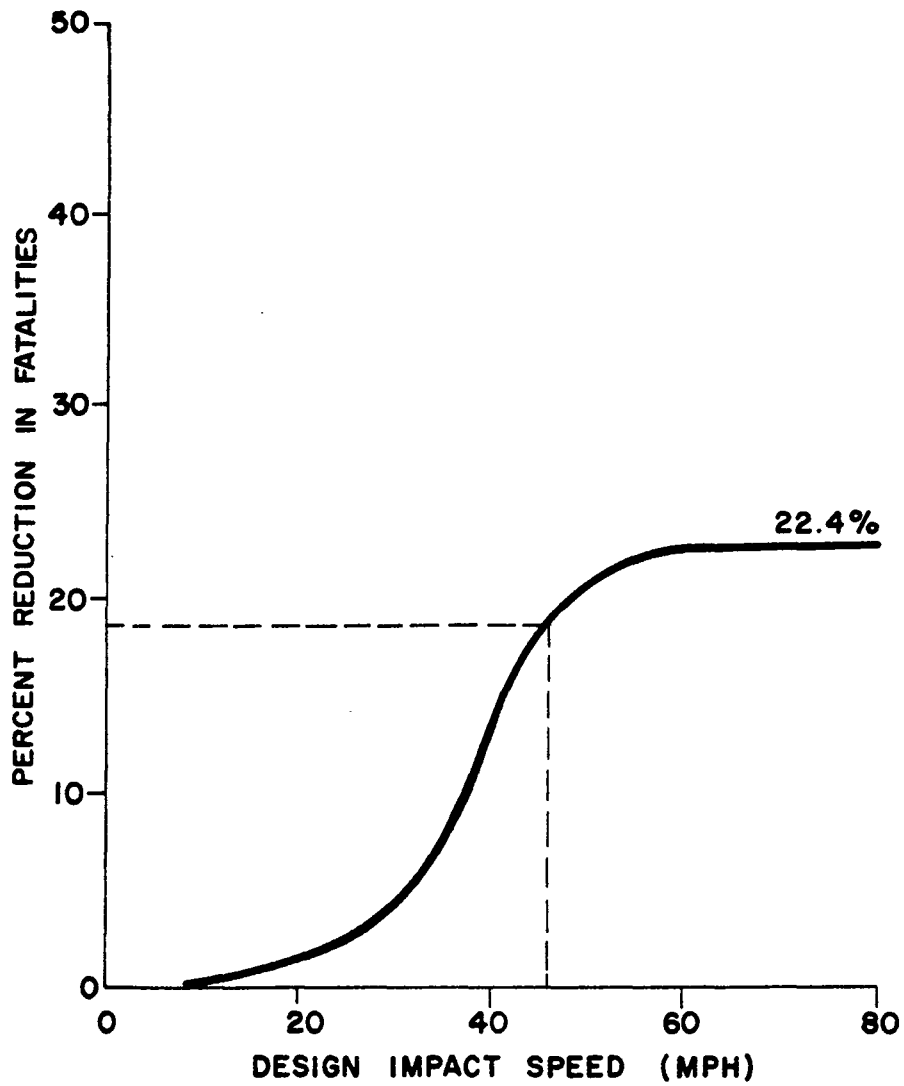


Figure B-8 . Engineering Estimate as to what the Percent Reduction in Fatalities Might be if a Rigid Barrier Underride Device were Used.

been established even though quite a bit of research has been done in this area.

Longitudinal deceleration tests have been conducted by Stapp (11) and crash tests have been performed by Severy (12). Most of the investigations conducted have dealt with longitudinal deceleration with well restrained vehicle occupants.

In actual automobiles, however, a variety of restrained as well as unrestrained vehicle occupants must be considered. A 1961 report published by Cornell Aeronautical Laboratory (13) provides tentative acceptable limits of combined lateral and longitudinal decelerations for human occupants as a function of restraint usage (unrestrained, restrained by lap belt, restrained by lap belt and shoulder harness) (see Table B-1). Note that the decelerations shown in Table B-1 are assumed not to exceed 0.2 seconds and the rate of onset is assumed not to exceed 500 g's per second.

Wyle Laboratories also recognized the need for adapting existing acceleration tolerance data to the automobile impact situation, so they planned a ten year program of research relating to the biodynamics of vehicular crashworthiness. In one of a series of initial reports on this program, Hyde (14) presented human body peak acceleration limits on a time-duration and direction basis. These limits are presented in Figure B-9.

The orientation of the axes in Figures B-9 and B-10 is such that the X-axis is forward or backward, the Y-axis is left or right, and the Z-axis is up or down. Positive and negative signs are used to show the direction of the acceleration vector. By convention, for vertical accelerations $+G_z$ indicates that the eyeballs are displaced down, and $-G_z$ indicates the eyeballs are displaced up. For longitudinal accelerations, $+G_x$ indicates the eyeballs are displaced in, and $-G_x$ indicates the eyeballs are displaced out. For lateral accelerations, $+G_y$ indicates displacement of the eyes to the right, and $-G_y$ indicates displacement of the eyes to the left.

The upper acceleration limits shown in Figure B-9 are those for which Hyde (14) says disabling injury or death may be expected. The limiting acceleration envelope which is derived from information in Figure B-9 is shown in Figure B-10 along with individual acceleration limits.

In view of the preceding discussion of the available literature, the writers have established tolerable longitudinal deceleration to be 20 to 25 g's for occupants restrained by lap belt and shoulder harness. These deceleration values may be used to arrive at a design closing speed for underride guards.

Table B-1. Limits of Tolerable Deceleration (Tentative)
Suggested by Cornell Aeronautical Laboratory.

RESTRAINT	MAXIMUM DECELERATION (g's)		
	Lateral	Longitudinal	Total
Unrestrained occupant	3	5	6
Occupant restrained by lap belt	5	10	12
Occupant restrained by lap belt and shoulder harness	15	25	25

Where: time of duration not exceeding 0.2 sec and the rate of onset not exceeding 500 g's per sec.

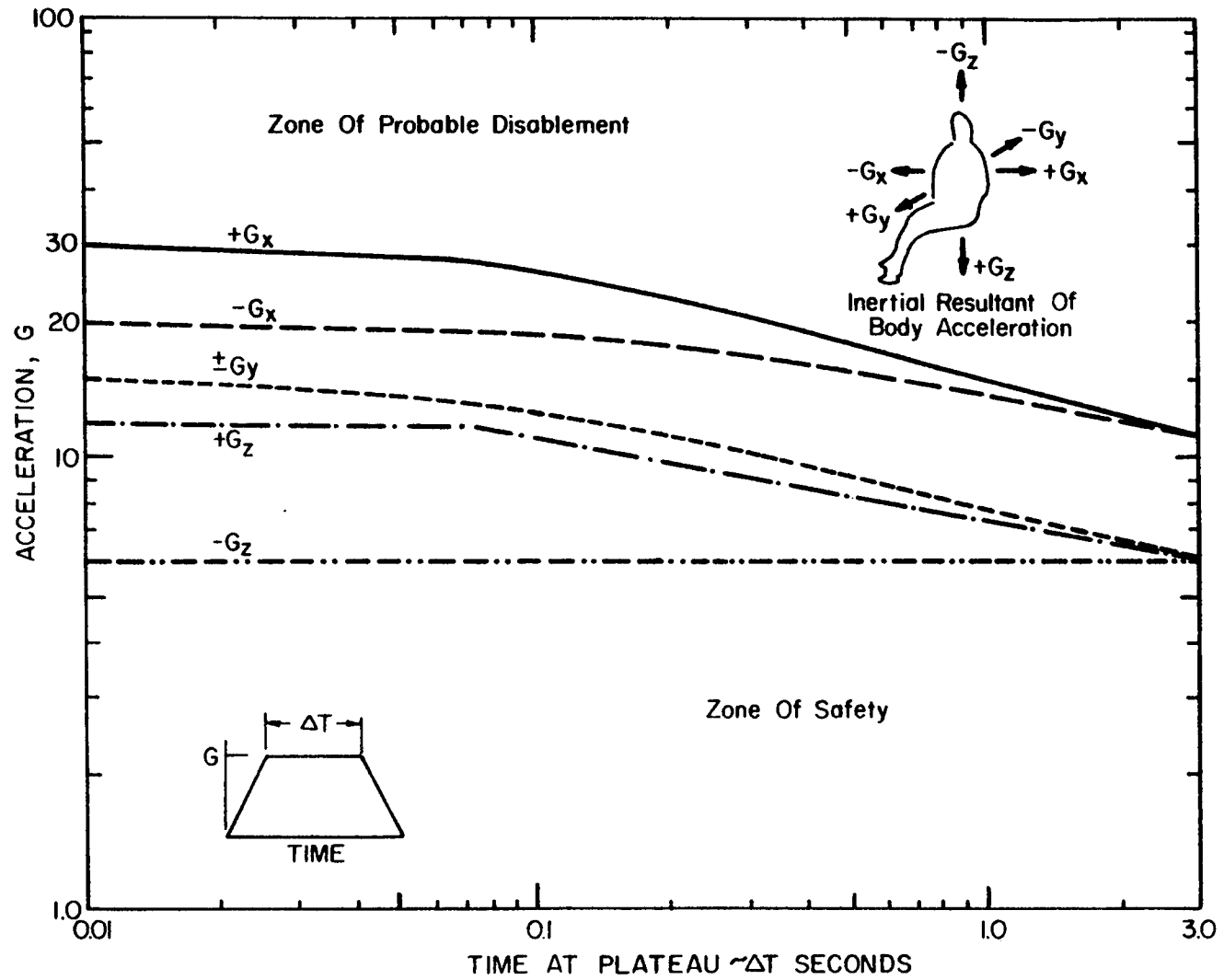
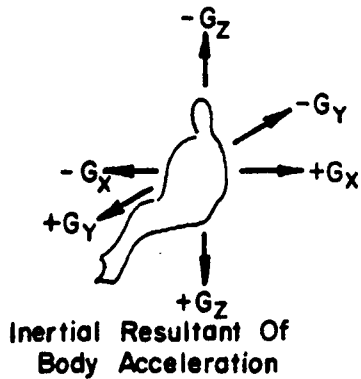
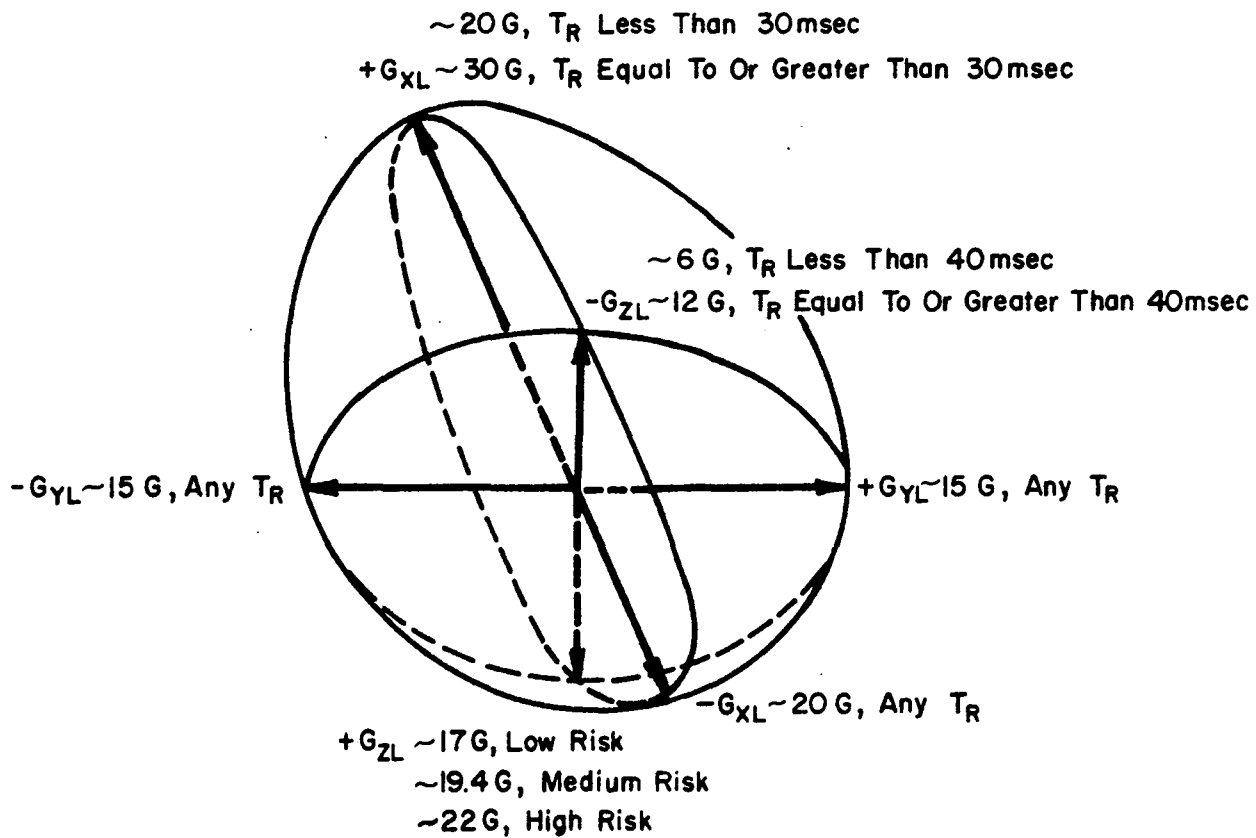


Figure B-9. Human Body Peak Acceleration Limits for Various Time Durations and Directions.



T_R Is The Rise Time Or Time Of Onset Acceleration

Figure B-10. Envelope for Defining the Multiaxial Acceleration Limits.

Chapter III and Appendix A have presented Emori's (3) simplified method of computing the approximate average deceleration (G_{avg}) of a vehicle impacting a rigid barrier.

$$G_{avg} = 0.58 V_{mph} \quad \text{--- --- --- --- --- Eqn B-2}$$

As indicated above, the maximum tolerable longitudinal deceleration for occupants restrained by lap belt and shoulder harness is about 20 to 25 g's (eyeballs out, duration not to exceed 200 ms, onset rate not exceeding 500 g's per second; and no secondary collision with car interior). Using this simple equation, it can be seen that the probable maximum automobile impact speed into a barrier is about

$$V_{mph} = \frac{G_{avg}}{0.58} = \frac{20}{0.58} = 35 \text{ mph}$$

or

$$V_{mph} = \frac{25}{0.58} = 43 \text{ mph}$$

Automobile Crashworthiness in Frontal Impacts

In order to design the underride protective device, the crashworthiness of automobiles should be considered. Automobile safety experts have suggested that present day automobiles have a built-in frontal crashworthiness of at least 48 km/h (30 mph) (barrier equivalent speed). Some experts are now suggesting that in the 1980's there is a high probability that vehicles will have a built-in crashworthiness of 64 km/h (40 mph) (barrier equivalent speed) or greater.

In discussion with engineers at Ford Motor Company, we asked: what is the probability that a person would live through 64 km/h (40 mph) frontal barrier crash? Response: That is difficult to answer quantitatively, but certainly a majority (see Figure B-11).

William Haddon of the Insurance Institute for Highway Safety (IIHS) partially corroborates the Ford statement:

"Seated adult males, decelerating while moving forward for the length of time typically involved in fatal crashes, about 100 milliseconds, can usually sustain forces of at least 30-35 g's without injury. Tolerances vary with the direction of force (e.g. longitudinal forces on the spine produce injury at far lower loadings) and with anatomical site and degree of localization. (Data are insufficient for localized forces, and for females, children, the elderly, and people with pathological conditions, but the values probably overlap those for adult males.) The equations show that the energy dissipated in crashes increases with the *square* of crash speed, an important determinant of both frequency and severity of injury.

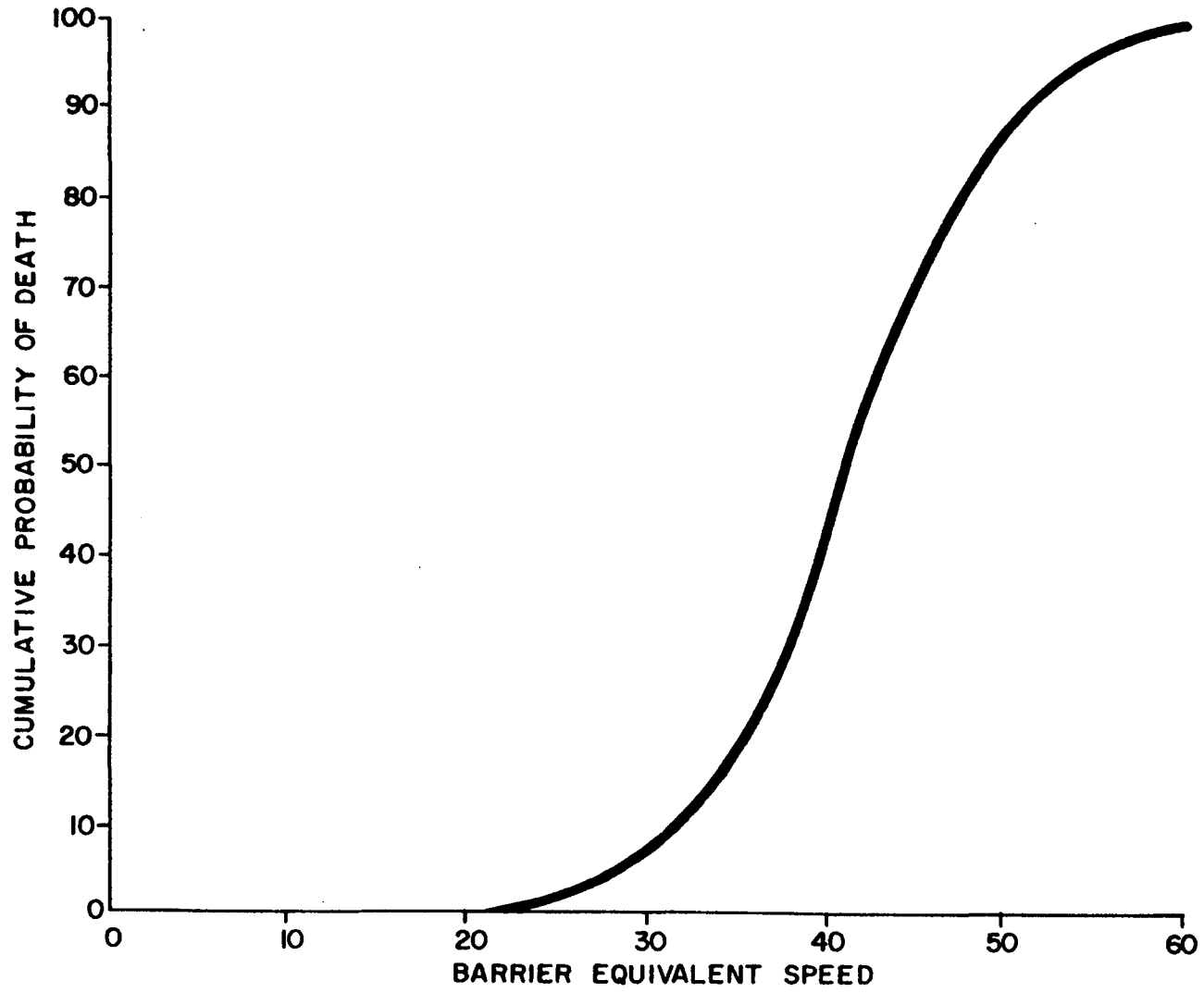


Figure B-11. Cumulative Probability of Death as a Function of Barrier Equivalent Speed (15).

It is not true that impact speeds in crashes producing injury to occupants are usually so great that crash-phase injury prevention measures have little to contribute. Although the risk of injury increases with speed, even high-speed crashes need not be fatal; at crash speeds of 110 km/h (70 mph) most motor vehicle occupants survive. Moreover, most injurious crashes occur at lower speeds." (16)

With the addition of the passive restraint requirement to FMVSS 208, there is good reason to believe that cars built in the 1980's will be more crashworthy in frontal collisions than current models.

"Air cushions were developed for the front seat passengers of a full-sized car, to obtain 72 to 80 km/h (45 to 50 mph) crash protection for normally seated occupants This required an ACRS (Air Cushion Restraint System) that inflated very quickly, to apply restraint loads early in the crash event. It was also necessary that the system operate in a controlled manner, so as not to injure an out-of-position occupant, such as a child leaning against the dash

During 1975, these systems were crash-tested. Full-sized 1974 production cars were fitted with the ACRS and impacted into rigid barriers at speeds up to 72 km/h (45 mph) The two systems performed well, meeting the injury criteria requirements of FMVSS 208. Additionally, when a 6-year-old child test dummy leaning against the dash was exposed to the inflating air-cushion, the loads were not injurious." (17, emphasis added).

In a recent speech to the Detroit Economic Club, Joan Claybrook Administrator of the National Highway Traffic Safety Administration (NHTSA) had this to say about the crashworthiness of 1980's passenger cars:

A "bright new horizon is ahead" if corporate managers "are willing to perceive their relation to it," Claybrook said. She cited a report of Calspan Corp. -- a vehicle design research firm -- which said that Americans in the 1980's may be riding in cars that protect passengers in head-on crashes up to 80 km/h (50 mph) and in side crashes up to 72 km/h (45 mph); protect pedestrians when they are struck at speeds up to 32 km/h (20 mph); offer protection against low-speed crash damage; and get good gas mileage. (18, emphasis added).

Summary

Estimates of a design closing speed for underride guards based on human tolerance to acceleration lead to values of 56 to 69 km/h (35 to 43 mph).

Studies of automobile crashworthiness in frontal impacts indicate survival of the occupants should be expected at impact speeds of 48 km/h (30 mph) or greater. Future automobiles are expected to exhibit adequate frontal crashworthiness at impact speeds of 64 to 72 km/h (40 to 45 mph) or greater.

Since FMVSS 208 requires that automobiles demonstrate an acceptable level of crashworthiness (i.e. $HIC \leq 1000$) in rigid barrier frontal impacts at 48 km/h (30 mph), this was considered to be the lower bound of a selected closing speed (9).

Based on the information summarized above, a design closing speed for underride guards of 64 km/h (40 mph) was initially chosen. During conduct of the test program, the design closing speed was reduced to 56 km/h (35 mph). For further discussion, the reader is referred to Appendix F.

APPENDIX C

VEHICLE DATA

Automobile Data

In specifying the performance requirements for a truck underride guard, four important questions concerning passenger car characteristics must be addressed:

- (1) What is the weight distribution for in-service passenger cars?
- (2) What is the distribution of vertical dimensions for in-service passenger cars?
- (3) What is the distribution of hood lengths for in-service passenger cars?

An answer to the first question is needed to determine the strength requirements for the guard. An answer to the second question is needed to determine the optimal height of the guard from the ground. An answer to the third question is needed to determine the optimal placement of the guard with respect to the rear most projection of the truck/trailer.

Automobile Weights

To calculate the distribution of passenger car weights in the United States for a given year, it was necessary to find both the weight and the number of all passenger cars registered in the United States for that year. Information on passenger car weights was obtained from Black Book Vehicle Identification Guide and Branham Automobile Reference Book (3 and 4). Registration information was obtained from Automotive News (19 and 20).

Figure C-1 is a plot of the cumulative percentage of new passenger car weights (i.e., vehicle shipping weights) for 1968 and 1976. From this figure it can be seen that passenger car weight increased between 1968 and 1976. In 1968, the 95th percentile car weight was approximately 4,300 pounds. In 1976, the 95th percentile weight had increased to 4,900 pounds.¹

¹All vehicle shipping weights used in these analyses represent the heaviest examples of given makes and models, e.g., shipping weights for V-8 rather than V-6 models were used in all calculations. Thus, a 95th percentile vehicle shipping weight reflected herein will be slightly greater than a 95th percentile vehicle shipping weight generally.

As a partial check on the methodology that was used to generate the 1968 and 1976 curves in Figure C-1, the distribution of passenger car weights for some 125,621 accident-involved passenger cars was also plotted in Figure C-1. This function was calculated from data provided in Single Variable Tabulations for 1973 North Carolina Accidents (6). The 1973 accident data reflect vehicle weights from model years 1967 through 1974. The curve for the 1973 accident data is remarkably similar to the curve representing 1968 new car registrations.

Since it is generally assumed that passenger car weight has been reduced since the energy crisis, the weights for twenty passenger car models which were manufactured between 1973 and 1977 (inclusive) were plotted as a function of model year. See Figure C-2 and Table C-1.² The dotted line in Figure C-2 represents the average weight of the twenty models for a given year. To the extent that passenger car weight has been reduced since the energy crisis, most of this reduction occurred in the 1977 model year. Furthermore, most of the reduction in the weight of the passenger car fleet seems to be provided by reductions in the weight of the heavier models, e.g., Lincoln Continentals, Cadillac DeVilles, Ford Thunderbirds, Buick Electra 225's.

The choice of a design weight for a heavy passenger car necessitates some assumptions. If one observes the 95th percentile shipping weight in Figure C-1, the value ranges from 4,200 to 5,000 lbs depending upon the data set used. The 90th percentile weight ranges from about 4,100 to 4,500 lbs. One might be encouraged to look at the lower end of these ranges because of trends in new car weights, but should also make some allowance for increasing the design weight (above shipping weight) to account for occupants and luggage. Present full-scale crash test procedures recommended in Transportation Research Circular 191 (7) for highway safety appurtenances specify a 4,500-lb automobile for evaluating the strength of barriers. For this project, a 4,100-lb design vehicle is recommended for establishing the required strength of an underride guard.

Vertical Dimensions of Automobiles

For an underride guard to prevent penetration of a vehicle beneath a truck or trailer, substantial portions (i.e., hard points) of the striking vehicle must make contact with the guard. If only the sheet metal (i.e., the hood) of the striking vehicle contacts the guard, the vehicle will tend to ride beneath the guard, and under the truck or trailer. On the other hand, if the engine block of the striking vehicle contacts the guard, the possibility exists of arresting the forward momentum of the vehicle, and thus preventing underride.

²Again, the heaviest examples of each of the twenty randomly chosen models was used in these calculations, e.g., V-8 models rather than V-6 models were plotted.

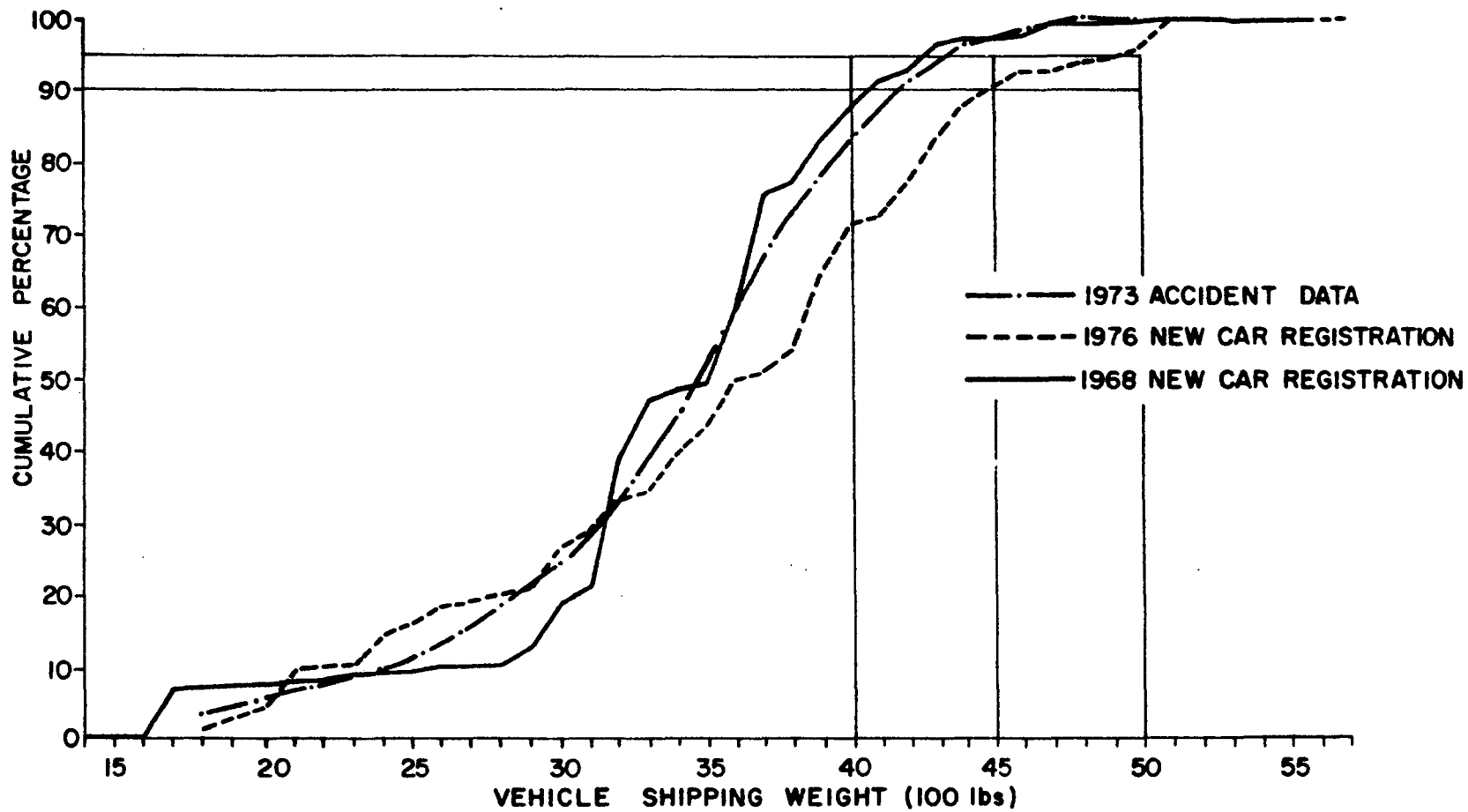


Figure C-1. Vehicle Shipping Weight (100 lbs).

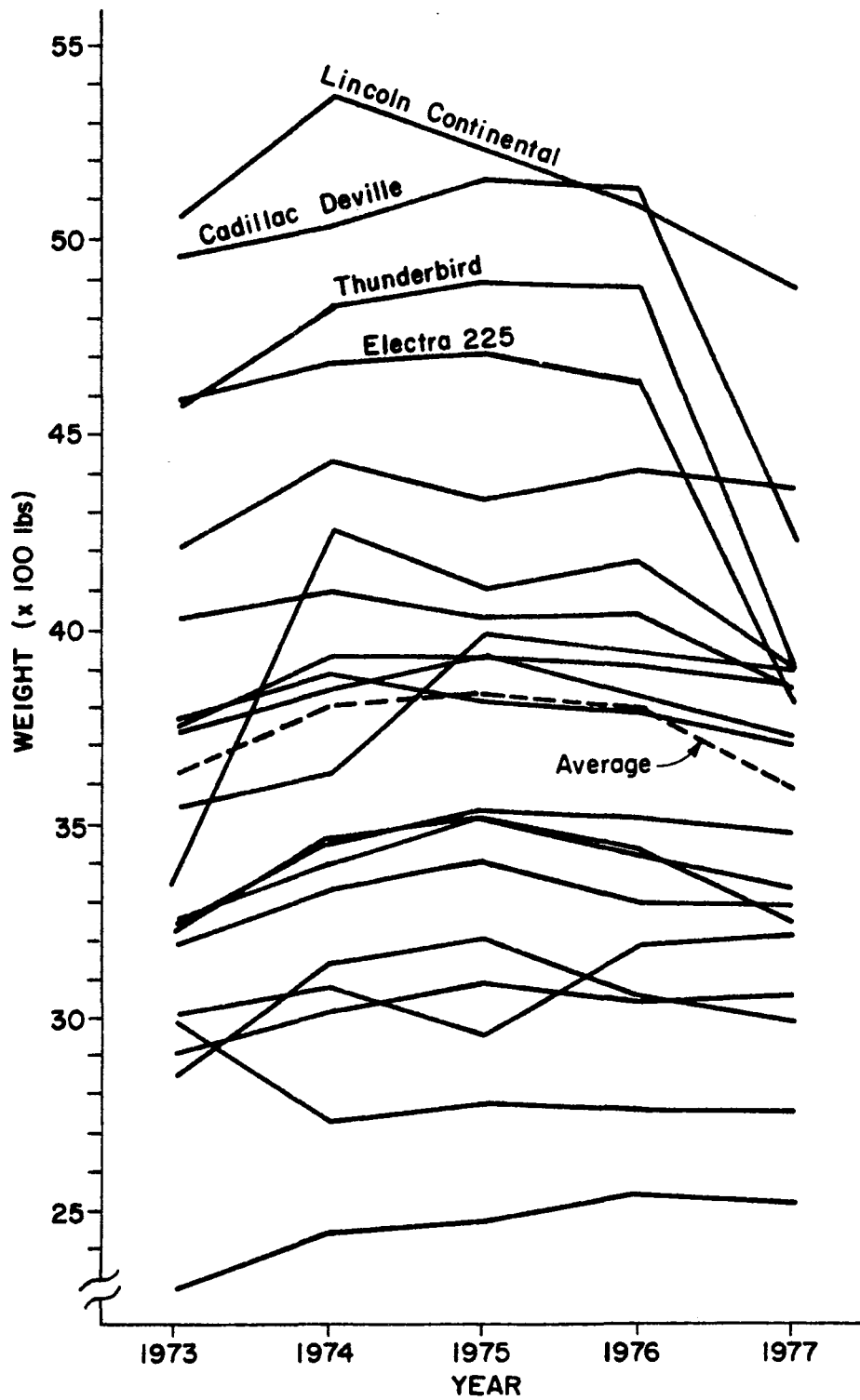


Figure C-2. Automobile Shipping Weights.

Table C-1. Automobile Shipping Weights.

MODEL	WEIGHT BY YEARS (lbs*)				
	1973	1974	1975	1976	1977
Chevy Nova	3194	3330	3408	3305	3292
Ford Thunderbird	4572	4825	4893	4808	3907
Dodge Charger	3540	3625	3985	3945	3895
Mercury Cougar XR7	3378	4255	4108	4168	3909
Pontiac Grand Prix	4025	4096	4032	4038	3804
Chevy Vega Hatchback	2313	2440	2478	2543	2522
Cadillac Deville	4953	5032	5146	5127	4222
Ford Maverick	2900	3014	3094	3040	3052
AMC Hornet	3008	3077	2946	3193	3214
Oldsmobile Cutlass	3761	3883	3816	3788	3703
Chevy Camaro	3238	3450	3532	3511	3476
Ford Mustang	2984	2727	2775	2756	2750
Buick Electra 225	4581	4682	4706	4641	3814
Mercury Comet	2838	3142	3201	3058	2988
Lincoln Continental	5055	5361	5229	5083	4880
Chevy Monte Carlo	3749	3926	3927	3907	3852
Pontiac LeMans	3731	3844	3948	3822	3723
Pontiac Ventura	3247	3398	3514	3436	3252
Chrysler Newport	4200	4430	4355	4400	4360
Oldsmobile Omega	3220	3462	3510	3421	3331
AVERAGE	3642	3800	3830	3800	3597

*Metric Conversion: 1 lb = 0.45 kg

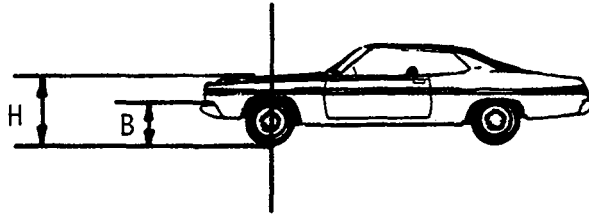
With this fact in mind, a brief field study was undertaken to determine the distribution of engine block heights. Because it is difficult to collect a large sample of engine block heights directly, an indirect method of collecting this information was defined. This indirect procedure involved the following steps:

- (1) Some 491, front-engine passenger cars located in parking lots in and around College Station, Texas were selected for purposes of this study. The hood height and bumper height for each of these vehicles was carefully recorded. See Figure C-3.
- (2) For an additional 25 passenger cars, hood heights, bumper heights, and engine block heights were measured directly. See Figure C-3.
- (3) On the basis of the data collected in the smaller sample, engine block height was defined as a percentage of the distance between the height of the bumper and the height of the hood. See Table C-2.
- (4) This percentage was then applied to the larger sample of hood heights and bumper heights. Figure C-4 is a cumulative percentage distribution of hood heights, bumper heights, and estimated engine block heights based upon the data of the larger sample.

It should be noted that the mean hood height, bumper height, and engine block height for the larger sample ($N = 491$) are, respectively, 0.89, 0.52, and 0.71 m (35.0, 20.5, and 27.8 in.) For the smaller sample ($N = 25$) the comparable means were: 0.90, 0.53, and 0.72 m (35.3, 21.0, and 28.3 in.)

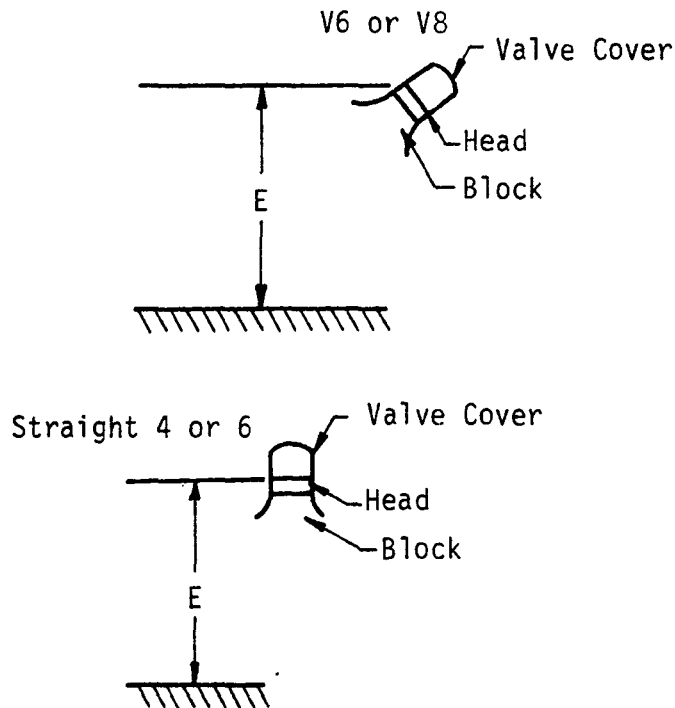
Based upon the data shown in Figure C-4, it can reasonably be concluded that 95 percent of all engine blocks are 0.66 m (26 in.) or more off the ground.

IHS information (film) shows that the front of impacting automobiles depress significantly upon impact with a guard. In more severe impacts, the automobile "bottoms out" on the pavement. Therefore one could argue that the ground clearance under the front of the automobile should be subtracted from the engine block height to arrive at the maximum ground clearance of a guard. Data from reference (21) indicate that for small cars the ground clearance is about 0.13 m (5 in.) and for larger cars it is about 0.15 m (6 in.) (see Table C-3). A cumulative distribution line 6 inches lower than the line indicating engine block height has been constructed in Figure C-4. This line indicates that engine block heights (bottomed out condition) are 0.51 m (20 in.) or higher for 90 percent of the sample. This dimension would be about 0.48 m (19 in.) for 95 percent of the sample.



All bumper heights measured from top of bumper to ground ("B").

All hood heights measured from hood to ground at center line of front tire ("H").



Engine block heights measured to highest point of "valve-cover-to-head" connection (@ front of engine).

Figure C-3. Vehicle Vertical Dimensions.

Table C-2. Distribution of Vertical Dimensions
For In-Service Automobiles.

(1) HOOD (in.*)	(2) BUMPER (in.*)	(3) BLOCK (in.*)	(4)** %
35.0	21.0	28.5	53.6
37.0	23.0	30.5	42.9
36.0	22.0	28.0	42.9
35.5	21.5	29.0	53.6
33.0	19.0	25.5	46.4
34.5	20.5	28.5	57.1
35.0	21.0	28.0	50.0
36.0	19.5	29.5	60.6
33.0	20.0	26.0	46.2
36.0	22.0	29.5	53.6
37.0	21.5	30.5	58.1
37.5	23.0	31.0	55.2
34.5	20.5	28.0	53.6
33.0	21.0	25.5	37.5
34.0	18.0	27.0	56.3
35.5	22.5	28.5	46.2
36.0	20.0	30.5	65.6
34.5	19.5	26.5	46.7
36.0	22.0	28.0	42.9
37.5	23.0	29.5	44.8
34.0	20.5	27.0	48.1
36.0	21.0	27.5	43.3
36.0	20.5	30.0	61.3
36.0	22.5	26.5	29.6
35.0	21.0	28.5	53.6
Sum 8835.0	526.0	707.5	1260.4
Average 35.3	21.0	28.3	50.4

*Metric Conversion: 1 in = 2.54 m

$$**(4) = \frac{(3) - (2)}{(1) - (2)} \times 100$$

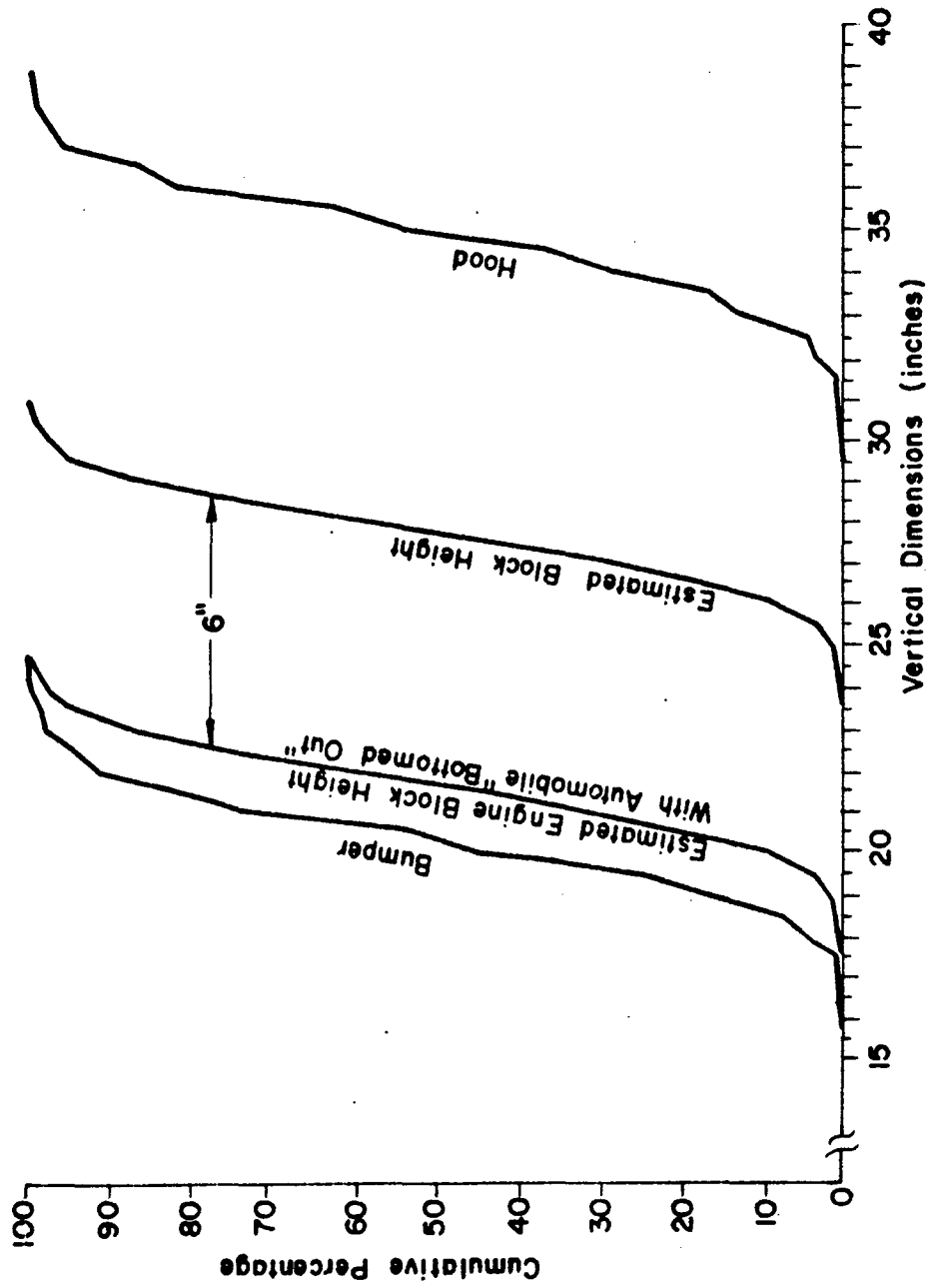


Figure C-4. Distribution of Vertical Dimensions of Automobiles.

Table C-3. Automobile Ground Clearances (21).

MODEL	GROUND CLEARANCE (in.*)	
	1973	1975
Chevy Nova	4.6	4.8
Ford Thunderbird	5.6	5.3
Dodge Charger	5.6	5.1
Mercury Cougar XR7	4.6	4.6
Pontiac Grand Prix	---	4.9
Chevy Vega Hatchback	5.2	4.9
Cadillac Deville	5.9	5.6
Ford Maverick	3.6	5.3
AMC Hornet	5.6	4.7
Oldsmobile Cutlass	5.4	5.4
Chevy Camaro	---	5.2
Ford Mustang	4.6	4.3
Buick Electra 225	5.6	5.7
Mercury Comet	3.6	5.3
Lincoln Continental	6.0	5.3
Chevy Monte Carlo	4.9	4.9
Pontiac LeMans	---	4.9
Pontiac Ventura	---	4.1
Chrysler Newport	6.0	5.4
Oldsmobile Omega	4.9	4.9
Sum	81.7	100.6
Average	5.1	5.0

*Metric Conversion: 1 in. = 25.4 mm

Longitudinal Dimensions of Automobiles

To obtain an estimate of the distribution of longitudinal dimensions of front portions of passenger cars, 100 vehicles in the local area were measured. These data are presented in Figure C-5 (see also Figure C-6). These data and the crush characteristics will be used to determine the optimal placement of the underride guard with respect to the rear of the truck or trailer.

It is observed from Figure C-5, that the 5th percentile hood length is about 1.20 m (3.95 ft) (i.e., the hood length on 95 percent of the automobiles surveyed was greater than 3.95 ft). If one assumes that this is the useable crush distance of an automobile and compares this with the tentatively computed crush distance of 0.73 m (2.39 ft), indications are that a guard might be placed as much as one foot forward of the rear of the truck or trailer. However, by placing the guard in this forward position, no margin of safety is provided. For this reason, it is recommended that the guard be mounted flush with, or aft of, the rear of the truck or trailer.

Truck and Trailer Data

Truck and Trailer Sales and Registration Data (22, 23)

In 1974, truck registrations in this country totaled 24,590,178 units. Most of these vehicles were small pickup trucks, vans, utility trucks, etc. However, 1,064,600 of the units (4.3 percent) were truck tractors.

In 1974, there were 2,490,849 commercial trailers registered in the United States. Some 2,189,816 of these units (87.9 percent) were semi-trailers; 301,033 units (12.1 percent) were full trailers.

In 1975, U.S. truck and bus factory sales equalled 2,272,160 units. Of this number, 1,190,835 units (52.4 percent) were pickup trucks, 196,525 units (8.7 percent) were general utility trucks, 383,956 units (16.9 percent) were panel trucks or vans, 120,261 units (5.3 percent) were multi-stop vehicles or station wagons, 40,530 units (1.8 percent) were buses, and 339,953 units (15.0 percent) were of some other body type.

In terms of gross vehicle weight (GVW pounds), 1,945,498 units (85.6 percent) weighed 10,000 lbs or less and 326,662 units (14.4 percent) weighed over 10,000 lbs. Table C-4 depicts 1975 U.S. truck and bus factory sales by body type and gross vehicle weight (GVW \leq 10,000 lbs or $>$ 10,000 lbs).

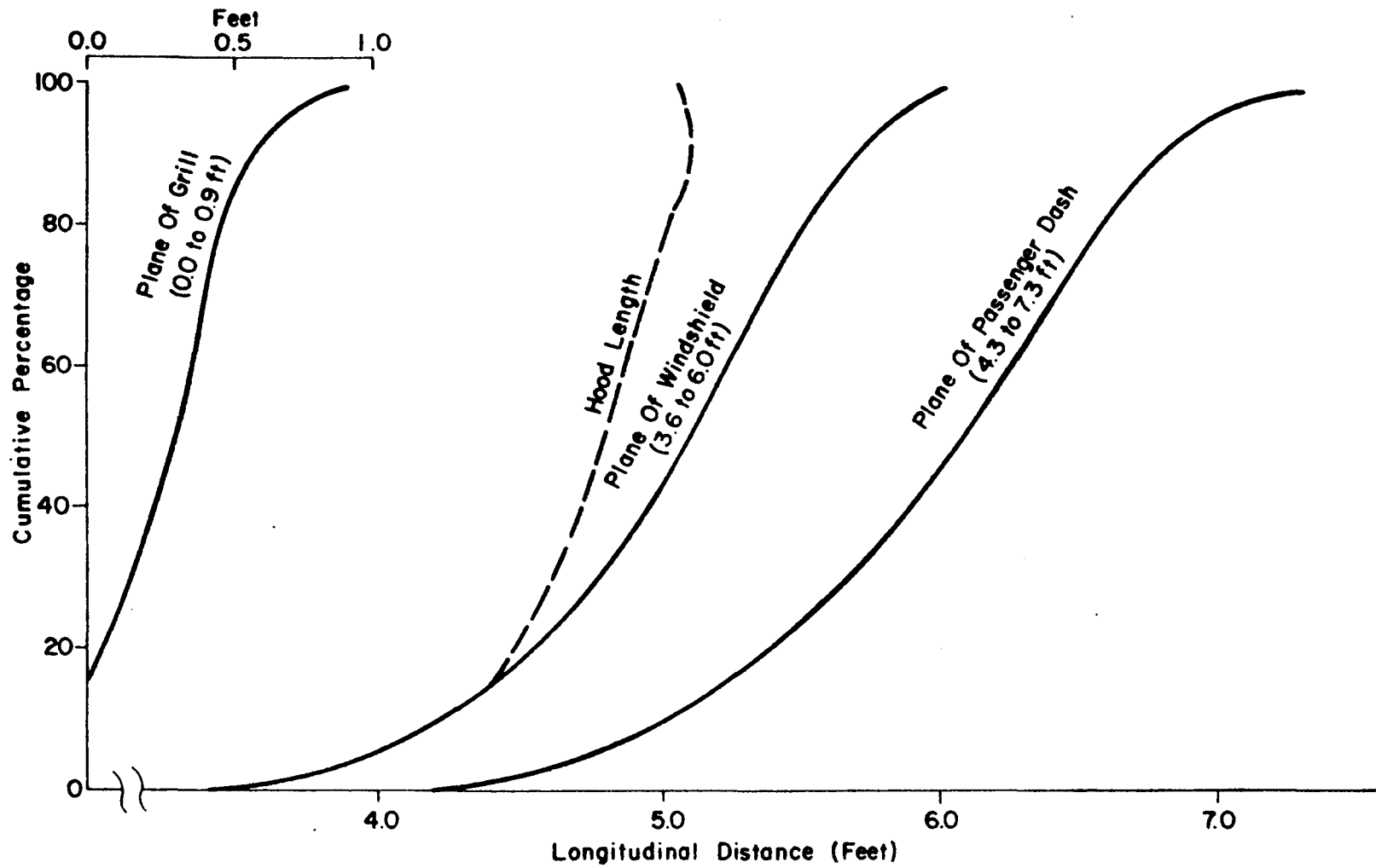


Figure C-5. Distribution of Longitudinal Dimensions of Front Portions of Passenger Cars.

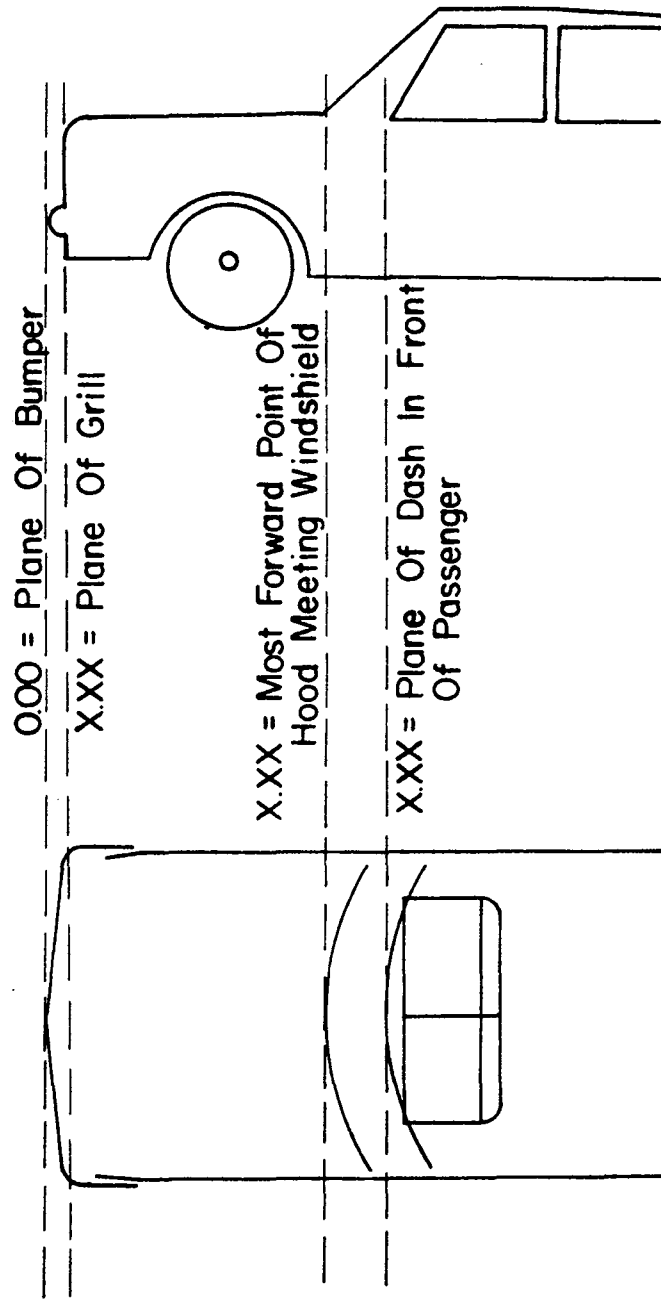


Figure C-6. Definition of Automobile Longitudinal Dimensions.

Table C-4. 1975 U. S. Truck and Bus Factory Sales by Body Type and Gross Vehicle Weight (lbs*) (22).

Body Type	Less than or Equal to 10,000 Pounds*		More than 10,000 Pounds*	
	Number	Percent	Number	Percent
Pickups	1,190,835	61.2	---	---
General Utility	196,626	10.1	---	---
Panel	1,143	0.1	---	---
Van	382,813	19.7	---	---
Multi-stop	23,184	1.2	13,835	4.2
Station Wagon (on truck chassis)	83,242	4.3	---	---
Buses (including school bus chassis)	---	---	40,530	12.4
Other	67,655	3.5	272,297	83.4
TOTAL	1,945,498	100.1	326,662	100.0

*Metric Conversion: 1 lb = 0.45 kg

Table C-5 is a further breakdown of truck body types by gross vehicle weight. All trucks represented in this table exceed 10,000 lbs. Both single unit trucks and combination trucks (i.e., truck-tractor with semi-trailers) are included in this table.

Table C-6 shows U.S. production of truck trailers by type. From this table it can be seen that vans constitute by far the largest portion of trailers currently being manufactured (58.6 percent), with platform trailers coming in second at 16.7 percent of production.

Truck and Trailer Mileage and Accident Data

In 1975, the truck fleet traveled km (274.5 billion miles). Single unit trucks (predominantly pickup trucks) amassed km (218,9 billion miles) (79.7 percent of the total) while truck combinations traveled 55.6 billion miles (20.3 percent of the total) (22). In 1974, the average single unit truck traveled km (8,985 miles) while the average truck-trailer combination traveled km (51,968 miles) (23).

According to the National Safety Council (24) 4,100,000 trucks were involved in accidents in the United States in 1976. Some 12,400 trucks (9.6 percent) were involved in a fatal accident. A total of 3,290,000 single unit trucks or truck tractors operated separately, were involved in accidents in 1976 -- 7,800 of these vehicles (0.2 percent) were involved in fatal accidents. Truck tractors and semi-trailers were involved in 530,000 accidents of which 3,600 (0.7 percent) were fatalities. Other truck combinations were involved in 280,000 total accidents and 1,000 (0.4 percent) fatal accidents.

In 1976, total motor vehicle miles traveled in this country equalled 1.412 trillion, and total accidents equalled 16,800,000. Or, in 1976, there were 11.90 accidents per million vehicle miles. For commercial truck fleets, the accident rate was 7.66 accidents per million vehicle miles (24).

Truck and Trailer Physical Dimensions

Federal government regulations define the size and weight limits for truck and truck-trailers operating on the interstate highway system. While the individual states are free to set their own size and weight limits for vehicles operating off the interstate system, 35 states have adopted the Federal limits. These limits specify that the maximum height of the vehicle shall not exceed 4.11 m (13 ft 6 in.), and the maximum width shall not exceed 2.44m (96 in.) Maximum axle weights are 9080 kg (20,000 lbs) for a single axle and 15,440 kg (34,000 lbs) for a tandem. Gross combined weight for truck and trailer shall not exceed 36,320 kg (80,000 lbs) (23).

Table C-5. Truck Size Class by Body Type
For Trucks in Excess of
10,000 lb* GVW. (22)

Body Type	Truck Size Class			TOTAL
	10,011- 20,000 lb* GVW	21,001- 26,000 lb* GVW	26,001- or More lb* GVW	
Pickup, Panel, Multi-Stop, or Walk-in	31.3%	4.4%	2.1%	18.5
Platform	27.4	28.9	21.0	25.8
Platform with added device	5.6	7.0	4.4	5.5
Cattlerack	6.7	6.7	2.4	5.4
Insulated Nonrefrigerated Van	1.2	1.2	3.1	1.8
Insulated Refrigerated Van	2.4	2.3	5.3	3.2
Furniture Van	3.7	2.8	3.2	3.4
Open Top Van	0.6	0.4	1.9	0.9
All Other Vans	6.3	7.2	18.6	10.0
Beverage Truck	1.4	3.0	1.6	1.7
Utility Truck	3.4	2.0	0.9	2.4
Garbage and Refuse Collector	1.3	1.4	1.2	1.3
Winch or Crane	0.8	3.5	1.8	1.5
Wrecker	2.3	0.6	0.2	1.4
Pole and Logging	0.3	1.4	2.4	1.1
Auto Transport	0.2	0.1	1.4	0.5
Dump Truck	3.1	17.3	14.0	8.6
Tank Truck for Liquids	2.3	9.7	9.1	5.5
Tank Truck for Dry Bulk	0.1	0.6	1.5	0.6
Concrete Mixer	0.2	0.1	4.1	1.3
All Other	0.6	0.5	0.6	0.6
TOTAL PERCENT	100.0	100.0	100.0	101.0
TOTAL TRUCKS	2,822	828	1,500	5,150

*Metric Conversion: 1 lb = 0.45 kg

Table C-6. U. S. Production of
Truck Trailers by
Type (1976) (23).

Type	Trailers	
	Number	Percent
Vans	61,726	58.6
Tank	6,520	6.2
Bulk Commodity	1,525	1.4
Pole, pipe, and logging	857	0.8
Platforms	17,586	16.7
Low-bed heavy haulers	4,424	4.2
Dump trailers	4,783	4.5
Other	7,980	7.6
TOTAL	105,401	100.0

According to the Truck Trailer Manufacturer's Association 73*, trailer lengths vary as indicated in the following table: (1976 production figures)

<u>Trailer Length</u>	<u>Percent</u>
≥ 45 ft	37.0
≥ 42 ft 6 in. 45 ft	18.5
≥ 40 ft 42 ft 6 in.	28.2
< 40 ft	<u>16.3</u>
	100.0

An appreciation for critical truck and tractor dimensions (e.g., height, width, overhang, wheel bases, etc.) can be obtained from reviewing Gasoline Truck Index (25) and Diesel Truck Index (26).

Truck and Trailer Departure Angles (Field Measurements)

For an underride guard to be effective, it must be sufficiently close to the ground to insure that it will restrain impacting vehicles. However, if the underride guard is too near the ground, the device may tend to drag or hang on the pavement when the truck/trailer to which it is attached is driven into loading locks, on and off ships, etc.

A second field study was conducted to determine the guard ground clearance for in-service trucks and trailers. The study was conducted as follows:

- (1) Some 229 trucks and trailers entering a weigh station near Spring, Texas were filmed by TTI personnel.
- (2) The film footage was then analyzed with the aid of a Vanguard Motion Analyzer to determine the departure angle for each of the 229 vehicles. See Figure C-7.
- (3) The vehicles were then subdivided into 10 major categories -- 5 major trailer categories and 5 major truck categories.

* Numerals in brackets refer to the entry number in reference (2).

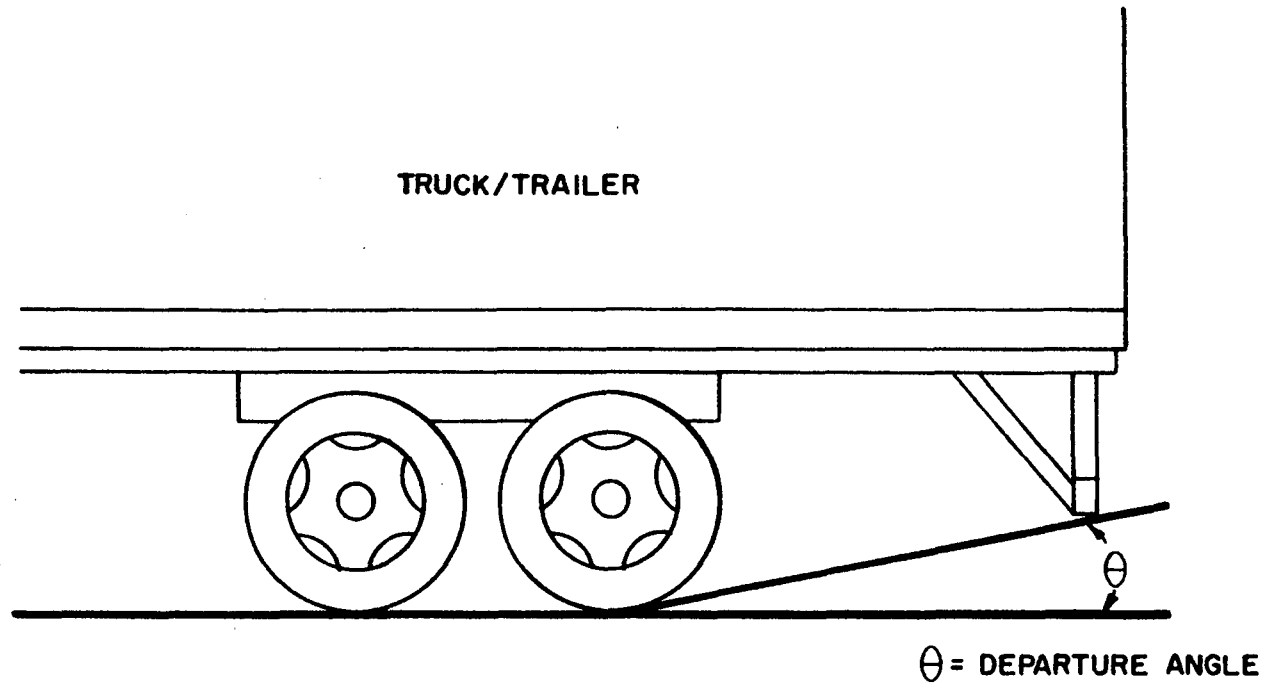


Figure C-7. Definition of Trailer Departure Angles.

<u>Trailer</u>	<u>Truck</u>
Box	Box
Flatbed	Flatbed
Tank	Tank
Dump	Dump
Special Purpose	Special Purpose

Trucks and trailers having cargo areas surrounded by solid walls and a roof were labeled "box". "Flatbed" vehicles were defined by the absence of solid walls and a roof in the cargo area. "Tank" trucks and trailers were defined by their ability to transport fluids. "Dump" trucks and trailers were characterized by solid wall cargo areas, and the absence of a solid roof. And, finally, the "Special Purpose" category was used for those vehicles which could not be subsumed under one of the four previous definitions.

Table C-7 and Figure C-8 depict the average departure angles for the ten categories of trucks and trailers which were just described. The brackets around the mean trailer departure angles (Figure C-8) indicate those values which lie within one standard deviation from the mean.

Figure C-8 is a cumulative percentage distribution of the departure angles for all 229 vehicles contained in the study.

Table C-7. Departure Angles for 5 Classes of Trailers and 5 Classes of Trucks.

Trailers	Average Departure Angle (°)	N
1. Box	30	91
(a) Tandem	(26)	(4)
(b) Other	(30)	(87)
2. Flatbed	36	44
3. Tank	40	17
4. Dump	47	13
5. Special Purpose	24	24
(a) Car Carrier	(15)	(6)
(b) Hopper	(54)	(4)
(c) Heavy Equipment Carrier	(24)	(7)
(d) Flatbed	(14)	(5)
(e) Other	(19)	(2)
SUBTOTAL		189
Trucks		
1. Box	14	12
2. Flatbed	24	13
3. Tank	14	1
4. Dump	43	5
5. Special Purpose	27	9
(a) Concrete Mixer	(30)	(7)
(b) Other	(14)	(2)
SUBTOTAL		40
TOTAL		229

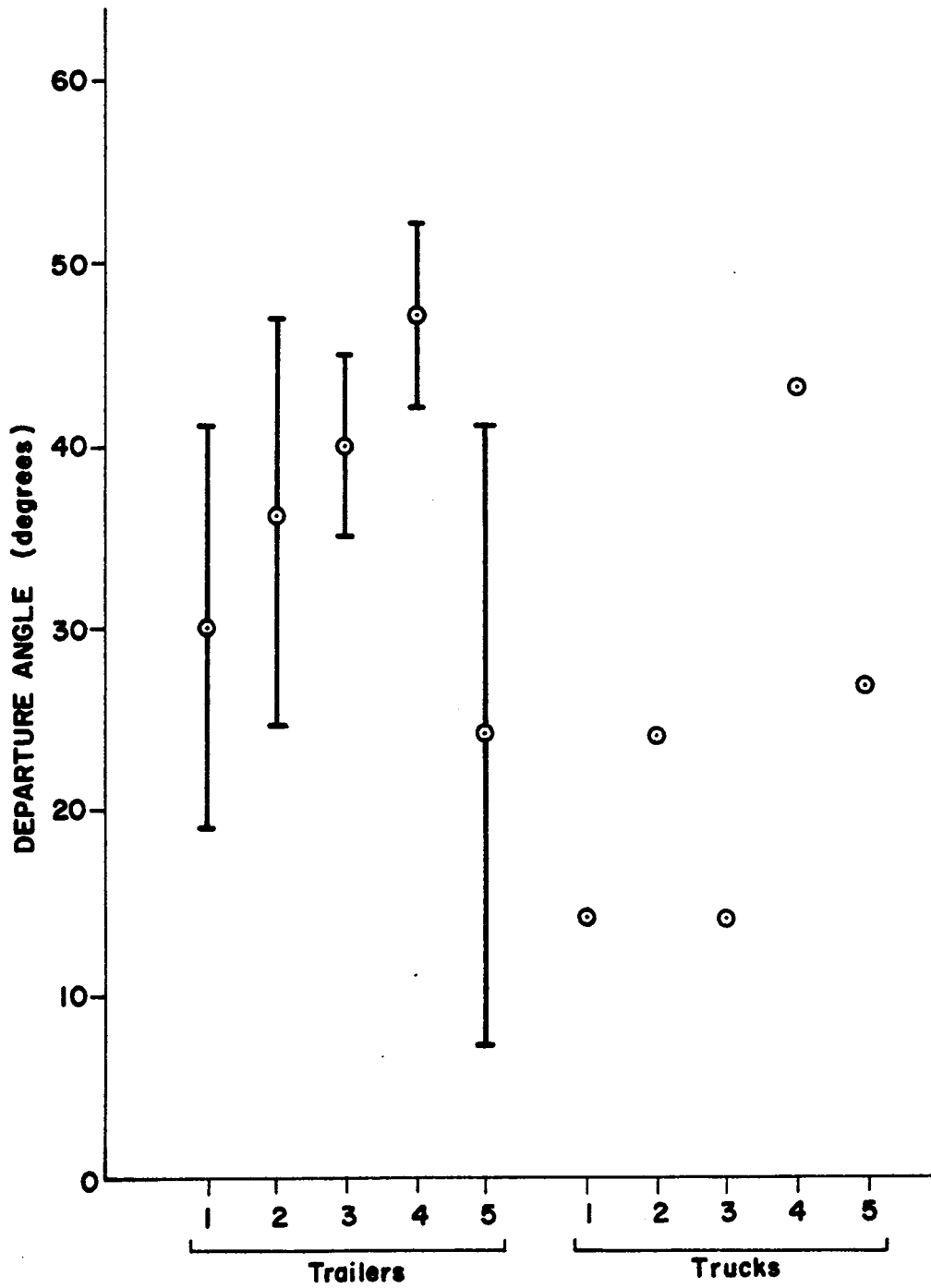


Figure C-8. Departure Angles for 5 Classes of Trailers and 5 Classes of Trucks.

APPENDIX D

RECOMMENDED PLASTIC ANALYSIS AND DESIGN PROCEDURE FOR REAR UNDERRIDE GUARDS

Section 1. TYPE OF CONSTRUCTION

Rigid frame structures or rigid connections between structural elements are recommended.

Section 2. LOADS AND FORCES

The recommended design impact force shall be considered as an ultimate load. No load factor or impact factor is required for this plastic analysis and design procedure. When the design impact force is applied, it is anticipated that the underride guard will deform plastically.

Section 3. MATERIAL

Structural steel or aluminum with at least 10 percent tested elongation is required. Metals with more ductility are desirable. High strength structural steel such as ASTM A514 with minimum $F_y = 100$ ksi or structural aluminum alloy known as 6061-T6 with minimum $F_y = 35$ ksi have desirable properties of high strength to low weight ratios.

Section 4. STRENGTH OF ELEMENTS

The strength of the structural elements may be computed as follows:

BENDING

$$M_p = F_y Z$$

COMPRESSION
AXIAL LOAD

$$P_u = F_y \left[1 - \frac{(kl/r)^2}{2C_c^2} \right] A$$

for

$$\frac{kl}{r} \leq C_c$$

where

$$C_c = \sqrt{\frac{2\pi^2 E}{F_y}}$$

when $\frac{k\ell}{r} > C_c$ then $P_u = \frac{\pi^2 E}{(\frac{k\ell}{r})^2} A$

TENSION $P_y = F_y A$

BENDING & AXIAL
COMPRESSION OR
AXIAL TENSION $\frac{P}{P_y} + \frac{M}{1.18 M_p} \leq 1.0$

SHEAR $V_u = .577 F_y A_{web}$

Section 5. LOCAL BUCKLING, WIDTH-THICKNESS RATIO

Width-thickness ratio of unstiffened projecting elements in compression--wide flange or I beams--shall not exceed:

Steel $\frac{b}{t} \leq \frac{65}{\sqrt{F_y}}$ Aluminum $\frac{b}{t} \leq 6.0$

Width-thickness ratio of axial compression flange of square or rectangular sections of uniform thickness shall not exceed:

Steel $\frac{b}{t} \leq \frac{190}{\sqrt{F_y}}$ Aluminum $\frac{b}{t} \leq 17$

Width-thickness ratio of projecting element single or double angle struts in compression shall not exceed:

Steel $\frac{b}{t} \leq \frac{76}{\sqrt{F_y}}$ Aluminum $\frac{b}{t} \leq 5.2$

Diameter-thickness ratio of circular tubes or pipes in compression shall not exceed:

Steel $\frac{D}{t} \leq \frac{3780}{F_y}$ Aluminum $\frac{D}{t} \leq 40$

Depth-thickness ratio of the web or webs of wide flange or I beams shall not exceed:

$$\text{Steel} \quad \frac{h}{t_w} \leq \frac{412}{\sqrt{F_y}}$$

$$\text{Aluminum} \quad \frac{h}{t_w} \leq 13$$

Section 6. LATERAL BUCKLING

The compression flange of beam elements shall be supported laterally at intervals not to exceed:

$$\text{Steel} \quad \ell \leq \frac{76 b_f}{\sqrt{F_y}}$$

$$\text{Aluminum} \quad \ell \leq \frac{44 b_f}{\sqrt{F_y}}$$

Section 7. CONNECTIONS

Welded connections are normally recommended so that rigid connections can be readily achieved. Some high strength metals achieve their high yield strengths through heat treating. The designer should be aware that when these metals are welded, the weld and adjacent metal will have a reduced yield strength. Special connection details or heat treating after welding may be required to regain the original strength.

Bolted connections may be desirable for attaching the underride guard to the truck or trailer.

Connections may be designed by a plastic design or ultimate strength procedure.

WELDS:

The capacity of groove or butt welds is equal to yield strength of the metal times the cross-sectional area of the weld.

$$P_y = F_y A$$

The capacity of a fillet weld is equal to the shear yield strength of the metal times the cross-sectional area of the fillet throat.

$$V_u = \frac{F_y}{\sqrt{3}} A_{\text{throat}}$$

BOLTS:

The tension capacity of a bolt is equal to yield strength of the metal times the tensile stressed area.

$$P_y = F_y A_t$$

$$\text{where: } A_t = 0.7854 \left[D - \frac{.9734}{n} \right]^2$$

The shear capacity of a bolt is equal to the shear yield strength of the bolt metal times the gross (nominal) area of the bolt.

$$V_u = \frac{F_y}{\sqrt{3}} A_g$$

The bearing capacity of a bolt is equal to the bearing yield capacity of the connecting metal times the bearing area.

$$P_b \approx 1.6 F_y D t \quad (\text{aluminum})$$

$$P_b \approx 2.0 F_y D t \quad (\text{steel})$$

NOMENCLATURE

A	Cross-sectional area, in. ²
A _g	Gross or nominal cross-sectional area of a bolt, in. ²
A _t	Tensile stress area of a bolt, in. ²
A _{throat}	Minimum cross-sectional area at throat of fillet weld, in. ²
A _{web}	Cross-sectional area of web of wide flange or beam, in. ²
b _f	Width of flange, in.
C _c	Column slenderness ratio dividing elastic and inelastic buckling
D	Diameter of pipe, usually outside diameter, in. or Diameter of bolt, in.
E	Modulus of elasticity of metal, kips/in. ²

F_y	Specified minimum yield strength of metal, kips/in. ²
h	Clear distance between flanges of a beam or girder (depth of beam), in.
k	Effective length factor
l	Unbraced length, in.
M	Moment, kip-in.
M_p	Plastic moment, kip-in.
n	Bolt threads per inch
P	Applied load, kips
P_b	Bearing capacity of bolt, kips
P_u	Ultimate axial compressive load, kips
P_y	Plastic axial load ($P_y = F_y A$), kips, yield load, kips
r	Governing radius of gyration, in.
t	Thickness of metal flange or wall thickness of metal pipe or square or rectangular tube, in.
t_w	Web thickness, in.
V_u	Ultimate shear strength of beam, kips or Ultimate shear strength of a weld or bolt, kips
Z	Plastic section modulus, in. ³
π	Ratio of circumference of a circle to its diameter, 3.1415927

APPENDIX E
UNDERRIDE GUARD DESIGN CALCULATIONS

General

Sample design calculations are included for guards 1ST, 1AL, 2ST, 2AL, 3AL, 5ST, and 7ST. Calculations for all except 7ST were made using tentative design guidelines which were established early in the program. They are intended to demonstrate the design procedure. The tentative design guidelines called for a 444,800 N (100,000 lb) uniform line load centered on the guard laterally and distributed over a 1.83 m (6 ft) width and a 111,200 N (25,000 lb) side load applied simultaneously for the centric impact. For the offset impact the tentative guidelines called for a 222,400 N (50,000 lb) uniform line load distributed over 0.61 m (2 ft) of the end of the guard and a 55,600 N (12,500 lb) side load applied simultaneously. These guidelines were revised to result in those presented in Chapter VII. Guard 7ST was designed in accordance with these revised guidelines.

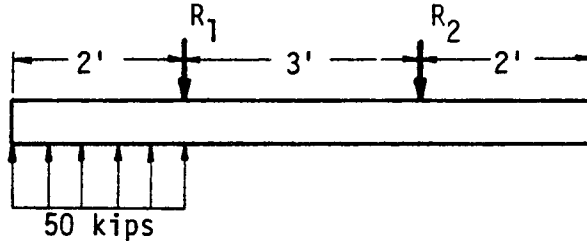
Subsequent calculations indicate that the latest versions of designs 5ST, 6ST, and 2AL are structurally adequate for tests specified in the performance criteria in Chapter VI. However, in test number 3661-6, an offset test, the guard proved to be inadequate.

It is emphasized to the reader that the following design calculations are for illustration of the recommended design procedure.

RIGID FRAME UNDERRIDE GUARD 1-ST

Design Calculations - Steel A514 $F_y = 100$ ksi

BEAM



$$R_1 = \frac{50 \times 4'}{3'} = 66.7 \text{ kips}$$

$$M_{\max.} = 50 \times 1^{ft} = 50\text{k-ft} = 600\text{k-in.}$$

$$Z_{\text{reqd.}} = \frac{600 \text{ k-in}}{100 \text{ ksi}} = 6 \text{ in.}^3 = \frac{M_p}{F_y}$$

PIPE 6" ϕ x 3/16" wall - 11.64 l_b/ft

$$S = 4.83 \text{ in.}^3 \quad Z = 4.83 \times 1.27 = 6.13 \text{ in.}^3$$

$$\frac{d}{t} = \frac{6''}{3/16} = 32 < 37.8 \text{ O.K.}$$

BOLTS 5/8 in. diam. ASTM A325 $F_y = 90$ ksi

$$A_{\text{tension}} = .226 \text{ in.}^2 \quad A_{\text{shear}} = .3068 \text{ in.}^2$$

$$P_{\text{tension}} = 0.226 \text{ in.}^2 \times 90 \text{ ksi} = 20.34 \text{ kips}$$

$$V_{\text{shear}} = 0.3068 \times \frac{90}{\sqrt{3}} = 15.94 \text{ kips}$$

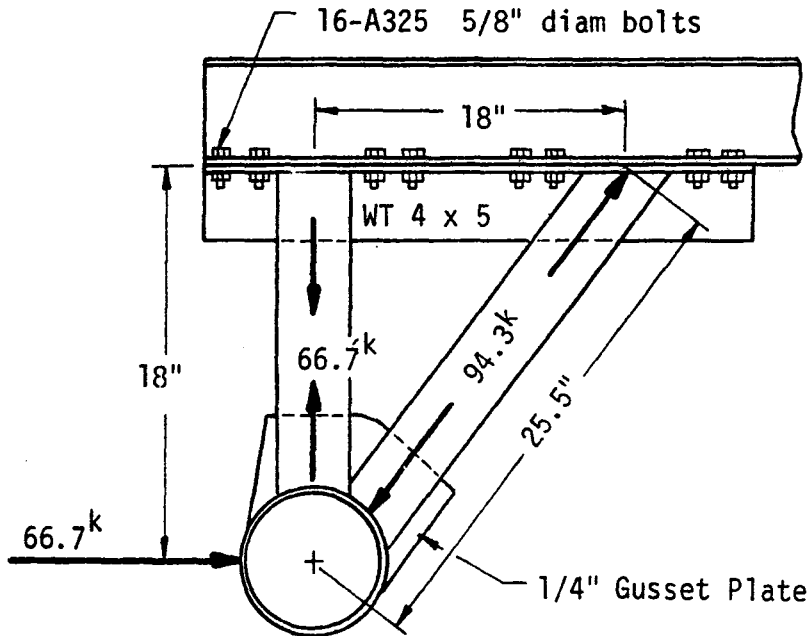
$$P_{\text{bearing}} = 5/8 \text{ in.} \times 1/4 \text{ in.} \times 56 \text{ ksi} = 8.8 \text{ kips (Alum.)}$$

Alum.

$$P_{\text{bearing}} = 5/8 \text{ in.} \times 1/4 \text{ in.} \times 70 \text{ ksi} = 10.9 \text{ kips (Steel)}$$

Steel

4 Bolts for Tension + 8 Bolts for Bearing = 12 total reqd.
Shear



STRUT 3" ϕ 3/16" wall - 5.63 lb/ft $Z = 1.39 \text{ in.}^3$

$A = 1.657 \text{ in.}^2$ $S = 1.097 \text{ in.}^3$ $r = 0.997 \text{ in.}$

$$\frac{kl}{r} = \frac{25.5}{0.997} = 25.6 \quad C_c = \sqrt{\frac{2\pi^2 \times 30,000}{100}}$$

$$= 76.95 \approx 77$$

$$P_u = 100 \left[1 - \frac{26^2}{2 \times 77^2} \right] 1.66$$

$$= 100 \times .94 \times 1.66$$

$P_u = 156 \text{ kips O.K.}$ $P_y = 166 \text{ kips O.K.}$

Lateral or Transverse Load on Strut

$$M = S f F_y \\ = 1.097 \times 1.27 \times 100 = 139.3 \text{ k-in}$$

$$P_{lat} = \frac{139.3 \text{ k-in}}{18 \text{ in}} = 7.74 \text{ kips per strut on side opposite impact}$$

$$M \leq \left[1.0 - \frac{P}{P_y} \right] 1.18 M_p$$

$$M = \left[1.0 - \frac{66.7}{166} \right] 1.18 M_p = .7 M_p \text{ Tension Strut}$$

$$M = \left[1.0 - \frac{94.3}{166} \right] 1.18 M_p = .51 M_p \text{ Compr. Strut}$$

$$P_{lat} = .7 \times \frac{139.3}{18} = 5.42 \text{ kips Tens. Strut}$$

$$P_{lat} = .51 \times \frac{139.3}{18} = 3.95 \text{ kips Compt. Strut}$$

$$\text{Tot. Transverse Capacity} = 7.74 + 7.74 + 5.42 + 3.95$$

$$= 24.85 \text{ kips}$$

$$\text{O.K.} \approx 25 \text{ kips}$$

Max. Centric Impact Capacity

$$P_{centric} = 2 \times 156 \times .707 = 220 \text{ kips}$$

$$P_{centric} = 12 \text{ bolts} \times 6.6 \text{ kips (Alum.)} \times 2 = 158 \text{ kips}$$

$$= 12 \text{ bolts} \times 10.9 \text{ kips (steel)} \times 2 = 261 \text{ kips}$$

$$\text{Impact Force} \approx .58 VW \approx 158 \text{ kips}$$

$$V = \frac{158 \text{ kips}}{.58 \times 4.5 \text{ kips}} \approx 60 \text{ mph}$$

Note: Truck Frame not this strong

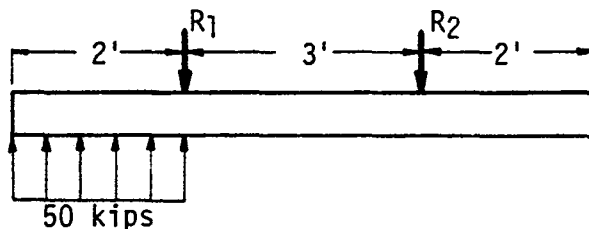
TOTAL WEIGHT

Beam	11.64 lb/ft x 7 ft	= 81.5
Struts	5.62 lb/ft x 2.12 ft x 2	= 23.8
	5.62 lb/ft x 1.5 ft x 2	= 16.9
Tee	5 lb/ft x 2.42 ft x 2	= 24.2
Plate		= 5.6
Bolts	16 lb/ft x .31 lb/ea. x 2	= <u>9.9</u>
	TOTAL	161.9 lb

RIGID FRAME UNDERRIDE GUARD 1-AL

Design Calculations - Aluminum 6061-TG $F_y = 35 \text{ ksi}$

BEAM



$$R_1 = 50 \times \frac{4}{3} = 66.7 \text{ kips}$$

$$M_{\max.} = 50 \times 1 \text{ ft} = 50 \text{ k-ft} = 600 \text{ k-in.}$$

$$Z_{\text{reqd.}} = \frac{600 \text{ k-in.}}{35 \text{ ksi}} = 17.14 \text{ in.}^3$$

$$\text{Pipe } S_{\text{reqd.}} = \frac{17.14 \text{ in.}^3}{1.27} = 13.50 \text{ in.}^3$$

$$\text{Use } 8" \phi \times 5/16" \text{ wall } S = 13.96 \text{ in.}^3 > 13.50 \text{ O.K.}$$

$$\text{Weight} = 8.875 \text{ lb/ft } A = 7.547 \text{ in.}^2$$

$$D/t = \frac{8}{5/16} = 25.6 \text{ O.K. } < 40$$

STRUT-COMPRESSION $P = 66.7 \times 1.414 = 94.3 \text{ kips}$

Try 4" $\phi \times 5/16$ wall

$$A = 3.62 \text{ in.}^2$$

$$S = 3.098 \text{ in.}^3$$

$$r = 1.308 \text{ in.}$$

$$\text{Wt.} = 4.257 \text{ lb/ft.}$$

$$\frac{KL}{r} = \frac{24"}{1.308} = 18.3 \approx 18 \quad D/t = \frac{4}{5/16} = 12.8 \text{ O.K.}$$

$$C_c = \sqrt{\frac{2 \times \pi^2 \times 10,000}{35}} = 75$$

$$P_u = 35 \left[1 - \frac{18^2}{2 \times 75^2} \right] = 3.62$$

$$P_u = 35 \times .971 \times 3.62 = 123 \text{ kips} > 94.3 \text{ O.K.}$$

STRUT-TENSION

Use 4" ϕ x 5/16"

$$P_y = 35 \text{ ksi} \times 3.62 = 126.7 \text{ kips} > 66.7 \text{ O.K.}$$

TRANSVERSE LOAD ON STRUTS

$$M_p = F_y f S = 35 \times 1.27 \times 3.098 = 137.7 \text{ k-in.}$$

$$P_{tr.} = \frac{M_p}{\text{arm}} = \frac{137.7 \text{ k-in.}}{17 \text{ in.}} = 8.1 \text{ kips}$$

per strut on side opposite impact

$$M = \left(1.0 - \frac{P}{P_y} \right) 1.18 M_p$$

$$= \left(1.0 - \frac{66.7}{126.7} \right) 1.18 \times 137.7 = 76.9 \text{ k-in.}$$

$$P_{lat.} = \frac{76.9 \text{ k-in.}}{17 \text{ in.}} = 4.5 \text{ kips on Tension Strut}$$

$$M = \left(1.0 - \frac{94.3}{126.7} \right) 1.18 \times 137.7 = 41.6 \text{ k-in.}$$

$$P_{lat.} = \frac{41.6 \text{ k-in.}}{17 \text{ in.}} = 2.4 \text{ kips on Compt. Strut}$$

$$\text{Tot. Transverse Load} = 8.1 + 8.1 + 4.5 + 2.4$$

$$= 23.1 \text{ kips O.K.}$$

BOLTS 5/8 in. diam. ASTM A 325 $F_y = 90$ ksi

$$A_{\text{tension}} = .226 \text{ in.}^2 \quad A_{\text{shear}} = .3068 \text{ in.}^2$$

$$P_{\text{tension}} = .226 \times 90 = 20.34 \text{ kips}$$

$$V_{\text{shear}} = .3068 \times \frac{90}{3} = 15.94 \text{ kips}$$

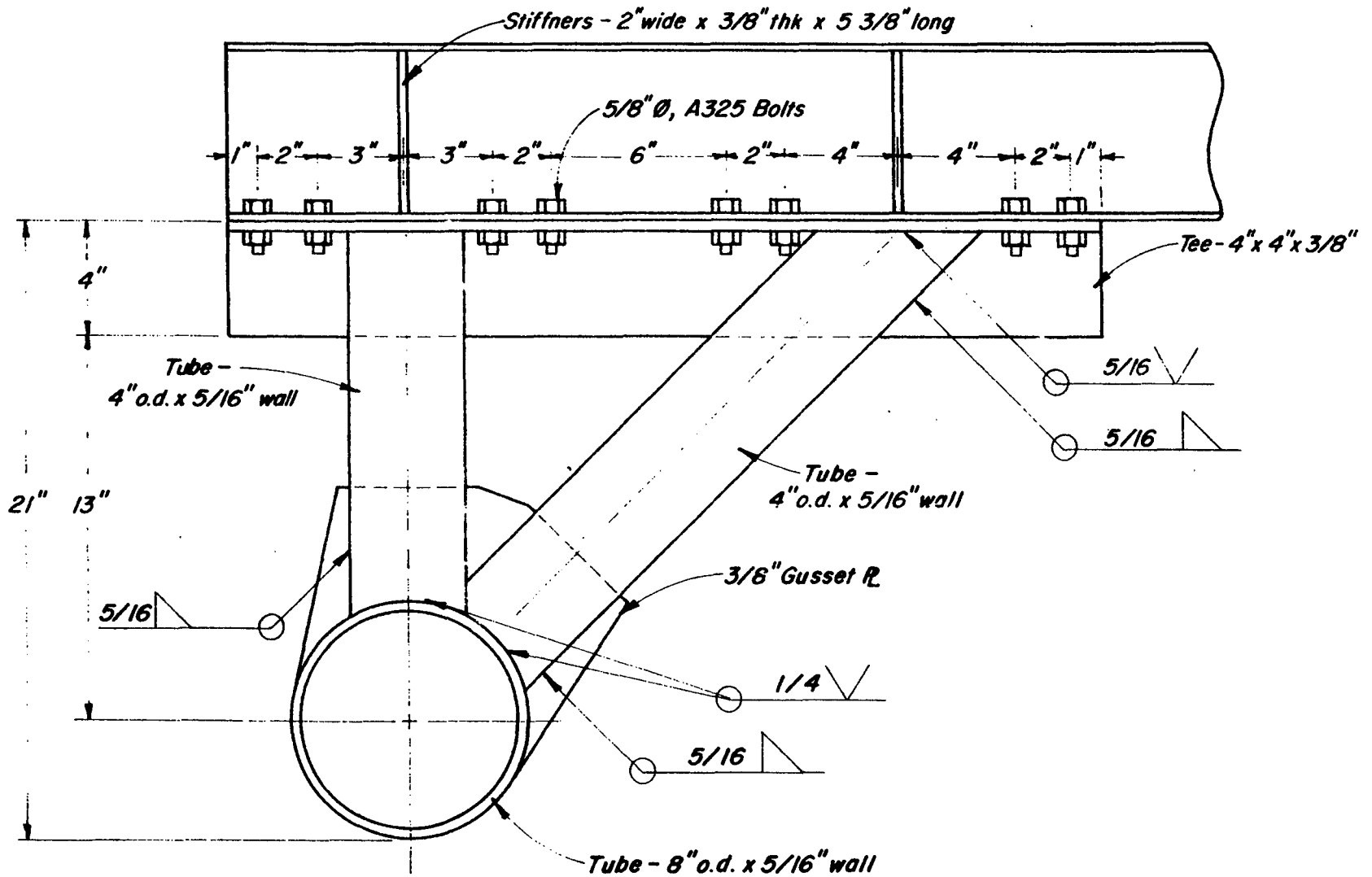
$$P_{\text{bearing}} = 5/8" \times 1/4" \times 56 = 8.8 \text{ kips}$$

Alum.

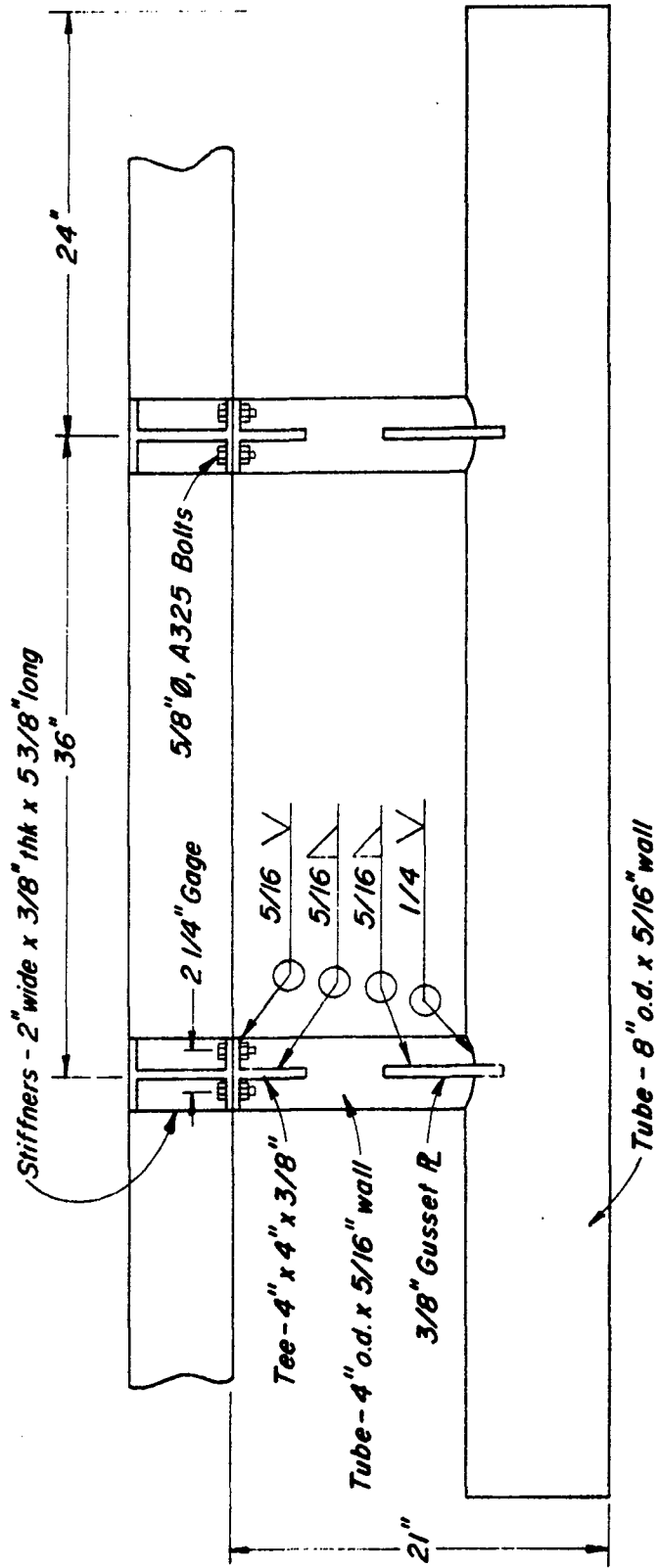
$$\text{No. Bolts for Compr. Strut} \frac{66.7 \text{ kips}}{8.8 \text{ kips}} = 7.6$$

$$\text{No. Bolts for Tension Strut} \frac{66.7 \text{ kips}}{20.34} = 3.3$$

Use 8 bolts



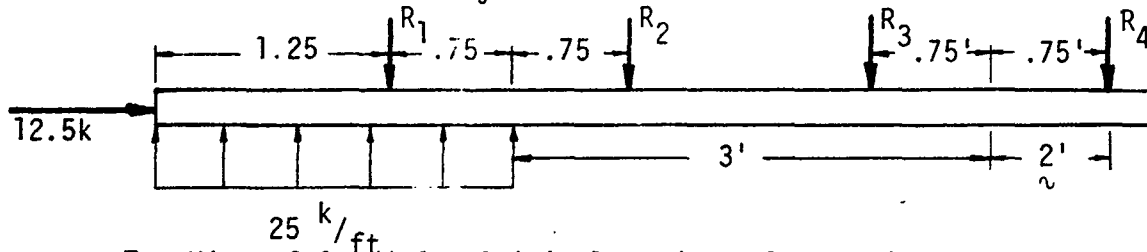
Guard 1AL



Guard IAL

RIGID FRAME UNDERRIDE GUARD 2-ST

Design Calculations Assume $F_y = 100$ ksi for Steel



Top View of Guard for Critical Loads on Beam and Struts

STRUTS

Try 2 1/2" O.D. x 1/8" wall tube $\frac{l}{r} = \frac{2.25 \text{ ft.} \times 12}{841} = 32$

Area = .933 in.² WT. = 3.05 lb/ft

I = 0.66 in.⁴ S = .528 in.³

$$F_u = \left[1 - \frac{(kl/r)^2}{\frac{4\pi^2 E}{F_y}} \right] F_y = 91.3 \text{ ksi}$$

Assume R_1 strut reaches yield strength of cross section in axial compression.

$R_1 = 91.3 \text{ ksi} (.933 \text{ in.}) (.707) (.89) = 54 \text{ kips}$

$R_2 = [25(2)4 - 54(3.75)]/2.25 = -1 \text{ kips}$

BEAM

$\Sigma M_2 = 0 = 25 \text{ k/ft} (2 \text{ ft}) (1.75 \text{ ft}) - 1.5 R_1 - M_2$

$M_2 = 87.5 - 1.5 R_1 = 87.5 - 1.5 (54) = 6.5 \text{ k-ft.}$

$M_1 = 25 \text{ k/ft.} (1.25 \text{ ft.}) (.625 \text{ ft.}) = 19.53 \text{ k-ft.}$

$Z_{\text{reqd.}} = \frac{M}{\sigma} = \frac{19.53 \text{ k-ft} \times 12 \text{ in./ft.}}{100 \text{ ksi}} = 2.34 \text{ in.}^3$

4" O.D. x 3/16" wall $Z = 1.27 (2.04) = 2.59 > 2.34 \text{ O.K.}$

WT. = 7.65 lb/ft., $I = 4.09 \text{ in.}^4$, $A = 2.24 \text{ in.}^2$

BOLTS 5/8" dia. ASTM A325 $F_y = 90$ ksi

$$A_{\text{tension}} = 0.226 \text{ in.}^2 \quad A_{\text{shear}} = .3068 \text{ in.}^2$$

$$P_{\text{tension}} = 0.226 \text{ in.}^2 (90 \text{ ksi}) = 2034 \text{ kips/bolt}$$

$$V_{\text{shear}} = 0.3068 \text{ in.}^2 (90 \text{ ksi}) = 15.94 \text{ kips/bolt}$$

$$P_{\text{bearing}} = (0.625 \text{ in.}) (.25 \text{ in.}) (56 \text{ ksi}) = 8.75 \text{ kips/bolt aluminum}$$

$$P_{\text{bearing}} = (0.625 \text{ in.}) (.25 \text{ in.}) (70 \text{ ksi}) = 10.9 \text{ kips/bolt steel}$$

$$\text{No. Bolts tension} = \frac{91.3 \text{ ksi} (.933 \text{ in.}^2)}{20.34 \text{ kips}} = 4 \text{ bolts for tension in vertical strut}$$

$$\text{No. Bolts shear} = \frac{54 \text{ kips} (2)}{10.9} = 10 \text{ bolts for shear bearing for steel frame}$$

$$\text{No. Bolts shear} = \frac{54 (2)}{8.75} = 12 \text{ bolts for shear bearing for aluminum frame}$$

Use 12 - 5/8" O.D. ASTM A325 bolts per V-brace assembly.

LATERAL OR TRANSVERSE LOAD ON STRUT

$$M_p = F_y f S = .528 (1.27) 100 = 67 \text{ k-in. per strut on side opposite impact.}$$

$$P_{\text{lat}} = \frac{67 \text{ k-in}}{18 \text{ in}} = 3.72 \text{ kips per strut on side opposite impact}$$

$$P_{\text{lat}} = \frac{[1 - P/P_y] 1.18 M_p}{18 \text{ in.}} = \frac{[1 - 54/93.3](67)}{18 \text{ in.}}$$

$$P_{\text{lat}} = 1.84 \text{ kips tension strut}$$

$$P_{\text{lat}} = \left[1 - \frac{85}{93.3} \right] \frac{1.18 (67)}{18} = .39 \text{ kips } R_1 \text{ comp. strut}$$

$$P_{\text{lat}} = \left[1 - \frac{1.6}{93.3} \right] \frac{1.18 (67)}{18} = 4.3 \text{ kips } R_2 \text{ strut}$$

$$\begin{aligned} \text{Total Transverse Capacity} &= 3(3.72) + 1.84 + .39 + 4.3 \\ &= 17.7 \text{ kips Horizontal} \end{aligned}$$

$$\text{Applied Transverse Load} = 12.5 \text{ kips} < 17.7 \text{ kips} \text{ O.K.}$$

MAXIMUM CENTRIC IMPACT CAPACITY (BOLTS)

$$P_{\text{centric strut}} = 2 (91.3 \text{ ksi}) (.933 \text{ in.}^2) (.707) (.89)$$

$$P_{\text{centric strut}} = 108 \text{ kips Capacity of VEE strut assembly.}$$

$$P_{\text{centric bolts}} = 12 \text{ bolts} \times 8.75 \text{ kips} = 105 \text{ kips}$$

O.K. for bolts.

MAXIMUM CENTRIC IMPACT CAPACITY OF BEAM

From engr. handbook using elastic analysis -

$$M_{\text{max}} = .1 w l^2 \text{ For dist. load on beam with four equally spaced reactions.}$$

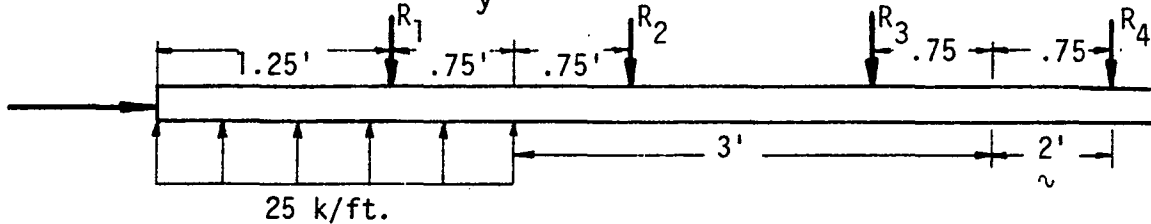
$$M_{\text{max}} = .1 \frac{100}{6\text{ft.}} (1.5 \text{ ft})^2 = 3.75 \text{ k-ft.} < 20 \text{ k-ft. used to design the beam. O.K.}$$

D/t RATIOS

$$\text{Struts } D/t = \frac{2.5}{.125} = 20 \leq \frac{3780}{100} = 37.8 \text{ O.K.}$$

RIGID FRAME UNDERRIDE GUARD 2-AL

Design Calculations Assume $F_y = 35$ ksi for Aluminum



Top View of Guard for Critical Loads on Strut and Beam

STRUTS

Try 3" O.D. x 1/4" wall tube, $\frac{l}{r} = \frac{2.25 (12)}{.976} = 27.66$

Area = 2.16 in.

$r = .976$

$$F_u = \left[1 - \frac{(27.66)^2}{\frac{4 \pi^2 10 \times 10^6}{35,000}} \right] 35,000 = 32,626 \text{ psi}$$

Assume R_1 strut reaches yield strength of cross section in axial compression.

$$R_1 = 32.63 \text{ ksi} (2.16 \text{ in.}) (.707) (.89) = 44.34 \text{ kips horizontal}$$

$$R_2 = [25(2)4 - 44.34 (3.75)]/2.25 = 14.98 \text{ kips horizontal}$$

BEAM

$$M_2 = 87.5 - 1.5 R_1 = 87.5 - 1.5 (44.34) = 21 \text{ k-ft.}$$

$$M_1 = 20 \text{ k-ft.}$$

$$Z = \frac{M}{\sigma} = \frac{21 \text{ k-ft.} \times 12 \frac{\text{in.}}{\text{ft.}}}{35,000} = 7.37 \text{ reqd.}$$

$$Z = 6.23 (1.27) = 7.9 \text{ for } 6" \text{ O.D. } \times 1/4" \text{ wall } (5.31 \text{ } 1b/ft)$$

BOLTS 5/8" dia. 2024-T4 Bolts

$$F_y = 44 \text{ ksi}, F_{us} = 60 \text{ ksi}, F_y \text{ shear} = 25 \text{ ksi}$$

$$A_{\text{tension}} = .207 \text{ in.}^2 \quad A_{\text{shear}} = .307 \quad F_y \text{ bearing} = 69 \text{ ksi}$$

$$P_{\text{tension}} = .207 \text{ in.}^2 (44 \text{ ksi}) = 9.11 \text{ kips strut}$$

$$V_{\text{shear}} = .307 \text{ in.}^2 (25 \text{ ksi}) = 7.67 \text{ kips}$$

$$P_{\text{bearing}} = .625 \text{ in.}^2 (.25 \text{ in.}) (56 \text{ ksi}) = 8.75 \text{ kips (Alum.)}$$

$$P_{\text{bearing}} = .625 \text{ in.}^2 (.25 \text{ in.}) (70 \text{ ksi}) = 10.9 \text{ kips (steel)}$$

$$\text{No. Bolts tension} = \frac{35 \text{ ksi} (2.16 \text{ in.}^2)}{9.11 \text{ kip/bolt}} = 8 \text{ bolts for vertical tension strut (Alum.)}$$

$$\text{No. Bolts shear} = \frac{44.34 \text{ kips} (2)}{7.67 \text{ kip/bolt}} = 12 \text{ bolts for shear per V-strut assembly (alum. truck frame)}$$

Use ASTM A325 steel bolts to reduce the number of bolts.

5/8" dia, ASTM A325

$$F_y = 90 \text{ ksi}, A_{\text{tension}} = .226 \text{ in.}^2, A_{\text{shear}} = .307 \text{ in.}^2$$

$$P_{\text{tension}} = .226 (90) = 20.34 \text{ kips}$$

$$V_{\text{shear}} = .307 \frac{90}{3} = 15.94 \text{ kips}$$

$$P_{\text{bearing}} = .625 (.25) (56 \text{ ksi}) = 8.75 \text{ for alum. frame}$$

$$P_{\text{bearing}} = .625 (.25) (70 \text{ ksi}) = 10.9 \text{ kips for steel frame}$$

$$\text{No. Bolts tension} = \frac{35 \text{ ksi} (2.16 \text{ in.}^2)}{20.34 \text{ kips}} = 4 \text{ bolts for vertical tension strut (steel bolt)}$$

$$\text{No. Bolts} = \frac{44.34 (2)}{8.75} = 10 \text{ bolts for alum. frame in bearing}$$

Use 14 ASTM A325 steel bolts.

LATERAL LOAD ON STRUTS

$$M_p = F_y f S = 1.373 (1.27) 35 = 61 \text{ k-in.}$$

$$P_{lat} = \frac{61 \text{ k-in.}}{18 \text{ in.}} = 3.39 \text{ kips per strut on opposite side of impact}$$

$$P_{lat} \leq \left[1.0 - \frac{P}{P_y} \frac{1.18 M_p}{18 \text{ in.}} \right] = \left[1.0 - \frac{59}{35 (2.16)} \right] \frac{1.18 (61)}{18}$$

$$P_{lat} = .9 \text{ kips tension strut}$$

$$P_{lat} \leq \left[1.0 - \frac{1.18 (61)}{18} \right] = 0.27 \text{ kips } R_1 \text{ strut}$$

$$P_{lat} \leq \left[1.0 - \frac{23.83}{35 (2.16)} \right] \frac{1.18 (61)}{18} = 2.73 \text{ kips } R_2 \text{ strut}$$

$$\text{Total Lateral Capacity} = 3(3.39) + .9 + 0.27 + 2.73$$

$$= 14.07 \text{ kips vs. 12 reqd. O.K.}$$

MAXIMUM CENTRIC CAPACITY (Long. C of car and truck centric)

$$P_{centric \text{ strut}} = 4 R_1 = 4(44.34 \text{ iips}) = 177 \text{ kips to induce yield strength in } R_1 \text{ thru } R_4 - \text{O.K.}$$

$$P_{centric \text{ bolts in shear}} = 10 \text{ bolts} \times 15.9 \text{ kips/bolt} \times 2$$

$$P_{centric \text{ bolts in shear}} = 318 \text{ kips}$$

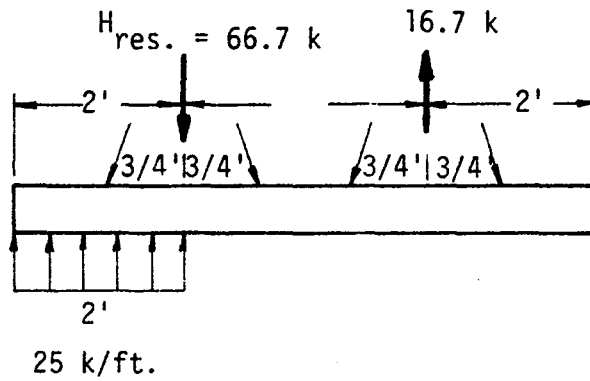
D/t RATIOS (Strut)

$$D/t = \frac{3}{.25} = 12 \leq 40 \text{ for aluminum O.K.}$$

VARIABLE ROAD CLEARANCE - TRUCK UNDERRIDE GUARD 3-AL

Design Calculations - Aluminum 6061-T6 $F_y = 35$ ksi

BEAM

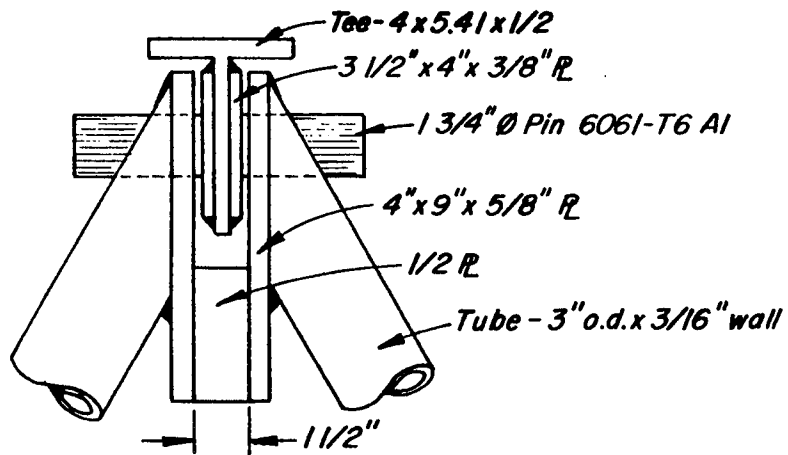
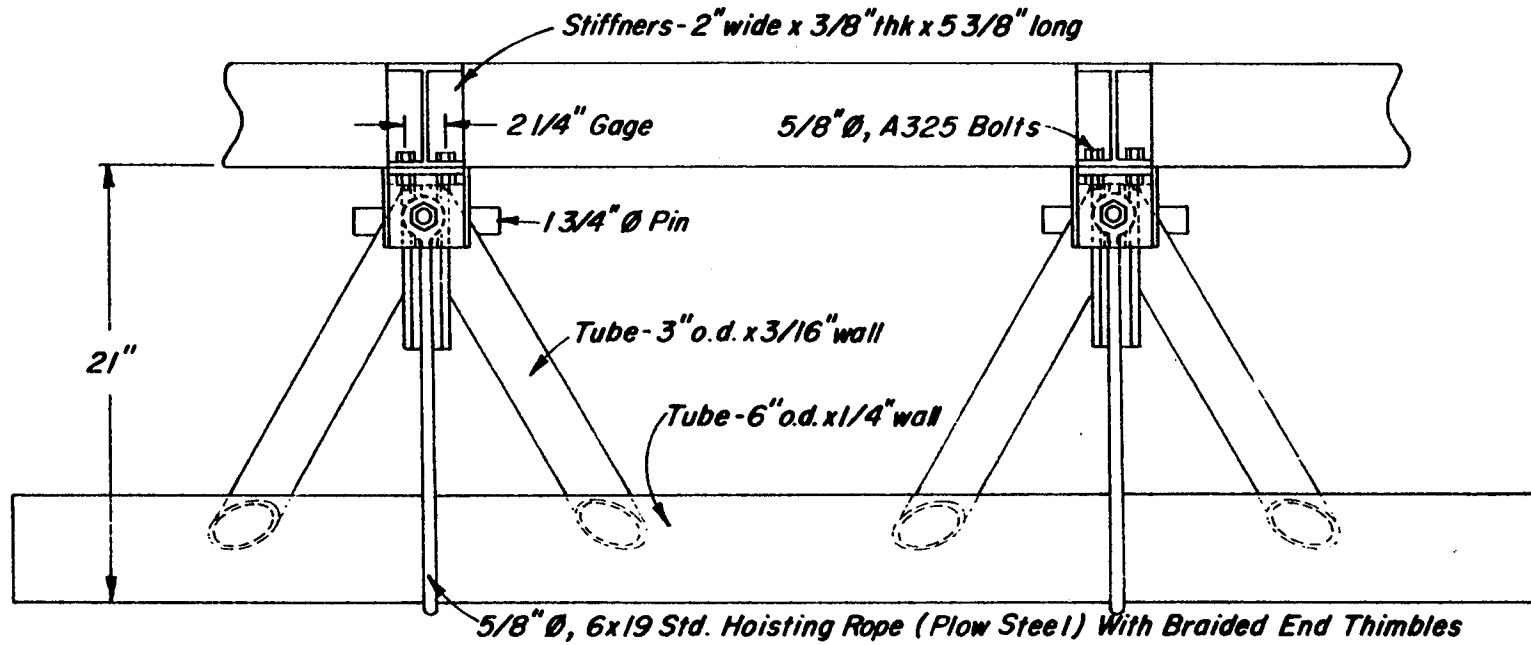


$$M = \frac{25 \text{ k/ft} (1.25 \text{ ft})^2}{2} = 19.53 \text{ k-ft.} = 234.4 \text{ k-in.}$$

$$Z = \frac{234.4 \text{ k-in.}}{35 \text{ ksi}} = 6.70 \text{ in.}^3 \quad S = \frac{6.70}{1.27} = 5.28 \text{ in.}^3$$

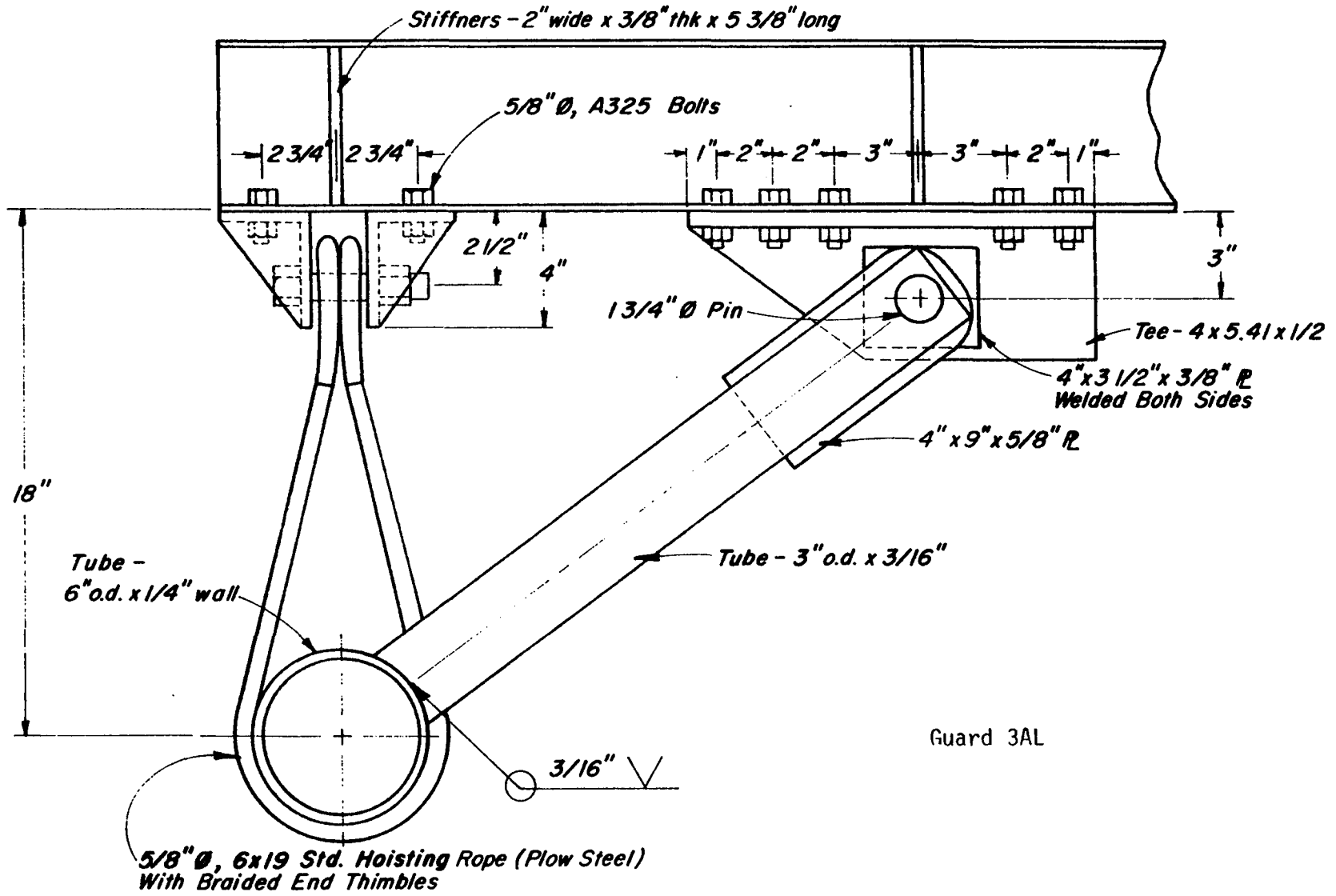
Use 6" ϕ 1/4" wall 6061-T6 Aluminum, $F_y = 35$ ksi;

$$D/t = \frac{6}{1/4} = 24 \text{ O.K.}$$



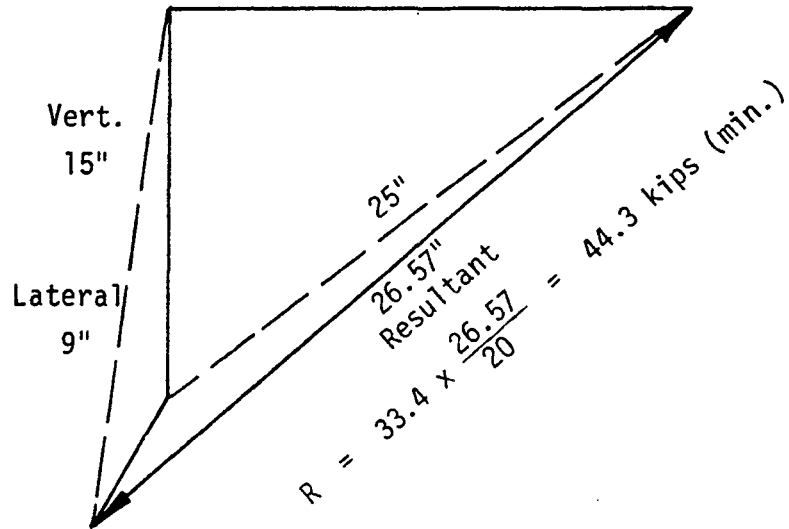
Guard 3AL

E-19



STRUT

Horz. 20" H = $\frac{66.7}{2} = 33.4$ kips



Try 3" ϕ 3/16" wall 1.949 lb/ft

$A = 1.657$ in.² $r = 0.997$ in. $D/t = 16$ O.K.

$\frac{k\ell}{r} = \frac{26.57}{.997} = 26.7 \approx 27$

$C_c = \sqrt{\frac{2\pi^2 \cdot 10,000}{35}} = 75$

$P_u = 35 \left[1 - \frac{27^2}{2 \times 75^2} \right] 1.657 = 35 \times .935 \times 1.657$

$P_u = 54.2$ kips > 44.3 kips O.K.

CABLE TENSION MEMBER

$$T_{\text{reqd.}} = 66.7 \times \frac{15''}{20''} = 50 \text{ kips (reqd.)}$$

Use 5/8" ϕ 6 x 19 standard hoisting rope (plow steel) with braided end thimbles 2 x 29 = 58 kips

BOLTS - Use 5/8" diam. steel ASTM A325

$$F_y = 90 \text{ ksi tension}$$

$$A_{\text{tension}} = .226 \text{ in.}^2 \quad A_{\text{shear}} = 0.3068 \text{ in.}^2$$

$$P_{\text{tension}} = .226 \times 90 = 20.34 \text{ kips}$$

Use 4 bolts to hold cable

$$V_{\text{shear}} = .3068 \times \frac{90}{\sqrt{3}} = 15.94 \text{ kips}$$

$$P_{\text{bearing}} = 5/8'' \times 1/4'' \times 56 \text{ ksi} = 8.8 \text{ kips aluminum}$$

Use at least 8 bolts for shear

BOLT FOR CABLE ATTACHMENT

$$T = 50 \text{ kips (reqd.)}$$

$$\frac{\pi D^2}{4} \times \frac{90}{\sqrt{3}} \times 2 = 50$$

$$D^2 = \frac{50}{.785 \times 51.97 \times 2} = .6$$

$$D = .783 \text{ in.}$$

Use 1" diam A325 Steel Bolt.

BEARING ON DOUBLE ANGLE

$$50^k = 1'' \times t \times 2 \times 35 \text{ ksi} \times 2$$

$$t = \frac{50}{70 \text{ ksi} \times 2} = .36 \text{ in.}$$

Use 2 \angle_s 4" x 3" x 3/8" or 6061-T6 Aluminum

PIN Double Shear 6061-T6 Aluminum

$$\text{Shear } 2 \times 44.3 \text{ kips} = \frac{\pi D^2}{4} \times \frac{35}{3} \times 2$$

$$D^2 = \frac{44.3}{.785 \times 20.2} = 2.79$$

$$D = 1.67 \text{ in.}$$

Use 1 3/4 in. diam. pin.

Bearing

$$1.75 \times t \times 1.6 \times 35 = 2 \times 44.3 \text{ kips}$$

$$t = \frac{88.6}{1.75 \times 56} = .90 \text{ in.}$$

Use 1/2" thick T + two 3/8" thick R's

1.25 in. total

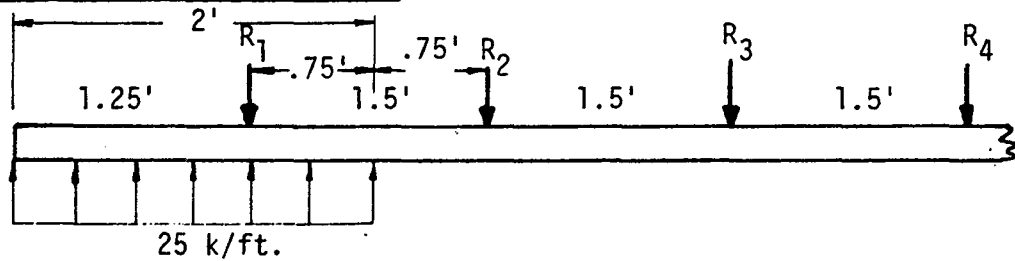
TOTAL WEIGHT

Beam	$7 \text{ ft} \times 5.311 \text{ lb/ft}$	=	37.18
Struts	$1.949 \text{ lb/ft} \times \frac{26.57 \text{ in.}}{12} \times 4$	=	17.26
Tee	$5.14 \text{ lb/ft} \times \frac{14 \text{ in.}}{12} \times 2$	=	11.99
Angles	$2.95 \text{ lb/ft} \times \frac{4 \text{ in.}}{12} \times 4$	=	2.93
Pin	$2.832 \text{ lb/ft} \times .67' \times 2$	=	3.80
Cable	$.63 \text{ lb/ft} \times \frac{42}{12} \times 2$	=	4.41
A325 Bolts	$14 \times 2 \times .31$	=	8.68
Thimble	$.38 \text{ lb.} \times 4$	=	1.52
1" Bolt	$1.5 \text{ lb.} \times 2$	=	<u>3.00</u>

TOTAL WEIGHT

90.77 lb.

RIGID FRAME UNDERRIDE GUARD 5-ST (100 ksi yield steel)



Top View of Guard for Critical Loads on Beam
(Note: Design Criteria has been Modified)

$$M_A = 25 \frac{k}{ft} (1.25 \text{ ft.}) (.625 \text{ ft.}) = 19.53 \text{ k-ft.}$$

$$M_B = 25(2)(1) - .75 R_1 = 50 - .75 R_1 \text{ k-ft.}$$

$$M_C = 25(2)(1.75) - 1.5 R_1 = 87.5 - 1.5 R_1 \text{ k-ft.}$$

DIAGONAL STRUTS

The R_1 strut will be designed to take the full load with a Yield strength stress throughout the cross section.

Try 2" O.D. x 1/8" sq. tube $\rightarrow b/t = 16 < 19$ O.K.

$$\frac{kl}{r} = \frac{2.25 \text{ ft.} \times 12 \text{ in./ft.}}{.585} = 46.15$$

$$A = .938 \text{ in.}^2 \quad \text{WT} = 3.2 \text{ lb/ft}$$

$$I = 0.55 \text{ in.}^4 \quad r = .585 \text{ in.}$$

$$F_u = \left[1 - \frac{\left(\frac{kl}{r}\right)^2}{\frac{4 \pi^2 E}{F_y}} \right] F_y = \left[1 - \frac{46.15^2}{\frac{4 \pi^2 29,000}{100}} \right] 100 = 99.98 \text{ ksi}$$

$$R_1 = 100 \text{ ksi} (.938 \text{ in.}) (.707) (.89) = 59 \text{ kips "Horizontal"}$$

R_1 strut can carry the design load.

Use 2" O.D. x 1/8" wall sq. tube

BEAM

$$M_A = 19.53 \text{ k-ft.}$$

$$M_B = 87.5 - .75 (50) = 12.5 \text{ k-ft.}$$

$$M_C = 87.5 - 1.5 (50) = 12.5 \text{ k-ft.}$$

$$Z_{\text{reqd.}} = \frac{M}{F_Y} = \frac{19.53 \text{ k-ft} \times 12 \text{ in/ft}}{100 \text{ ksi}} = 2.34$$

Try 3 x 3 x 1/4 tube

$$Z = \frac{(3^4 - 2.5^4)1.15}{12(1.5)}$$

$$Z = 2.68$$

$$WT = 9.35 \text{ lb/ft}$$

$$\frac{b}{t} = \frac{3}{1/4} = 12 < 19 \text{ O.K.}$$

Try 3 1/2 x 3 1/2 x 3/16 tube

$$Z = \frac{(3.5^4 - 3.125^4)1.15}{12(1.875)}$$

$$Z = 2.79$$

$$WT = 8.5 \text{ lb/ft}$$

$$\frac{b}{t} = \frac{3.5}{3/16} = 18.67 < 19 \text{ O.K.}$$

Try 4 x 4 x 1/8 tube

$$Z = \frac{(4^4 - 3.75^4)1.15}{12(2)}$$

$$Z = 2.79$$

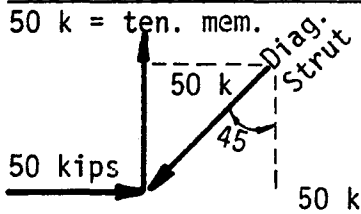
$$WT = 6.33 \text{ lb/ft}$$

$$\frac{b}{t} = \frac{4}{1/8} = 32 \nless 19 \text{ NO}$$

Based on weight and stability (b/t) choose 3 1/2 x 3 1/2 x 3/16 tube.

VERTICAL TENSION MEMEBER

50 k = ten. mem.



Try 2" O.D. x 1/8" sq. tube

$$\sigma = \frac{P}{A} = \frac{50 \text{ kips}}{.938 \text{ in}^2} = 53.3 \text{ ksi vs. } 100 \text{ ksi}$$

O.K.

Side View with Full Load
on 2 diag. Struts.

LATERAL LOADING

$$M_p = \frac{.55}{1} (1.15) (100 \text{ ksi}) = 63.25 \text{ k-in.}$$

$$P_{lat} = \frac{M_p}{d} = \frac{63.25 \text{ k-in.}}{18 \text{ in.}} = 3.51 \text{ kip per strut on impact side}$$

$$P_{lat} = 0 \text{ ten. strut on impact side}$$

$$P_{lat} = 0 \text{ for } R_1$$

$$P_{lat} = \left[1 - \frac{9.4}{59} \right] \frac{1.8 (67)}{18} = 3.7 \text{ kip for } R_2$$

Total lateral load capacity $3.51 (3) + 3.7 = 14.25 \text{ kip} > 12.5 \text{ kip}$ O.K.

TOTAL WEIGHT

Beam $8.5 \frac{\text{lb}}{\text{ft}} \times 7 \text{ ft.} = 59.5 \text{ lbs.}$

Struts $3.2 (2.25) (6) = 43.2 \text{ lbs.}$

Tees = 24.0 lbs.

Six Plates = 9.0 lbs.

Bolts, Washers = 8.0 lbs.

TOTAL LBS. 143.7 lbs.

BOLTS

$$5/8" \text{ dia. ASTM A325} \quad F_y = 90 \text{ ksi}$$

$$A_{\text{tension}} = 0.226 \text{ in}^2 \quad A_{\text{shear}} = .307 \text{ in}^2$$

$$P_{\text{tension}} = (90 \text{ ksi}) (.226 \text{ in}^2) = 20.34 \text{ kips/bolt}$$

$$V_{\text{shear}} = .307 (90 \text{ ksi}) = 15.94 \text{ kips/bolt}$$

$$P_{\text{bearing}} = .625 (.25) (70 \text{ ksi}) = 10.9 \text{ kips/bolt}$$

$$\begin{array}{l} \text{No. Bolts ten.} \\ \text{vert. Ten strut} \end{array} = \frac{100 \text{ ksi} (.938)}{20.34 \text{ kips/bolt}} = 4.6 \text{ Bolt for vert. ten.} \\ \text{strut to strength of} \\ \text{member}$$

Use 4 bolts on vertical tension strut since actual load is less than capacity.

$$\text{No. Bolt Shear} = \frac{59 \text{ kips} (2) (.707)}{10.9 \text{ kips/bolt}} = 7.65 \text{ or } 8 \text{ bolts}$$

Use 8 bolts for shear

Total Bolts = 12 ASTM A325 5/8" dia.

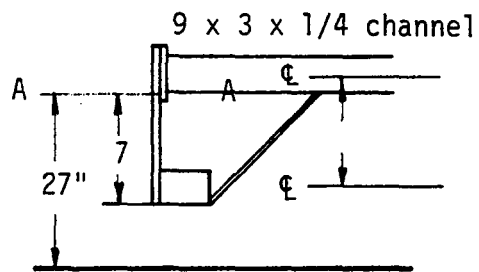
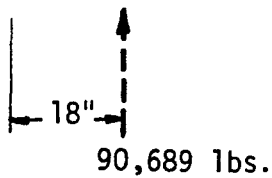
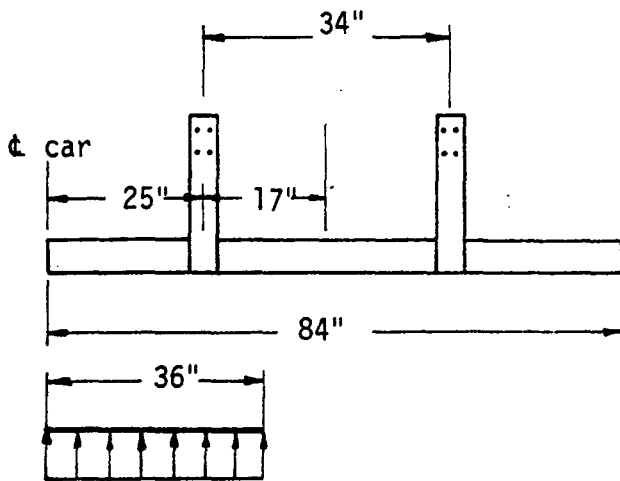
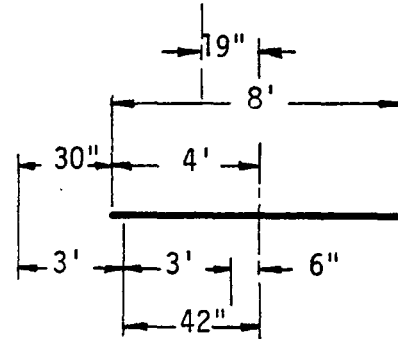
GUARD 7-ST for IH 1610 TRUCK

FOR CENTRIC COLLISION

$$\begin{aligned}
 F_{\max} &= 0.967 (V) (W_A) \sqrt{\frac{\Delta}{D}} \frac{W_T}{W_T + W_A} \\
 &= 0.967 (35) (4500) (1) \frac{24,000}{24,000 + 4,500} \\
 &= 128,255 \text{ lbs.}
 \end{aligned}$$

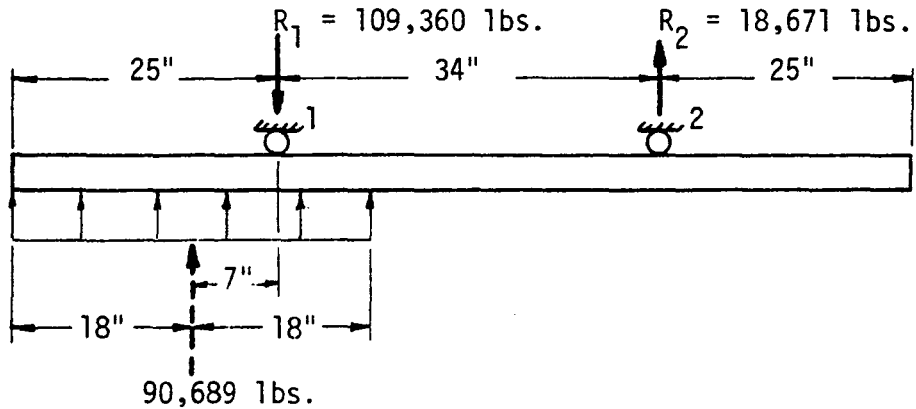
FOR OFFSET (42") COLLISION

$$\begin{aligned}
 F_{\max} &= 128,254 \text{ lbs.} \sqrt{\frac{\Delta}{D}} \\
 &= 128,254 \sqrt{\frac{1}{2}} \\
 &= 90,689 \text{ lbs.}
 \end{aligned}$$

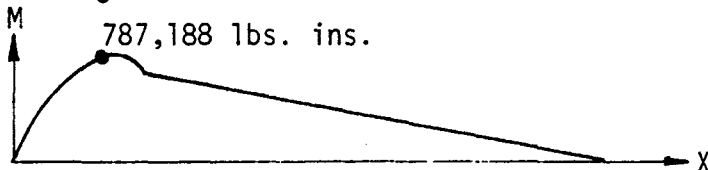
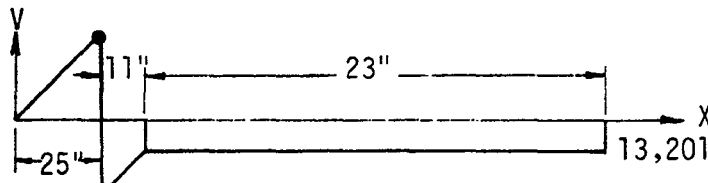


42" OFFSET DESIGN

BEAM



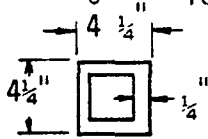
$$\sum M_2 = 0 = 90,689 \text{ lbs.} (41) - 34 (R_1) \rightarrow R_1 = 109,360 \text{ lbs.}$$



Max. Moment = 787,188 lbs. in. or 65.6 k-ft.

Assume plastic hinge forms @ Section 1

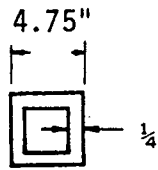
$$Z = \frac{M}{\sigma} = \frac{787,188}{100,000} = 7.87 \text{ in}^3 \text{ req'd.}$$



$$Z = \frac{(4.25^4 - 3.75^4) 1.15}{12 (2.125)} =$$

$$Z = 5.80 \text{ in}^3$$

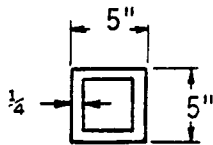
$$b/t = 17 \text{ vs. } 19 \text{ max.}$$



$$Z = \frac{(4.75^4 - 3.75^4) 1.15}{12 (2,375)}$$

$$Z = 7.37 \text{ in}^3$$

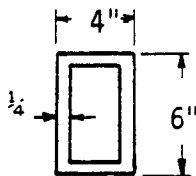
$$b/t = 19 \text{ vs. } 19 \text{ max.}$$



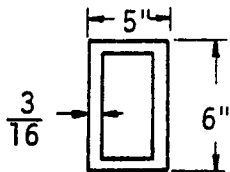
$$Z = \frac{(5^4 - 4.5^4) 1.15}{12 (2.5)}$$

$$Z = 8.23$$

$$b/t = 20 \text{ vs. } 19 \text{ max.}$$

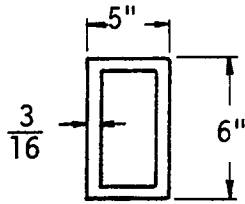


$$Z = \left[\frac{4 (6)^3 - 3.625 (5.625)^3}{12 (3)} \right] 1.15 = 6.99 \text{ in}^3 < 7.87 \text{ NO!}$$



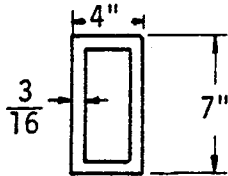
$$Z = \left[\frac{4 (6)^3 - 3.5 (5.5)^3}{12 (3)} \right] 1.15 = 8.99 > 7.87 \text{ O.K.}$$

$$A = 4 \times 1/4 \times 2 + 5.5 \times 1/4 \times 2 = 4.75 \text{ in}^2$$



$$Z = \left[\frac{5 (6)^3 - 4.625 (5.625)^3}{12 (3)} \right] 1.15 = 8.2 > 7.87 \text{ O.K.}$$

$$A = 5 \times 3/16 \times 2 + 5.625 \times 3/16 \times 2 = 3.98 \text{ in}^2$$

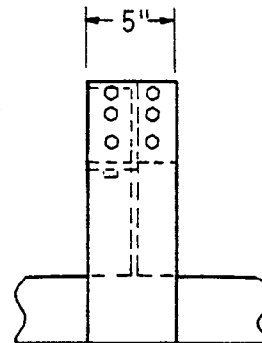
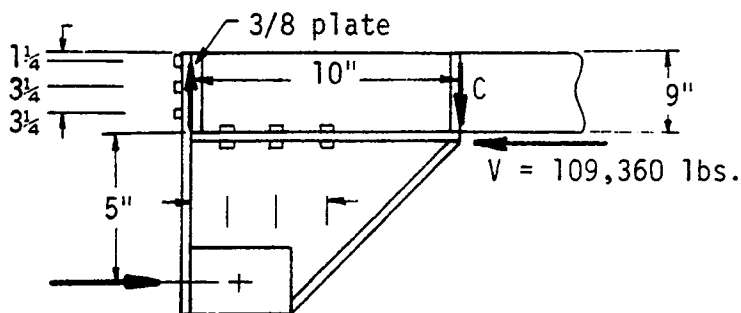


$$Z = \left[\frac{4 (7)^3 - 3.625 (6.625)^3}{12 (3.5)} \right] 1.15 = 8.7 > 7.87 \text{ O.K.}$$

$$A = 4 \times 3/16 \times 2 + 6.625 \times 3/16 \times 2 = 3.98$$

$$b/t = \frac{4}{3/16} = 4.3$$

CONNECTIONS FOR 42" OFFSET COLLISION



SHEAR CAPACITY THRU BOLT HOLES (# 3 BOLT)

$$V_{\text{allow}} = (5 - 22/16) (1/4) 100,000 = 90,625 \text{ vs. } 103,892 \text{ lbs.}$$

$$\text{MAX. MOMENT IN CHANNEL} = 109,360 \text{ lbs.} (5 + 4.5) = 1,038,920$$

$$T = C = \frac{1,038,920 \text{ lbs. in.}}{10 \text{ in.}} = 103,892 \text{ lbs.}$$

$$\text{For ASTM A325 } 5/8 \text{ } \emptyset \quad V_{\text{allow}} = 15.94 \text{ kips/bolts}$$

$$\text{No. Bolts for } T = \frac{103.89 \text{ kips bolt}}{15.94 \text{ kips}} = 6.5 \text{ bolts}$$

SHEAR CAPACITY @ Section i-j

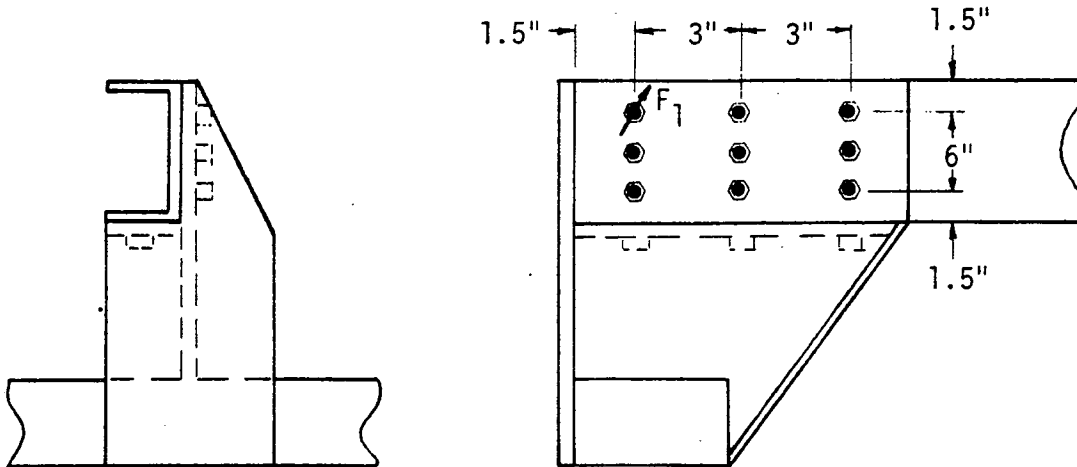
$$V_{\text{allow}} = (5" \times 1/4") 100,000 \text{ psi} = 125,000 \text{ lbs. vs. } 109,360 \text{ lbs.}$$

BEARING CAPACITY OF VERT. PLATE

$$P_{\text{bearing}} = \frac{103,892 \text{ lbs.}}{8 \text{ bolts}} = 12,986 \text{ lbs./bolt or}$$

$$12.9 \frac{\text{kips}}{\text{bolt}} \text{ vs. } 11 \text{ kips allow}$$

ALTERNATE CONNECTION PATTERN



$$\text{Max Moment} = 1,038,920 = F_1 \overset{\text{Bolts}}{1, 3, 6 \ \& \ 8} 3 \sqrt{2} (4) + \frac{3}{3\sqrt{2}} \overset{\text{Bolts}}{2,4,5,7,9, 10 \ \& \ 11} F_1 3 (7)$$

$$F_{\text{max}} = 32 \text{ kips shear vs. } 16 \text{ kips shear allow}$$

To many bolts req'd!

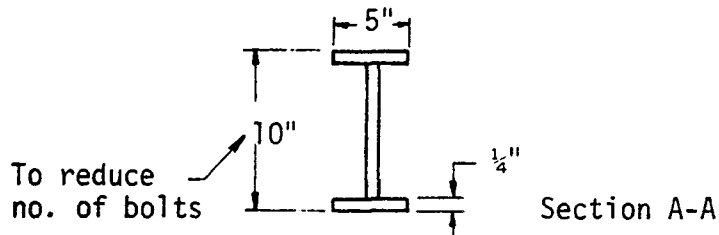
DESIGN OF VERTICAL BRACE

$$\text{Max. Moment} = 109,360 \text{ lbs. } (7 + 4.5 - 2.125)$$

in channel

$$= 1,025,250 \text{ lbs. in. or } 85.4 \text{ k/ft.}$$

$$F = \frac{M}{\sigma_y} = \frac{1,025,250 \text{ lbs. in.}}{100,000 \text{ psi}} = 10.25 \text{ in}^3 \text{ req'd.}$$



$$M_p = \left[5'' \times \frac{1}{4}'' \times 5.125'' \times 2 + 5 \times \frac{1}{4} \times 2.5 \times 2 \right] 100,000 \text{ psi}$$

$$M_p = 19.062 (100,000)$$

$$Z_p = \frac{19.062 (100,000)}{100,000} = 19.062 \text{ in}^3$$

$$\frac{b}{t} = \frac{2.5}{1/4} = 10 > 6.5 \text{ req'd.}$$

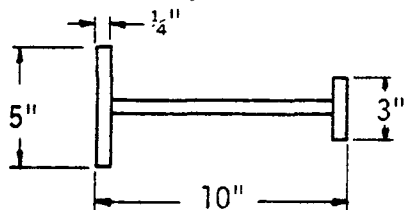
But Comp. Flg. is stiffened by attached (welded) 1/4" plate which bolts to channel. See P. 4.

LATERAL BENDING

$$\frac{P}{4} = 128,254/4 = 32,063 \text{ lbs.}$$

$$\text{Lateral Moment} = \frac{32,063 (5)}{2} = 80,158 \text{ lbs. in.}$$

$$S = \frac{M}{\sigma} = \frac{80,158}{100,000} = .8 \text{ in}^3 \text{ req'd.}$$



$$S = \left[\frac{1}{4} (5)^3 + \frac{1}{4} (3)^3 \right] = 1.05 \text{ O.K.}$$

Bolts O.K. too!

WEIGHT

Beam	=	95	lbs.
Vert. Brace	=	30	lbs.
Bolts	=	10	lbs.
Plates	=	<u>11.5</u>	<u>lbs.</u>
TOTAL		146.5	lbs.

APPENDIX F

DETAILS OF FULL-SCALE CRASH TESTS

Test Program

Table F-1 gives a summary of the twelve full-scale crash tests that were conducted in the program. The first three columns in this Table give the test number; identify the trailer or truck and total test weight for that vehicle; and identify the underride guard design used in the test. The fourth column gives the guard ground clearance measured immediately prior to testing. The distance given is from the pavement surface to the lower extremity of the guard. The fifth through seventh columns identify the automobile and its total test weight including instrumentation and dummies, the actual test closing speed (or impact speed), and the relative alignment of the two vehicles at impact.

The target closing speed for tests 1 and 2 was 64 km/h (40 mph). For tests 3 through 12, the target closing speed was 56 km/h (35 mph). There were several reasons for lowering the design closing speed. The decision included input from other underride research that was being conducted by the National Highway Traffic Safety Administration (NHTSA). Secondly, in 64 km/h (40 mph) impacts where excessive underride did not occur, dummy injury indices were well above normally acceptable values. That is to say, even though a rigid guard was effective in preventing excessive underride of an automobile at 64 km/h (40 mph), it was ineffective in reducing dummy injury indices to acceptable levels. This finding indicated that the 64 km/h (40 mph) design closing speed should be lowered. Finally impact forces generated on the underride guard and the vehicle framework in 64 km/h (40 mph) tests were quite high and necessitated the use of heavier guards than would be required by lower closing speeds.

The eighth column in this table gives the maximum force that was imposed on the automobile during the collision. This force is based on the highest value of the average acceleration taken over a 0.050 sec interval and is computed using the following equation:

$$F = \left[\frac{1}{0.050 \text{ sec}} \int_{t_1}^{t_1 + 0.050} a \, dt \right] W$$

Where:

- a = acceleration value from accelerometer trace (g's)
- t = time variable (sec)
(t = 0 at impact)
- t₁ = the time value within collision event that produces max value of the interval (sec)

Table F-1. Summary of Full-Scale Tests and Results.

TEST	TRUCK/TRAILER	GUARD DESIGN	GUARD GROUND CLEARANCE	AUTOMOBILE	CLOSING SPEED	ALIGNMENT	MAX .050 SEC FORCE ON AUTO	MIN TRAILER TO WINDSHIELD DIST. (ft)	PENETRATION OF OCCUPANT COMPARTMENT	DRIVER						PASSENGER					
										HEAD			CHEST			HEAD			CHEST		
										HIC	GADD	.003 SEC G	HIC	GADD	.003 SEC G	HIC	GADD	.003 SEC G	HIC	GADD	.003 SEC G
3661-1	Fruehauf FB-9-F2-40 54,830 lbs	5ST-1 163 lb	18.0 in	1977 VW Rabbit 2250 lbs	40.8 mph	Centric	29.2 g's 65,700 lbs	0.7	No	----	----	---	---	---	---	2901	3819	149	495	636	60
3661-2	Fruehauf FB-9-F2-40 54,830 lbs	5ST-2 163 lb	17.6 in	1977 Ford LTD 4500 lbs	40.4 mph	62 in Offset left	11.1 g's 50,000 lbs	---	Yes	----	----	---	---	---	---	477	791	65	32	60	28
3661-3	Fruehauf FB-9-F2-40 54,830 lbs	5ST-3 173 lb	17.8 in	1979 Chev. Impala 4090 lbs	33.8 mph	Centric	25.2 g's 103,000 lbs	2.5	No	1941	2353	105	406	492	59	1372	1712	66	No Instrumentation		
3661-4	Fruehauf FB-9-F2-40 54,830 lbs	5ST-3 215 lb	17.0 in	1979 Chev. Impala 4090 lbs	35.2 mph	42 in Offset left	18.1 g's 74,000 lbs	1.2	No	552	680	69	109	128	27	1225	1610	94	No Instrumentation		
3661-5	Fruehauf FB-9-F2-40 23,960 lbs	6ST 210 lb	18.5 in	1977 VW Rabbit 2300 lbs	36.3 mph	Centric	26.3 g's 60,500 lbs	0.5	No	1150	1456	99	541	609	53	1794	2263	91	No Instrumentation		
3661-6	Fruehauf FB-9-F2-40 23,960 lbs	6ST 210 lb	18.5 in	1979 Chev. Impala 4090 lbs	33.4 mph	42 in Offset left	8.6 g's 35,200 lbs	---	Yes	241	330	29	18	24	10	135	204	25	36	54	15
3661-7	Fruehauf FB-9-F2-40 56,240 lbs	Q-H 315 lb	15.1 in	1979 Chev. Impala 4090 lbs	34.2 mph	Centric	18.2 g's 74,400 lbs	1.9	No	333	403	34	151	186	29	594	758	57	190	255	37
3661-8	Fruehauf FB-9-F2-40 20,140 lbs	Q-H 315 lb	15.2 in	1979 Chev. Impala 4010 lbs	34.6 mph	42 in Offset left	15.7 g's 63,000 lbs	1.9	No	637	760	59	38	53	20	480	617	53	152	194	31
3661-9	IH Str. Truck C01610A 20,140 lbs	7ST 159 lb	17.0 in	1979 Chev. Impala 4070 lbs	35.0 mph	Centric	18.8 g's 76,900 lbs	2.6	No	937	1131	75	213	278	49	666	899	64	175	219	33
3661-10	Trailmobile A11-A1-CAH 54,460 lbs	None	N/A	1977 VW Rabbit 2260 lbs	33.0 mph	Centric	22.7 g's 51,300 lbs	0.4	No	916	1217	67	323	383	47	852	1023	49	254	293	34
3661-11	Trailmobile A11-A1-CAH 54,460 lbs	None	N/A	1979 Chev. Impala 4060 lbs	35.2 mph	42 in Offset left	15.0 g's 60,900 lbs	1.5	No	501	650	59	158	178	26	730	946	67	244	267	35
3661-12	Fruehauf FB-9-F2-40 56,400 lbs	2AL 119 lb	18.0 in	1979 Chev. Impala 4090 lbs	34.6 mph	Centric	22.6 g's 92,000 lbs	2.0	No	1921	2377	114	509	638	65	1528	1857	88	374	447	44

F-2

$F = \text{max } .050 \text{ sec average force on the automobile (lbs)}$
 $W = \text{weight of automobile (lbs)}$

Values of a time interval other than 0.050 sec could be used for computation of maximum force. However, the 0.050 sec interval produces forces that compare favorably with mathematical models of automobile collisions and these forces, when used to design structures which exhibit some ductility, result in structures which behave as expected.

Other techniques for arriving at a maximum force have been proposed and are sometimes used. One such technique is to use the highest peak acceleration from the accelerometer trace. This technique will result in higher forces than the 0.050 sec average and the value varies with the amount and kind of filtering of the accelerometer signal. Peak forces, if desired, may be read from the accelerometer traces for each individual test.

The ninth column in Table F-1 gives the minimum distance, during the collision, between the most forward point on the automobile windshield and the lower, rear edge of the trailer body. In other words the dimensions given represent the distance remaining before excessive underride as defined in Chapter VI would occur.

The eleventh through twenty-second columns in Table F-1 contain dummy injury indices computed from head and chest acceleration in accordance with FMVSS 208 (9).

General Test Procedures

All tests were conducted on a concrete parking apron at the Texas A&M Research and Extension Center, Bryan, Texas. The tractor/trailer unit (or other commercial vehicle test unit) with prototype underride guard installed (or other configuration) was parked on the concrete pavement. In tests involving a tractor/trailer unit the normal operating air brakes on the trailer were set on. Brakes were not applied on the tractor. In tests 1 through 8 and in 12, the trailer was a 1968 Fruehauf Model FB-9-F2-40. It was set on a 1965 International Harvester tractor with a single rear axle. In tests 10 and 11, a 1971 Trailmobile trailer Model A11-A1-CAH was used on the same tractor. No guard was installed on this trailer. In test 9, a 1971 International Harvester Model C01610A single unit truck was used. The mechanical parking brake on this unit was set on during the test.

The automobile was towed into the parked trailer or truck using a cable guidance and tow system. One cable, connected to the pavement and stretched along the intended path of the automobile, passed through an attachment to the front wheel spindle of the automobile to provide guidance. Another cable, attached near the front of the frame of the automobile, was threaded around a pulley on the pavement to accomplish a change in direction and was connected to the tow vehicle. Both cables were disconnected immediately prior to impact.

Data Acquisition and Processing

Electronic Instrumentation: Measurement of the accelerations, angular rotations, and speed of the automobile were made by means of precision transducers coupled to a telemetry system transmitter in the test automobile. At the base station the data were received, demultiplexed, processed, and recorded on magnetic tape and high speed oscillographs.

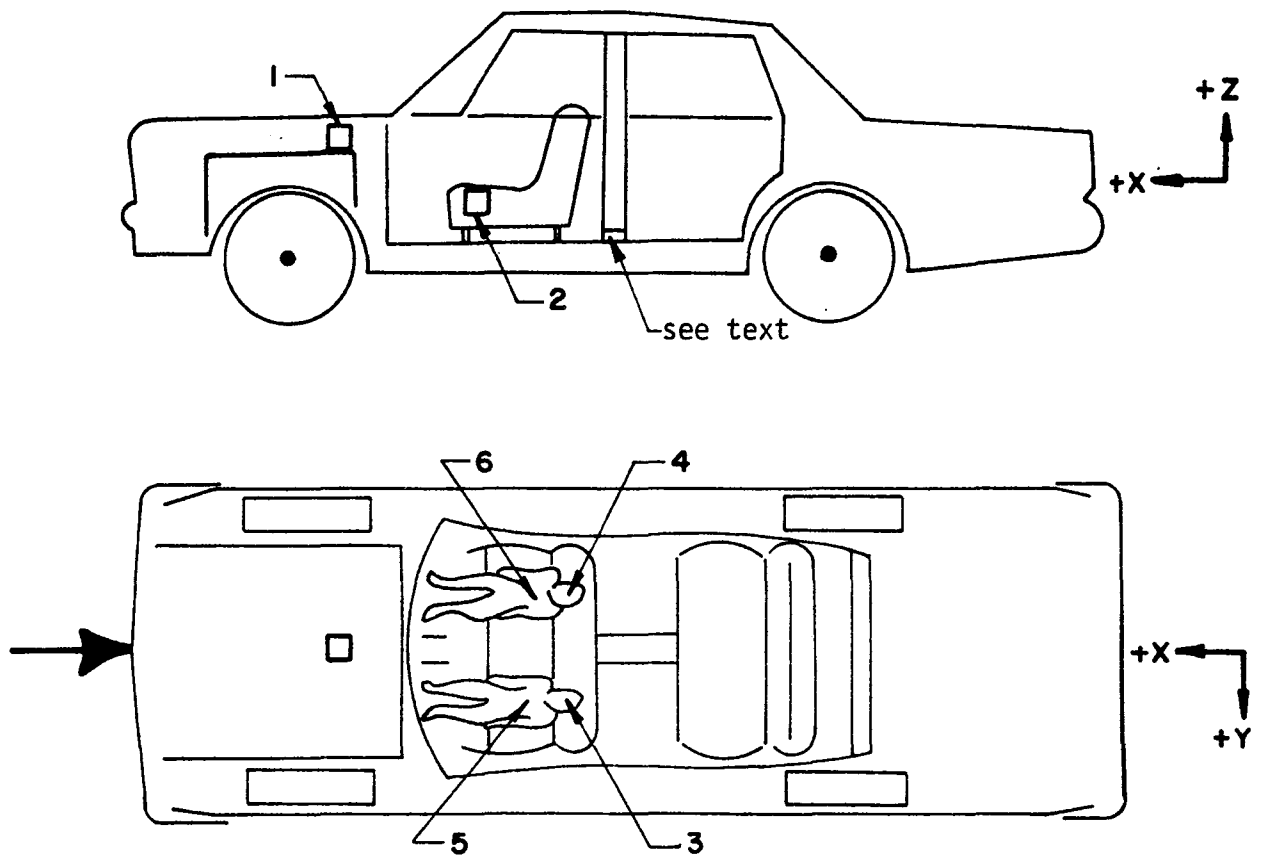
The various transducers used in this test series are described in Table F-2. Typical locations and transducer ranges are illustrated in Figure F-1 along with vehicle coordinate system sign conventions.

In test 9 through 12, a modified automobile accelerometer location was used. The automobile longitudinal accelerometer at the center of gravity was replaced with two longitudinal accelerometers -- one at the base of each B-pillar. This was done to take advantage of more suitable mounting structure for the accelerometers.

The Statham and C.E.C. accelerometers are of the strain gage type providing a linear millivolt output proportional to acceleration. The nature of the transducer allows the output to accurately indicate steady state acceleration complying with the lower limit specifications of SAE J211 and allowing calibration on a precision centrifuge. The accelero-

Table F-2. Automobile-Mounted and Occupant-Mounted Transducers.

ABVR.	MEASUREMENT	TRANSDUCER
AXv	Automobile Accel, X Axis	Statham A69TC
AYv	Automobile Accel, Y Axis	Statham A5
AZv	Automobile Accel, Z Axis	Statham A5
AXe	Engine Accel, X Axis	Statham A69TC
AXe	Engine Accel, Z Axis	Statham A69TC
AHX	Dummy Alpha, Head, X Axis	CEC 4-204-0001
AHY	Dummy Alpha, Head, Y Axis	
AHZ	Dummy Alpha, Head, Z Axis	
ACX	Dummy Alpha, Chest, X Axis	CEC 4-204-0001
ACY	Dummy Alpha, Chest, Y Axis	
ACZ	Dummy Alpha, Chest, Z Axis	
BHX	Dummy Beta, Head, X Axis	CEC 4-204-0001
BHY	Dummy Beta, Head, Y Axis	
BHZ	Dummy Beta, Head, Z Axis	
BCX	Dummy Beta, Chest, X Axis	CEC 4-204-0001
BCY	Dummy Beta, Chest, Y Axis	
BCZ	Dummy Beta, Chest, Z Axis	
PITCH	Automobile Pitch Rate	Humphrey, RT03
ROLL	Automobile Roll Rate	Humphrey, RT03
YAW	Automobile Yaw Rate	Humphrey, RT03



AUTOMOBILE ACCELEROMETER LOCATION AND
PHYSICAL COORDINATES

ACCELEROMETER RANGES

<u>NO.</u>	<u>DESCRIPTION OF LOCATION</u>	<u>X</u>	<u>Y</u>	<u>Z</u>
1.	On top of rear portion of engine	+250 g		+100 g
2.	Near automobile c.g.	+100 g	+ 50 g	+ 50 g
3.	Inside driver's head	+100 g	+100 g	+ 50 g
4.	Inside passenger's head	+250 g	+250 g	+100 g
5.	Inside driver's chest	+100 g	+100 g	+ 50 g
6.	Inside passenger's chest	+100 g	+100 g	+ 50 g

Figure F-1. Transducer Locations and Ranges,
and Sign Conventions in the Automobile Coordinate System.

meters are physically calibrated at periodic intervals on a Genisco model 1074 Accelerometer Calibrator located at this facility.

The angular rate transducers are solid-state rather than a conventional spinmotor type to remain accurate and operational during the high levels of acceleration incurred during the crash test. The rate transducers operate by internally generating a fine-stream laminar flow of gas molecules along the cylindrical axis of the sensor through the nozzle chamber and pass between the two parallel, heated wires of the sensor element. As the unit is rotated about the sensitive axis, the parallel wires move into and out of the gas stream causing a differential resistance change proportional to the angular rate. This type of rate transducer is insensitive to linear velocity and acceleration and capable of withstanding 10,000 g shock.

Vehicle speed and contact indication are provided by pressure sensitive switches in strip form that are applied to the front bumper with the speed switch lower than the impact switch. Vehicle speed immediately prior to impact is measured by contacting and breaking off small wooden dowels with the bumper switch. With the dowels a known distance apart and precise timing of the interval between contacts, the speed can be calculated. The impact switch is actuated only upon contacting the test target.

Amplification and signal conditioning for each data channel is provided in the vehicle to obtain a high signal-to-noise ratio. Calibration levels for each separate channel are also provided in the vehicle to compensate for any gain changes anywhere in the data system. These calibration levels are transmitted immediately prior to and after each vehicle crash test.

The data is transmitted between the test vehicle and the data acquisition station by means of a constant band width FM/FM telemetry link. The aerospace quality telemetry system was specially designed for vehicle crash test work. A great deal more durability is required for vehicle crash testing than in-flight testing where this type of system is normally found

The multiplex of data channels, transmitted on one radio frequency, is received at the data acquisition station, demultiplexed into separate tracks of Intermediate Range Instrumentation Group (I.R.I.G.) tape recorders. The data are also displayed on a high-speed strip chart recorder for quick-look, real-time information. After the test, the data is played back from the tape machines, one channel at a time, filtered according to Table F-3, on the strip chart recorder. FMVSS procedures specify that dummy head acceleration signals be filtered at 1000 Hertz. The telemetry system has a built-in 500 Hertz filter; however, a head drop test was the 50 Hertz filter met the Part 572 performance requirements.

Table F-3. Filter Characteristics.

TYPE	Fco	0.6Fco	1.0Fco	2.0Fco	4.0Fco	Class	USE
4 Pole LowPass Butterworth	100Hz	-0.25db	-3.0db	-24.0db	-48.0db	60	Vehicle structural Accelerations and Rate Transducers
4 Pole LowPass Butterworth	300Hz	+0.5db	-3.0db	-24.0db	-48.0db	180	Dummy Chest Accelerations and Engine Accelerations
5 Pole LowPass Bessel (Telemetry Output Filter)	500Hz	-1.0db	-3.0db	-15db	-45db	---	* Dummy Head Accelerations

* Note: Part 572 Head Drop test is acceptable using these filters.

Along with the data trace on each chart, the data channel calibrations, precise timing in the form of a square wave and the contact pulse are recorded. These charts are then forwarded to the data reduction groups for subsequent digitizing and computations.

Photographic Instrumentation: High-speed film documents the test from the various cameras shown in Figure F-2. The documentary camera records pre-test configurations, pans with the automobile motion during the test, and records damage to the test article and the test automobile after the test. The oblique view of the front of the guard (camera 1) provides details of the automobile deformation and dummy movements. The view perpendicular to the vehicle motion (camera 2) is used for frame-by-frame analysis resulting in time-displacement data from which speeds and events as a function of time or displacement may be obtained. The oblique frontal view of the approaching car (camera 3) provides details of behavior of the guard and shows the transverse point of contact between the vehicle and guard. The overhead view is also used to collect frame-by-frame data for speeds and displacements and is compared to that computed from the perpendicular view data. The overhead camera is particularly useful when the car yaw significantly distorts data from the perpendicular camera. The on-board camera records dummy action. In tests 1 and 2 the on-board camera was positioned in the left rear corner of the passenger compartment and photographed the action of the single dummy in the passenger seat. Tests 3 through 12 included both a driver and passenger dummy and the camera was repositioned to a central rear location (see Figure F-3). Sequential photographs are presented from the overhead view, the interior view and the angular view for the approaching car to illustrate the car motion, dummy motion, and guard damage.

Data Processing - Electronic: Strip charts of analog data that correspond to the transducers described in Table F-2 are analyzed. These charts are digitized on a Gerber digitizer (Model GDDRS-3B). The "Impact" computer program uses the data decks from the vehicle x, y, and z charts and the engine x and z charts to compute accelerations, area beneath the curve, change in velocity, average acceleration, average speed, change in momentum, instantaneous force, and average force at 0.001 sec intervals on each chart. Peak acceleration and the maximum average acceleration over a 0.050 sec interval are also computed for each chart. The "Crash Test" program computes acceleration for 0.002-sec intervals using digitized data of dummy head or chest x, y, and z charts, and provides these three accelerations at each interval in printout form and in punched-deck form. The "Crash Test" program computes accelerations for each chart independently and combines acceleration of the dummy head or chest. The "Injury" program uses the accelerations assembled in the "Crash Test" output deck to compute HIC and GADD injury indices (9) and the maximum acceleration for a 0.003 sec interval. The "Plotangle" program uses the digitized data from the roll, pitch, and yaw displacement charts to compute angular velocity (deg/sec) and displacement (deg) at 0.001 sec intervals and then instructs the Houston Instruments DP-7 plotter to produce three reprodu-

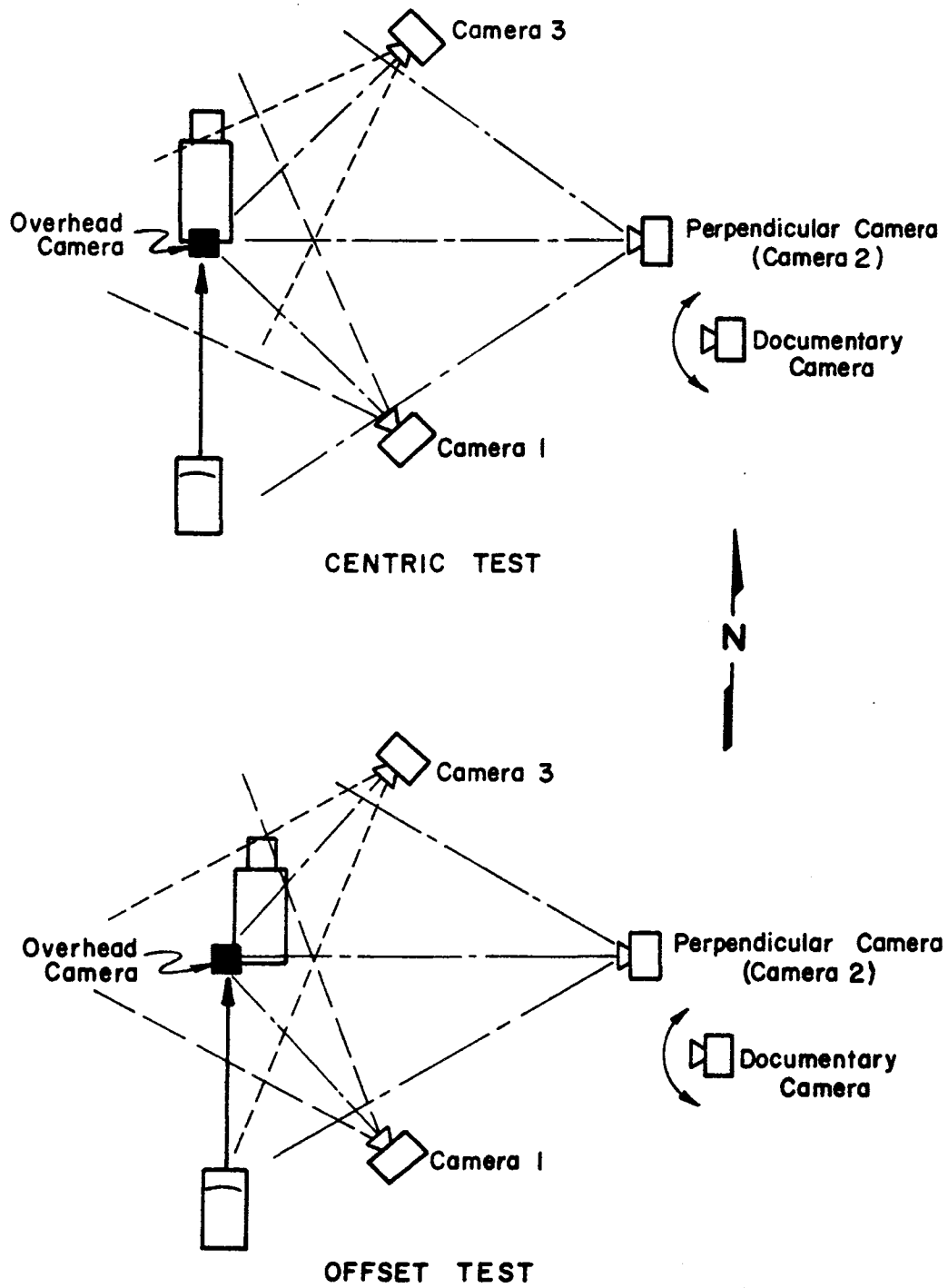
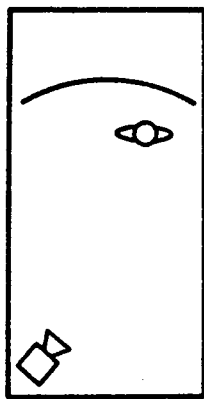


Figure F-2. Typical Camera Positions.



Tests 1 & 2



Tests 3 thru 12

Figure F-3. On-Board Camera Positions.

cible plots: roll (deg) versus time (sec); pitch (deg) versus time (sec); and yaw (deg) versus time (sec). The vehicle and dummy charts are then traced by hand with appropriate grids for display in the final report.

Data Processing - Photographic: There are two kinds of information obtained from the photographic instrumentation. First, the films are used to observe and document events during the collision. Second, frame by frame analyses of films from the perpendicular and/or overhead cameras are performed to obtain time-displacement data and then used to compute velocity and/or acceleration as functions of time. The frame by frame analyses are made using a Vanguard Motion Analyzer. Each frame, or selected frames, are viewed in turn with measurements being made using movable crosshairs on the viewing screen. The measurements are recorded and processed by hand to obtain the tabulations of data mentioned above.

Test Results

The following sections present detailed results of Tests 3661-1 through 3661-12. Each section includes:

- Underride guard design configurations
- Summaries of test results
- Still and sequence documentary photographs
- Accelerometer traces
- Time-displacement-event summaries
- Dummy injury indices

Test 3661-1

Fruehauf Trailer - 24,890 kg (54,830 lb)
Rigid Guard Design 5ST-1 - 74 kg (163 lb)
Ground Clearance - 0.45 m (18.0 in)
1977 Volkswagen Rabbit - 1022 kg (2250 lb)
65.7 km/h (40.8 mph) closing speed
Centric alignment
Tested January 5, 1979

A prototype 5ST-1 guard (Figure F-4) mounted on the loaded Fruehauf trailer was used in this test. The guard successfully prevented excessive underride during the collision. Results of the test are summarized in Table F-5.

The maximum dynamic crush of the front of the automobile was 0.9 m (2.9 ft) as determined from the high-speed data film.

Photographs documenting the test are presented in Figures F-5 through F-8. Damage to the guard was nil. However, the trailer frame members were slightly deformed in bending at the forward extreme of the guard (Figure F-6). Front portions of the automobile occupant compartment received significant damage.

Accelerometer traces for the automobile are presented in Figures F-9 through F-11. The highest 0.050 sec average acceleration imposed on the automobile during the collision was -29.2 g's. For the 1022 kg (2250 lb) automobile this amounts to a force of 292,234 N (2250 x 29.2 = 65,700 lbs).

Accelerometer traces for the passenger dummy (Beta) are presented in Figures F-13 through F-16 and dummy injury indices are given in Table F-8. The HIC value for the head is excessively high in this test.

Sequential photographs of the collision are presented in Figure F-12 and a summary of events are given in Table F-6. Sequential photographs of the dummy are shown in Figure F-17. The photographs and dummy accelerometer traces indicate significant contact of the dummy with the instrument panel.

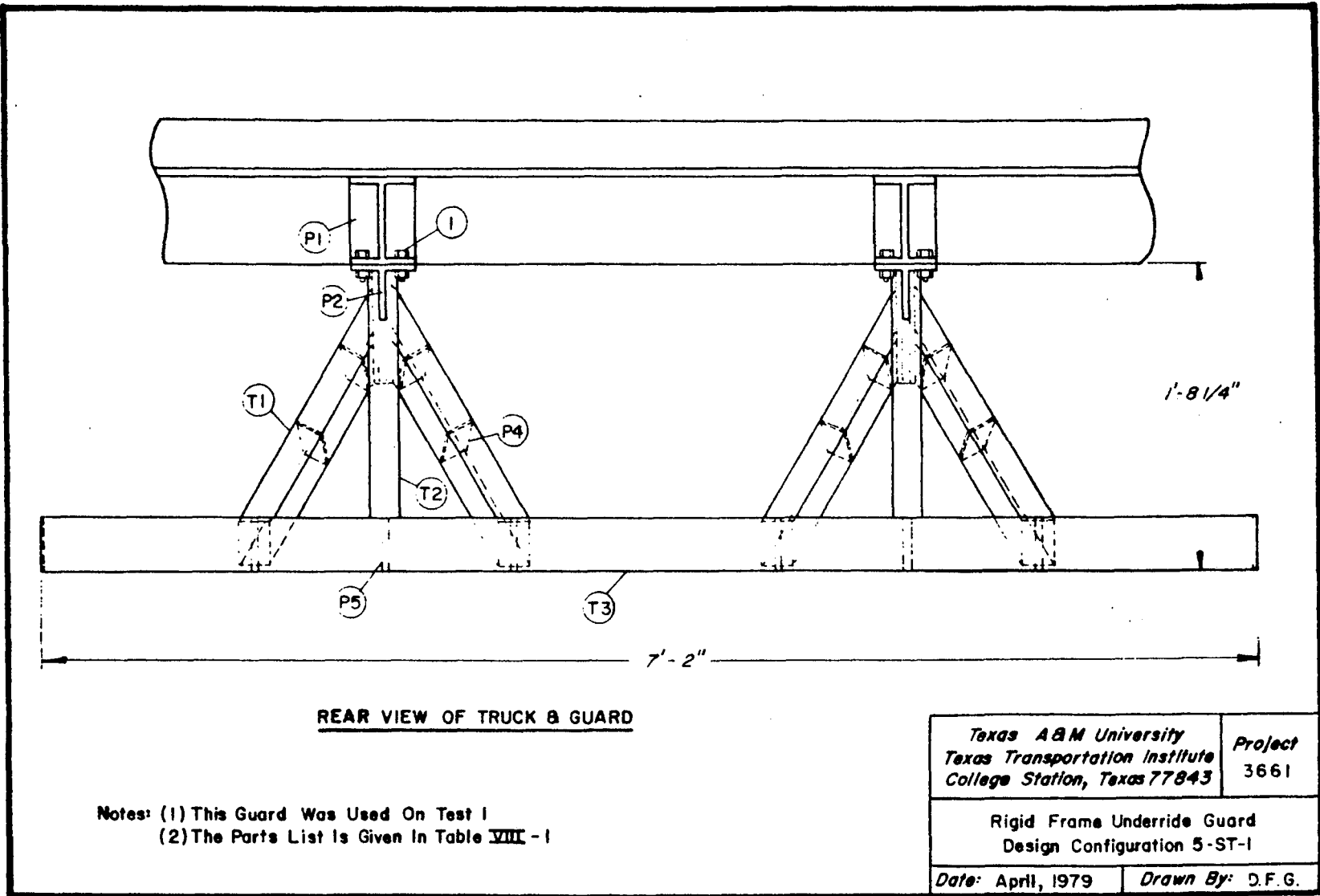
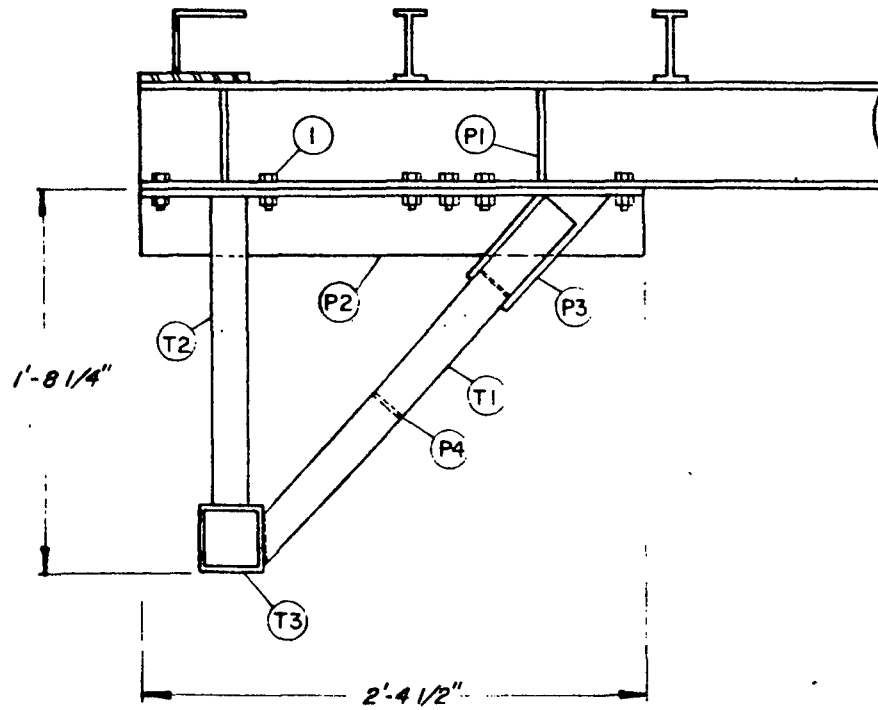


Figure F-4. Underride Guard Design 5ST-1.



RIGHT SIDE VIEW

<i>Texas A&M University Texas Transportation Institute College Station, Texas 77843</i>		Project 3661
Rigid Frame Underride Guard Design Configuration 5-ST-1		
<i>Date: April, 1979</i>		<i>Drawn By: D.F.G.</i>

Figure F-4. Underride Guard Design 5ST-1 (continued).

Table F-4. Parts List for Guard 5ST-1

DESIGNATION	DESCRIPTION	MATERIAL	NUMBER REQUIRED
T1	Fabricated Tubing, 2"x2"x3/16"	ASTM A514 100 ksi yield	4
T2	Fabricated Tubing, 2"x2"x3/16"	ASTM A514 100 ksi yield	2
T3	Fabricated Tubing, 3 1/2"x3 1/2"x3/16"	ASTM A514 100 ksi yield	1
P1	Stiffener, 2"x5 3/8"x3/8"	ASTM A514 100 ksi yield	8
P2	Fabricated Tee, 4"x4"x3/16"	ASTM A514 100 ksi yield	2
P3	Gusset, 4"x9"x3/16"	ASTM A514 100 ksi yield	12
P4	Stiffener, 1 5/8"x1 5/8"x3/16"	ASTM A514 100 ksi yield	12
P5	Stiffener, 3 1/8"x3 1/8"x3/16"	ASTM A514 100 ksi yield	8
1	Bolt, 5/8"	ASTM A325-N, 104 ksi yield	24

Table F-5. Summary of Results, Test 3661-1.

AUTOMOBILE	1977 Volkswagen Rabbit 1022 kg (2250 lb)		
FILM DATA			
Impact angle	0 deg (Centric Impact)		
Initial speed of passenger car	65.7 km/h (40.8 mph) 18.2 m/s (59.8 fps)		
Average speed of trailer after impact	2.6 km/h (1.6 mph) 0.7 m/s (2.4 fps)		
Max. penetration (stopping distance) of auto. c.g. at time after impact	0.93 m (3.04 ft) 0.087 sec		
Avg. longitudinal accel. from impact to max. penetration*	-23.3 g		
Trailer movement began at	0.028 sec		
Max. movement of trailer during contact at	0.04 m (0.14 ft) 0.087 sec		
Max. distance trailer moved	0.18 m (0.60 ft) at 0.504 sec		
Final location of trailer	0.18 m (0.58 ft) at 0.571 sec		

ELECTRONIC DATA -- Class 60 Filter

Impact speed	64.2 km/h (39.0 mph) 17.9 m/s (58.6 fps)		
	<u>Ax</u>	<u>Ay</u>	<u>Az</u>
Max. 0.050 sec acceleration over time interval	-29.2 g 0.036 sec 0.086 sec	-1.8 g 0.047 sec 0.097 sec	-6.6 g 0.022 sec 0.072 sec
Peak acceleration at time after impact	-43.5 g 0.070 sec	28.2 g 0.043 sec	36.7 g 0.074 sec

AUTOMOBILE DAMAGE

Max. dynamic crush	0.89 m (2.9 ft)	
Residual auto. deformation	0.74 m (2.42 ft)	
Damage classification	SAE -- 12FDAW8	TAD -- 12FD6.3

$$* G_{avg} = \left(\frac{2}{\pi}\right) \frac{V^2}{gd}$$

where V is impact speed in m/s (ft/sec)
g is acceleration due to gravity
in m/s² (ft/sec²)
d is stopping distance in m (ft)

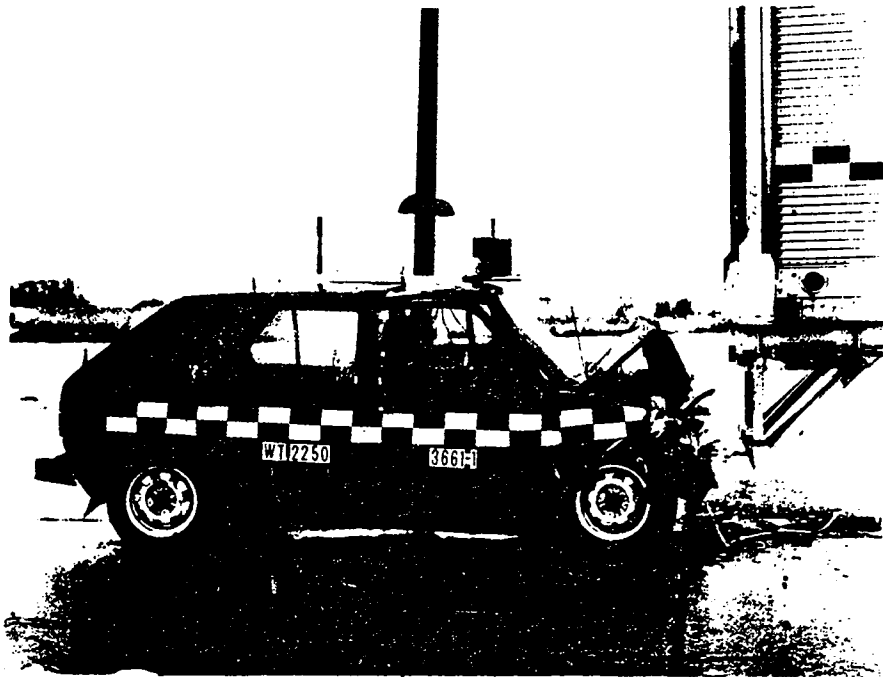
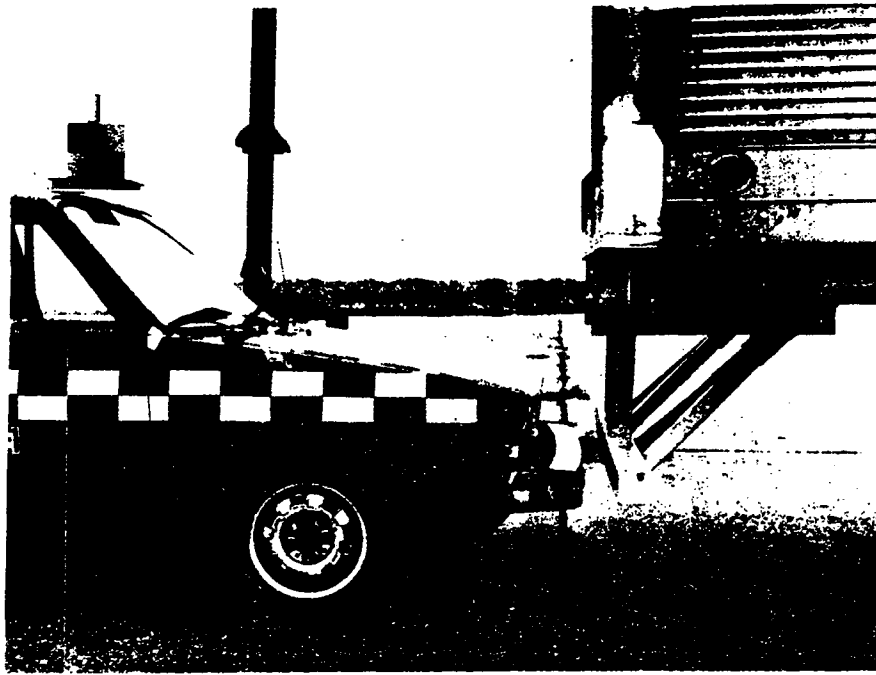


Figure F-5. Automobile and Guard Before and After Test 3661-1.

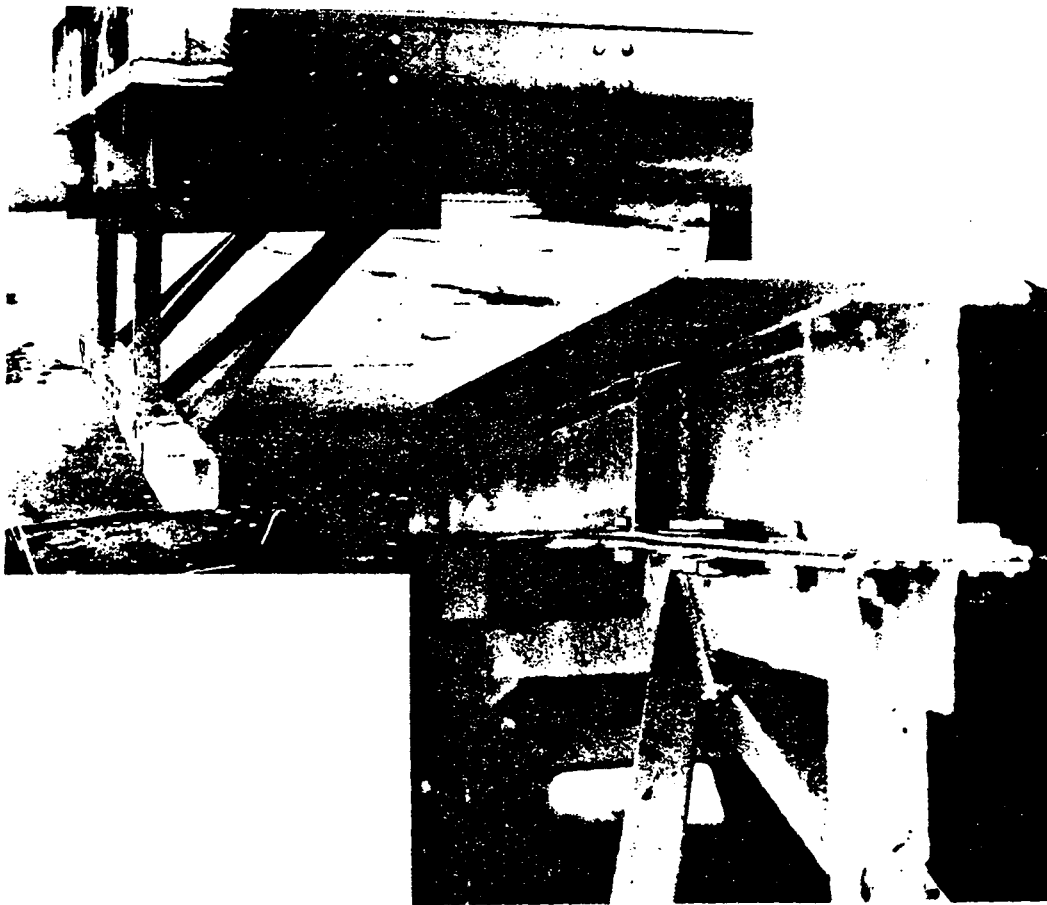
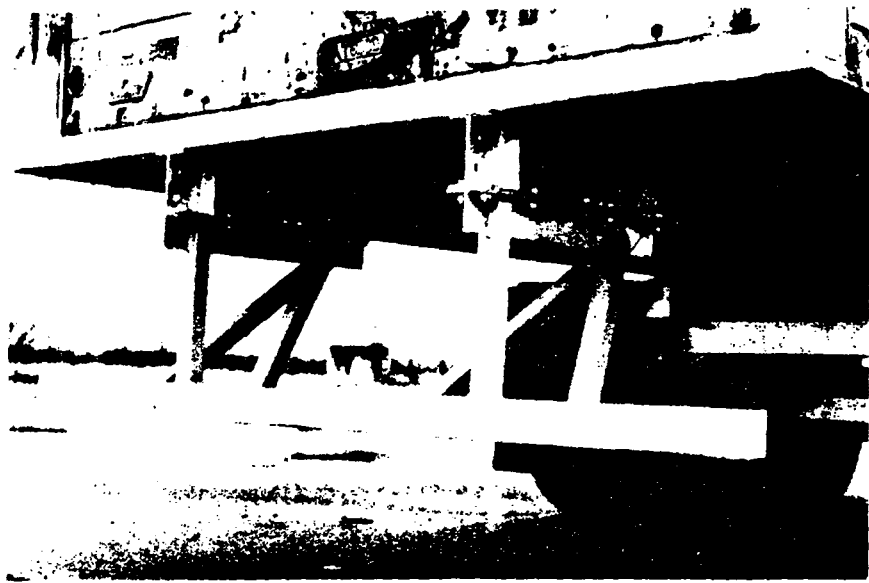


Figure F-6. Guard Before and After Test 3661-1.



Figure F-7. Automobile Before and After Test 3661-1

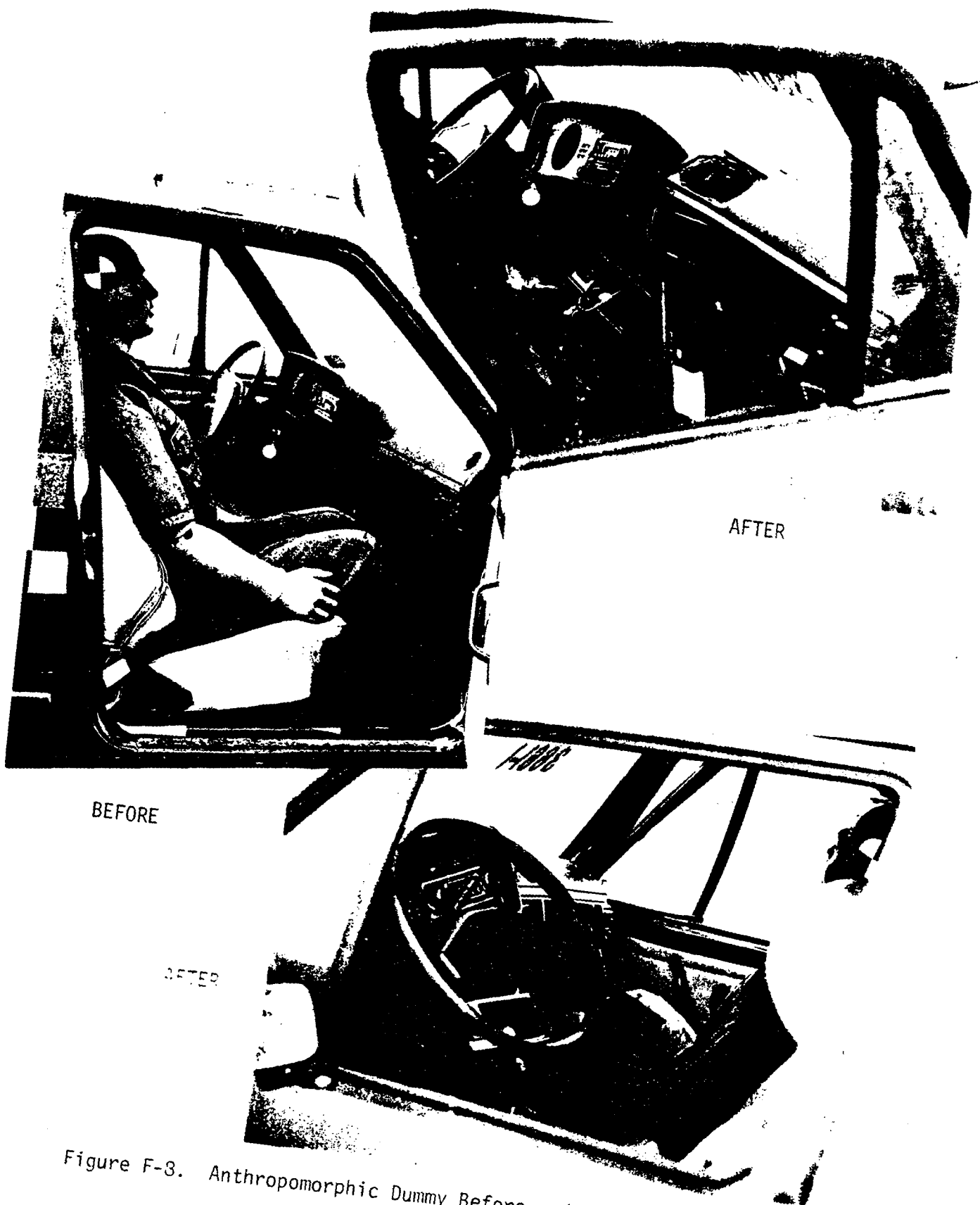


Figure F-3. Anthropomorphic Dummy Before and After Test 3661-1.

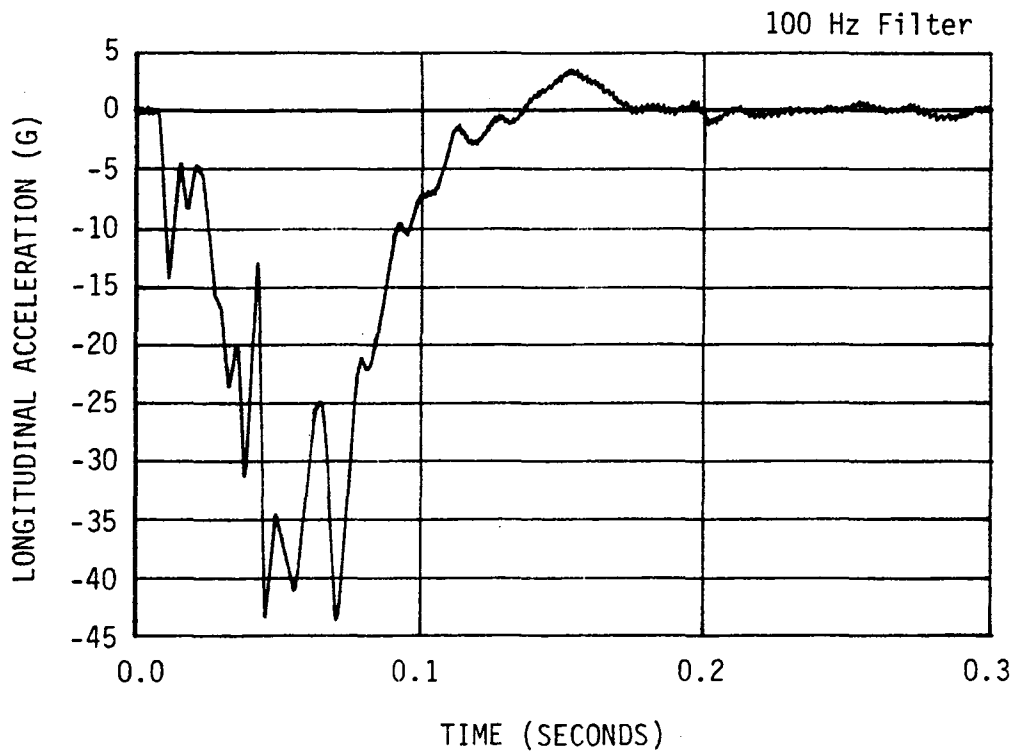


Figure F-9. Longitudinal Automobile Accelerometer Trace for Test 3661-1.

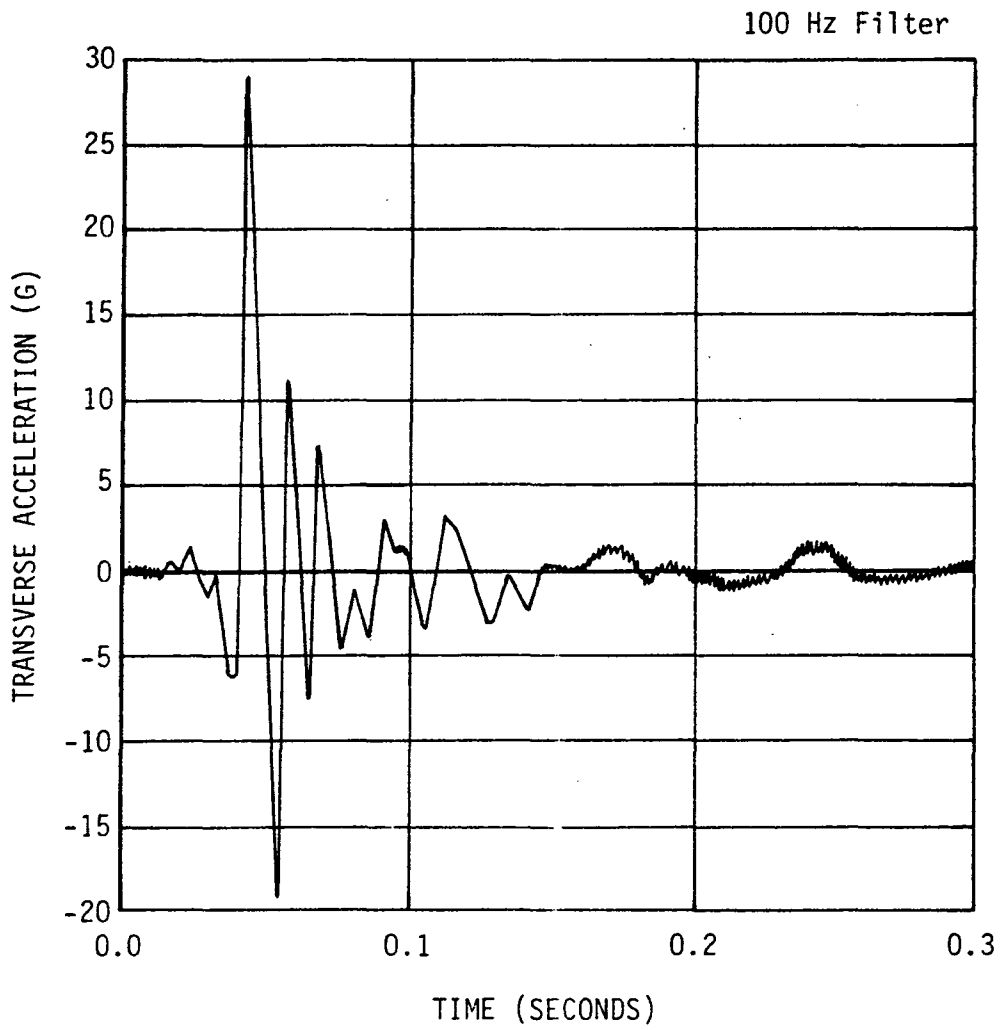


Figure F-10. Transverse Automobile Accelerometer Trace for Test 3661-1.

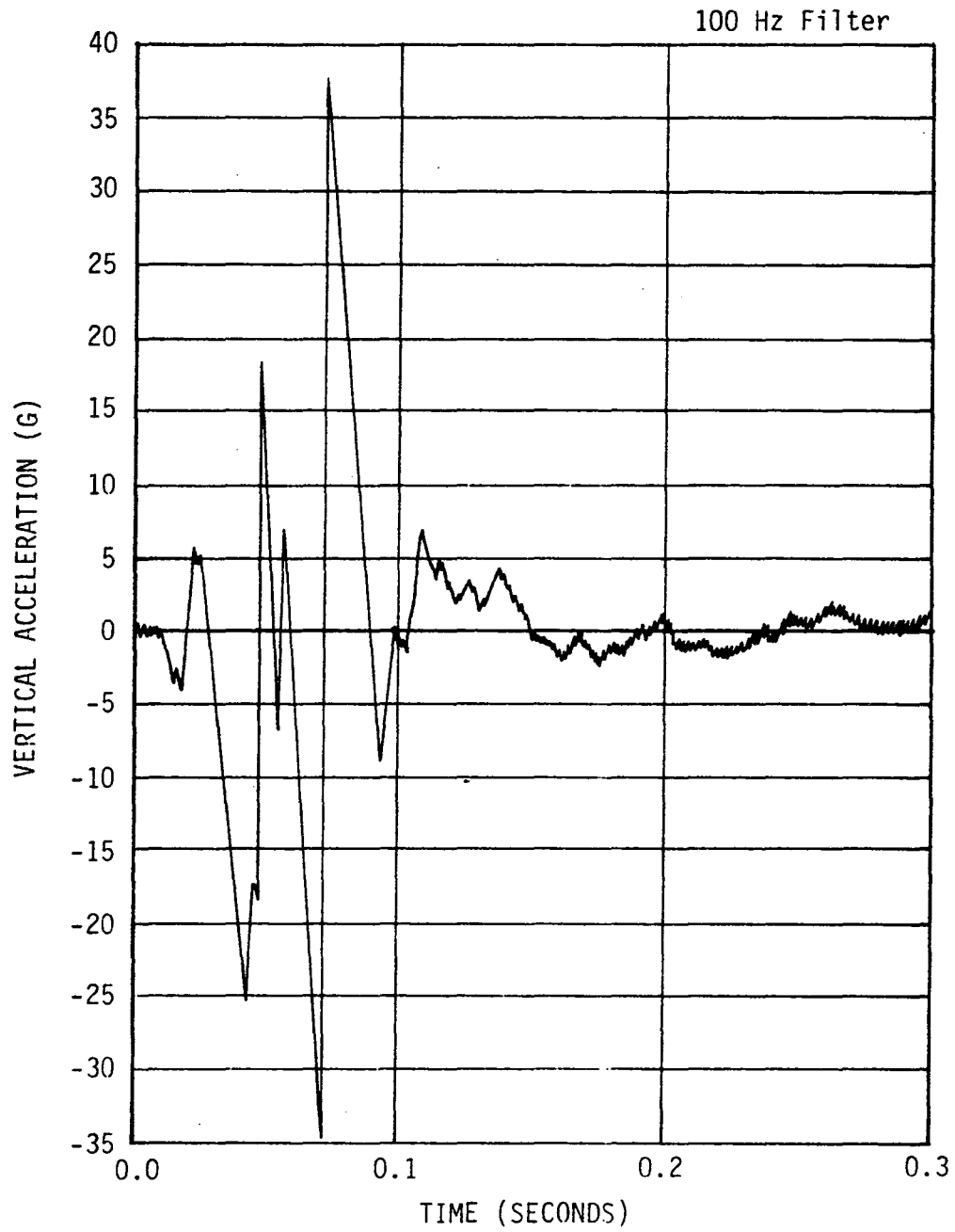


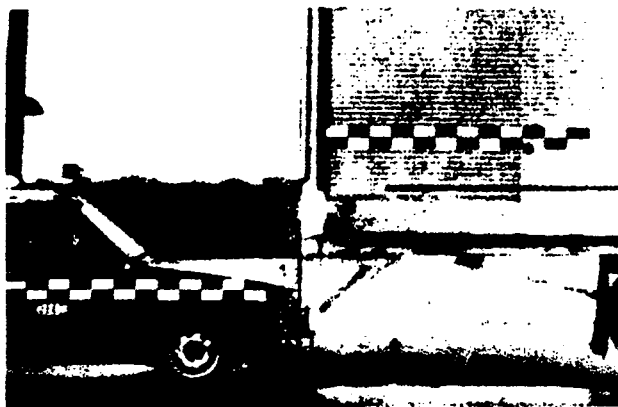
Figure F-11. Vertical Automobile Accelerometer Trace for Test 3661-1.

Table F-6. Time, Displacement, Event Summary
for Test 3661-1.

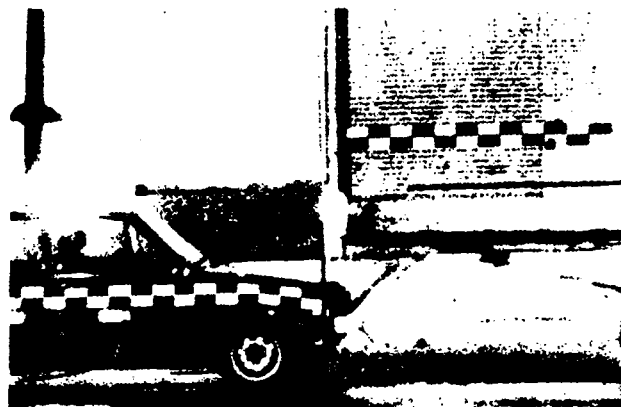
TIME (SEC)	CAR DISPLACEMENT (FT)	TRAILER DISPLACEMENT (FT)	EVENT
-0.010	-0.58	0.00	
-0.008	-0.46	0.00	
-0.006	-0.34	0.00	
-0.004	-0.23	0.00	
-0.002	-0.09	0.00	
0.000	0.00	0.00	Impact
0.006	0.37	0.00	
0.014	0.81	0.01	Hood buckles
0.022	1.25	0.01	
0.028	1.54	0.03	Trailer movement
0.034	1.82	0.02	Car begins to pitch
0.040	2.08	0.04	Dummy and seat pitch
0.047	2.38	0.06	
0.055	2.64	0.08	Dummy no longer resting on seat
0.061	2.77	0.09	
0.069	2.91	0.10	
0.079	3.02	0.13	
0.087	3.04	0.14	Stopping distance for car
0.099	3.02	0.17	Car rebounds & dummy contacts dash
0.128	2.86	0.24	
0.168	2.73	0.30	
0.208	2.66	0.37	
0.257	2.55	0.44	
0.306	2.39	0.49	
0.356	2.29	0.54	
0.405	2.20	0.57	
0.455	2.11	0.59	
0.504	2.02	0.60	Max. forward motion of trailer
0.571	2.15	0.58	Stopping distance for trailer

Metric Conversion:

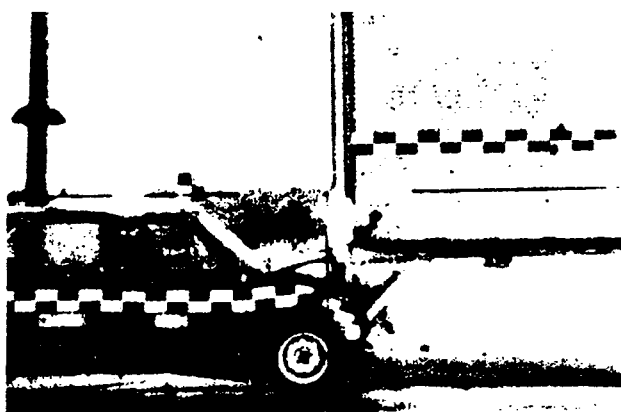
1 ft = 0.305 m



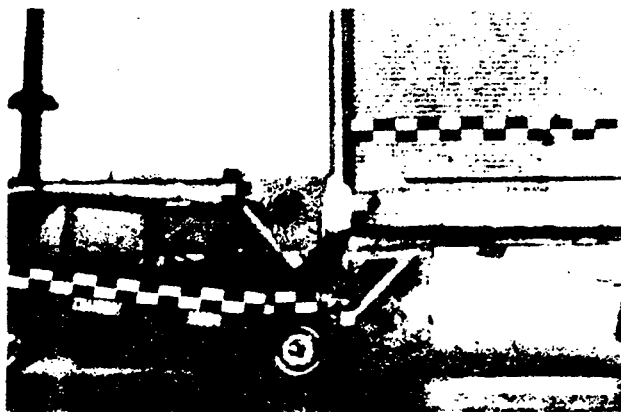
0.000 sec



0.013 sec



0.039 sec



0.087 sec

Figure F-12. Sequential Photographs for Test 3661-1.

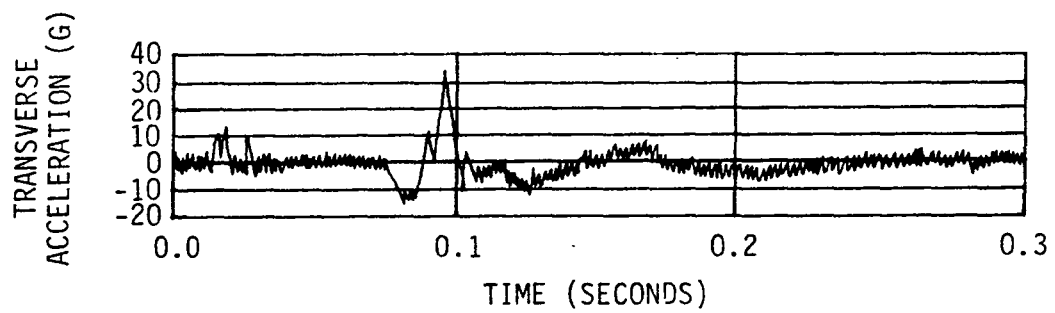
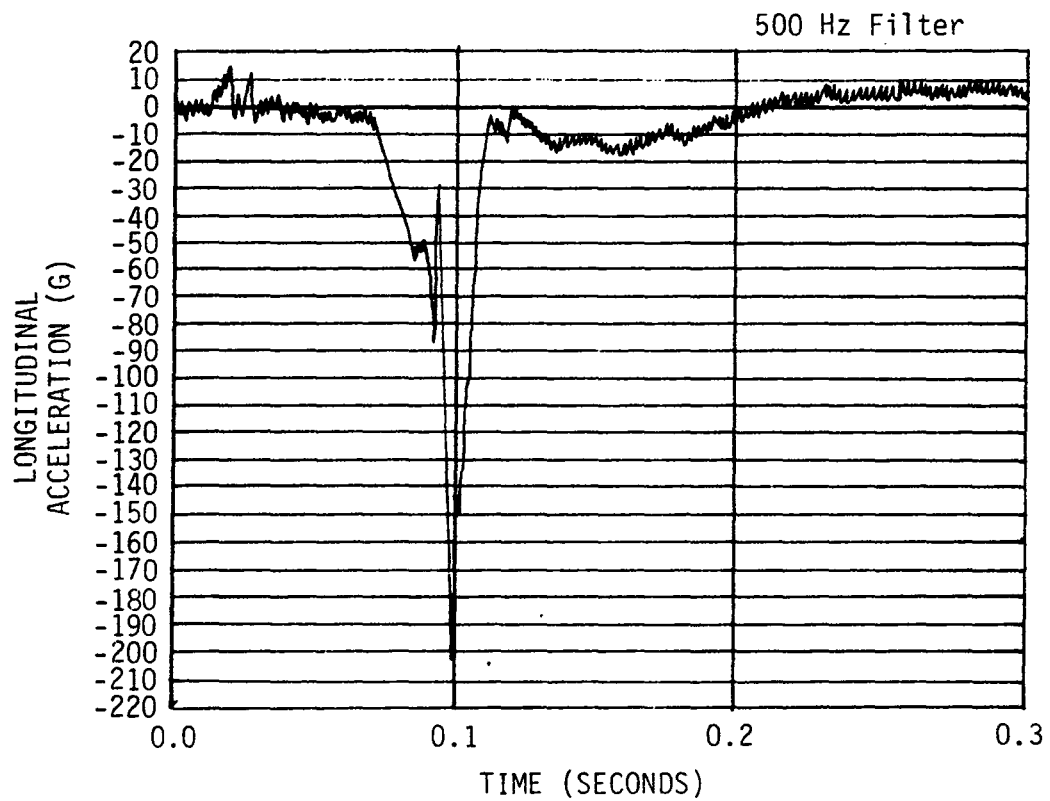


Figure F-13. Beta Head Longitudinal and Transverse Accelerometer Trace for Test 3661-1.

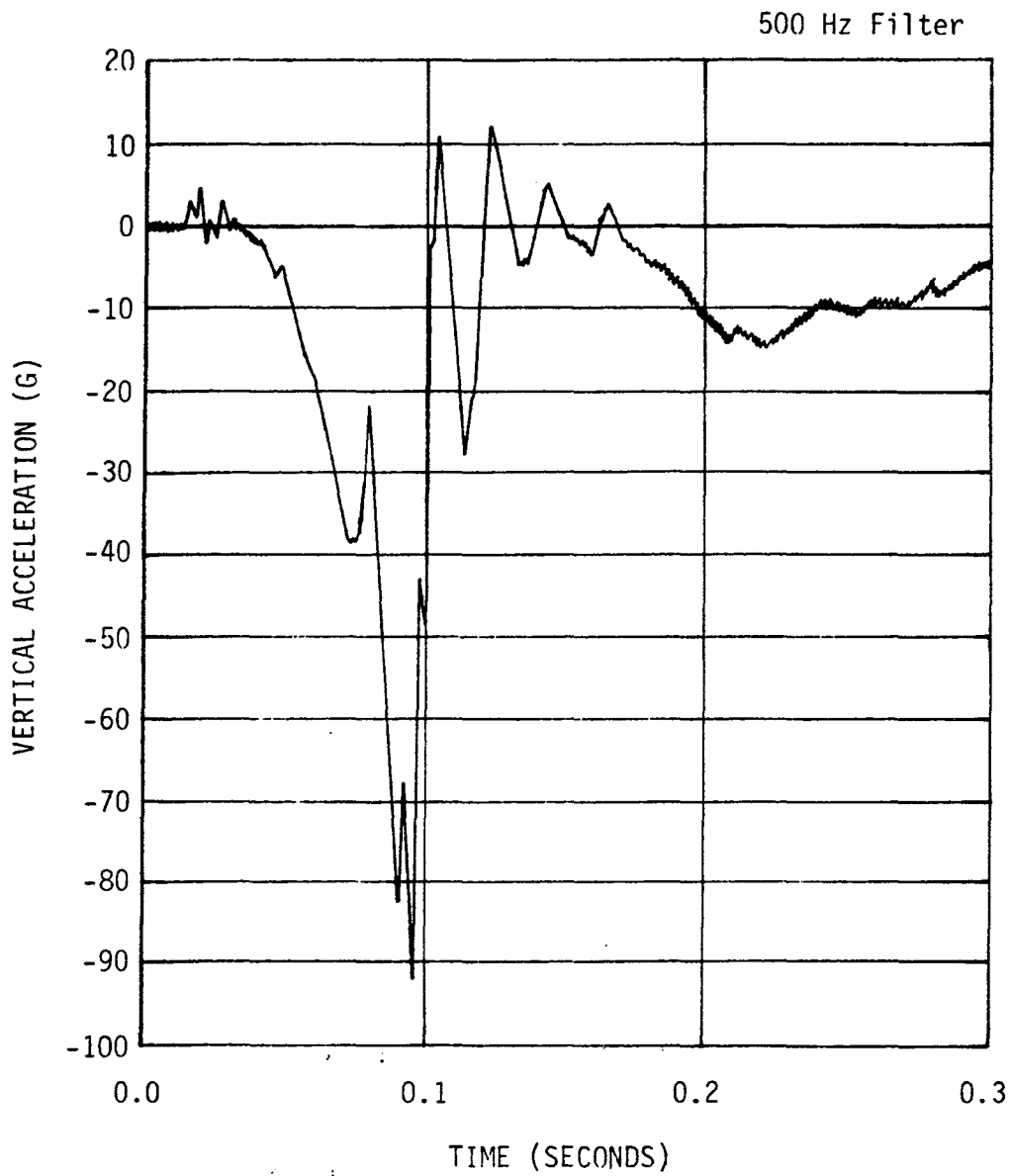


Figure F-14. Beta Head Vertical Accelerometer Trace for Test 3661-1.

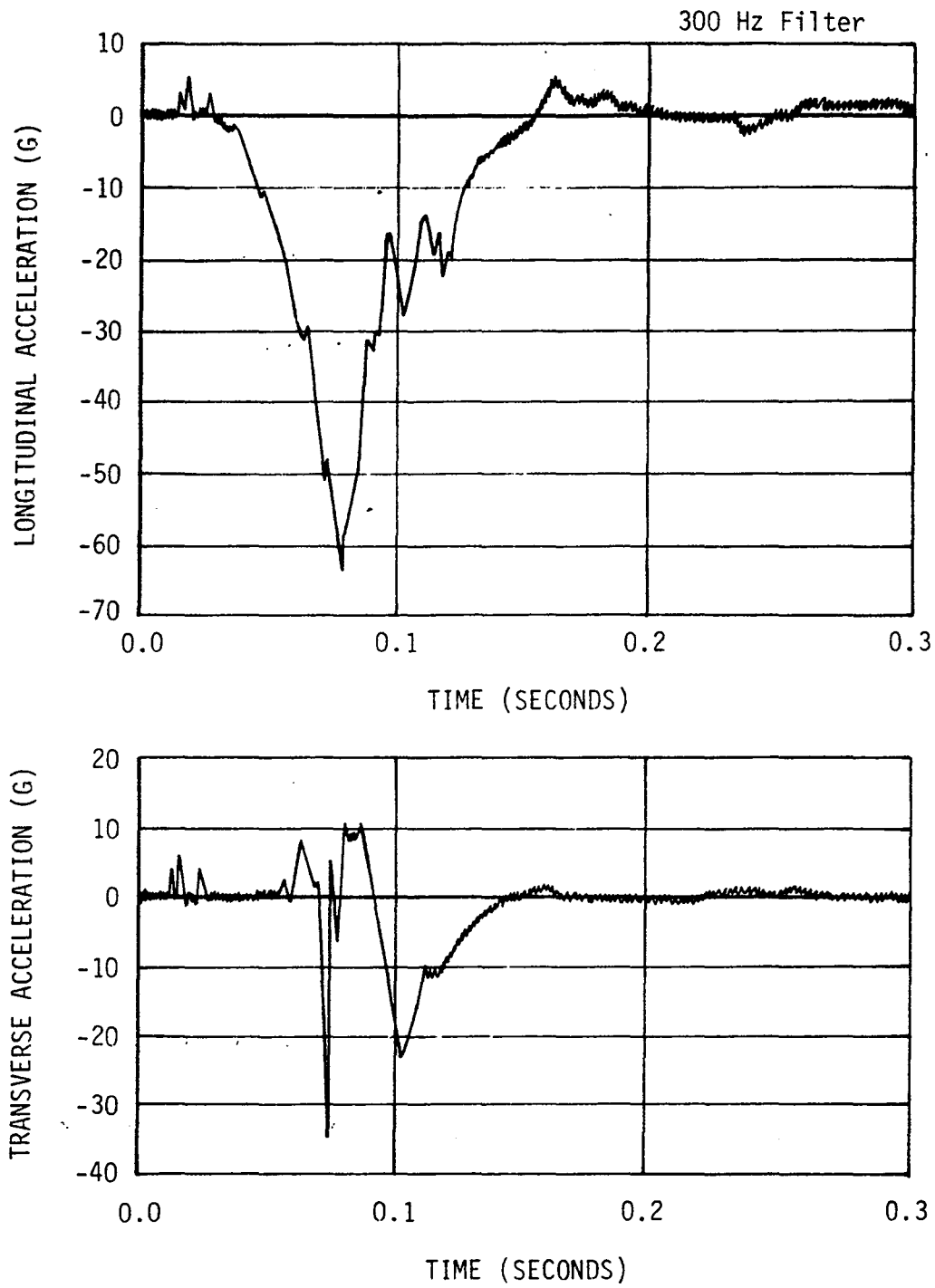


Figure F-15. Beta Chest Longitudinal and Transverse Accelerometer Traces for Test 3661-1.

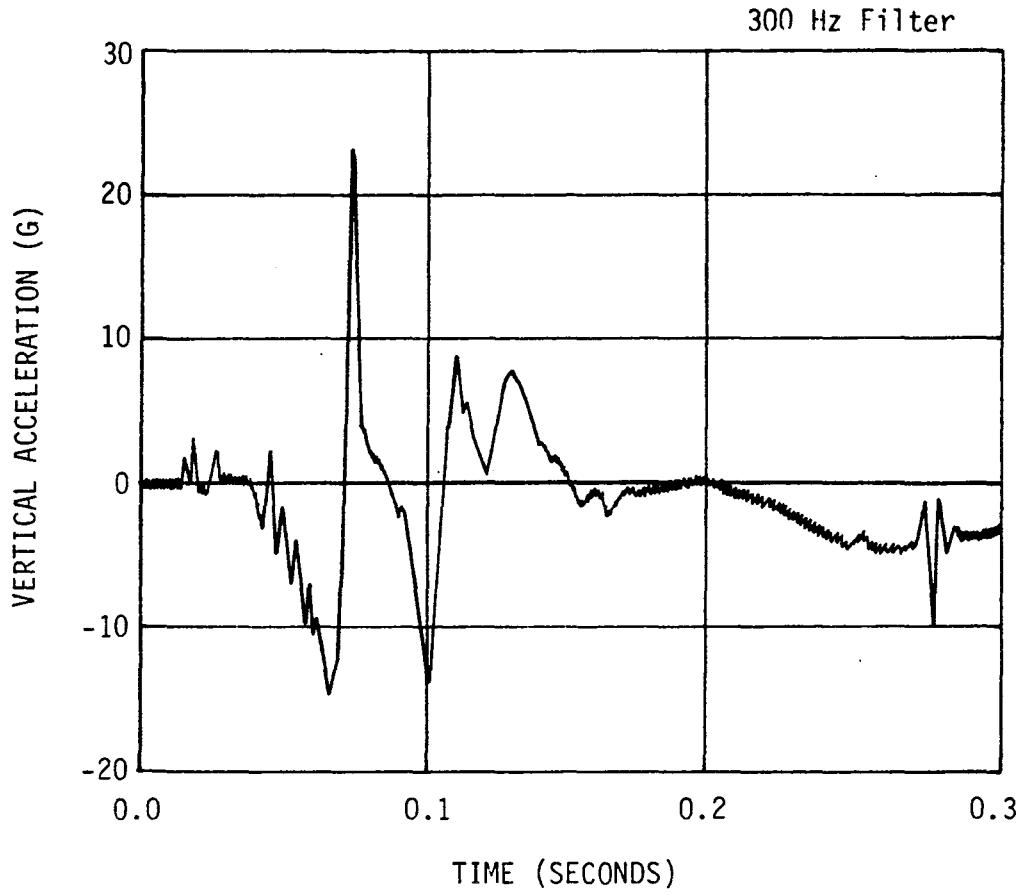


Figure F-16. Beta Chest Vertical Accelerometer Trace for Test 3661-1.

Table F-7. Dummy Time-Event Summary
For Test 3661-1.

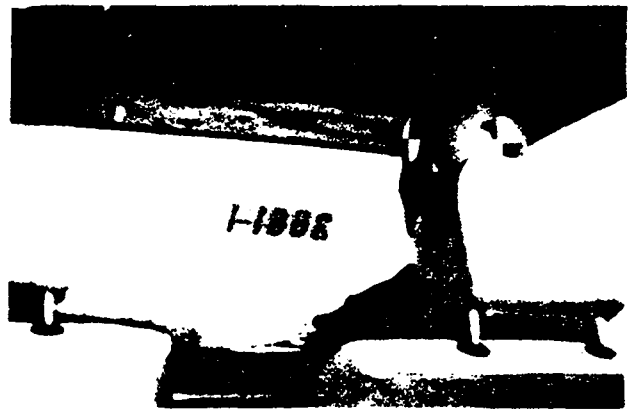
TIME (SEC)	EVENT
	<u>Beta</u>
0.030	Initial movement
0.065	Shoulder harness tightens on chest
0.071	Upper body is turned to right because of shoulder harness pulling on right shoulder
0.100	Left shoulder and left side of head impact dash

Table F-8. Dummy Injury Indices

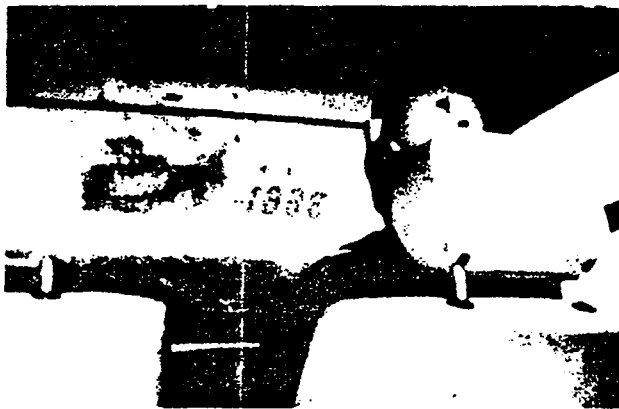
	HIC	GADD	0.003 sec G
Beta Head	2901 from 0.086 sec to 0.104 sec	3819 from 0.000 sec to 0.282 sec	149 from 0.098 sec to 0.101 sec
Beta Chest	495 from 0.056 sec to 0.110 sec	636 from 0.000 sec to 0.200 sec	60 from 0.076 sec to 0.079 sec



0.000 sec



0.013 sec



0.039 sec



0.087 sec

Figure F-17. Interior Sequential Photographs for Test 3661-1.

Test 3661-2

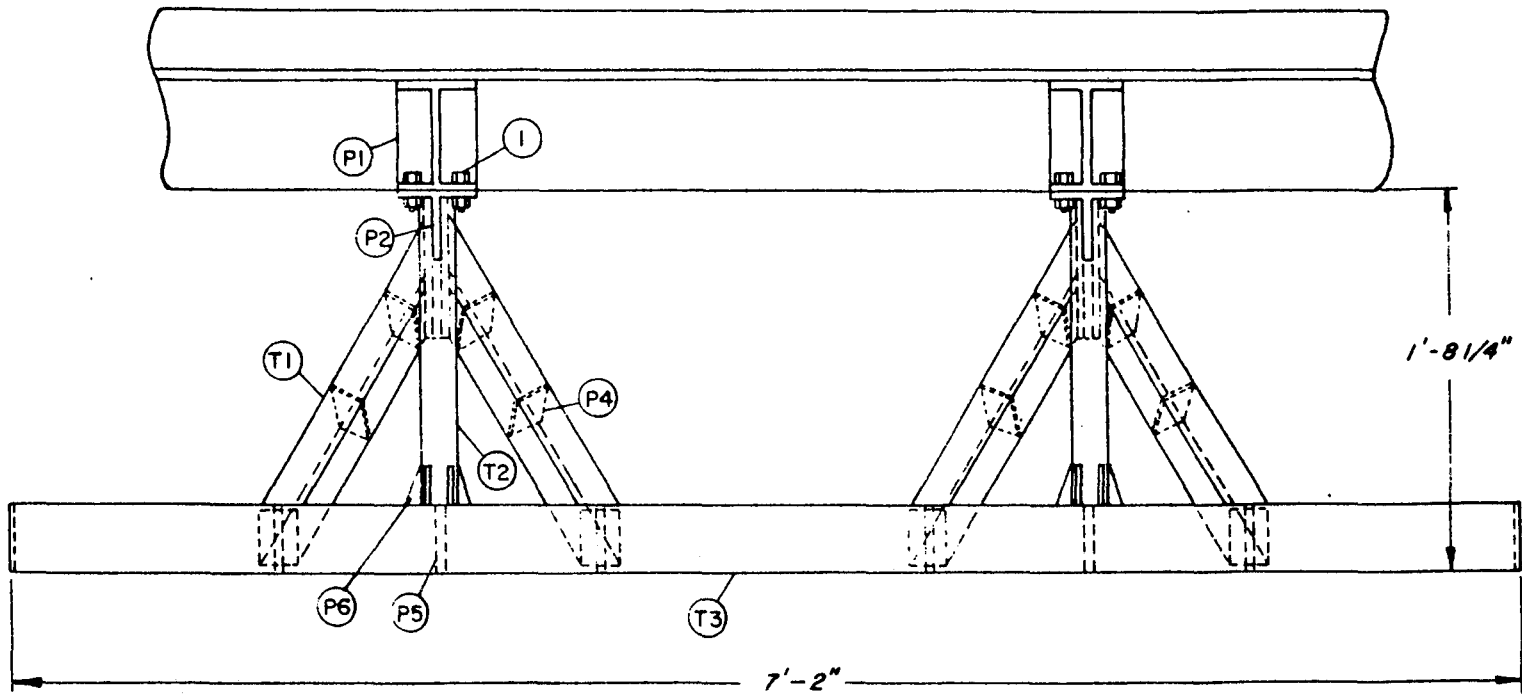
Fruehauf Trailer - 24, 890 kg (54,830 lb)
Rigid Guard Design 5ST-2 - 74 kg (163 lb)
Ground Clearance - 0.45 m (17.6 in)
1977 Ford LTD - 2043 kg (4500 lb)
65.1 km/h (40.4 mph) closing speed
Alignment - 1.58 m (62 in) offset to left
Tested January 25, 1979

Results of the test are summarized in Table F-10 and sequential photographs of the collision are shown in Figure F-26. From impact until 0.091 sec after impact, the automobile traveled forward with little yaw displacement. During this time interval, the automobile, the truck frame and the guard were deformed. At about 0.091 sec, the vertical strut was separated from the lateral member in the guard. At this time, the automobile had decelerated to 42.6 km/h (26.4 mph) and the amount of under-ride was approximately 1.4 m (4.6 ft). If one uses these data in the equation $G_{\max} = (V_2^2 - V_1^2)/gd$, the resulting maximum acceleration is -13.7 g's, which would indicate a maximum force of 273,997 N (61,600 lbs). After this the automobile continued to underride and yaw.

At about 0.148 sec, the windshield contacted the trailer. As the automobile continued forward, the corner of the trailer penetrated the occupant compartment and contacted the passenger dummy's head, pushing the dummy back into the seat. The automobile finally contacted the left rear wheels of the trailer, displacing the undercarriage and causing some distress in its attachment to the left rail.

The automobile longitudinal acceleration trace in Figure F-23 shows a -20 g peak at about 0.08 sec and similar peaks between 0.25 and 0.30 sec. The first peak occurred slightly before structural integrity of the guard was lost. The -20 g's would indicate that the peak force applied to the guard was about 400,320 N (90,000 lbs).

Dummy injury indices given in Table F-13 are within acceptable limits because of the relatively long stopping distance that resulted from structural failure of the guard. The high peaks in the dummy acceleration traces at slightly less than 0.200 sec (Figures F-28 through F-30) are evidently a result of penetration of the occupant compartment by the corner of the trailer.

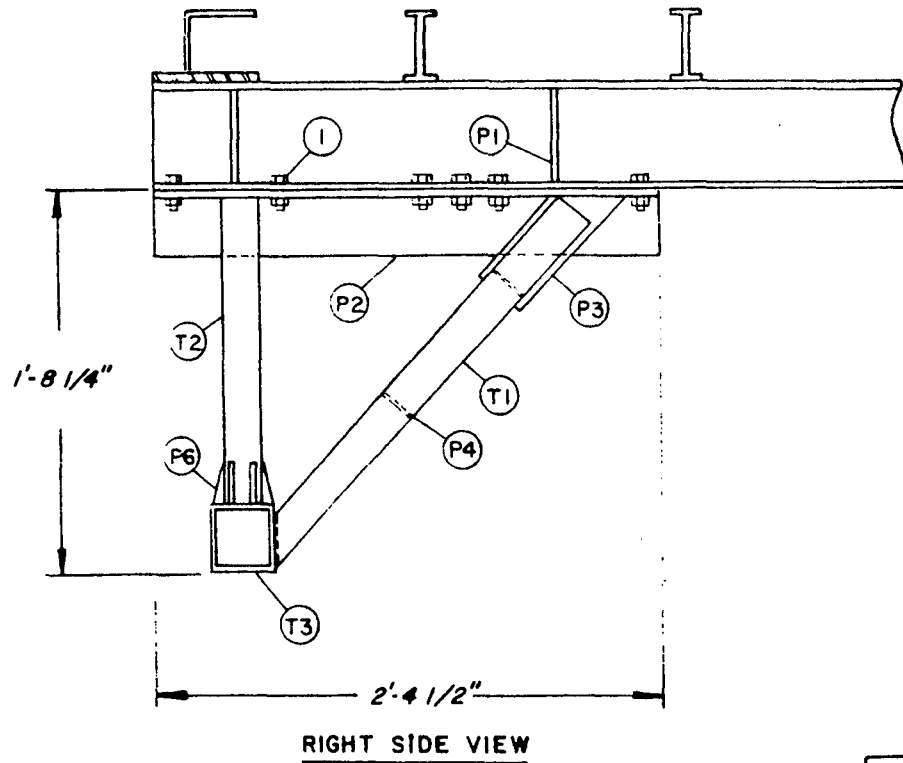


REAR VIEW OF TRUCK & GUARD

Notes: (1) This Guard Was Used On Test 2
 (2) The Parts List Is Given In Table F-9

Texas A&M University Texas Transportation Institute College Station, Texas 77843		Project 3661
Rigid Frame Underride Guard Design Configuration 5-ST-2		
Date: April, 1979	Drawn By: D.F.G.	

Figure F-18. Underride Guard Design 5ST-2.



Texas A&M University Texas Transportation Institute College Station, Texas 77843	Project 3661
Rigid Frame Underride Guard Design Configuration 5-ST-2	
Date: April, 1979	Drawn By: D.F.G.

Figure F-18. Underride Guard Design 5ST-2 (continued).

Table F-9 . Parts List for Guard 5ST-2.

DESIGNATION	DESCRIPTION	MATERIAL	NUMBER REQUIRED
T1	Fabricated Tubing, 2"x2"x3/16"	ASTM A514 100 ksi yield	4
T2	Fabricated Tubing, 2"x2"x3/16"	ASTM A514 100 ksi yield	2
T3	Fabricated Tubing, 3 1/2"x3 1/2"x3/16"	ASTM A514 100 ksi yield	1
P1	Stiffener, 2"x5 3/8"x3/8"	ASTM A514, 100 ksi yield	8
P2	Fabricated Tee, 4"x4"x3/16"	ASTM A514 100 ksi yield	2
P3	Gusset, 4"x9"x3/16"	ASTM A514 100 ksi yield	12
P4	Stiffener, 1 5/8"x1 5/8"x3/16"	ASTM A514 100 ksi yield	12
P5	Stiffener, 3 1/8"x3 1/8"x3/16"	ASTM A514 100 ksi yield	8
P6	Gusset, 1"x2"x3/16"	ASTM A514 100 ksi yield	16
1	Bolt, 5/8"	ASTM A325-N, 104 ksi yield	24

Table F-10. Summary of Results, Test 3661-2.

AUTOMOBILE	1977 Ford LTD 3043 kg (4500 lb)
FILM DATA	
Impact angle	0 deg (1.58 m (62 in) offset to left)
Initial speed of passenger car	65.1 km/h (40.4 mph) 18.1 m/s (59.3 fps)
Average speed of trailer after impact	1.4 km/h (0.8 mph) 0.4 m/s (1.2 fps)
Max. penetration (stopping distance) of auto. c.g. at time after impact	3.05 m (9.99 ft) 0.367 sec
Avg. longitudinal accel. from impact to max. penetration*	-6.96 g
Trailer movement began at	0.017 sec
Max. movement of trailer during contact at time	0.21 m (0.69 ft) 0.567 sec
Max. deflection of guard	0.30 m (0.99 ft) down 0.63 m (2.06 ft) back
Max. distance trailer moved	0.21 m (0.69 ft)
Final location of trailer	0.16 m (0.52 ft)
Amount of underride when strut broke at time	1.39 m (4.56 ft) 0.091 sec
Speed of car at 0.091 sec	42.6 km/h (26.4 mph) 11.8 m/s (38.8 fps)

ELECTRONIC DATA -- Class 60 Filter

Impact speed	65.2 km/h (40.5 mph) 18.1 m/s (59.4 fps)		
	<u>Ax</u>	<u>Ay</u>	<u>Az</u>
Max. 0.050 sec acceleration over time interval	-11.1 g 0.025 sec 0.301 sec	3.0 g 0.255 sec 0.305 sec	-4.9 g 0.288 sec 0.338 sec
Peak acceleration at time after impact	-20.2 g 0.077 sec	13.7 g 0.275 sec	16.5 g 0.278 sec

AUTOMOBILE DAMAGE

Residual auto. deformation	0.23 m (0.75 ft)
Damage classification	SAE -- 00TYHA9 TAD -- 12FR5/12RT7

$$* G_{avg} = \left(\frac{2}{\pi}\right) \frac{V^2}{gd}$$

where V is impact speed in m/s (ft/sec)
g is acceleration due to gravity
in m/s² (ft/sec²)
d is stopping distance in m (ft)

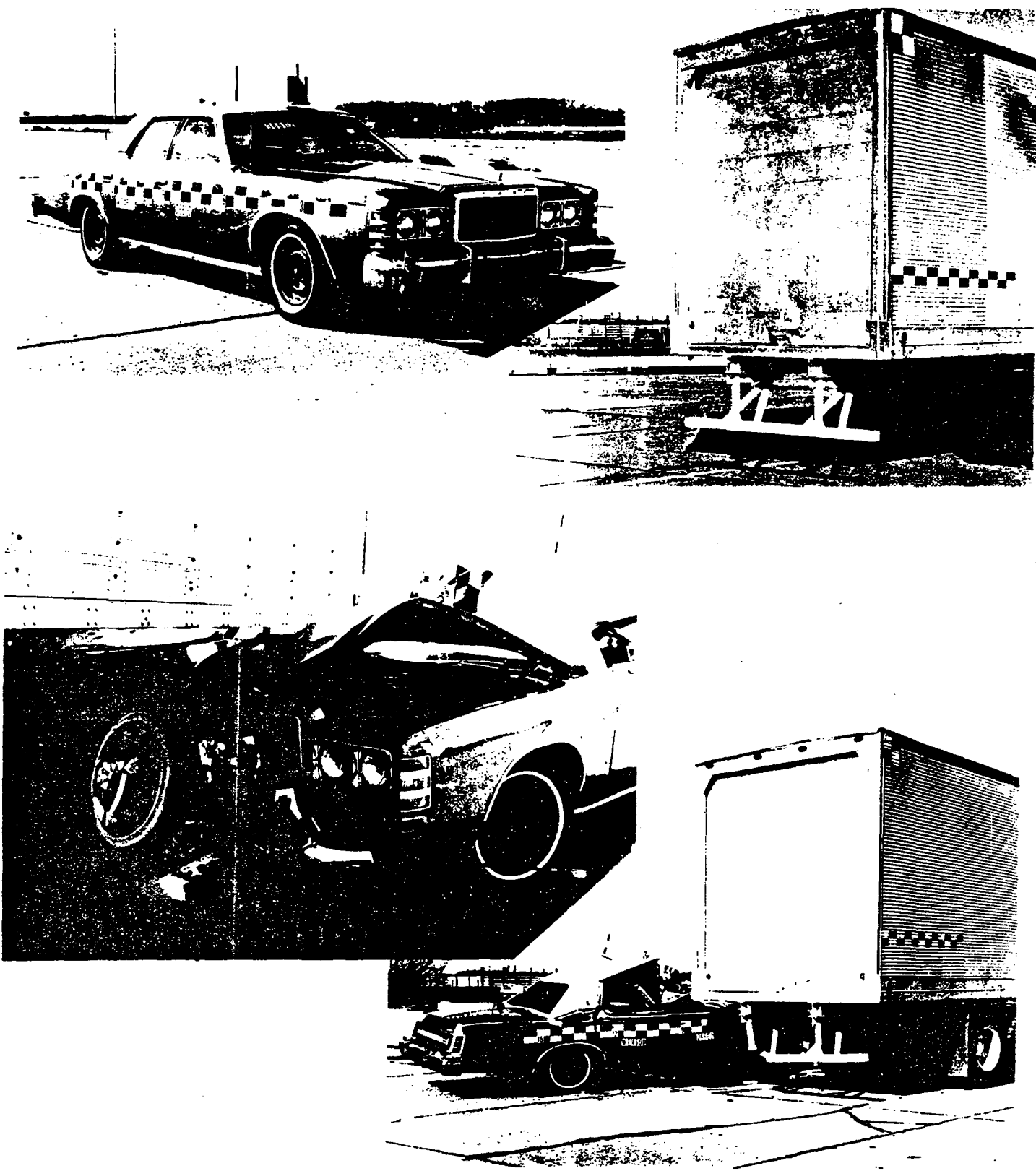


Figure F-19. Automobile and Guard Before and After Test 3661-2.

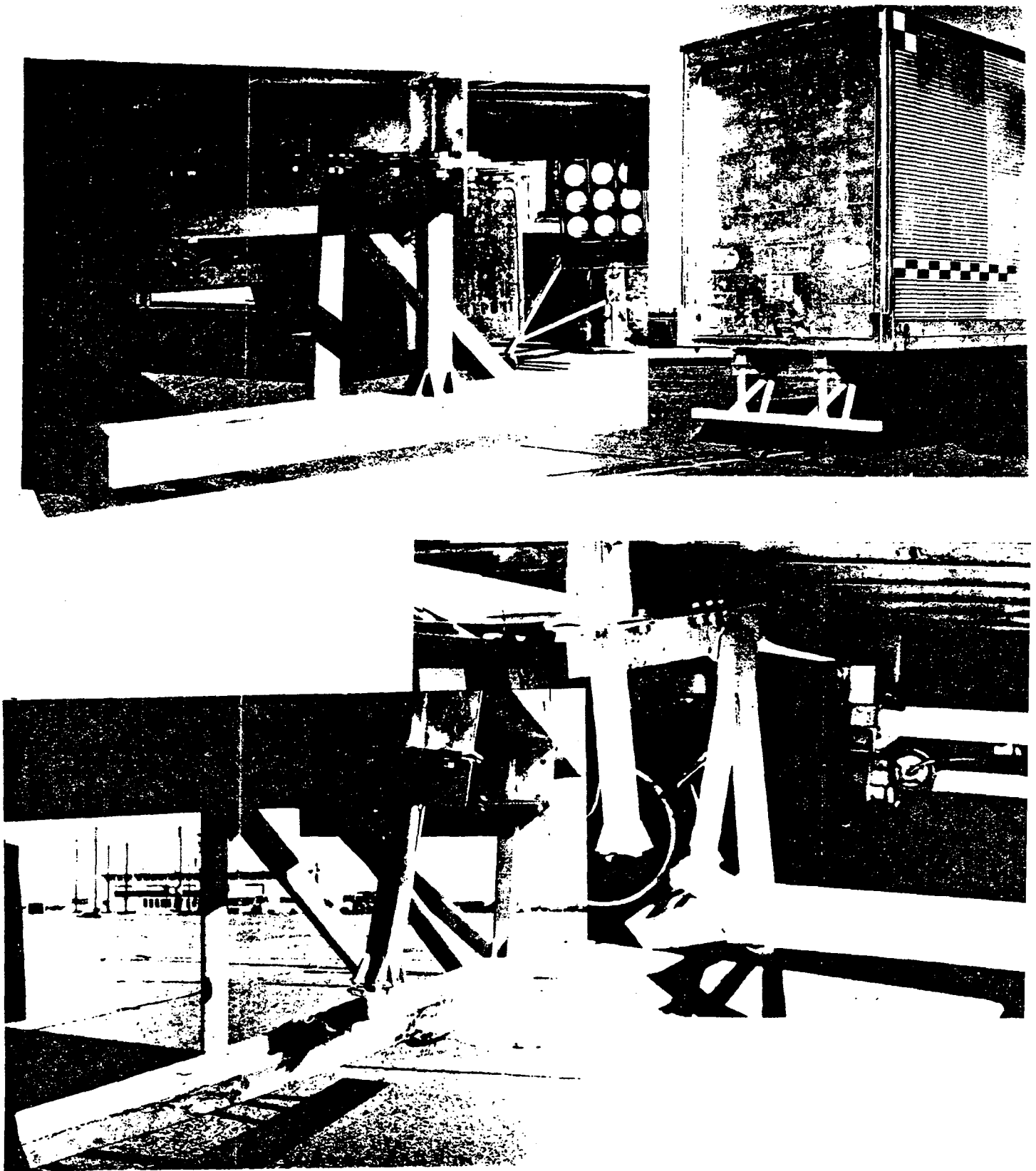


Figure F-20. Guard Before and After Test 3661-2.

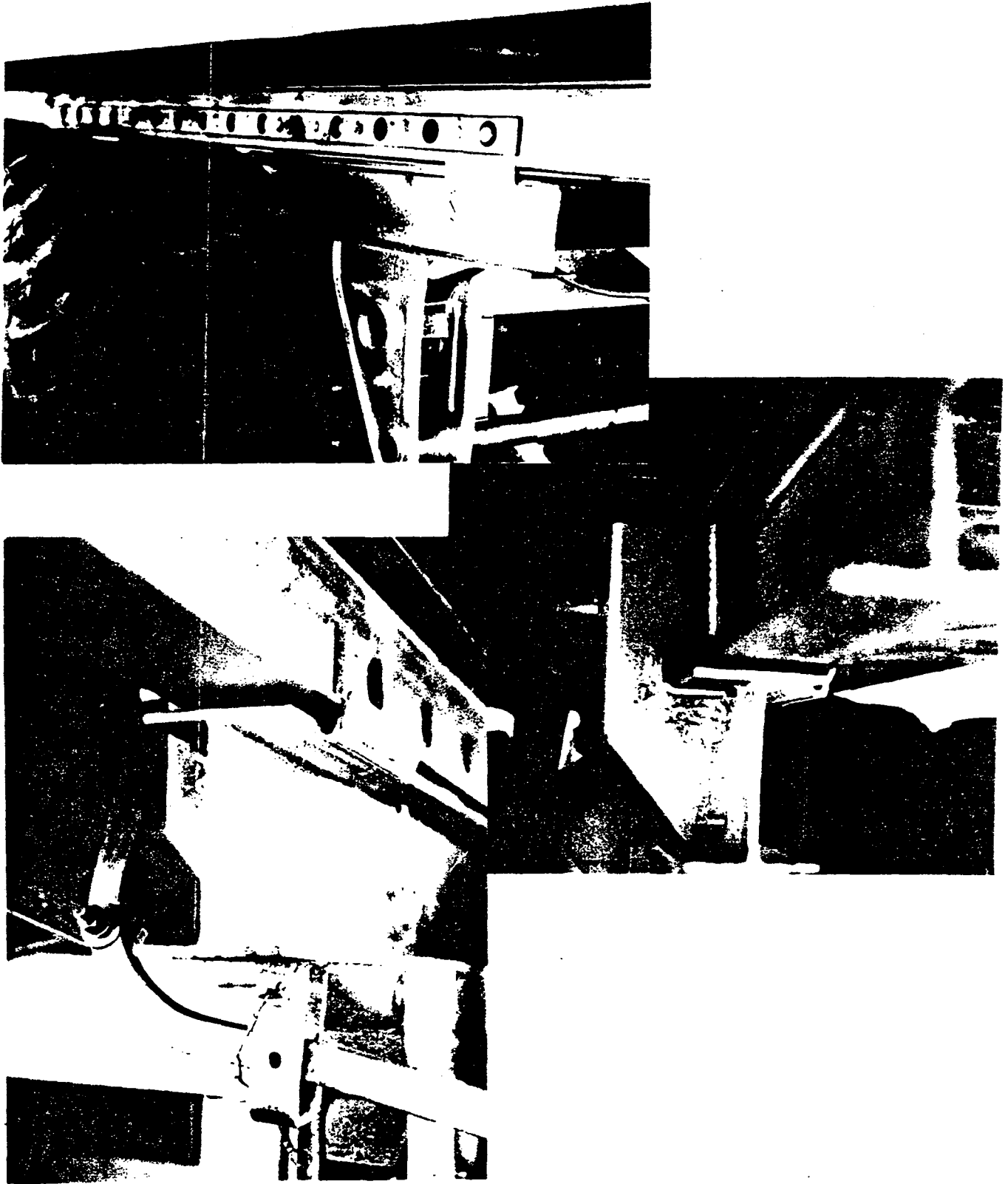


Figure F-21. Details of Damage to Trailer Undercarriage, Test 3661-2.



Figure F-22. Anthropomorphic Dummy Before and After Test 3661-2.

F-42

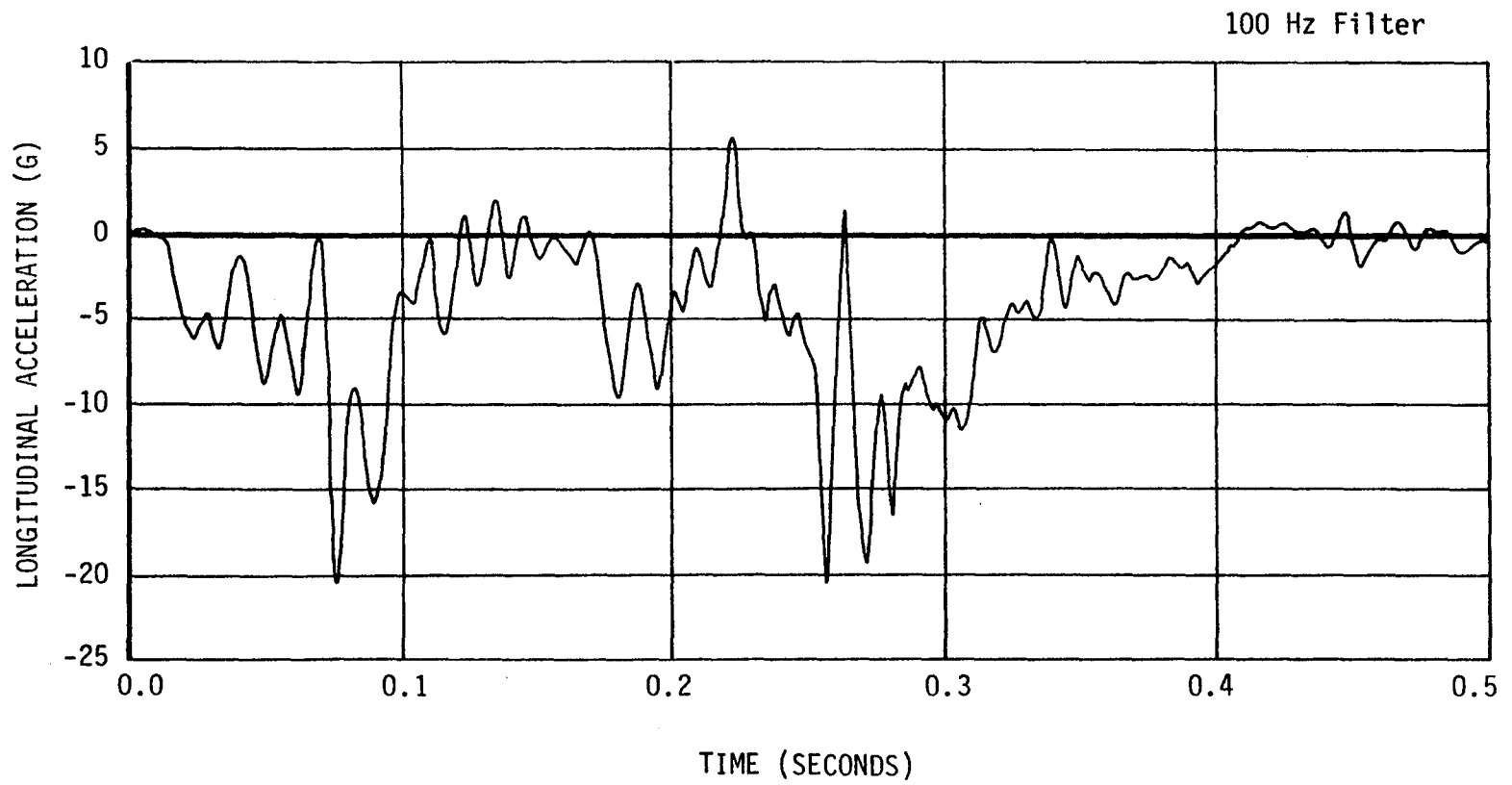


Figure F-23. Longitudinal Automobile Accelerometer Trace for Test 3661-2.

F-43

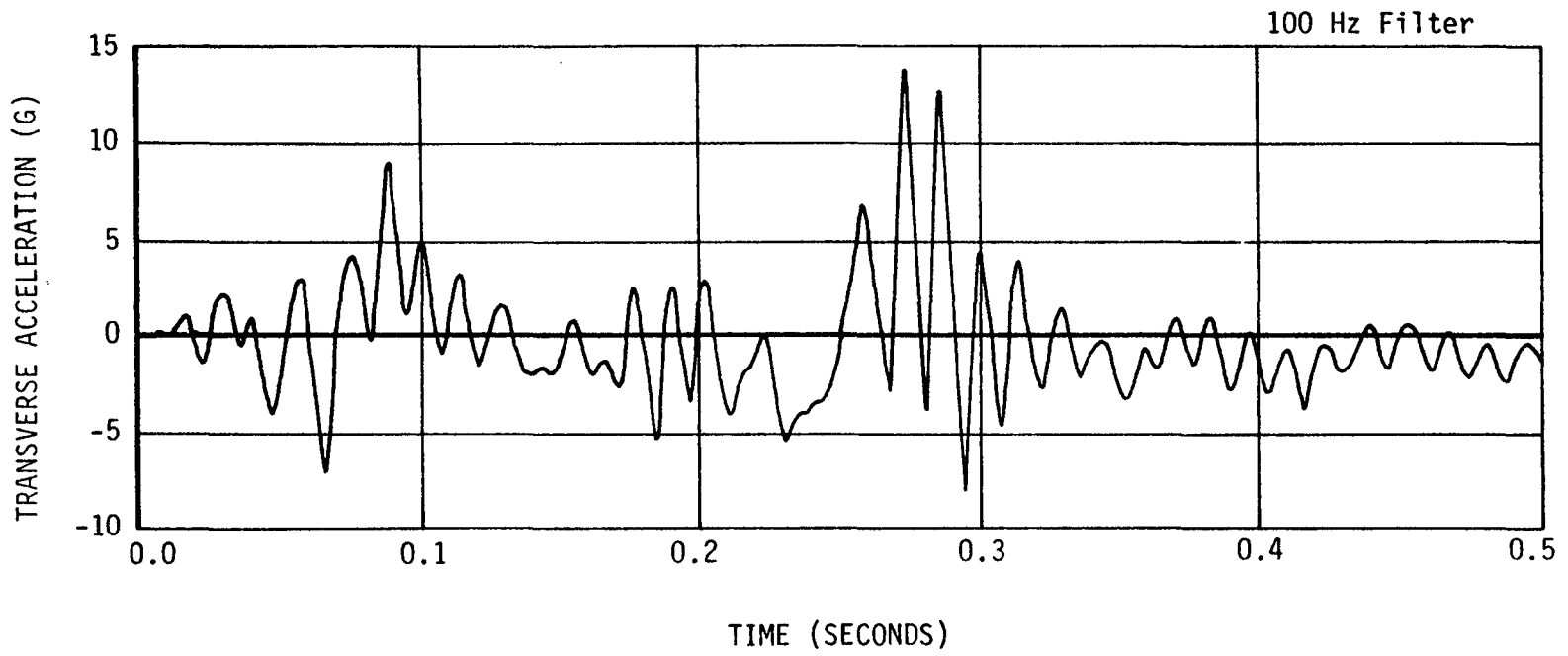


Figure F-24. Transverse Automobile Accelerometer Trace for Test 3661-2.

F-44

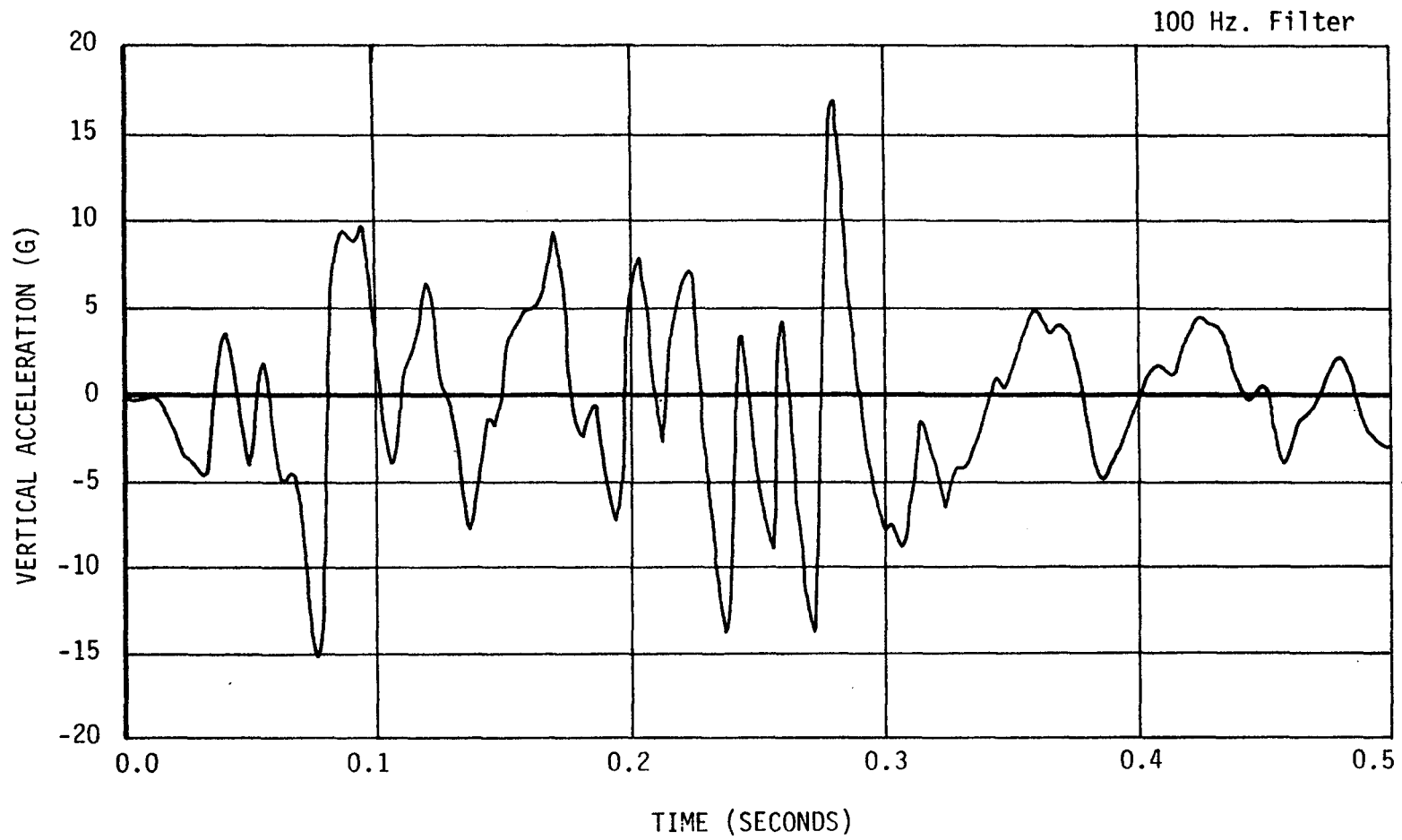


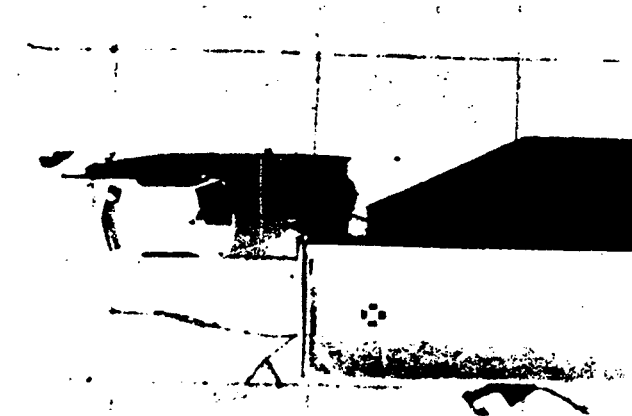
Figure F-25. Vertical Automobile Accelerometer Trace for Test 3661-2.

Table F-11. Time, Displacement, Event Summary
for Test 3661-2.

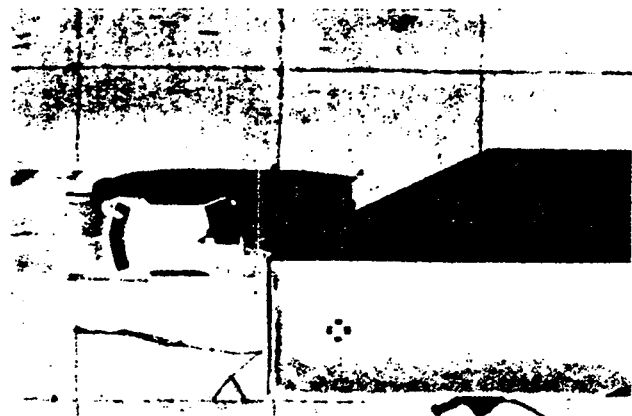
TIME (SEC)	X-DISPLACEMENT (FT)	Y-DISPLACEMENT (FT)	YAW ANGLE (DEG)	EVENT
-0.103	-5.78	0.00	0	
-0.082	-4.58	0.00	0	
-0.062	-3.45	0.00	0	
-0.041	-2.31	0.00	0	
-0.021	-1.15	0.00	0	
0.000	0.00	0.00	0	Impact
0.029	1.54	0.00	0	
0.058	3.03	0.00	0	Trailer frame buckles
0.091	4.49	0.12	-2	Vert. support tube pulls out
0.107	5.14	0.27	-3	Upper plate broken
0.128	5.96	0.44	-4	Lower tube buckling
0.148	6.78	0.66	-5	Windshield hits trailer
0.173	7.73	0.90	-6.5	
0.202	8.79	1.25	-9.75	
0.231	9.81	1.55	-11.25	
0.260	10.78	1.84	-13.25	
0.289	11.39	2.08	-14.75	
0.313	11.69	2.23	-16.25	
0.342	11.87	2.48	-18.75	
0.371	12.00	2.66	-19.25	Maximum penetration
0.400	12.10	2.89	-20.50	
0.433	12.14	3.16	-20.75	
0.462	12.17	3.44	-21.50	
0.491	12.20	3.65	-21.75	
0.524	12.24	3.94	-21.75	
0.553	12.29	4.20	-21.75	Car rebounding

Metric Conversion:

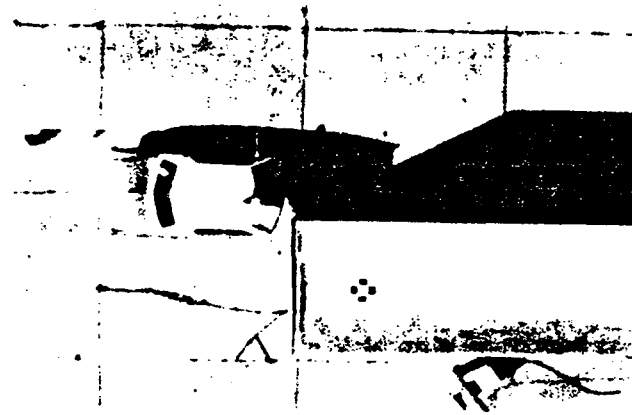
1 ft = 0.305 m



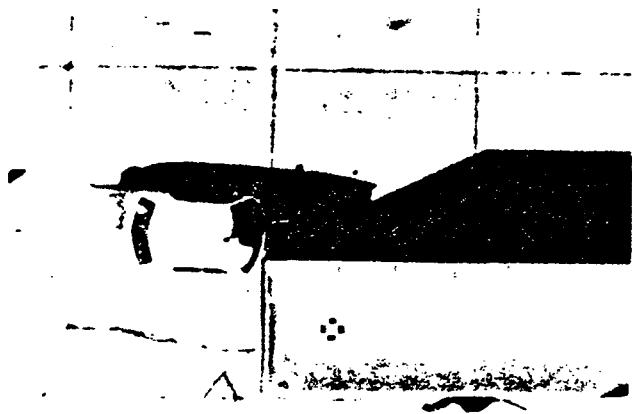
0.000 sec



0.058 sec

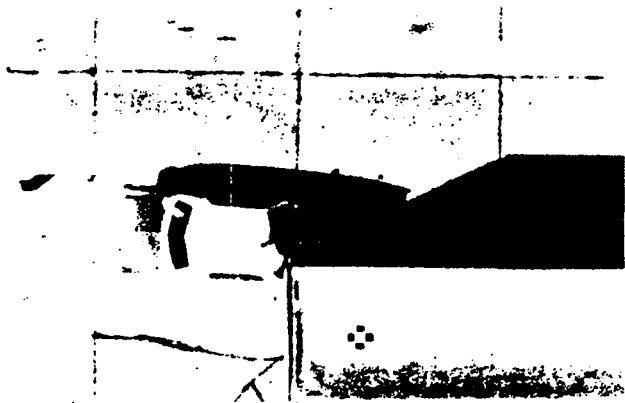


0.091 sec



0.107 sec

Figure F-26. Sequential Photographs for Test 3661-2.



0.128 sec



0.148 sec



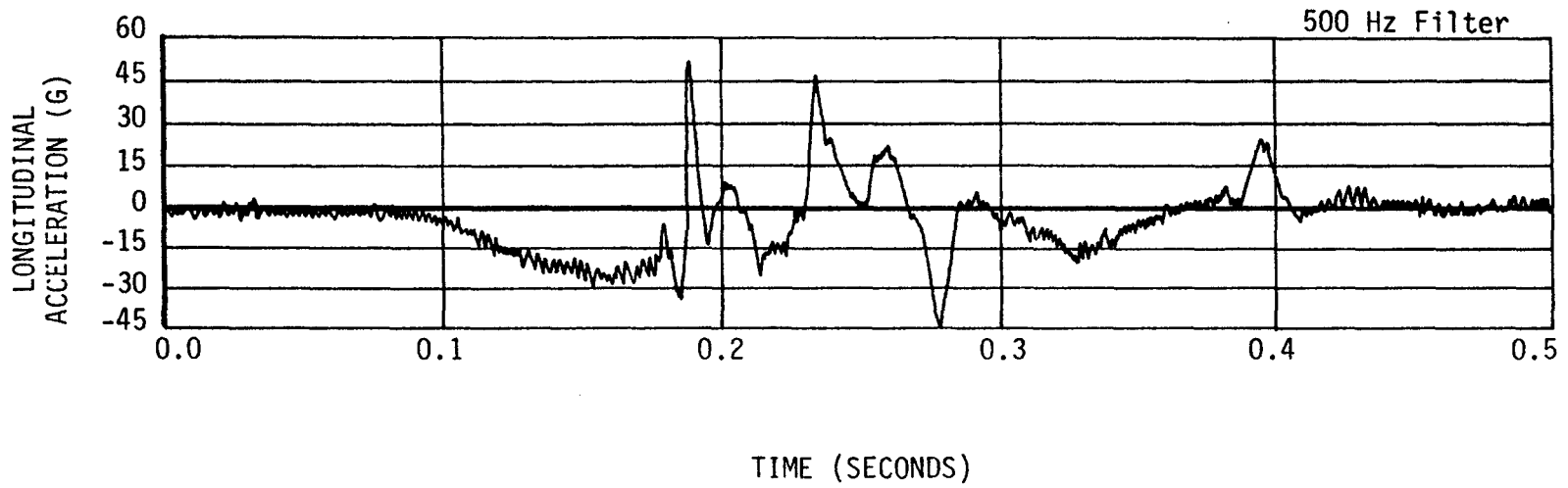
0.371 sec



0.553 sec



Figure F-26. Sequential Photographs for Test 3661-2 (continued).
F-47



F-48

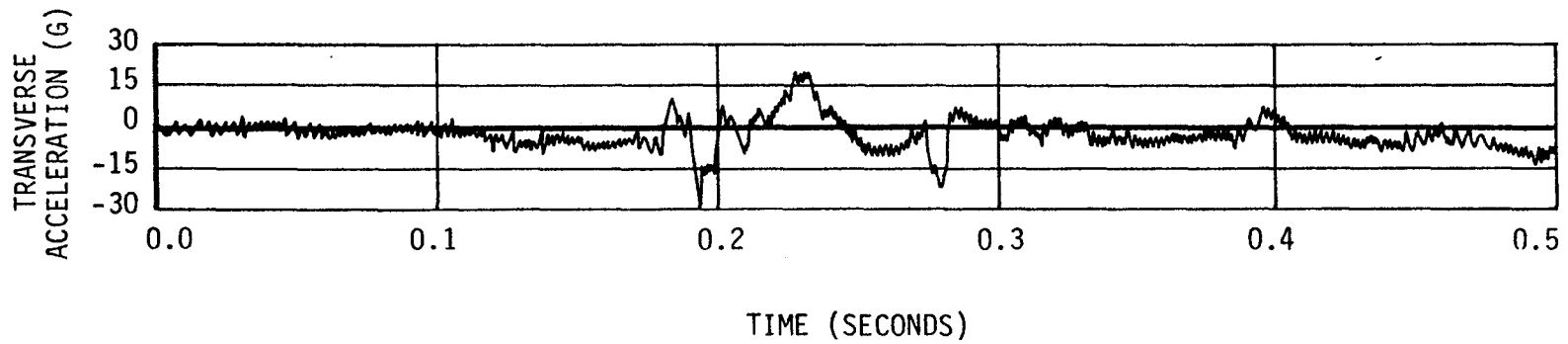


Figure F-27. Beta Head Longitudinal and Transverse Accelerometer Trace for Test 3661-2.

F-49

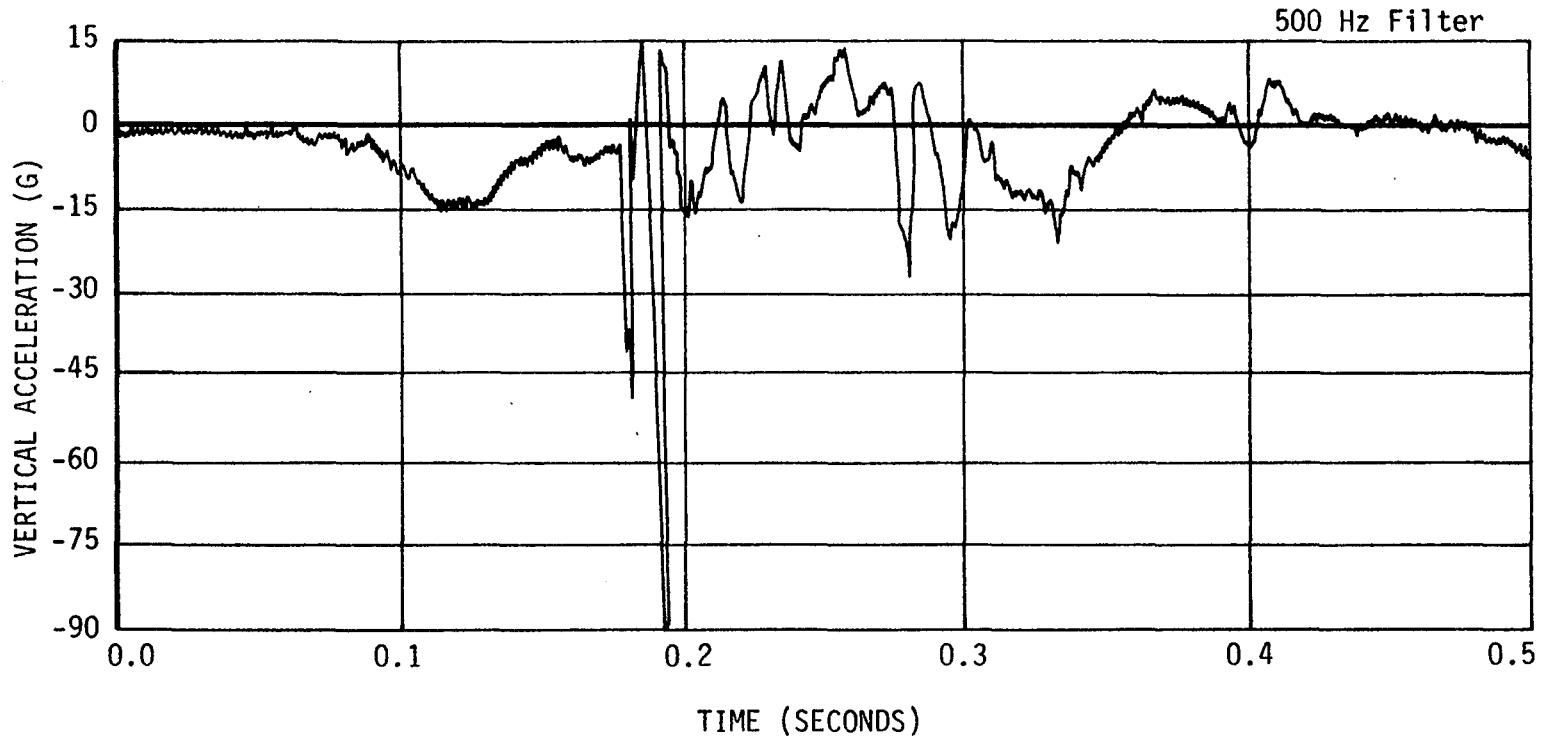


Figure F-28. Beta Head Vertical Accelerometer Trace for Test 3661-2.

F-50

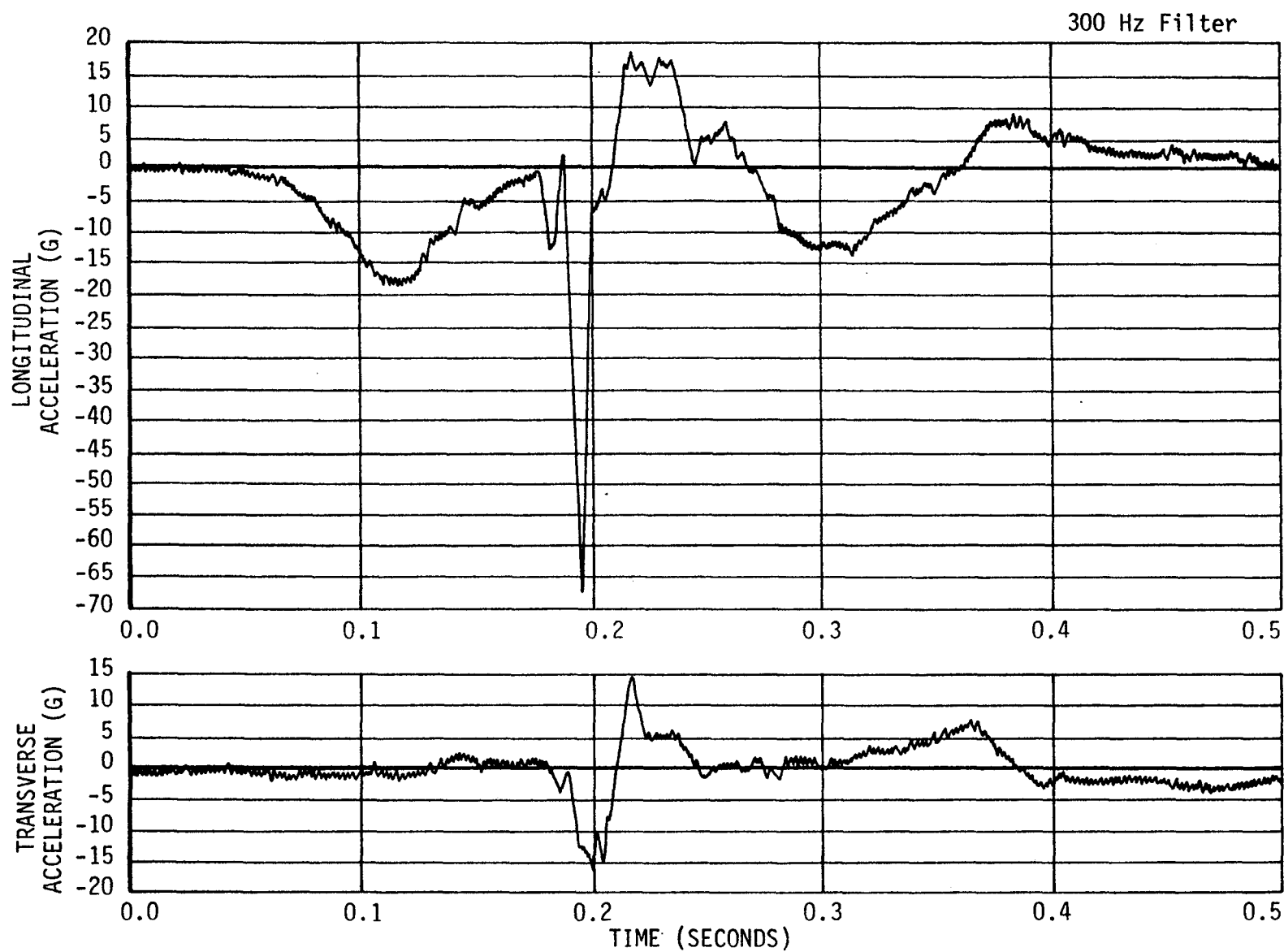


Figure F-29. Beta Chest Longitudinal and Transverse Accelerometer Trace for Test 3661-2.

F-51

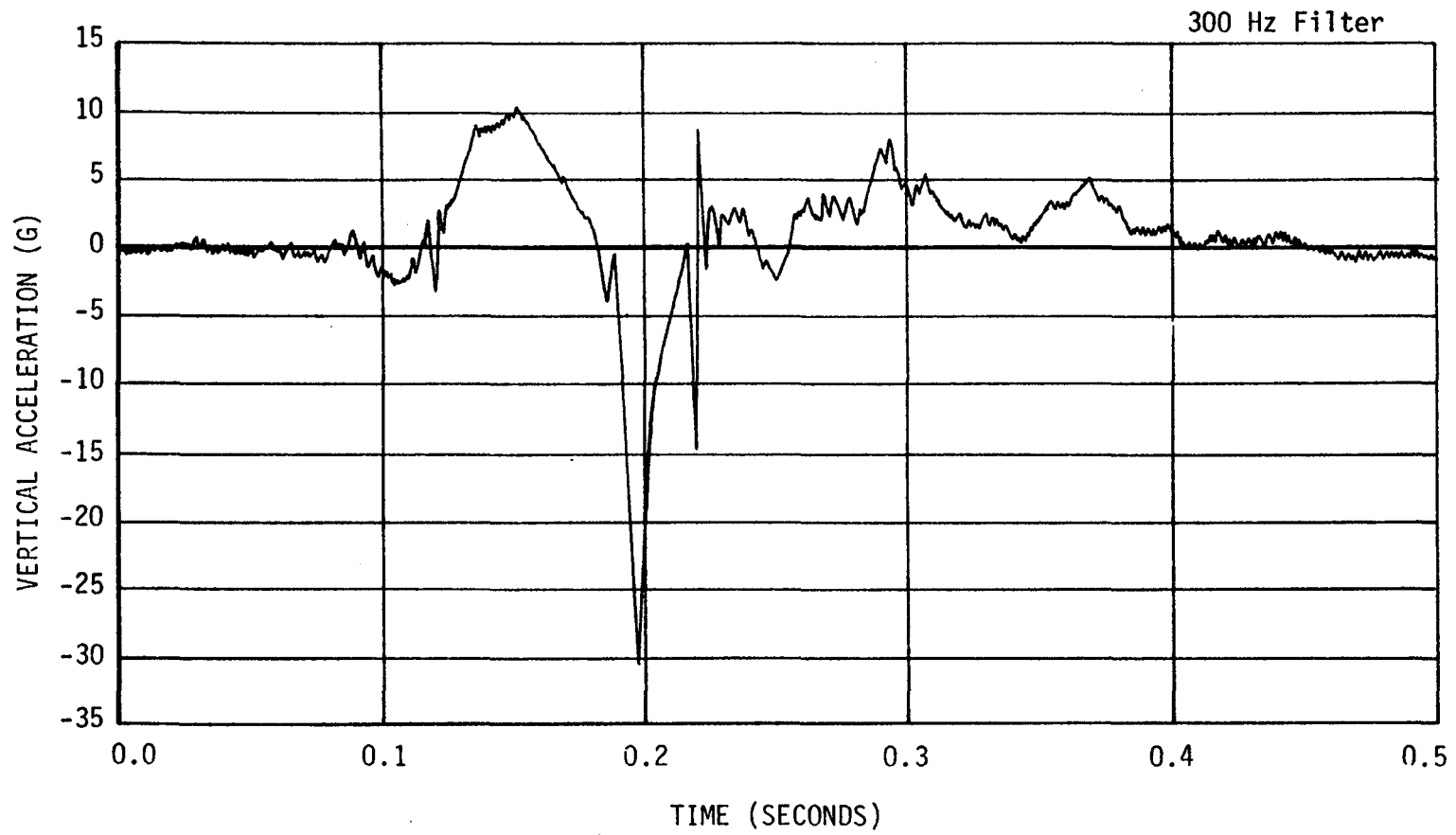


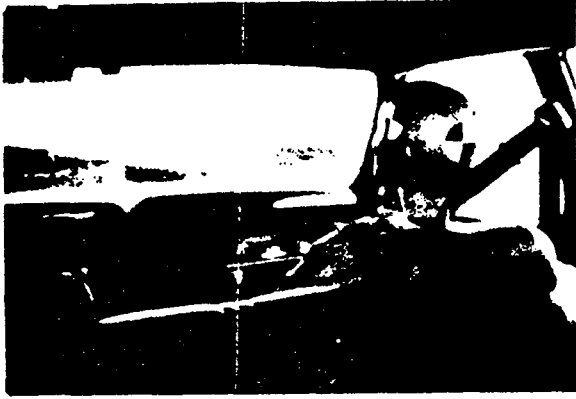
Figure F-30. Beta Chest Vertical Accelerometer Trace for Test 3661-2.

Table F-12. Dummy Time-Event Summary
For Test 3661-2.

TIME (SEC)	EVENT
	<u>Beta</u>
0.03	Initial movement
0.10 - 0.17	Falling forward but restrained by shoulder harness
0.17	Full forward motion, seat belt begins pulling body backward
0.18	Shattered glass hits forehead and face
0.19	Forehead impacts with rear end of trailer
0.20	Deforming car top impacts forehead
0.21 on	Car top has deformed to completely block Beta from view

Table F-13. Dummy Injury Indices.

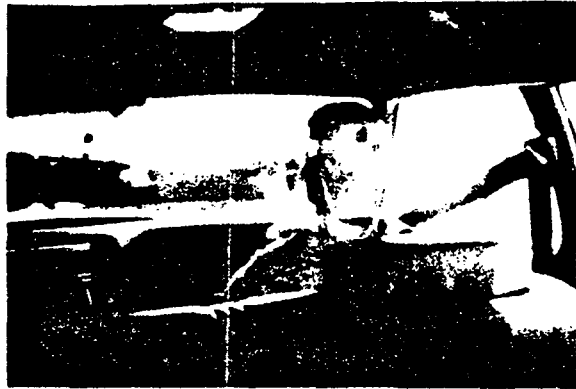
	HIC	GADD	0.003 sec G
Beta Head	477 from 0.106 sec to 0.344 sec	791 from 0.000 sec to 0.512 sec	65 from 0.188 sec to 0.191 sec
Beta Chest	32 from 0.194 sec to 0.206 sec	60 from 0.000 sec to 0.552 sec	28 from 0.197 sec to 0.200 sec



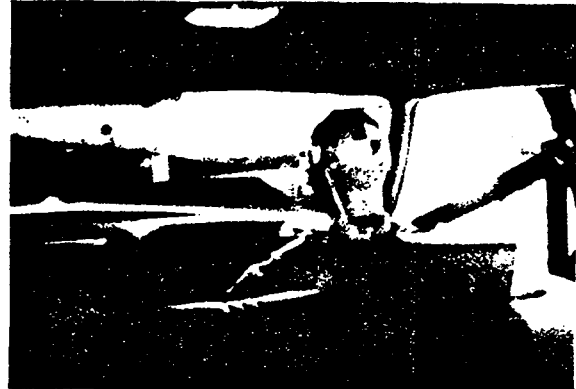
0.000 sec



0.056 sec



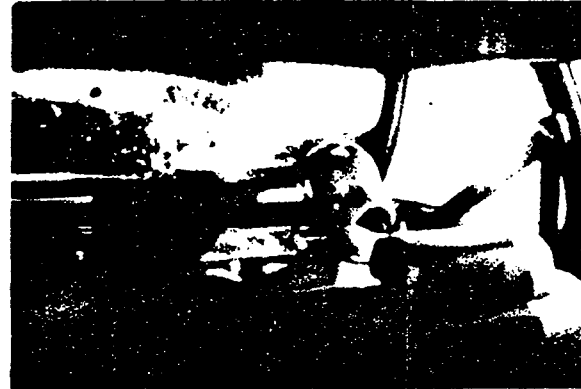
0.093 sec



0.106 sec



0.131 sec



0.150 sec



0.374 sec



0.555 sec

Figure F-31. Interior Sequential Photographs for Test 3661-2.

Test 3661-3

Fruehauf Trailer 24,890 kg (54,830 lb)
Rigid Guard Design 5ST-3 - 79 kg (173 lb)
Ground Clearance - 0.45 m (17.8 in)
1979 Chevrolet Impala - 1857 kg (4090 lb)
54.3 km/h (33.8 mph) closing speed
Centric Alignment
Tested March 21, 1979

Results of the test are summarized in Table F-15. Sequential photographs of the collision are shown in Figure F-40. The trailer began to move forward 0.028 sec after impact. Subsequently, the automobile received a maximum dynamic crush of 0.81 m (2.64 ft) at 0.089 sec after impact. At this time the trailer had moved forward 0.05 m (0.15 ft). The maximum forward movement of the automobile (0.86 m [2.82 ft]) occurred some 0.109 sec after impact, while the maximum forward movement of the truck (0.23 m [0.76 ft]) occurred at 0.434 sec. Inspection of the guard after impact indicated that the guard sustained negligible permanent deformation.

The automobile longitudinal acceleration trace in Figure F-35 shows a peak acceleration of approximately -72 g, at 0.08 sec after impact. This would indicate a peak force of approximately 1,302 kN (294,500 lbs). The highest 0.050 sec average acceleration of 24.5 g's would indicate an average of 445,700 N (100,200 lbs).

Accelerometer traces from the two dummies, driver (Alpha) and passenger (Beta), are given in Figures F-41 through F-46. For both dummies, the vertical acceleration traces have truncated peaks. This resulted from inappropriate settings of instrumentation prior to the test. Dummy injury indices were computed using the data as shown.

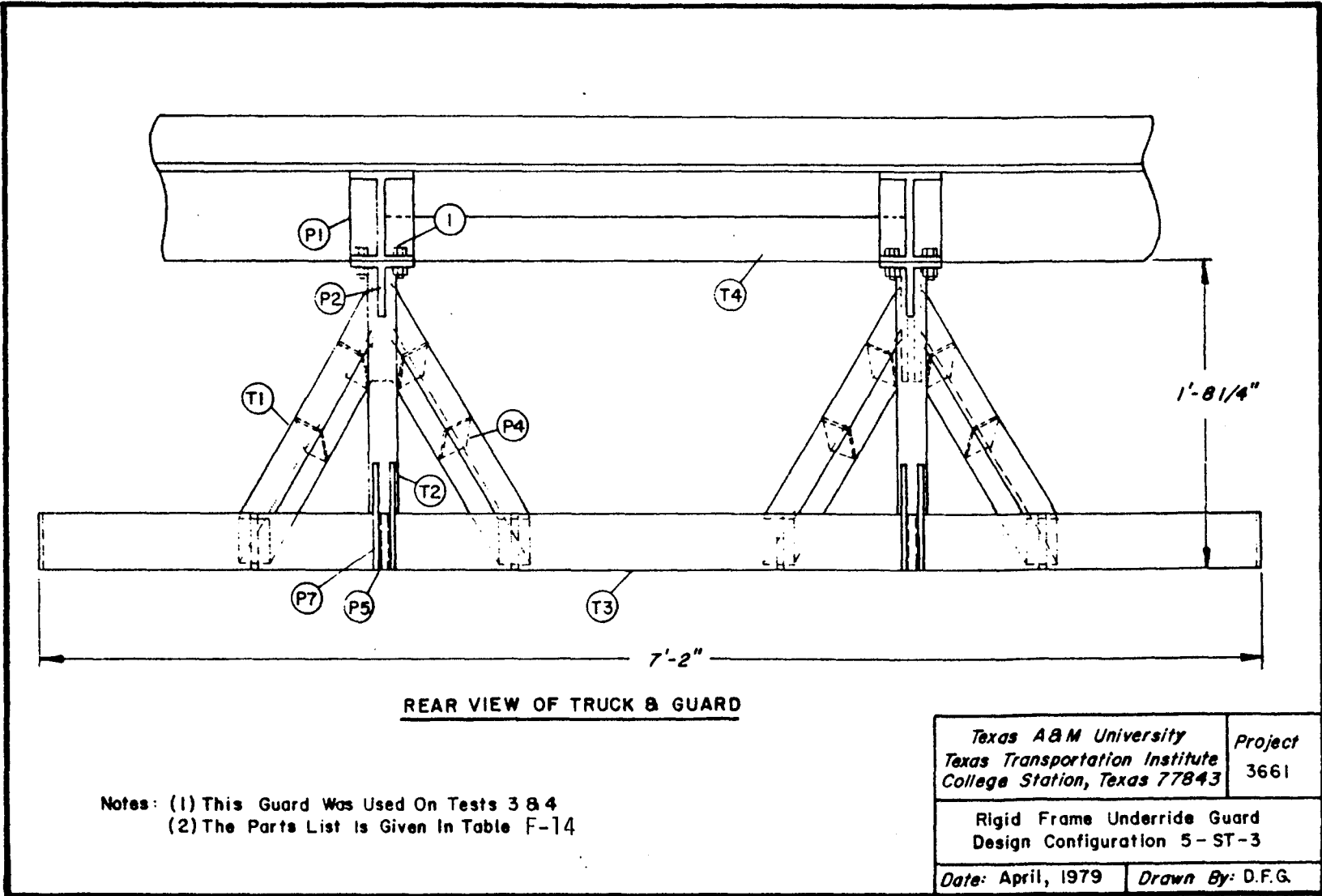
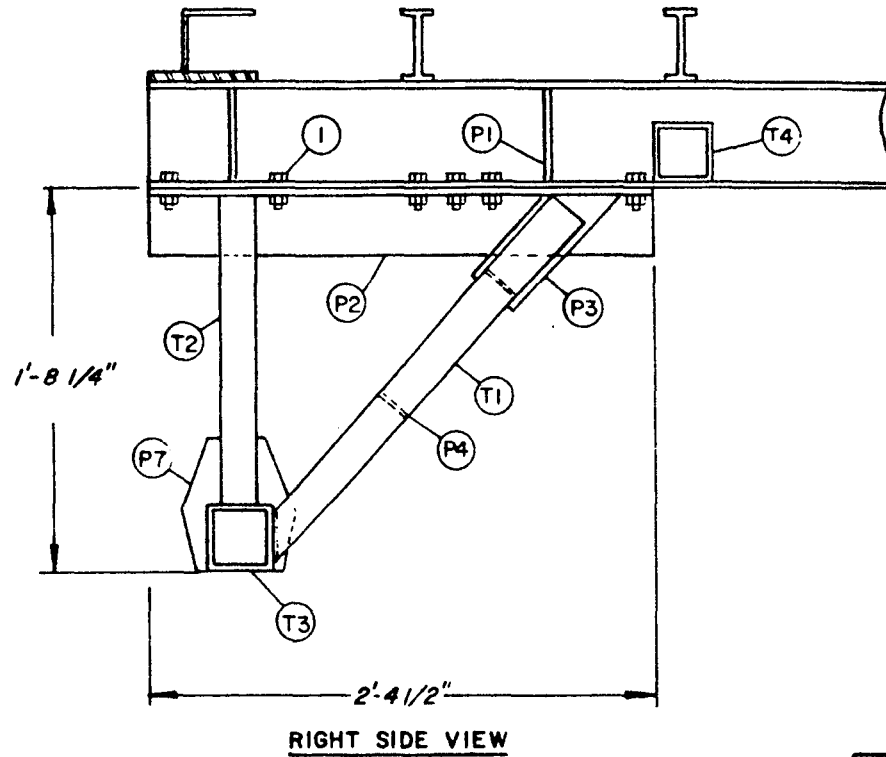


Figure F-32. Underride Guard Design 5ST-3.



Texas A & M University Texas Transportation Institute College Station, Texas 77843		Project 3661
Rigid Frame Underride Guard Design Configuration 5-ST-3		
Date: April, 1979	Drawn By: D. F. G.	

Figure F-32. Underride Guard Design 5ST-3 (continued).

Table F-14. Parts List for Guard 5ST-3.

DESIGNATION	DESCRIPTION	MATERIAL	NUMBER REQUIRED
T1	Fabricated Tubing, 2"x2"x3/16"	ASTM A514 100 ksi yield	4
T2	Fabricated Tubing, 2"x2"x3/16"	ASTM A514 100 ksi yield	2
T3	Fabricated Tubing, 3 1/2"x3 1/2"x3/16"	ASTM A514 100 ksi yield	1
T4	Fabricated Tubing 3"x3"x3/16"	ASTM A514 100 ksi yield	1
P1	Stiffener, 2"x5 3/8"x3/8"	ASTM A514 100 ksi yield	8
P2	Fabricated Tee, 4"x4"x3/16"	ASTM A514 100 ksi yield	2
P3	Gusset, 4"x9"x3/16"	ASTM A514 100 ksi yield	12
P4	Stiffener, 1 3/4"x1 3/4"x3/16"	ASTM A514 100 ksi yield	12
P5	Stiffener, 3 1/8"x3 1/8"x3/16"	ASTM A514 100 ksi yield	8
P7	Gusset, 2"x7"x3/16"	ASTM A514 100 ksi yield	8
1	Bolt, 5/8"	ASTM A325-N, 104 ksi yield	24

Table F-15. Summary of Results, Test 3661-3.

AUTOMOBILE	1979 Chevrolet Impala 1857 kg (4090 lb)					
FILM DATA						
Impact angle	0 deg (centric alignment)					
Initial speed of passenger car	54.3 km/h (33.8 mph) 15.1 m/s (49.5 fps)					
Average speed of trailer after impact	2.8 km/h (1.8 mph) 0.4 m/s (1.2 fps)					
Max. penetration (stopping distance) of auto. c.g. at time after impact	0.86 m (2.82 ft) 0.109 sec					
Avg. longitudinal accel. from impact to max. penetration*	-17.2 g					
Trailer movement began at	0.027 sec					
Max. movement of trailer at max. penetration at time	0.07 m (0.23 ft) 0.109 sec					
Max. distance trailer moved	0.23 m (0.76 ft) at 0.134 sec					
Final location of trailer	0.18 m (0.58 ft)					
ELECTRONIC DATA -- Class 60 Filter						
Impact speed	54.7 km/h (34.0 mph) 15.2 m/s (49.8 fps)					
		<u>Ax(v)</u>	<u>Ay(v)</u>	<u>Ax(v)</u>	<u>Ax(e)</u>	<u>Az(e)</u>
Max. 0.050 sec accel. over time interval	g	-24.5	1.8	-14.5	-28.6	7.0
	sec	0.032	0.044	0.035	0.022	0.072
	sec	0.082	0.094	0.085	0.072	0.122
Peak acceleration at time after impact	g	-71.6	-21.0	51.8	49.6	24.7
	sec	0.078	0.040	0.092	0.040	0.092
AUTOMOBILE DAMAGE						
Max. dynamic crush	0.81 m (2.64 ft) at 0.089 sec					
Residual auto. deformation	0.67 m (2.19 ft)					
Damage classification	SAE -- 12FDMW5 TAD -- 12FD5.5					

$$* G_{avg} = \left(\frac{2}{\pi}\right) \frac{V^2}{gd}$$

where V is impact speed in m/s (ft/sec)
g is acceleration due to gravity
in m/s² (ft/sec²)
d is stopping distance in m (ft)

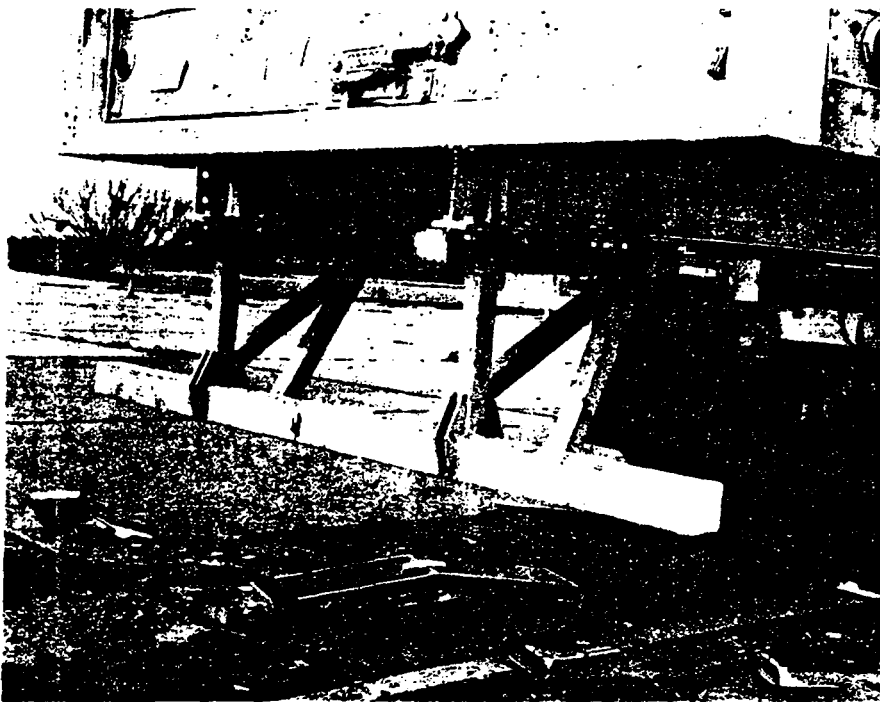
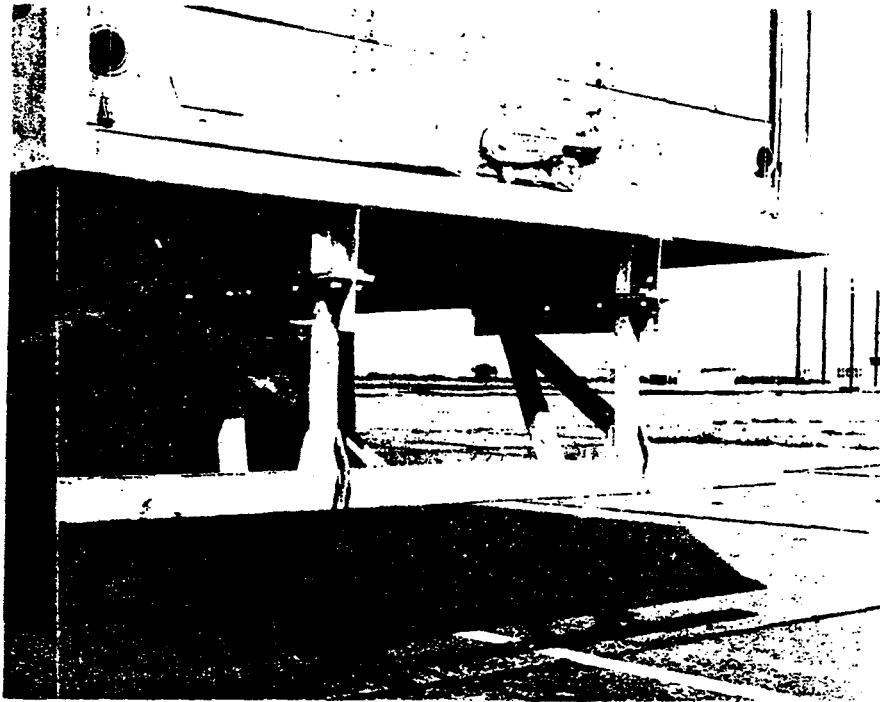


Figure F-33. Guard Before and After Test 3661-3.

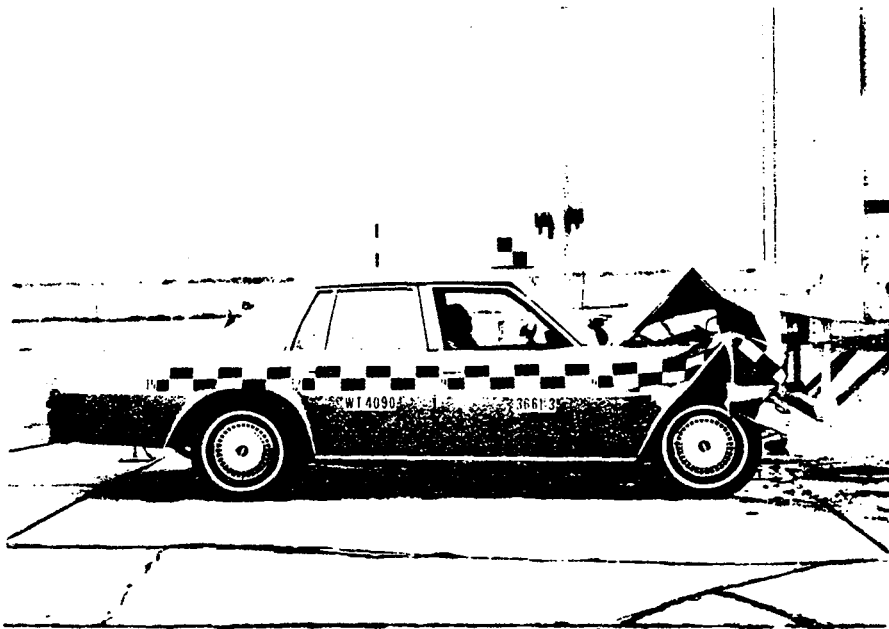


Figure F-34. Automobile Before and After Test 3661-3.

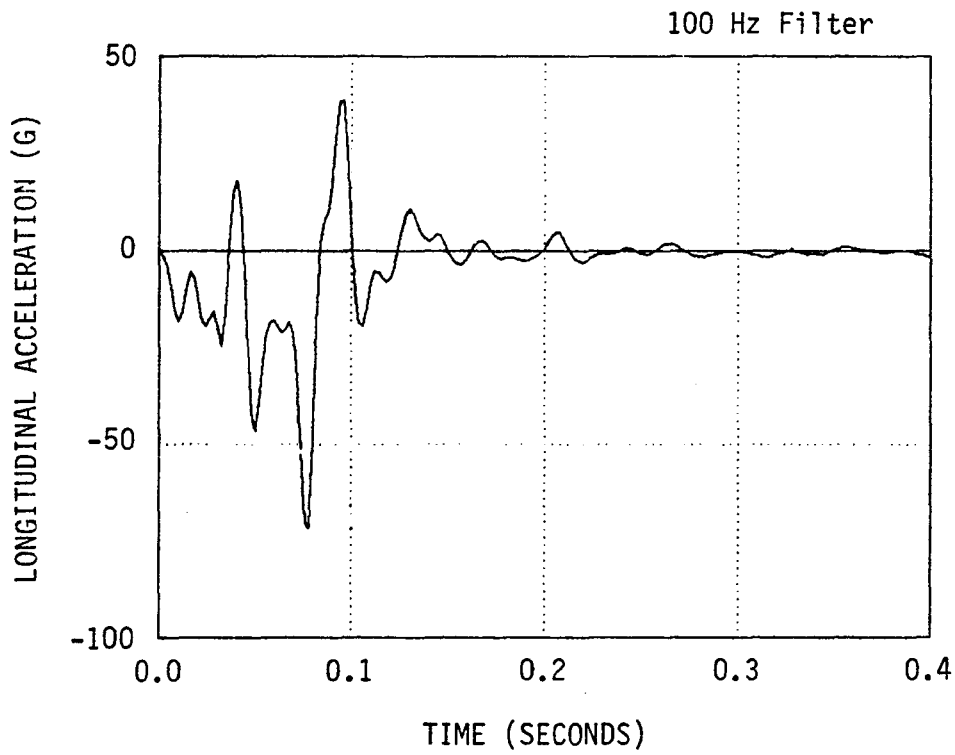


Figure F-35. Longitudinal Automobile Accelerometer Trace for Test 3661-3.

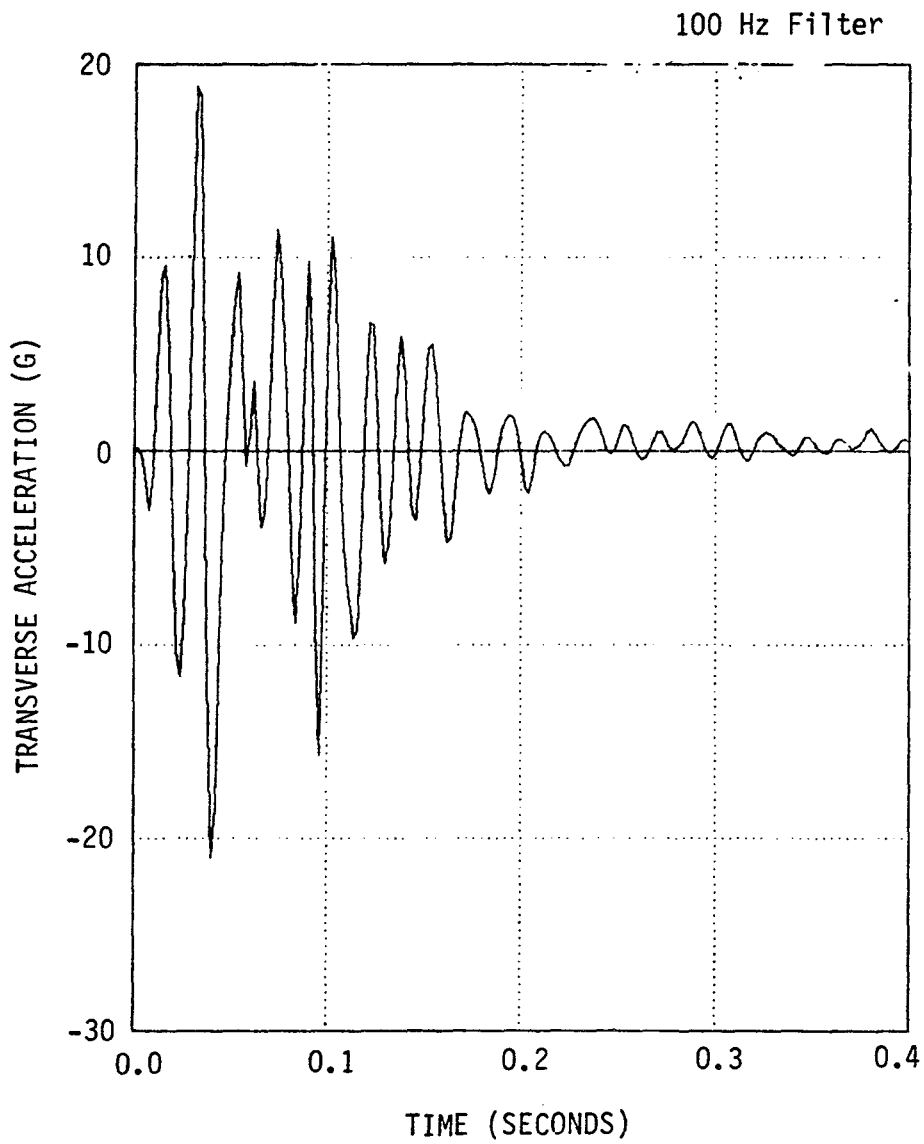


Figure F-36. Transverse Automobile Accelerometer Trace for Test 3661-3.

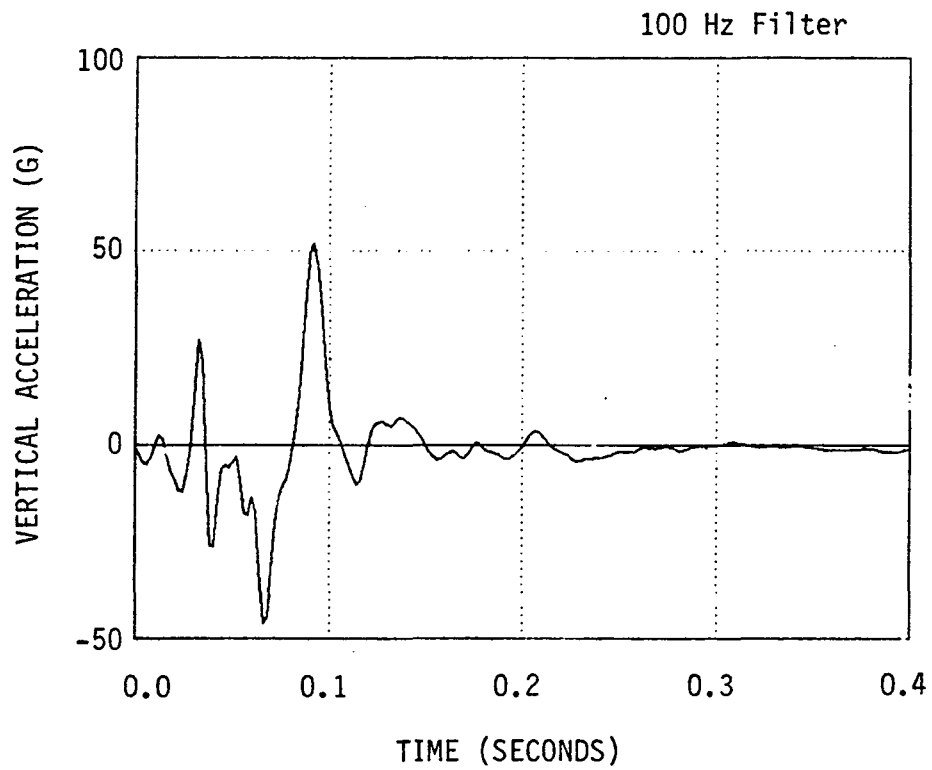


Figure F-37. Vertical Automobile Accelerometer Trace for Test 3661-3.

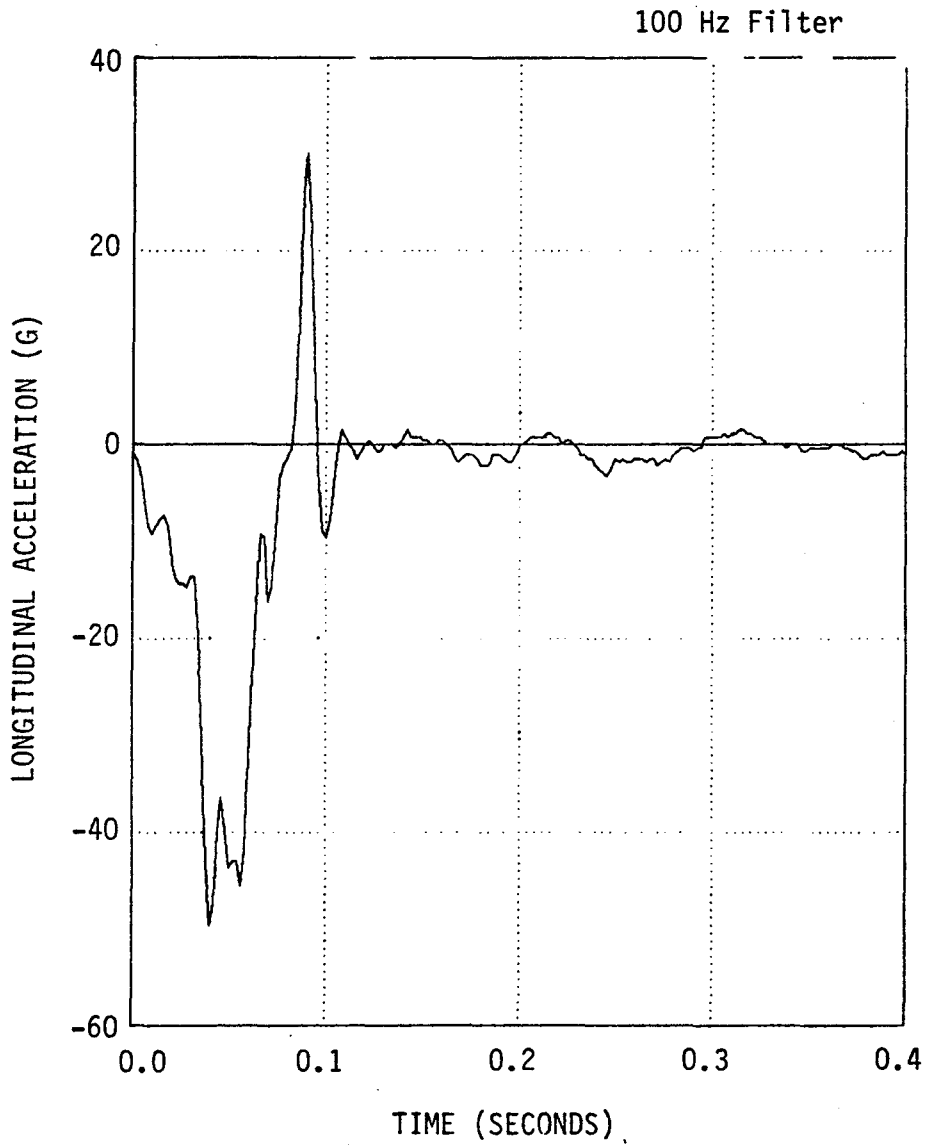


Figure F-38. Longitudinal Engine Accelerometer Trace for Test 3661-3.

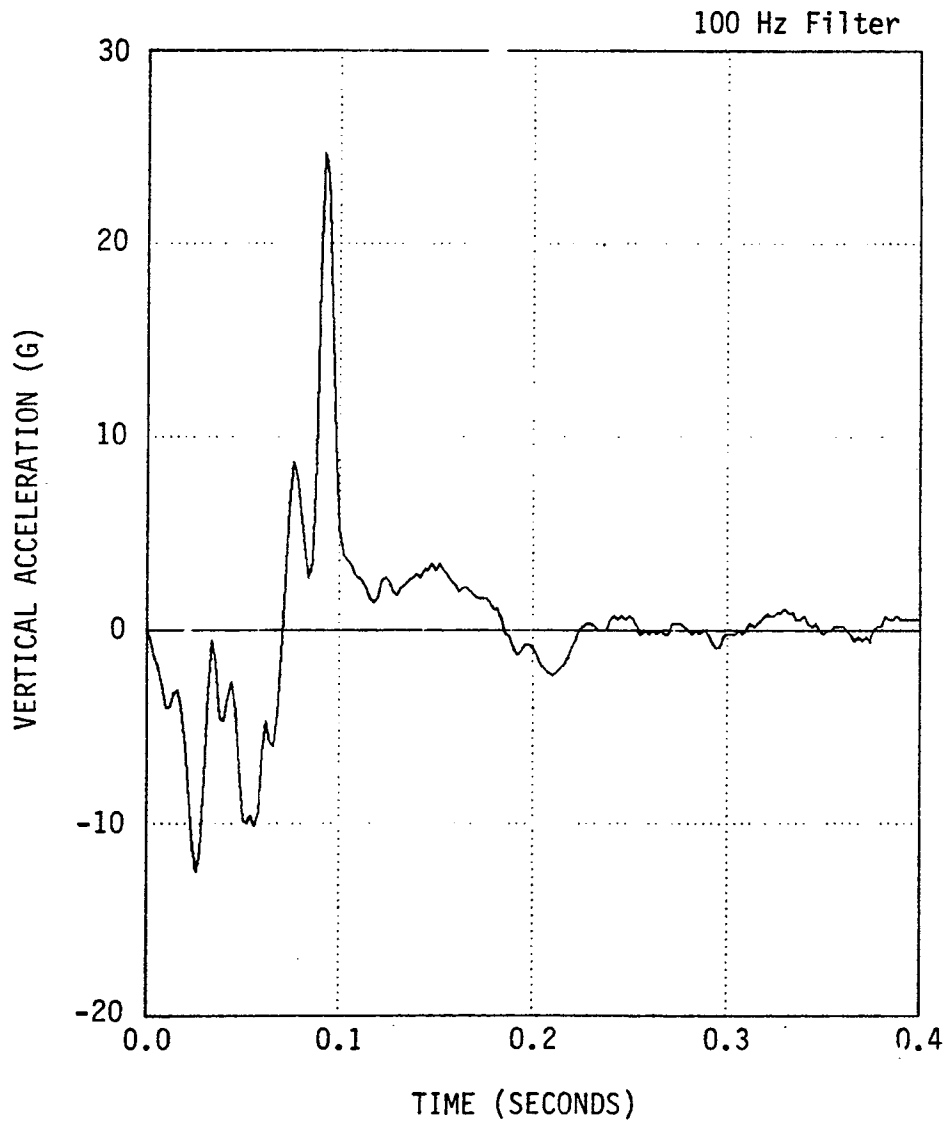


Figure F-39. Vertical Engine Accelerometer Trace for Test 3661-3.

Table F-16. Time, Displacement, Event Summary
for Test 3661-3.

TIME (SEC)	CAR DISPLACEMENT (FT)	TRAILER DISPLACEMENT (FT)	EVENT
-0.097	-4.80	0.00	
-0.078	-3.84	0.00	
-0.058	-2.89	0.00	
-0.039	-1.93	0.00	
-0.019	-0.96	0.00	
0.000	0.00	0.00	Impact
0.019	0.93	0.00	
0.027	1.26	0.01	Trailer movement begins
0.045	1.90	0.03	Bumper pushed under guard
0.064	2.45	0.07	
0.076	2.67	0.10	
0.089	2.79	0.15	Maximum crush of car
0.109	2.82	0.23	Maximum forward motion of car
0.124	2.78	0.26	
0.155	2.73	0.35	Car rear wheels off ground
0.175	2.68	0.40	
0.190	2.63	0.43	
0.204	2.59	0.46	
0.250	2.48	0.57	
0.300	2.38	0.64	
0.349	2.29	0.71	Car rebounding
0.400	2.18	0.75	
0.434	2.09	0.76	Trailer stopped
0.450	2.05	0.76	
0.500	1.95	0.76	

Metric Conversion:

1 ft = 0.305 m

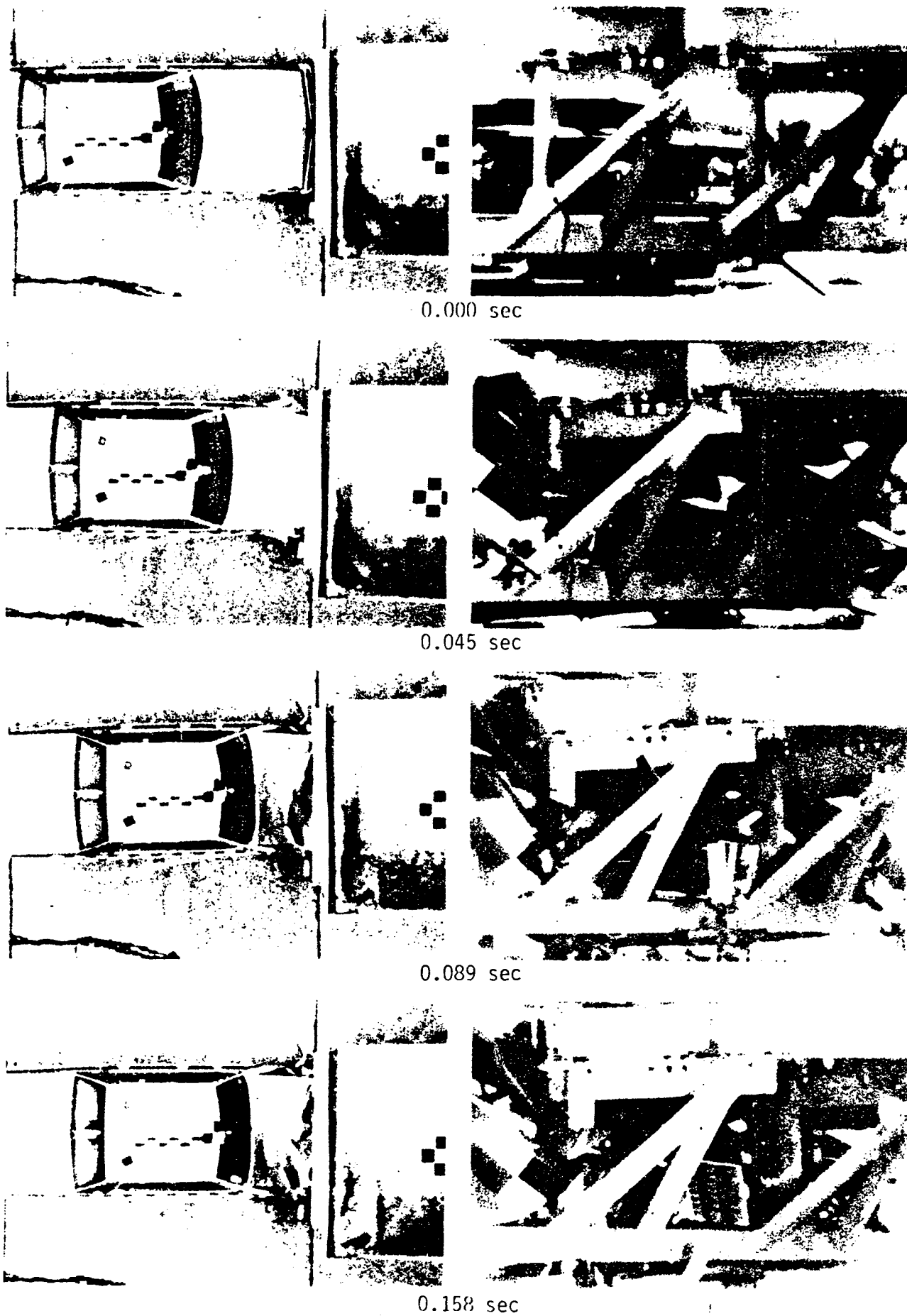
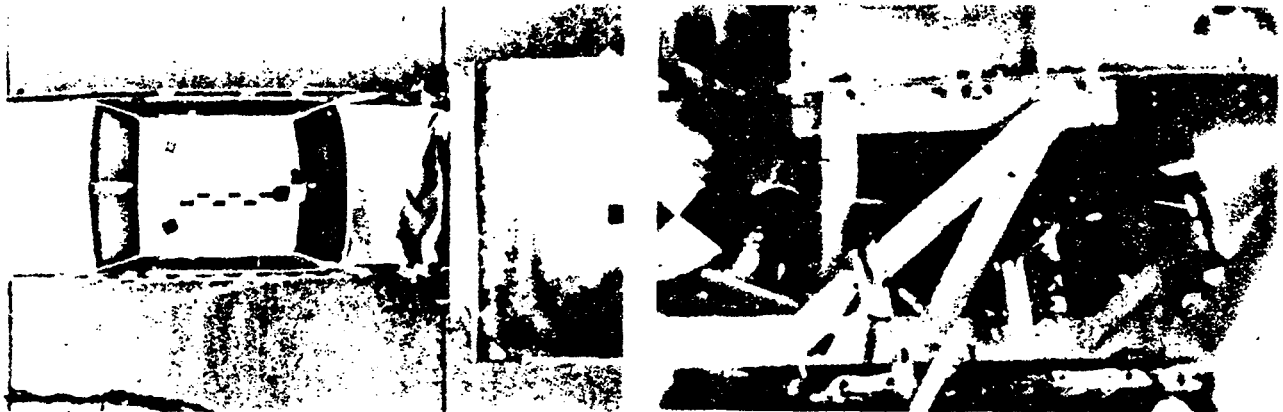


Figure F-40. Sequential Photographs for Test 3661-3.
F-67



0.228 sec



0.295 sec



0.365 sec



0.435 sec

Figure F-40. Sequential Photographs for Test 3661-3 (continued).

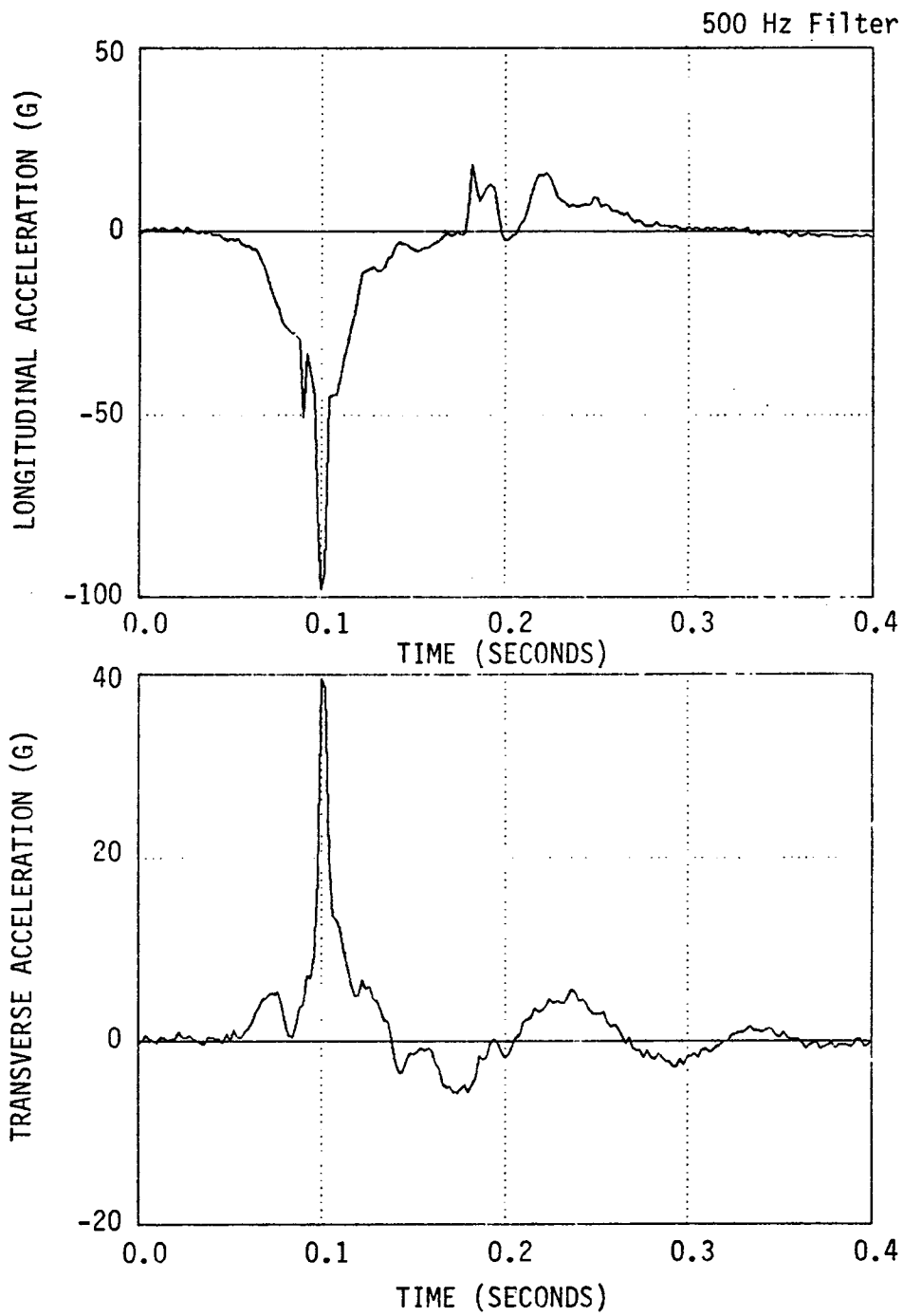


Figure F-41 . Alpha Head Longitudinal and Transverse Accelerometer Traces for Test 3661-3.

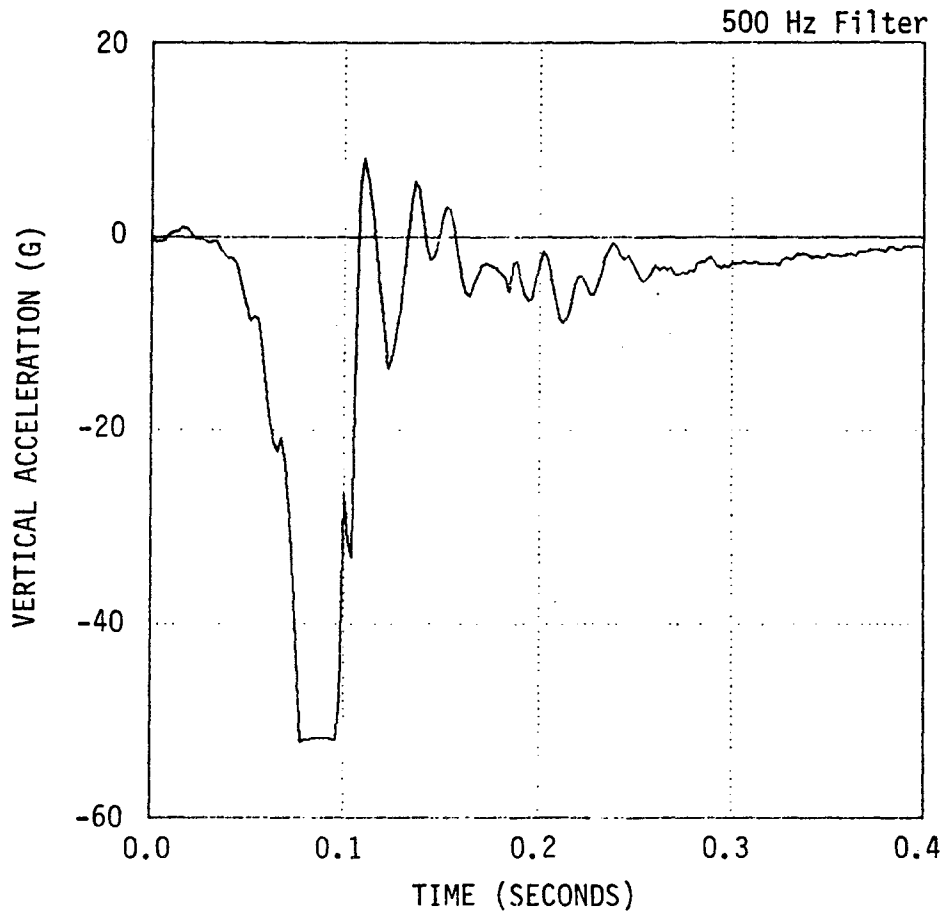


Figure F-42. Alpha Head Vertical Accelerometer Trace for Test 3661-3.

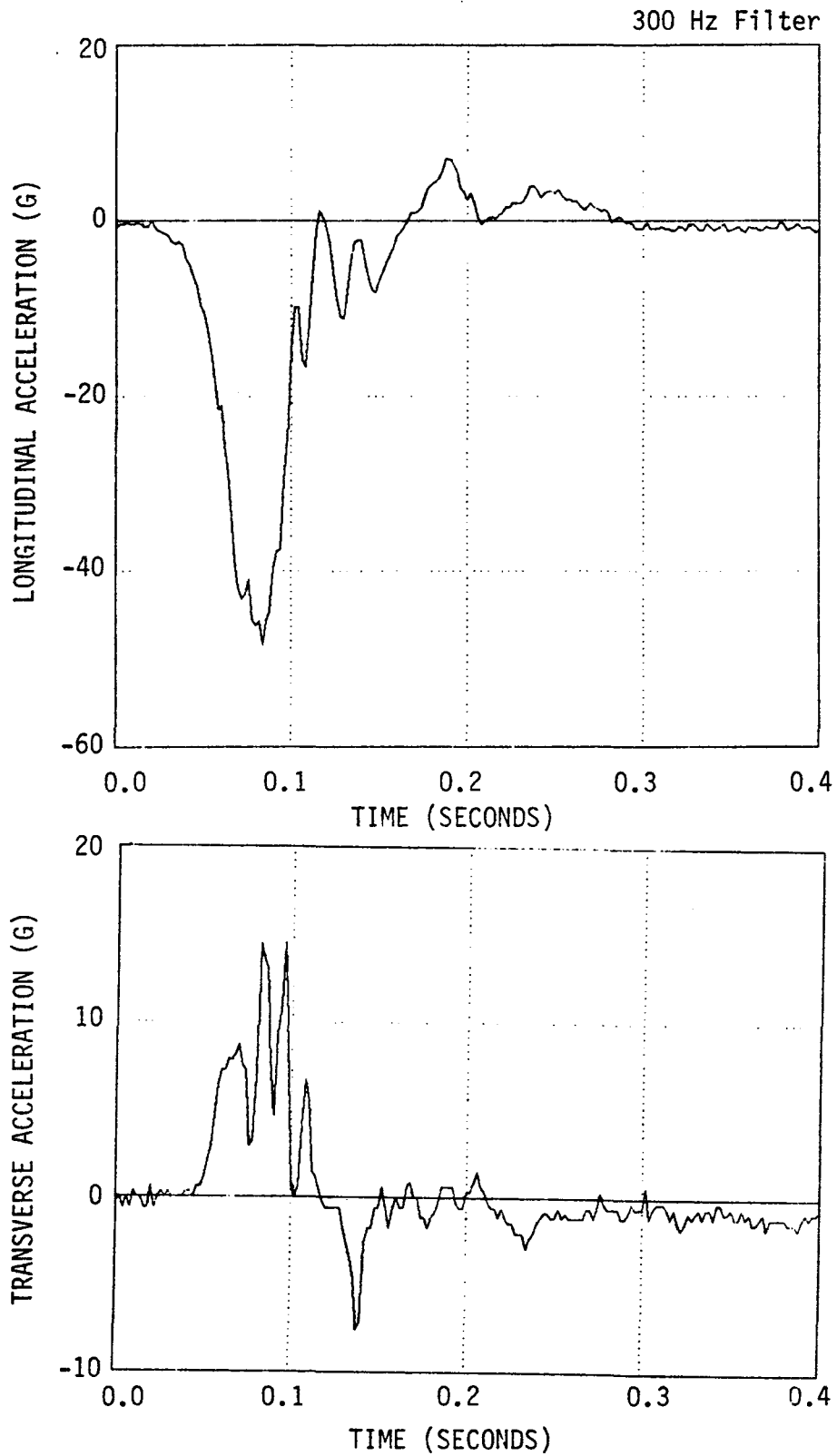


Figure F-43. Alpha Chest Longitudinal and Transverse Accelerometer Traces for Test 3661-3.

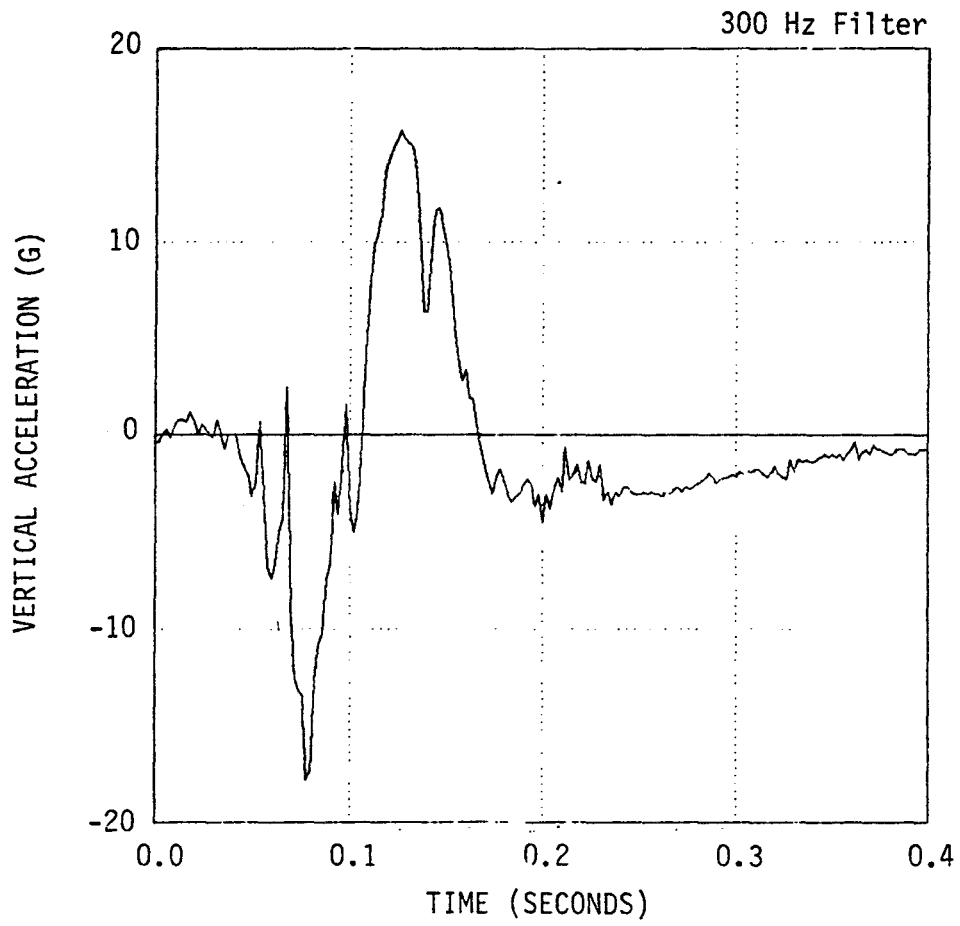


Figure F-44. Alpha Chest Vertical Accelerometer Trace for Test 3661-3.

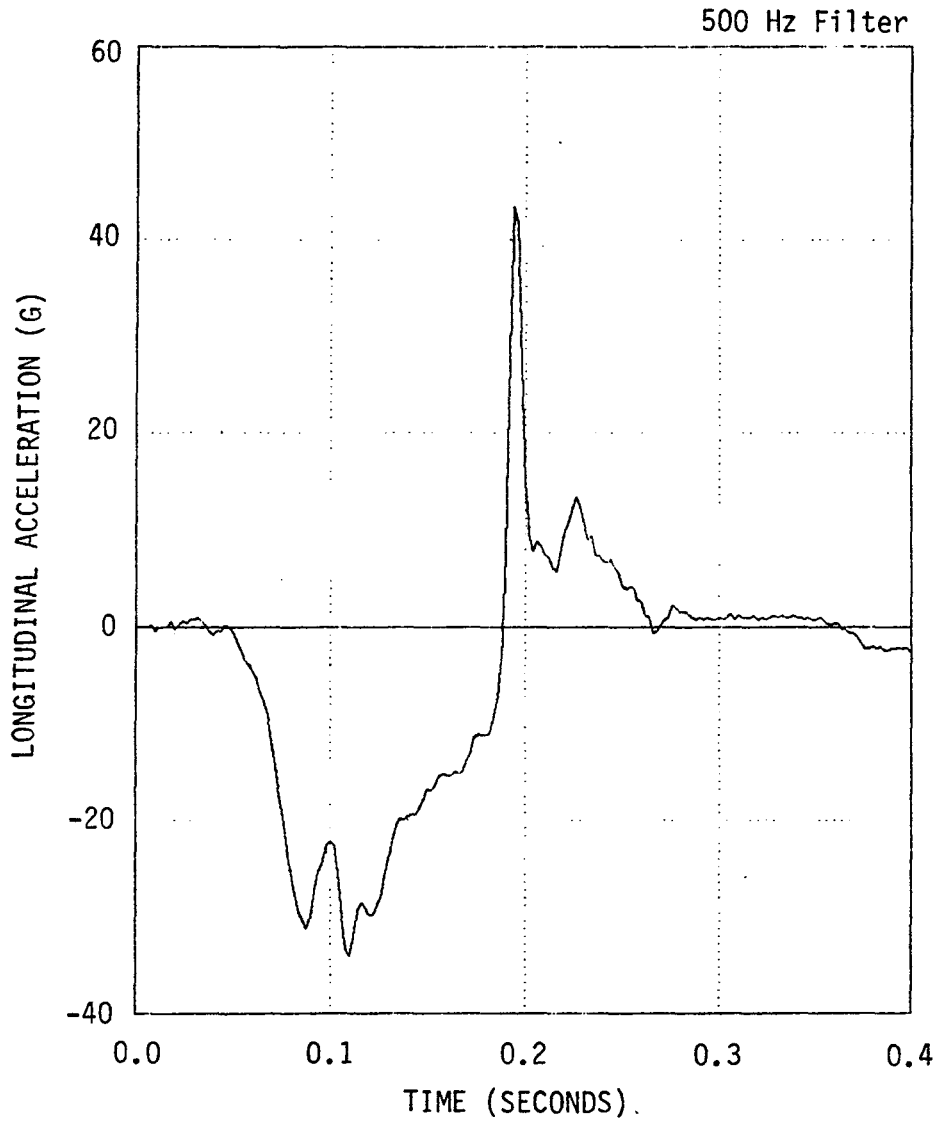


Figure F-45. Beta Head Longitudinal Accelerometer Trace for Test 3661-3.

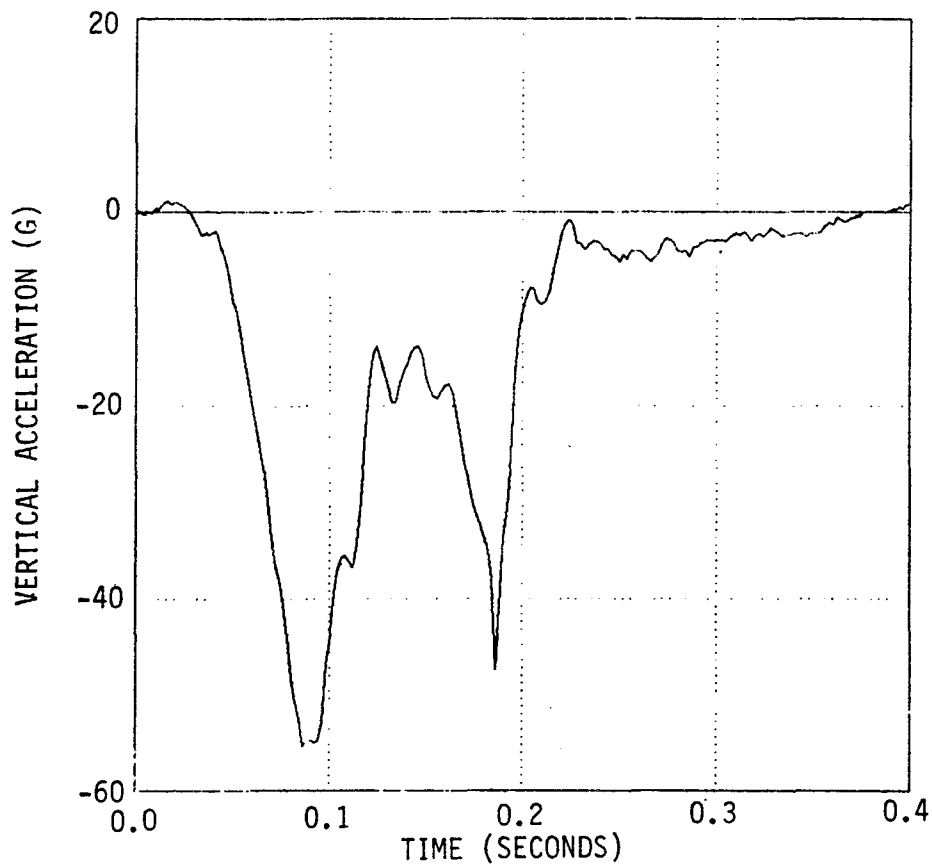
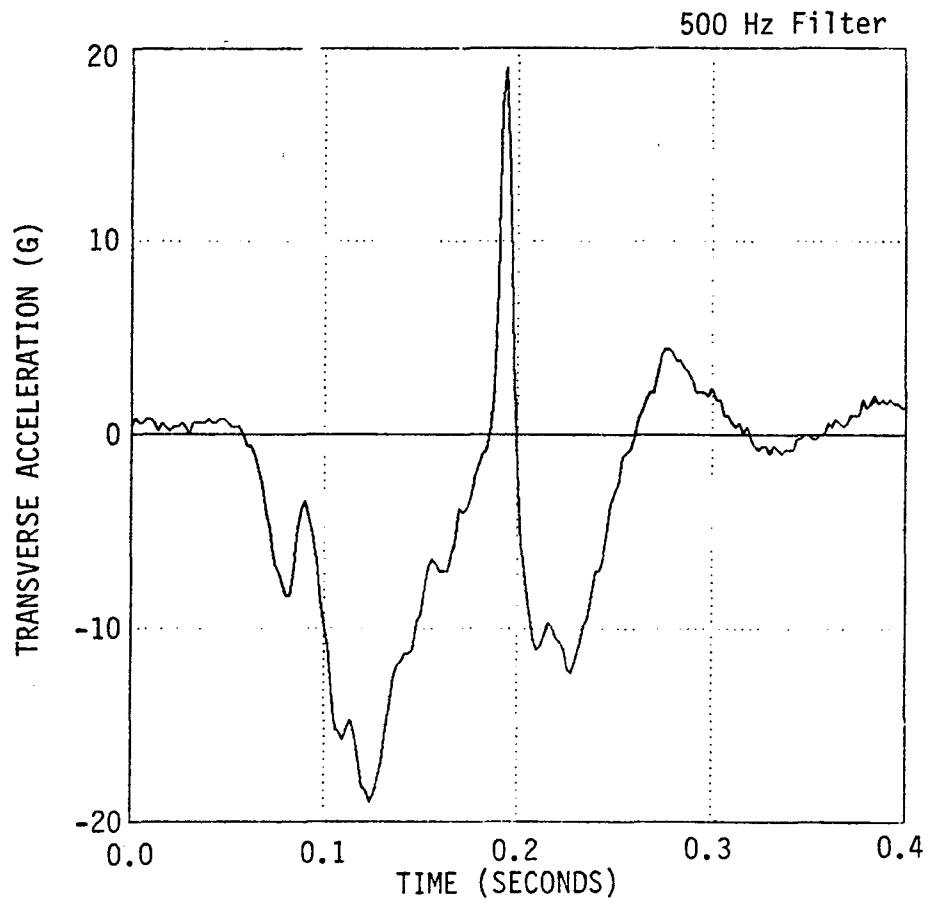


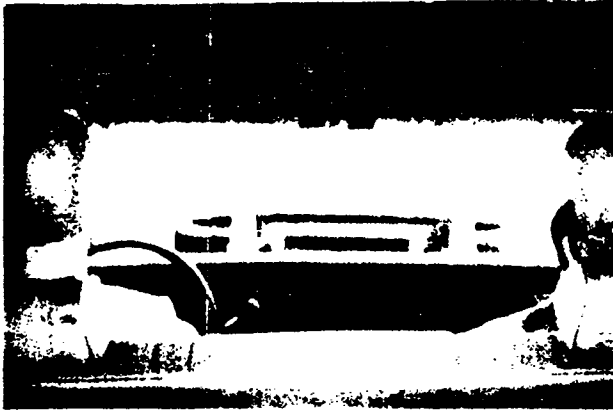
Figure F-46. Beta Head Transverse and Vertical Accelerometer Traces for Test 3661-3.

Table F-17. Dummy Time-Event Summary
For Test 3661-3.

TIME (SEC)	EVENT
	<u>Alpha</u>
0.03	Initial movement
0.09	Head impacts steering wheel
0.11	Steering wheel deforms to allow head to impact dash
0.15 - 0.19	Back impacts with seat
	<u>Beta</u>
0.03	Initial movement
0.12 - 0.20	Beta is bent forward and out of view
0.22	Back of head is impacting top portion of front seat

Table F-18. Dummy Injury Indices.

	<u>HIC</u>	<u>GADD</u>	<u>0.003 sec G</u>
Alpha Head	1235 from 0.074 sec to 0.112 sec	1551 from 0.000 sec to 0.396 sec	101 from 0.099 sec to 0.102 sec
Alpha Chest	412 from 0.060 sec to 0.098 sec	501 from 0.000 sec to 0.396 sec	50 from 0.082 sec to 0.085 sec
Beta Head	1322 from 0.062 sec to 0.200 sec	1600 from 0.000 sec to 0.396 sec	63 from 0.086 sec to 0.089 sec
Beta Chest	No instrumentation		



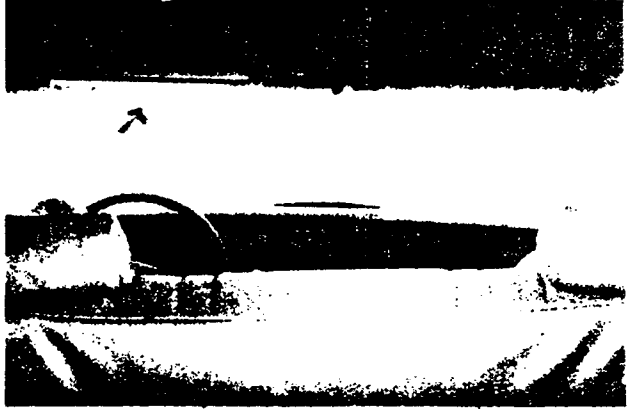
0.000 sec



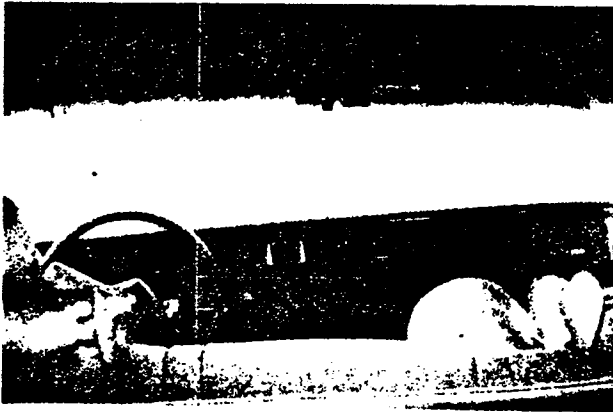
0.044 sec



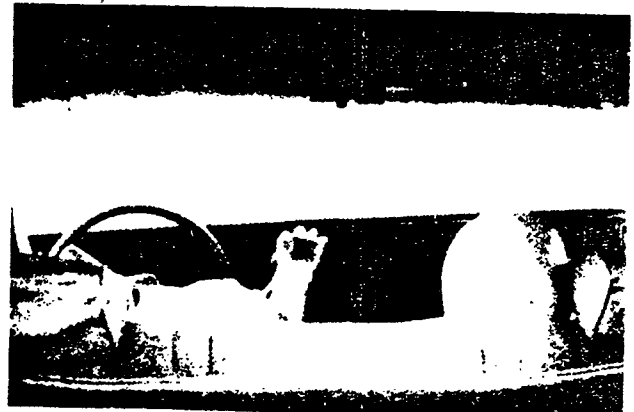
0.089 sec



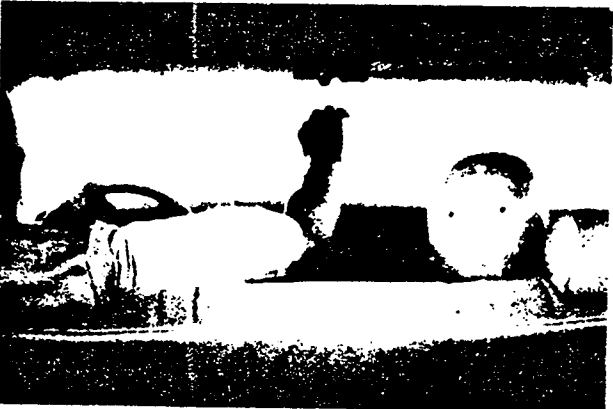
0.166 sec



0.217 sec



0.299 sec



0.365 sec



0.437 sec

Figure F-47. Interior Sequential Photographs for Test 3661-3.

Test 3661-4

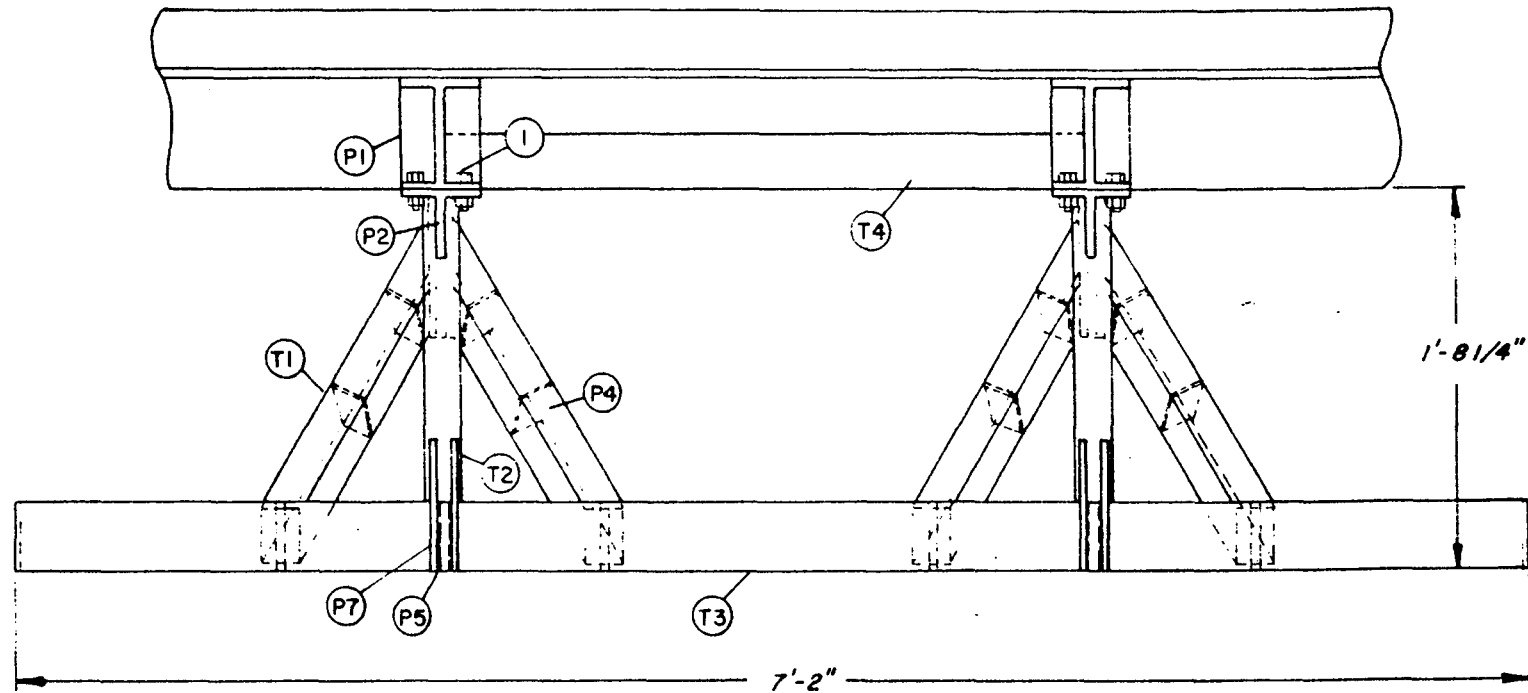
Fruehauf Trailer - 24,890 kg (54,830 lb)
Rigid Guard Design 5ST-3 - 98 kg (215 lb)
Ground Clearance - 0.43 m (17.0 in)
1979 Chevrolet Impala - 1857 kg (4090 lb)
56.8 km/h (35.2 mph) closing speed
1.07 m (42 in) offset to left
Tested May 3, 1979

Study of the structural failure that occurred in test 2 indicated that the lack of lateral support for the trailer frame member was one of the weak points in the structure. For this reason a cross member was added between the truck frame members for test 4 as shown in the drawing in Figure F-48.

Results of the test are summarized in Table F-20. Sequential photographs of the collision are shown in Figure F-57. The trailer began to move forward 0.031 sec after impact. Subsequently, the automobile received a maximum dynamic crush of 1.52 m (5.41 ft) at 0.866 sec after impact. At this time the trailer had moved forward 0.08 m (0.27 ft). The maximum forward movement of the automobile (1.73 m [4.68 ft]) occurred some 0.866 sec after impact, while the maximum forward movement of the truck (0.13 m [0.42 ft]) occurred at 0.364 sec. The guard prevented underride although a segment of the beam did fracture (see Figure F-51) and the trailer frame member on the left side was deformed significantly.

The automobile longitudinal acceleration trace in Figure F-53 shows a peak acceleration of approximately -57.9 g, at 0.84 sec after impact. This would indicate a peak force of 1,053 kN (236,800 lbs). The highest 0.050 sec average acceleration of 18.1 g's would indicate a force of 329 kN (74,000 lbs).

Examination of the motion picture film indicates that both dummies' heads contacted the instrument panel. Driver dummy (Alpha) struck the right half of the steering wheel with his chest and left shoulder (time = 0.1 sec), slid out of his shoulder harness and struck the instrument panel just to the right of the steering wheel. The instrument panel was permanently deformed as shown in Figure F-52. Passenger dummy (Beta) also, struck the instrument panel (time = 0.12 sec)

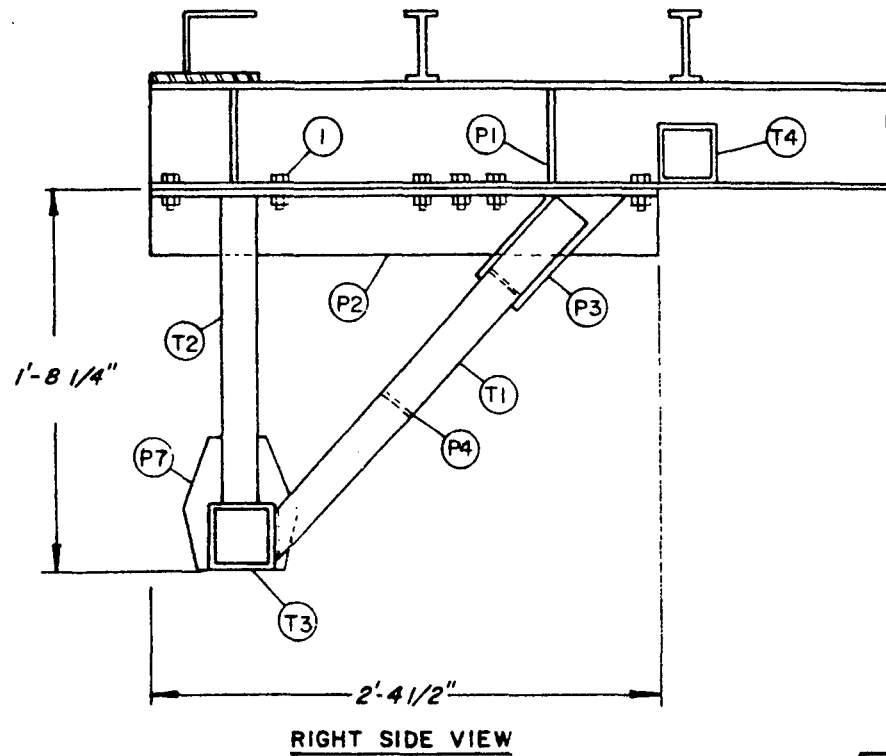


REAR VIEW OF TRUCK & GUARD

Notes: (1) This Guard Was Used On Tests 3 & 4
 (2) The Parts List Is Given In Table F-19

Texas A&M University Texas Transportation Institute College Station, Texas 77843		Project 3661
Rigid Frame Underride Guard Design Configuration 5-ST-3		
Date: April, 1979	Drawn By: D.F.G.	

Figure F-48. Underride Guard Design 5ST-3.



<i>Texas A & M University Texas Transportation Institute College Station, Texas 77843</i>		<i>Project 3661</i>
Rigid Frame Underride Guard Design Configuration 5-ST-3		
Date: April, 1979		Drawn By: D.F.G.

Figure F-48. Underride Guard Design 5ST-3 (continued)

Table F-19. Parts List for Guard 5ST-3.

DESIGNATION	DESCRIPTION	MATERIAL	NUMBER REQUIRED
T1	Fabricated Tubing, 2"x2"x3/16"	ASTM A514 100 ksi yield	4
T2	Fabricated Tubing, 2"x2"x3/16"	ASTM A514 100 ksi yield	2
T3	Fabricated Tubing, 3 1/2"x3 1/2"x3/16"	ASTM A514 100 ksi yield	1
T4	Fabricated Tubing 3"x3"x3/16"	ASTM A514 100 ksi yield	1
P1	Stiffener, 2"x5 3/8"x3/8"	ASTM A514 100 ksi yield	8
P2	Fabricated Tee, 4"x4"x3/16"	ASTM A514 100 ksi yield	2
P3	Gusset, 4"x9"x3/16"	ASTM A514 100 ksi yield	12
P4	Stiffener, 1 3/4"x1 3/4"x3/16"	ASTM A514 100 ksi yield	12
P5	Stiffener, 3 1/8"x3 1/8"x3/16"	ASTM A514 100 ksi yield	8
P7	Gusset, 2"x7"x3/16"	ASTM A514 100 ksi yield	8
1	Bolt,	ASTM A325-N, 104 ksi yield	24

Table F-20. Summary of Results, Test 3661-4.

AUTOMOBILE	1979 Chevrolet Impala 1857 kg (4090 lb)
FILM DATA	
Impact angle	0 deg (1.07 m (42 in) offset to left)
Initial speed of passenger car	56.8 km/h (35.2 mph) 15.8 m/s (51.7 fps)
Average velocity of trailer after impact	1.5 km/h (0.9 mph) 0.4 m/s (1.3 fps)
Max. penetration (stopping distance) of auto. c.g. at time after impact	1.73 m (5.68 ft) 0.866 sec
Avg. longitudinal accel. from impact to max. penetration*	-12.9 g
Trailer movement began at	0.031 sec
Max. movement of trailer during contact at time	0.08 m (0.27 ft) 0.866 sec
Max. distance trailer moved	0.13 m (0.42 ft) at 0.364 sec
Final location of trailer	0.08 m (0.27 ft)
Amount of underride when guard broke at time	1.07 m (3.50 ft) 0.094 sec
Speed of car at 0.094 sec	24.5 km/h (15.2 mph) 6.8 m/s (22.4 fps)

ELECTRONIC DATA -- Class 60 Filter

Impact speed		55.8 km/h (34.6 mph) 15.5 m/s (50.8 fps)
		<u>Ax(v)</u> <u>Ay(v)</u> <u>Az(v)</u> <u>Ax(e)</u> <u>Az(e)</u>
Max. 0.050 sec accel. over time interval	g	-18.1 5.0 -6.0 -19.3 6.5
	sec	0.078 0.085 0.053 0.027 0.095
	sec	0.128 0.135 0.103 0.177 0.145
Peak acceleration at time after impact	g	-57.9 -25.7 -24.8 -35.1 15.3
	sec	0.084 0.161 0.101 0.060 0.132

AUTOMOBILE DAMAGE

Maximum dynamic crush	1.62 m (5.41 ft) at 0.866 sec
Residual automobile deformation	0.84 m (2.75 ft)
Damage classification	SAE -- 12FZEW9 TAD -- 1FR6

$$* G_{avg} = \left(\frac{2}{\pi}\right) \frac{V^2}{gd}$$

where V is impact speed in m/s (ft/sec)
g is acceleration due to gravity in m/s² (ft/sec²)
d is stopping distance in m (ft)

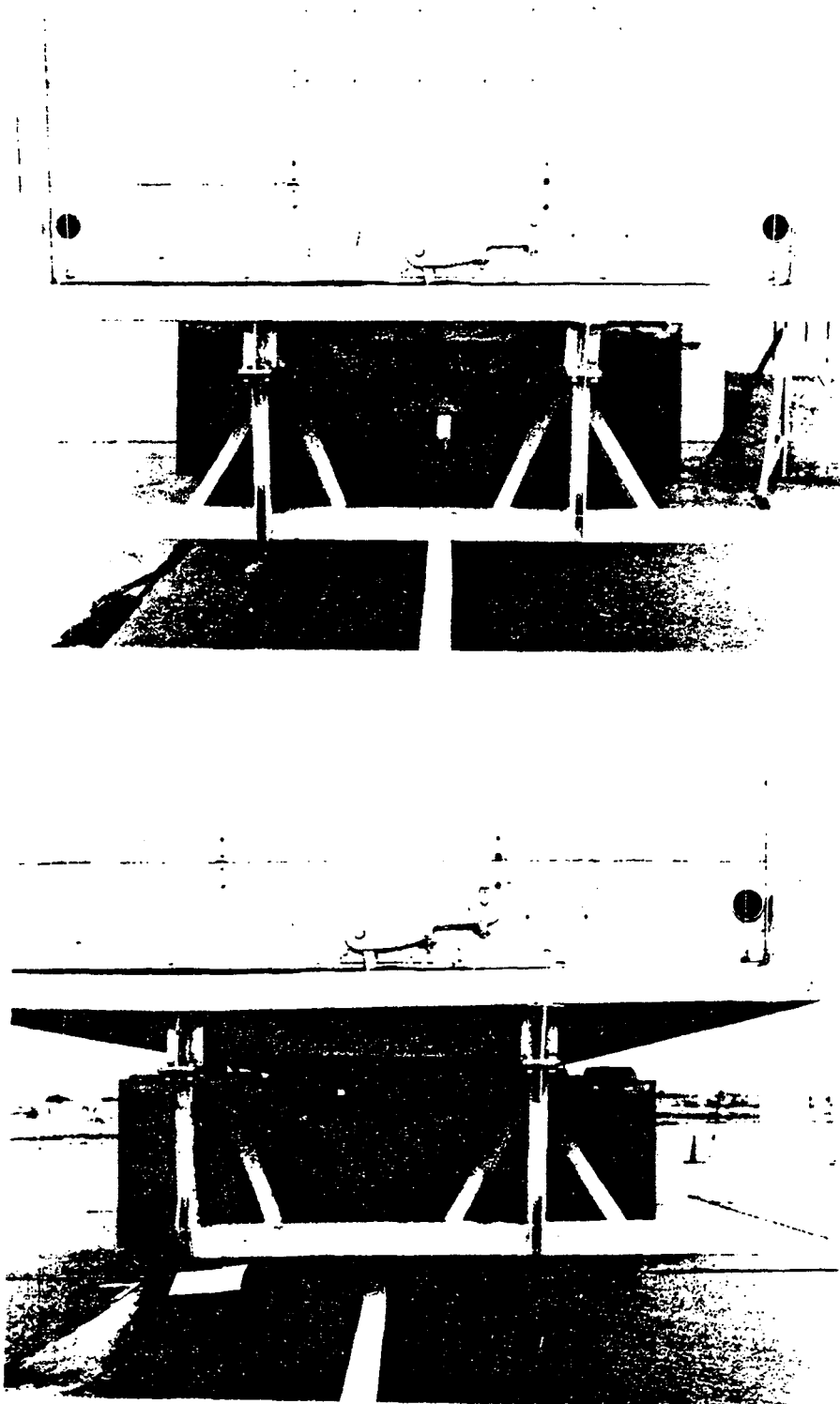


Figure F-49. Guard Before and After Test 3661-4.

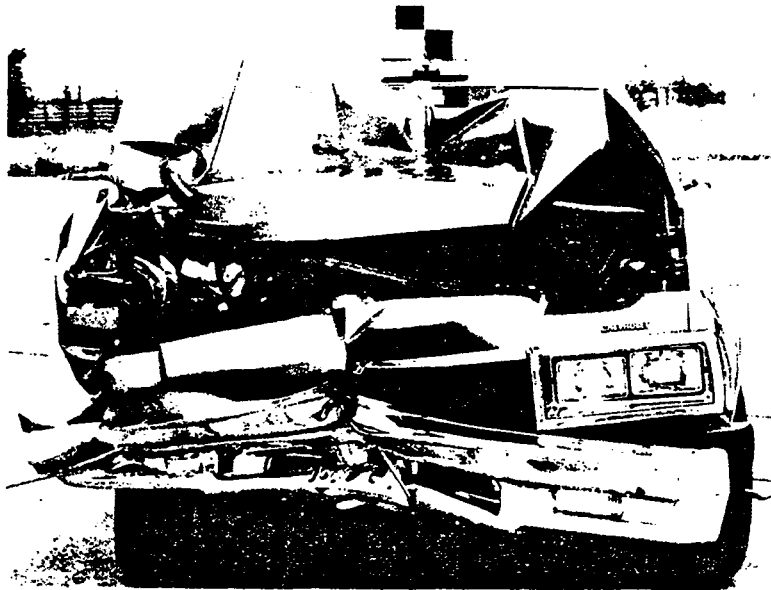


Figure F-50. Automobile Before and After Test 3661-4.

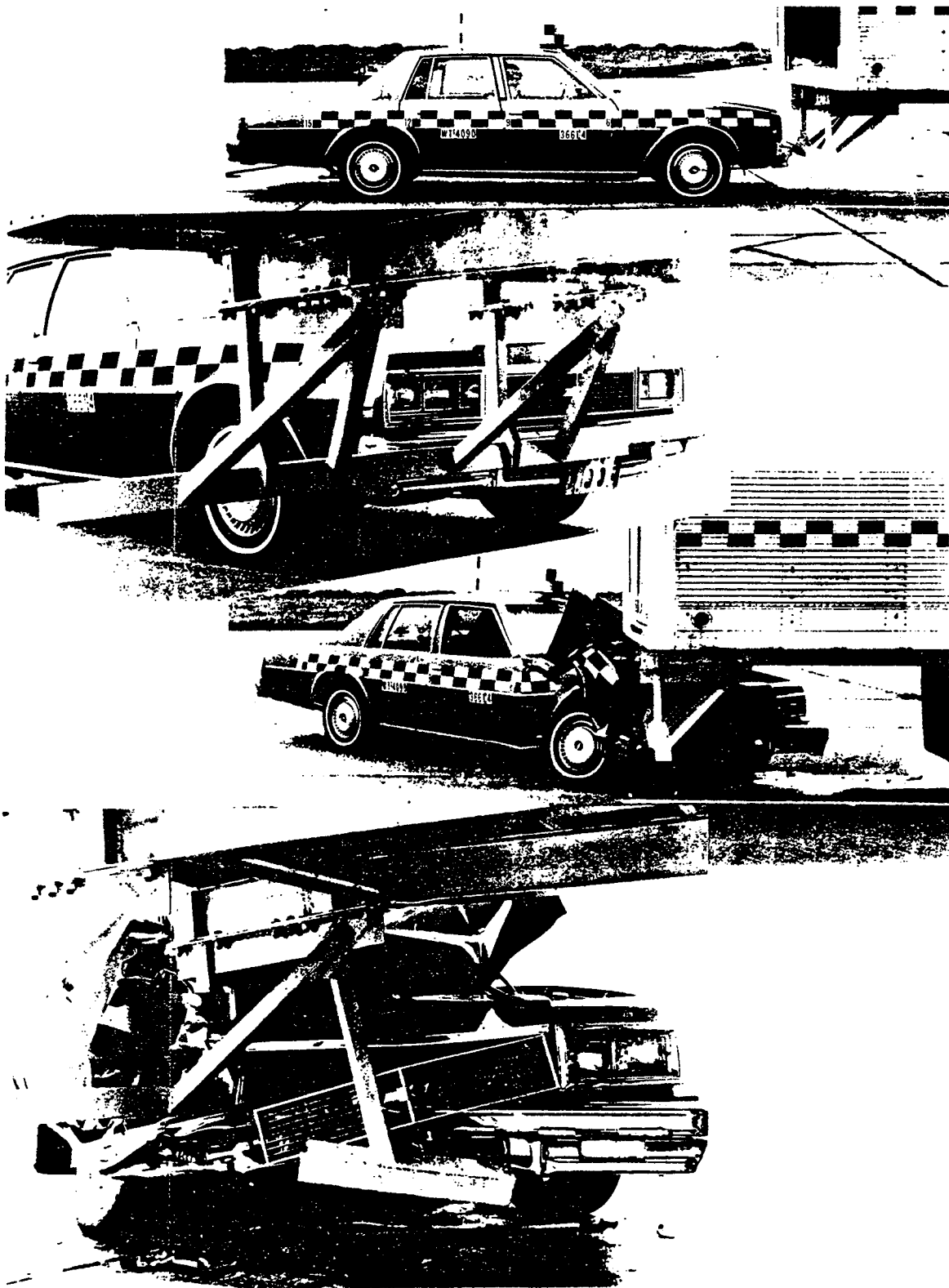


Figure F-51. Automobile and Guard Before and After Test 3661-4.



Figure F-52. Automobile Interior Before and After Test 3661-4.

F-86

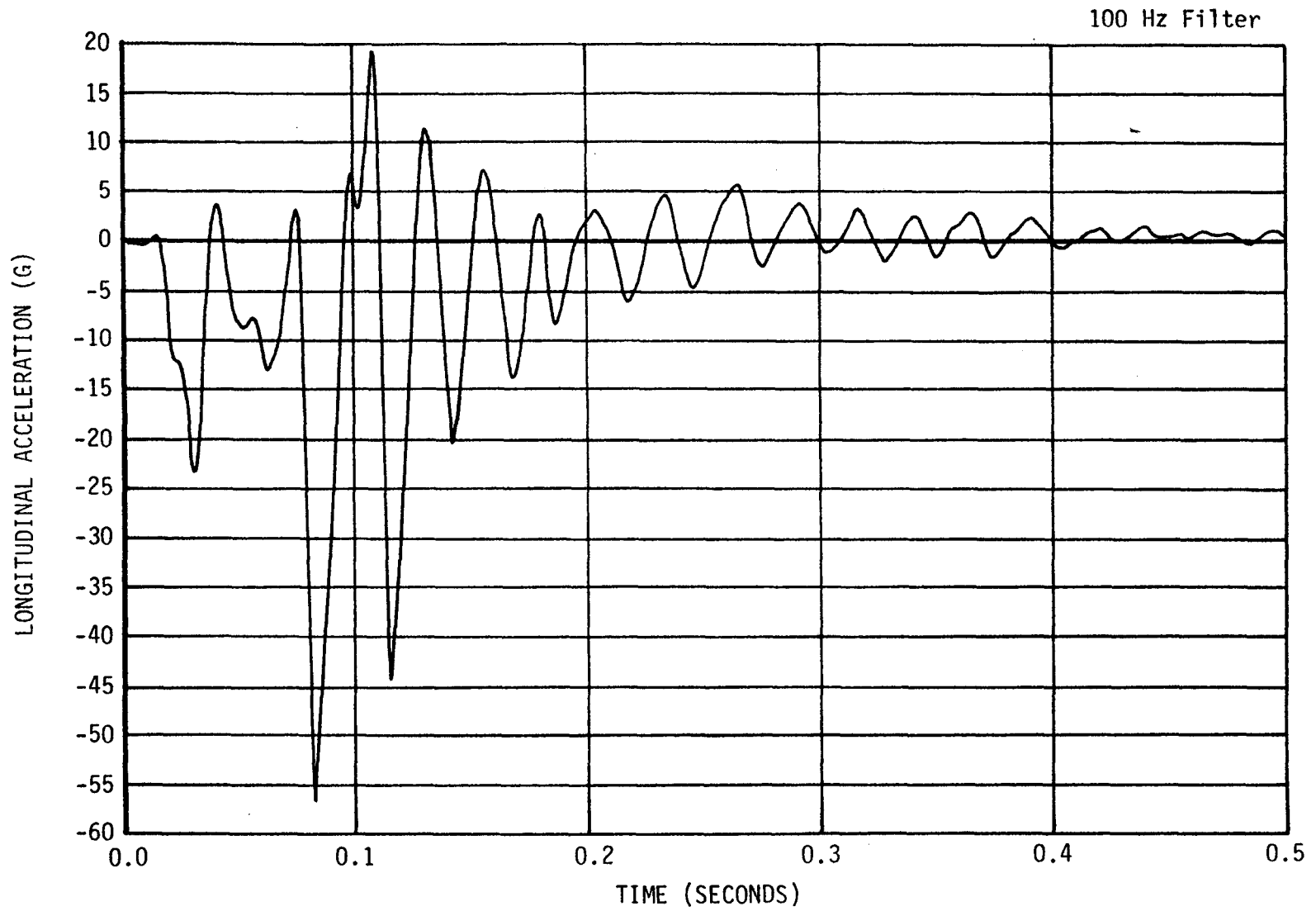


Figure F-53. Longitudinal Automobile Accelerometer Trace for Test 3661-4.

F-87

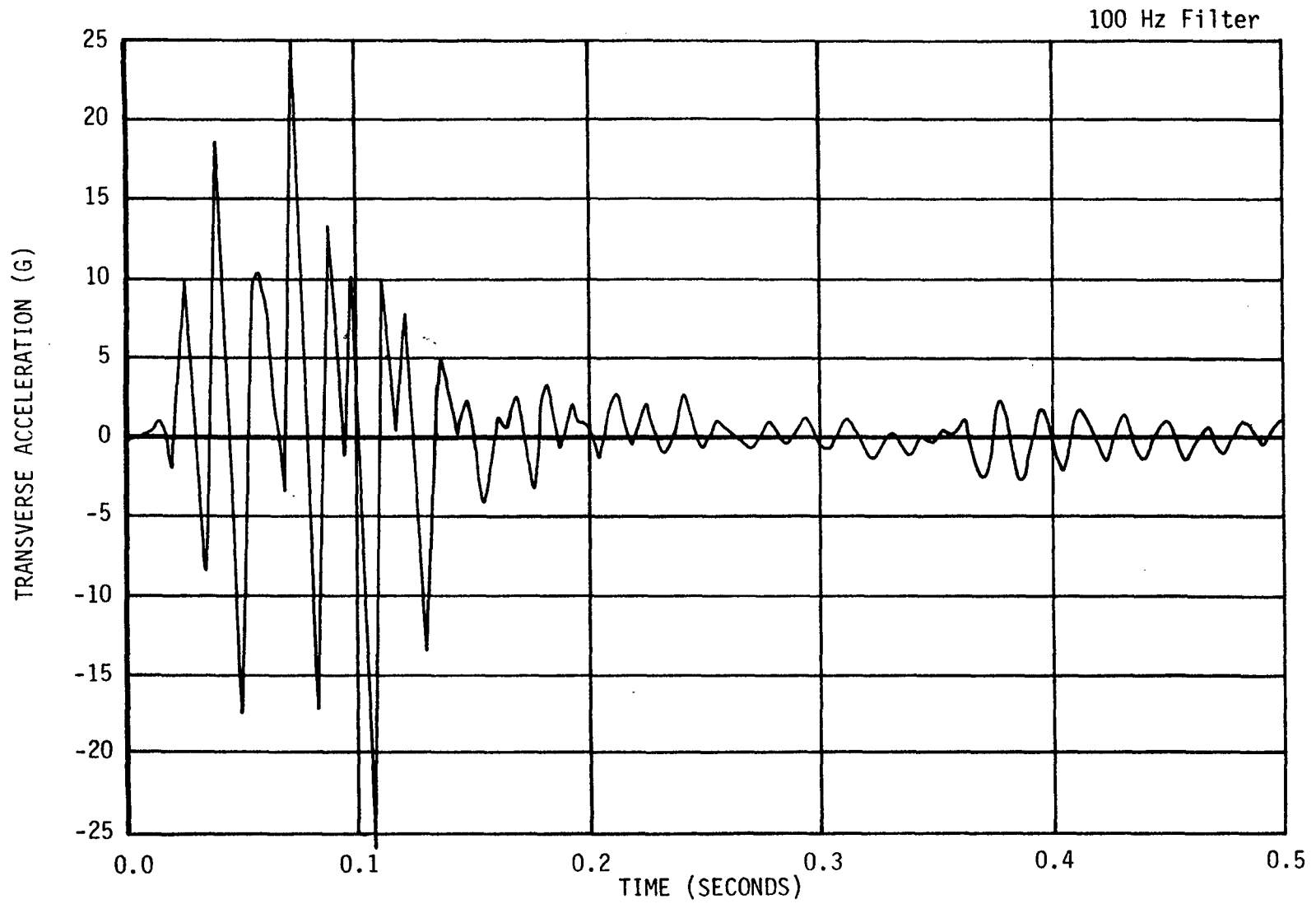


Figure F-54. Transverse Automobile Accelerometer Trace for Test 3661-4.

F-88

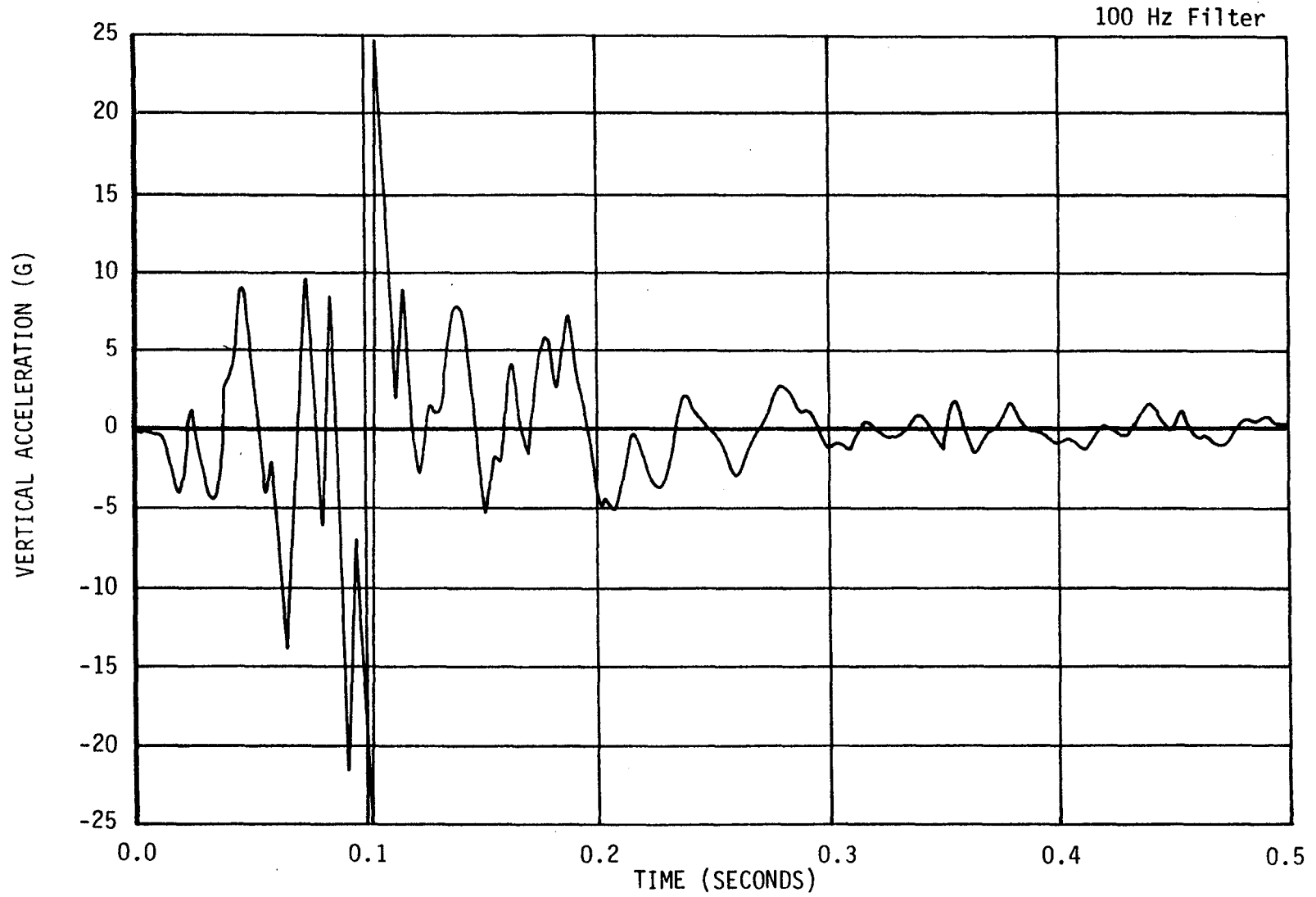


Figure F-55. Vertical Automobile Accelerometer Trace for Test 3661-4.

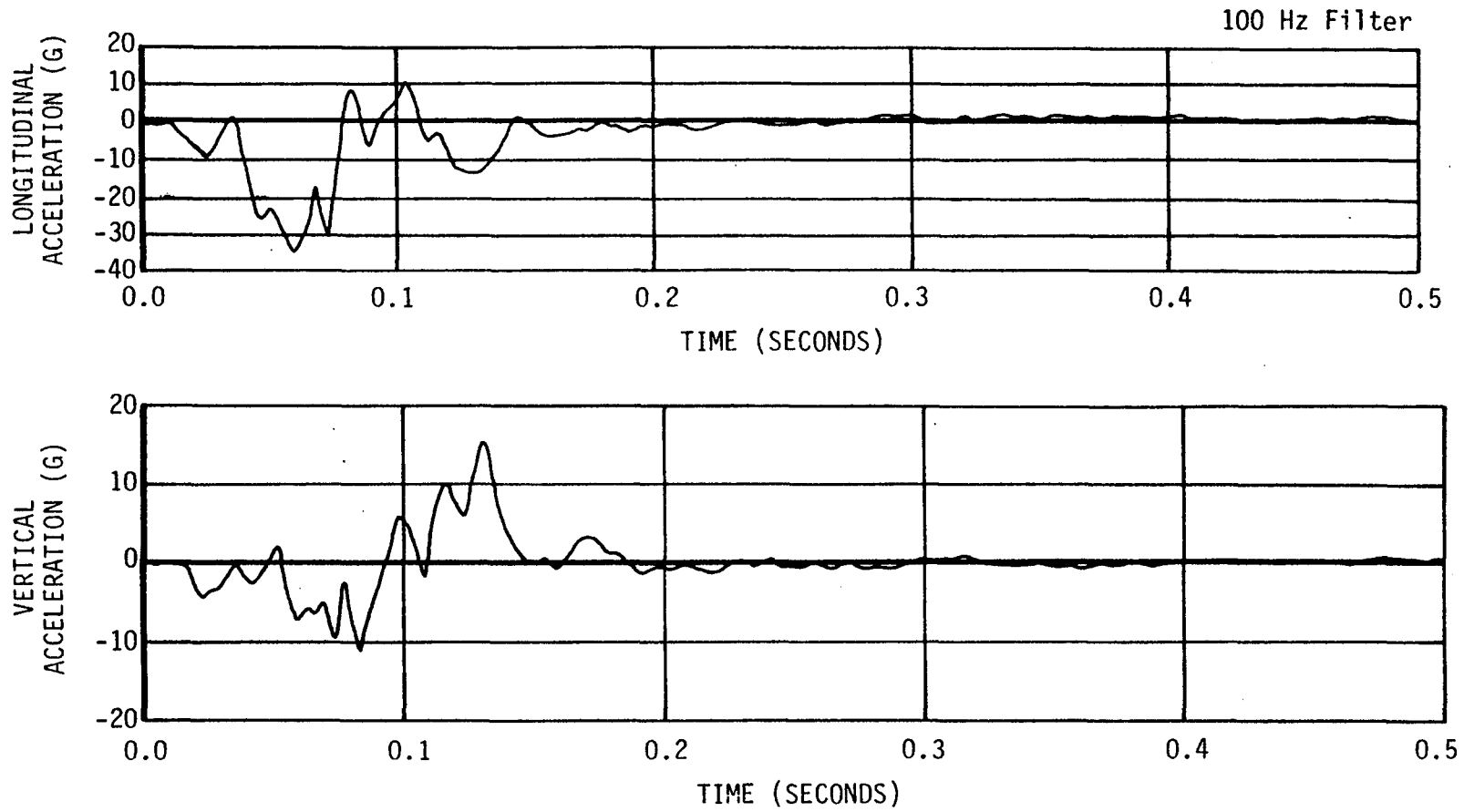


Figure F-56. Engine Accelerometer Traces for Test 3661-4.

Table F-21. Time, Displacement, Event Summary
for Test 3661-4.

TIME (SEC)	X-DISPLACEMENT (FT)	Y-DISPLACEMENT (FT)	YAW ANGLE (DEG)	EVENT
-0.046	-2.30	0.00	0	
-0.036	-1.79	0.00	0	
-0.025	-1.29	0.00	0	
-0.015	-0.79	0.00	0	
-0.005	-0.26	0.00	0	
0.000	0.00	0.00	0	Impact
0.007	0.26	0.00	0	Bumper bending
0.031	1.44	0.00	0	Trailer movement
0.036	1.67	0.01	0	Hood buckling
0.056	2.47	0.03	0	Dummies move
0.081	3.31	-0.01	1/4	Front of car down
0.097	3.60	0.02	1/2	Guard has broken
0.127	4.11	0.22	3	Dummy hits dash
0.143	4.26	0.32	4-1/4	
0.153	4.30	0.39	5-1/4	
0.168	4.38	0.48	6-3/4	
0.188	4.42	0.61	8-3/4	
0.209	4.44	0.68	11-1/2	
0.239	4.50	0.88	14-3/4	
0.260	4.50	1.00	16-3/4	
0.285	4.54	1.10	19	
0.292	4.53	1.13	19-1/2	Max. deflection of guard
0.326	4.63	1.37	23	
0.367	4.66	1.52	26-1/4	
0.448	4.80	2.04	33	
0.524	5.01	2.53	38	Rear wheels touch down
0.585	5.22	2.91	40-3/4	
0.641	5.39	3.14	43	
0.692	5.53	3.19	44-1/2	
0.764	5.60	3.10	45	
0.804	5.62	3.03	44-1/2	
0.866	5.68	2.92	44	Max. penetration & crush
0.927	5.65	2.83	43-1/4	
0.988	5.58	2.72	42-1/2	

Metric Conversion:

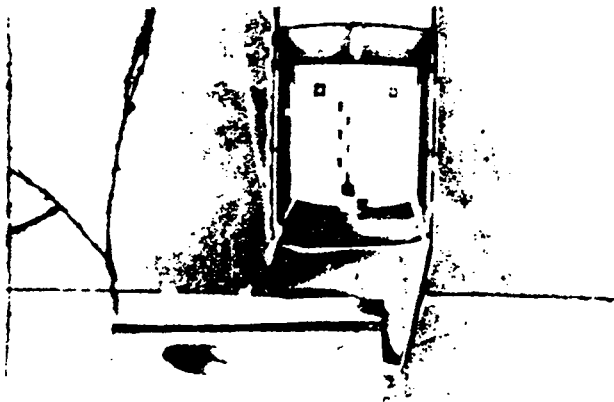
1 ft = 0.305 m



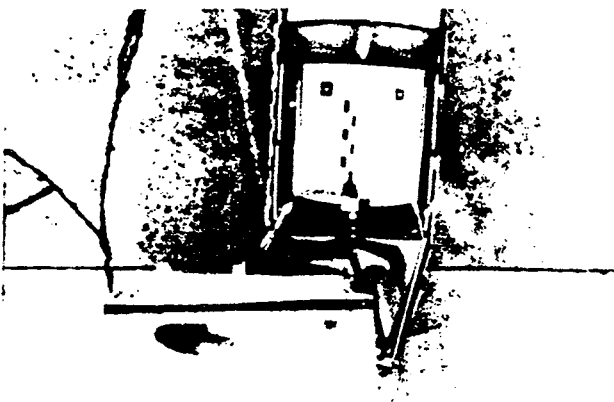
0.000 sec



0.031 sec



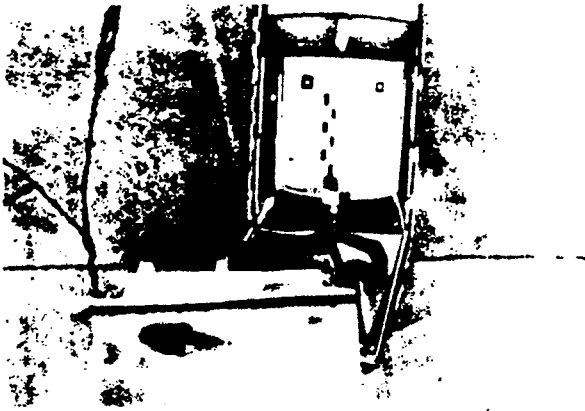
0.081 sec



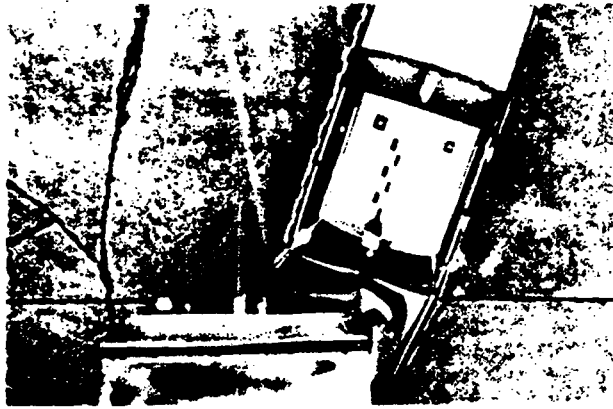
0.132 sec



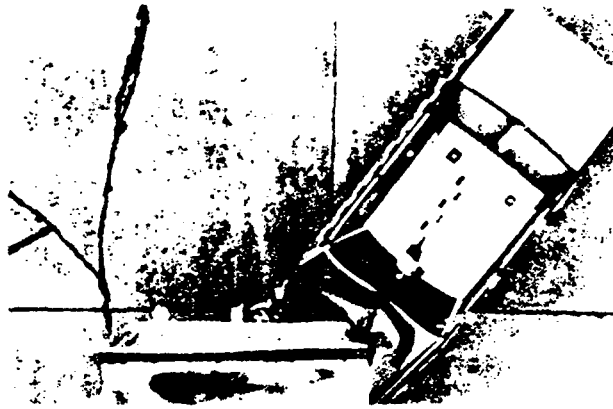
Figure F-57. Sequential Photographs for Test 3661-4.
F-91



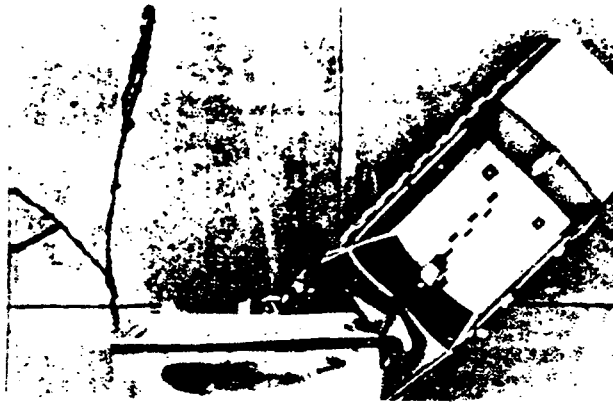
0.143 sec



0.285 sec



0.524 sec



0.748 sec



Figure F-57. Sequential Photographs for Test 3661-4 (continued)

F-93

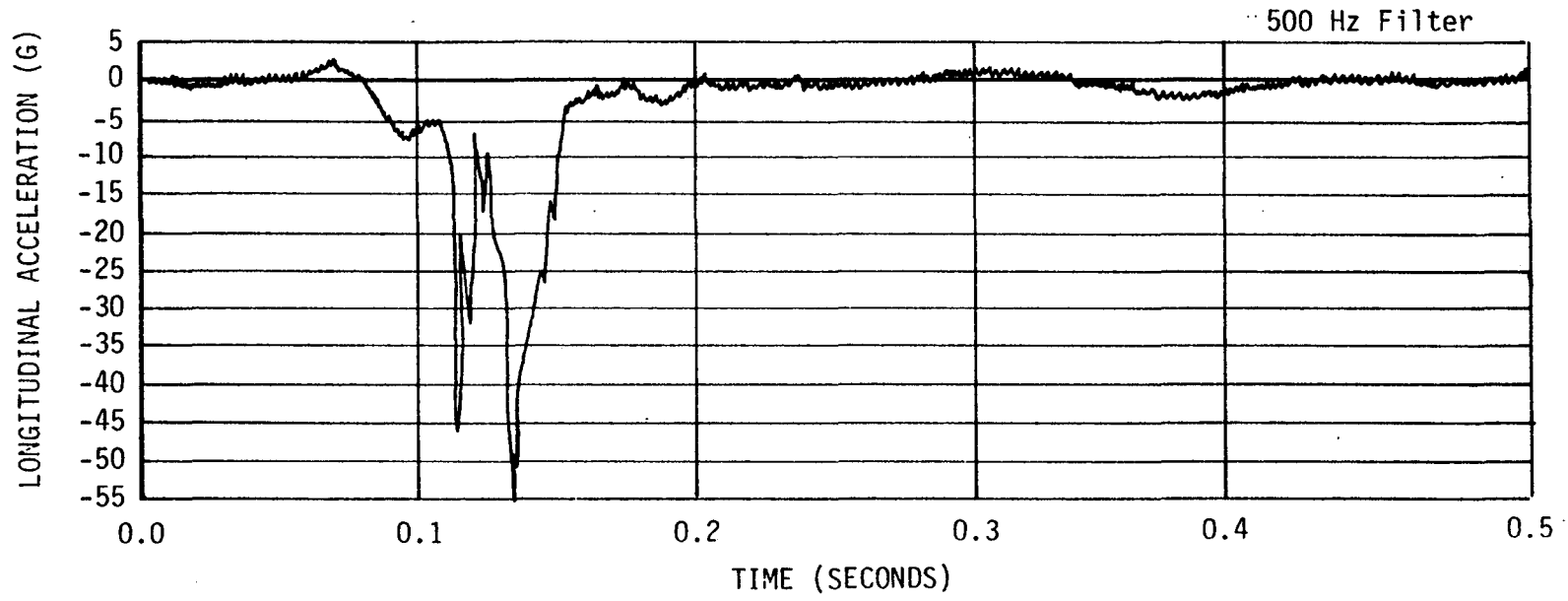


Figure F-58. Alpha Head Longitudinal Accelerometer Trace for Test 3661-4.

F-94

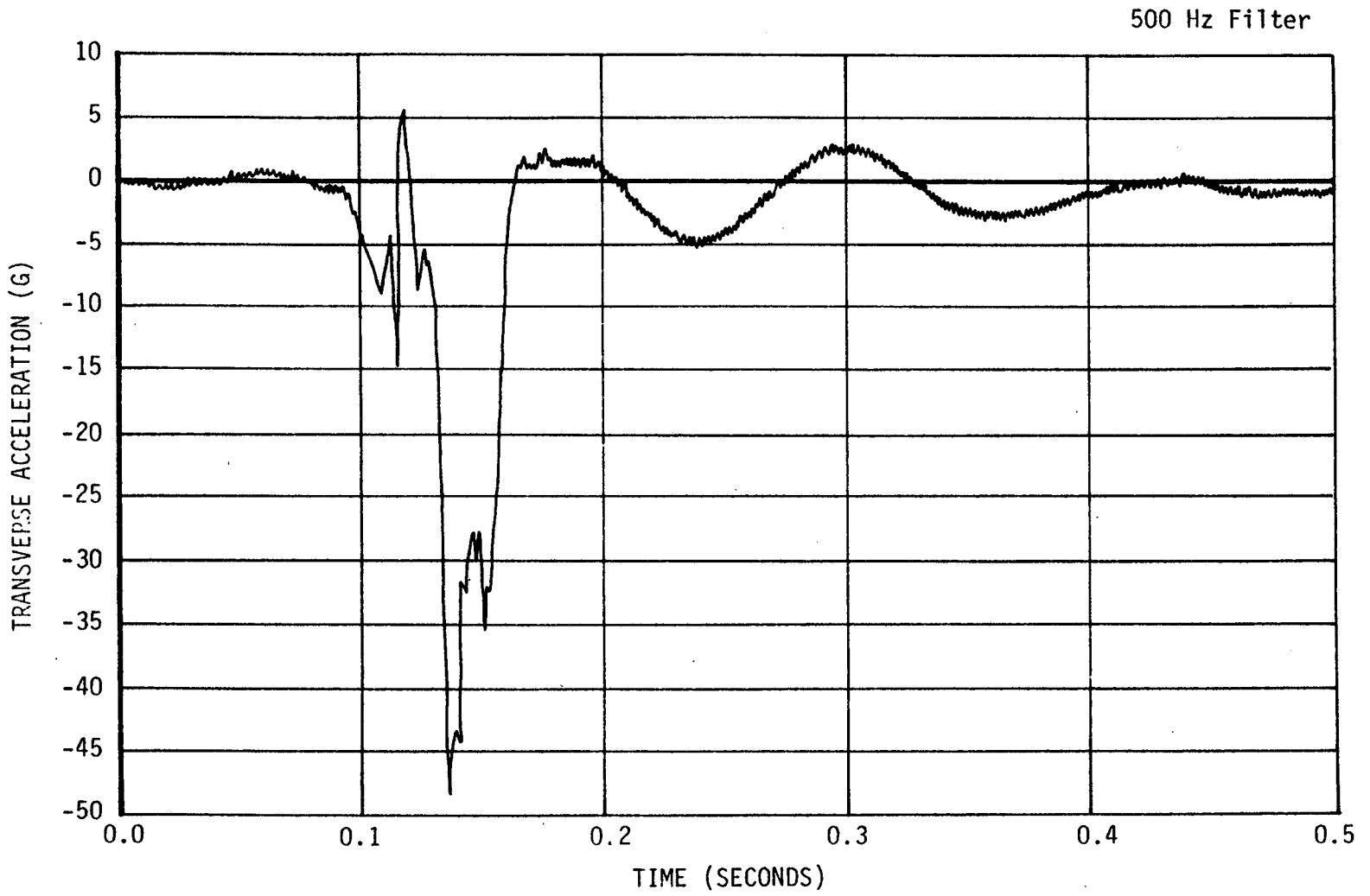


Figure F-59. Alpha Head Transverse Accelerometer Trace for Test 3661-4.

F-95

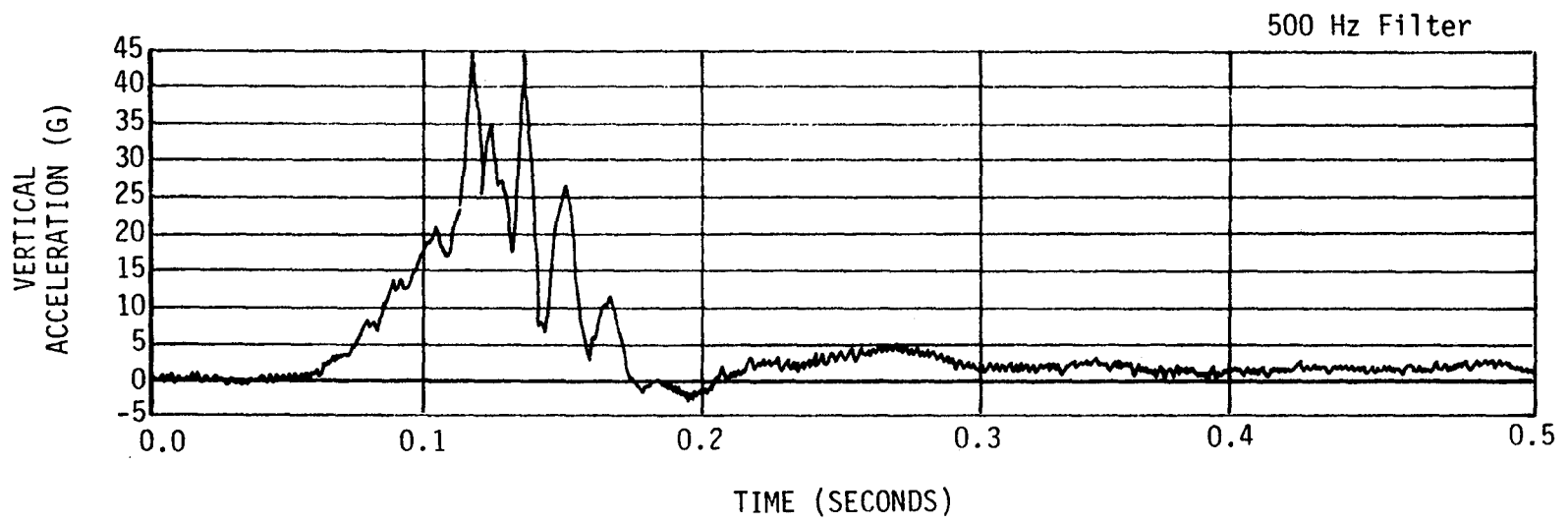


Figure F-60 . Alpha Head Vertical Accelerometer Trace for Test 3661-4.

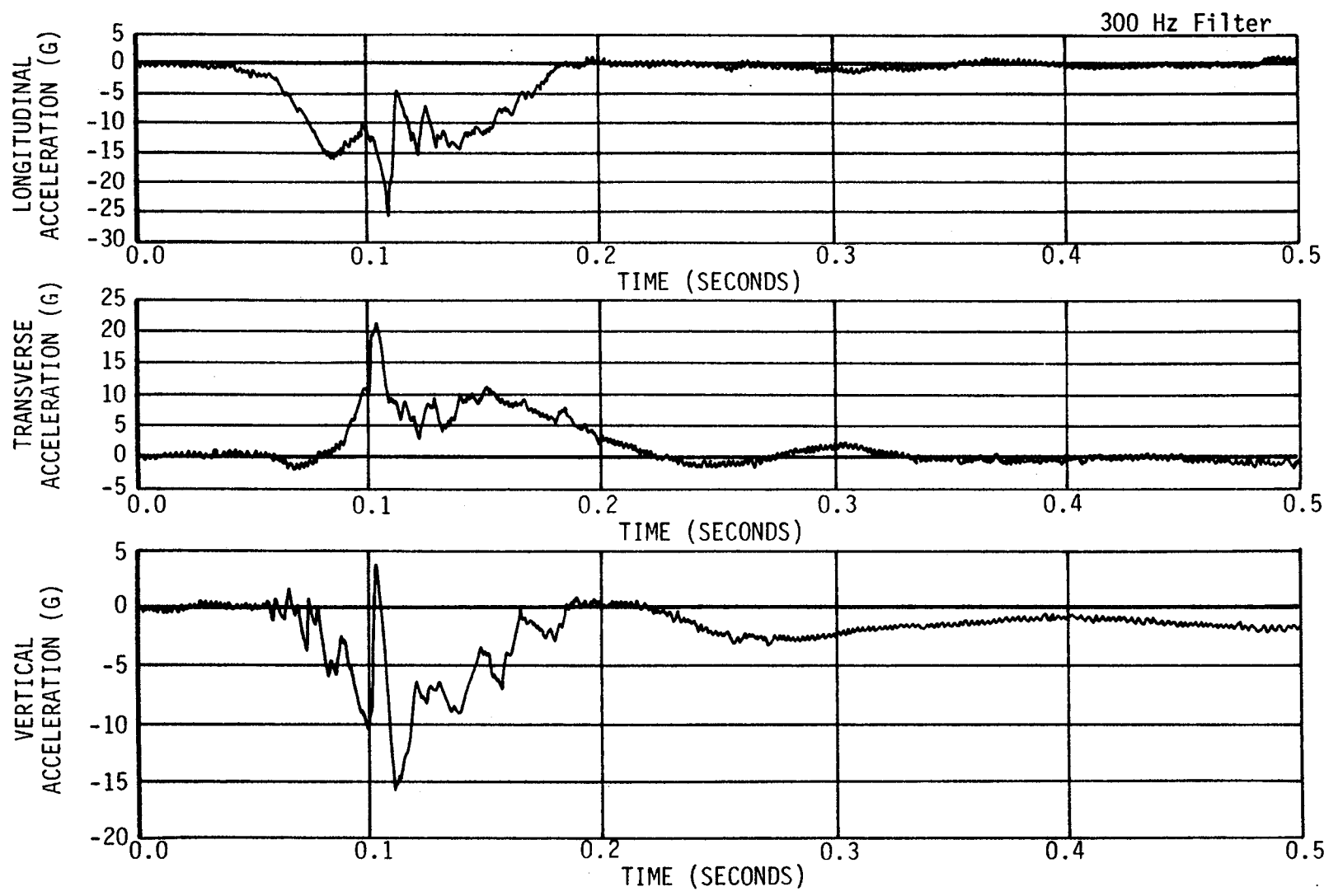


Figure F-61 . Alpha Chest Accelerometer Traces for Test 3661-4.

F-97

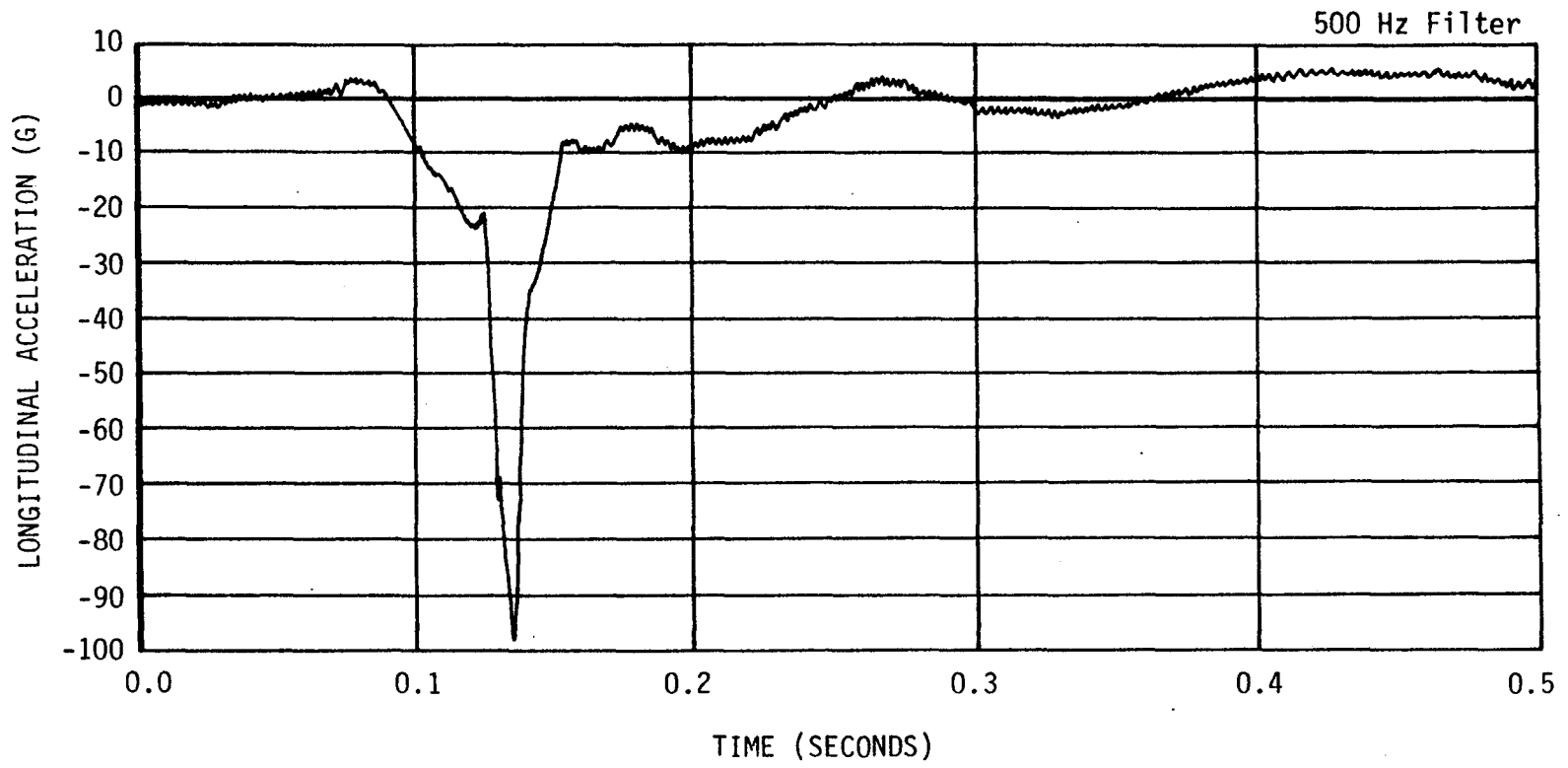


Figure F-62 . Beta Head Longitudinal Accelerometer Trace for Test 3661-4.

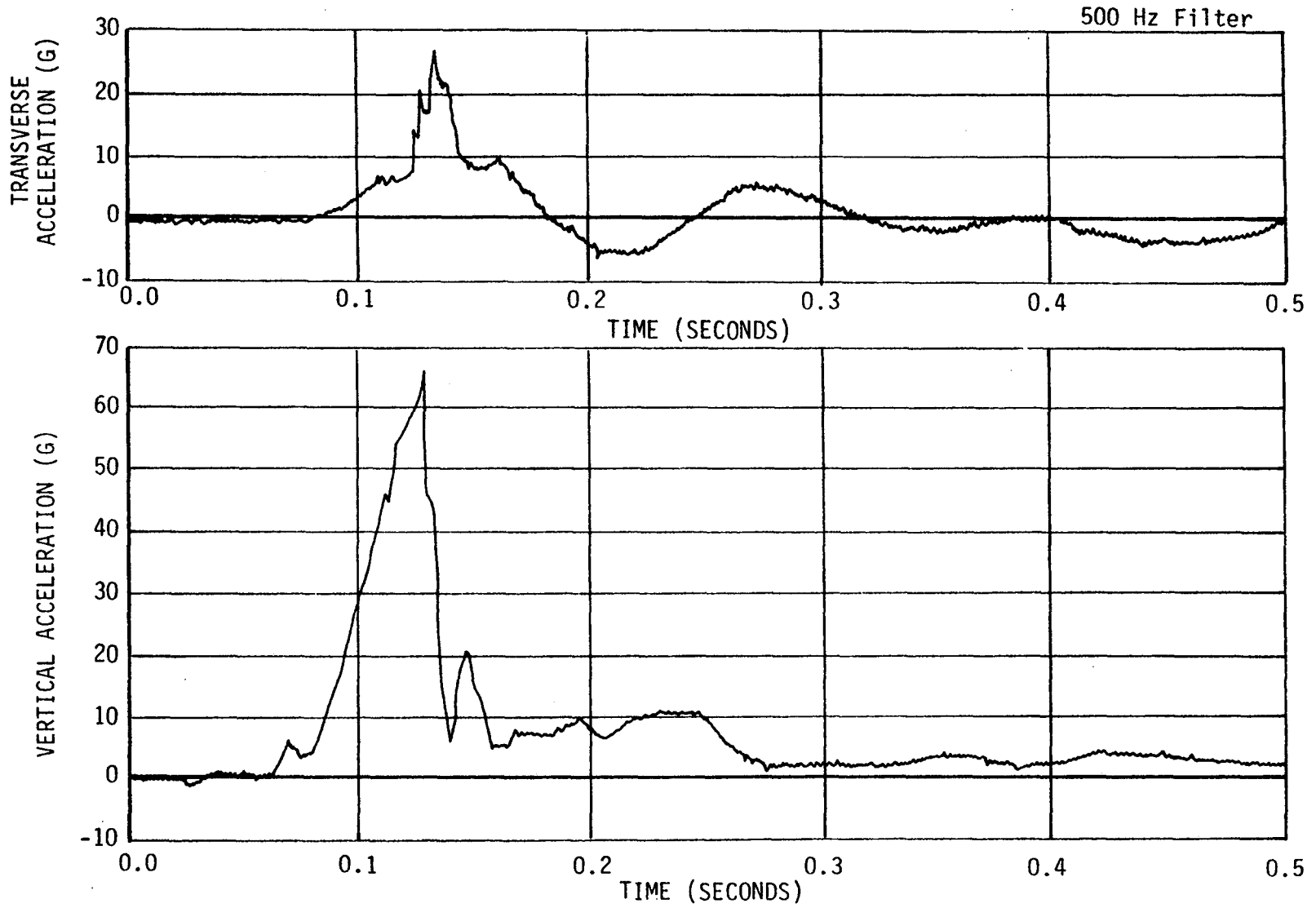


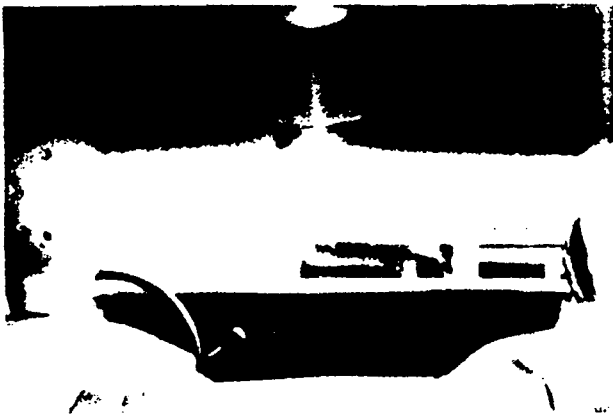
Figure F-63. Beta Head Transverse and Vertical Accelerometer Traces for Test 3661-4.

Table F-22. Dummy Time-Event Summary
For Test 3661-4.

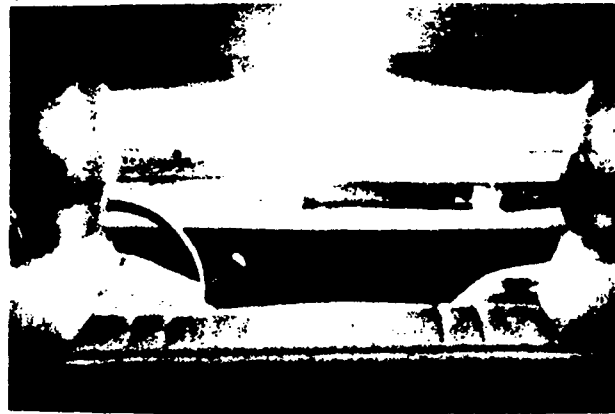
TIME (SEC)	EVENT
	<u>Alpha</u>
0.03	Initial movement
0.09	Head and chest impact steering wheel
0.13	Right side of head impacts dash
0.14	Right shoulder impacts dash
0.13 - 0.24	Head and shoulder remain against dash
0.57	Right shoulder and upper back impact top portion of front seat
0.72	Right side of head impacts left side of Beta's head
	<u>Beta</u>
0.03	Initial movement
0.12	Forehead impacts top of dash
0.37	Back impacts seat
0.72	Left side of head impacts right side of Alpha's head

Table G25. Dummy Injury Indices.

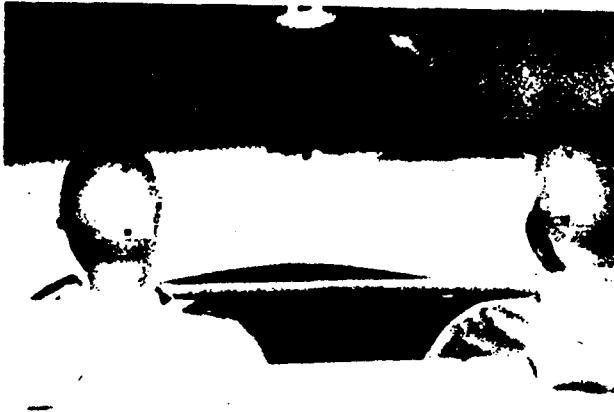
	HIC	GADD	0.003 sec G
Alpha Head	552 from 0.112 sec to 0.156 sec	680 from 0.000 sec to 0.652 sec	69 from 0.134 sec to 0.137 sec
Alpha Chest	109 from 0.074 sec to 0.170 sec	128 from 0.000 sec to 0.620 sec	27 from 0.108 sec to 0.111 sec
Beta Head	1225 from 0.104 sec to 0.142 sec	1610 from 0.000 sec to 0.602 sec	94 from 0.134 sec to 0.137 sec
Beta Chest	No instrumentation		



0.000 sec



0.028 sec



0.079 sec



0.135 sec



0.141 sec



0.287 sec



0.523 sec



0.748 sec

Figure F-64. Interior Sequential Photographs for Test 3661-4.